SLIP VELOCITIES IN PNEUMATIC TRANSPORT

A THESIS SUBMITTED IN FULFILMENT

OF THE REQUIREMENT FOR THE DEGREE OF

DOCTOR OF PHILOSOPHY

S. Ravi Sankar

M. Tech. (Chem. Eng.)

(I.I.T Madras, India)

MAY 1984

DEPARTMENT OF CHEMICAL ENGINEERING

UNIVERSITY OF ADELAIDE

AUSTRALIA

CERTIFICATE OF CONSENT

I agree that this thesis may be made available for consultation within the University.

I agree that the thesis may be made available for photo-copying.

I note that my consent is required only to cover the three-year period following approval of my thesis for the award of my degree.

S. Ravi Sankar

TABLE OF CONTENTS

LIST OF FIGURES

LIST OF TABLES

NOMENCLATURE

A	Parameter in the correlation 2.8
B	Parameter in the correlation 2.8
A_c	Cross sectional area of transport tube (m^2)
A_p	Projected area of a particle (m^2)
C	Volume fraction of solids
$C_{D\infty}$	Drag coefficient in an infinite medium
C_{min}	Lower limit of the concentration
D_p	Particle diameter (m)
D_t	Tube diameter (m)
f_D	Doppler shift
f_s	Solid-wall friction factor
f_g	Gas-wall friction factor
f_m	Combined friction factor
f	Frequency of contact of particles in the test section
f_{2N}	Frequency of contacts between clusters of size "N"
$F_{D\infty}$	Drag force on a particle in an infinite medium (N)
F_r	Froude number
F_t	Total thrust on the impact plate (N)
F_g	Thrust due to gas phase (N)
F_s	Thrust due to solid phase (N)
g	Acceleration due to gravity (ms^{-2})
k	Parameter derived from solid phase momentum equation.*(It is the ratio of slip velocity to solid velocity)*
K_f	Ratio of observed thrust to theoretical thrust
K_{2N}	Equilibrium constant for formation and break up of clusters.

L	Length of test section between pressure taps (m)
M_g	Mass flow rate of air through the tube (kgs^{-1})
n	Number concentration of particles in the test section
n_N	Number concentration of clusters in the test section
N	Number of particles in a cluster
$(\Delta P)_t$	Total pressure drop (Nm^{-2})
$(\Delta P)_{gs}$	Pressure drop due to static head of gas (Nm^{-2})
$(\Delta P)_{ss}$	Pressure drop due to static head of solids (Nm^{-2})
$(\Delta P)_{fg}$	Pressure drop due to gas-wall friction (Nm^{-2})
$(\Delta P)_{fs}$	Pressure drop due to solid-wall friction (Nm^{-2})
R	Loading ratio
Re_g	Tube Reynolds number based on gas velocity
Re_p	Particle Reynolds number
Re_t	Tube Reynolds number based on terminal velocity
T	Turbulent intensity
U_g	Superficial gas velocity (ms^{-1})
$\overline{u^2}$	Mean square fluctuation velocity (ms^{-1})
v_p	Volume of a single particle (m^3)
V_g	Gas velocity (ms^{-1})
V_s	Solid velocity (ms^{-1})
V_t	Terminal velocity of a particle (ms^{-1})
V_r	Slip velocity (ms^{-1})
V_0	Terminal velocity of a particle in the presence of wall (ms^{-1})
μ_g	Gas viscosity $(Nm^{-1}s^{-1})$
τ	Velocity gradient (s^{-1})
ρ_g	Gas density (kgm^{-3})
ρ_s	Solid density (kgm^{-3})
Φ_g	Volumetric flux of air in the test section (ms^{-1})
Φ_s	Volumetric flux of solid in the test section (ms^{-1})

SUMMARY

Slip velocities of solids in a vertical transport line were correlated to solid volume fraction and the effect of pertinent parameters such as tube diameter, particle properties and transport velocity were investigated.

Slip velocities were determined from pressure drop measurements in a counter-current flow apparatus with solid flow against rising air stream. Particles of sand, glass and steel ranging from 100microns to 700microns in diameter were investigated in 12.7, 19.1, 25.4 and 38.1mm transport tubes. The maximum solid volume fraction realised in these tests was about 10%. A strong dependence of slip velocity on solid volume fraction was observed. Its value was larger than single particle terminal velocity and increased with concentration.

The large slip velocities are due to formation of clusters of particles near the transport walls observed in the tests. A mathematical model based on gradient coagulation theory is presented to explain these trends. The significance of the concentration-slip velocity relationship for the definition of "choking" in forward transport is discussed.

It is established that Richardson & Zaki's correlation which describes the effect of concentration on slip velocity although appropriate for sedimentation and fluidization processes, can not be extended to transport of solids in the tubes where velocity gradients are considerably large. A correlation of the form $\frac{V_r}{V_t} = AC^B$ is proposed which represents the obtained data with reasonable accuracy. The parameters "A" and "B" are in turn correlated to dimensionless groups involving only system properties $(D_p, D_t, V_t, \rho_s, \rho_g, \mu_g)$.

The effect of transport velocity on slip velocity was investigated with cocurrent transport apparatus. Solid velocity and volume fraction were determined from the measurement of thrust due to solid phase on an impact plate which deflects the solid particles right angles to their flight path. This technique proved to be simple and accurate. Transport velocities as high as 15 m/s were investigated.

At large transport velocities solid-wall friction is significant and its effect is to

increase slip velocity. An attempt was made to determine the individual contributions of transport velocity and solid volume fraction from solid phase momentum balance. A correlation for the slip velocity due to solid-wall friction is proposed to help estimate the energy losses due to solid-wall friction. Some qualitative understanding of the mechanism of solid-wall frictional losses is presented and the need for independent determination of these losses and the associated mechanisms is stressed.

The usefulness of the concentration-slip velocity relationship obtained from simple countercurrent flow experiments is demonstrated by comparing the predicted trends with those obtained from cocurrent transport experiments. The observed minimum transport velocities are in good agreement with those predicted from concentration-slip velocity relationship obtained with countercurrent flow arrangement.

DECLARATION

This thesis contains no material which has been accepted for the award of any other degree or diploma in any University and, to the best of the author's knowledge and belief, the thesis contains no material previously published or written by another person, except where due reference is made in the text or where common knowledge is assumed.

S. Ravi Sankar

ACKNOWLEDGEMENTS

The author wishes to express his appreciation for the assistance that was received throughout this work.

Special thanks are due to Dr. T.N. Smith, the supervisor of this research, for his excellent guidance and encouragement throughout this work. Thanks are also due to Dr. B.K. Oneill, for his assistance when Dr. Smith moved to Perth to head the Chemical Engineering Department at Western Australian Institute of Technology.

The author wishes to thank the workshop staff, Fred Steer and Brian Inwood in particular for helping to build and revise the experimental equipment. Thanks are due to Mechanical Engineering department for lending him the expensive pressure transducer which made the task of data collection less tedious.

The author wishes to convey his appreciation for the assistance in typing and proof reading of the document from his wife Padma. The moral support and understanding obtained from her throughout his work are also very much appreciated.

The scholarship provided by the Adelaide University which enabled him to pursue this study is gratefully acknowledged.

CHAPTER 1

SLIP VELOCITY

1.1 Introduction

Pneumatic transport as a means of transporting solids is of great interest to process industries. The use of riser reactors with attractive features, such as better heat-transfer and continuous operation, placed further emphasis on the need for a better understanding of fluid-solid systems. The literature covering this subject is vast and includes both horizontal and vertical pneumatic conveying. However, the scope of the present work is confined to vertical pneumatic conveying.

One of the main objectives in the design of solid transport systems is to predict the key parameters, such as pressure drop in the line and slip velocity of solids, with reasonable confidence. The pressure drop is important in determining the power requirements and in specifying the capacity of driving machinery. The slip velocity is useful for the estimation of the amount of solids that can be conveyed at a given gas flow rate. Also it is important that a lower limit to transport is specified for trouble free and economic operation.

Some design methods have been proposed (Yang 1975, Leung & Wiles 1976) based on correlations derived from a large collection of data. However, these procedures are limited to a certain range of parameters and require caution in their application. The aim of this work is to investigate the problem of determining the slip velocity and its dependence on pertinent variables. Delineation of the effects of these variables is of great value to the design of pneumatic transport systems.

1.2 Definition

Slip velocity in pneumatic transport is the velocity of the carrying fluid relative to the moving solid. In the case of fluidization where the net movement of the solids is

zero, its value is equal to the gas velocity in the fluidized bed.

$$V_r = V_g - V_s \tag{1.1}$$

where

V_r is the Slip velocity

V_g is the Gas velocity

V_s is the Solid velocity

1.3 Significance of Slip Velocity

Slip velocity is a prime factor in the design of transport systems, for it represents the minimum gas velocity at which any transport is feasible. When a substantially greater fluid velocity is chosen for practical transport of solid at a specified rate through a conduit, the slip velocity may be used to calculate the solid velocity and the volumetric concentration in the conduit. These in turn may be used to calculate the contributions of solid-wall friction and solid weight, to the pressure gradient which must be applied to the motive fluid in order to maintain transport. While solid weight can simply be estimated from concentration and solid density, estimation of solid-wall frictional loss requires that its dependence on solid velocity is established.

It is therefore, a fundamental requirement for design of transport systems to identify the factors that influence the slip velocity, and to establish a quantitative relationship with those factors.

A systematic analysis of vertical pneumatic system will be presented, accompanied by a review of related works.

1.4 Factors Influencing Slip Velocity

Consider the situation of solids transported up against gravity, by a gas in a vertical conduit . Under steady state conditions, with zero acceleration of solids, the

slip velocity (V_r) should ideally be equal to the single particle terminal velocity (V_t), if all the particles behaved as if they were surrounded by an infinite fluid medium. Therefore:

$$V_r = V_t \tag{1.2}$$

where

V_t is the Particle terminal velocity

1.4.1 Single Particle Terminal Velocity

Terminal velocity is defined as the equilibrium velocity of a particle, moving under gravity relative to an infinite fluid medium subject to the influence of drag. Its value is determined by equating the fluid drag ($F_{D\infty}$) on the particle to the net weight (including buoyancy) of the particle. For a spherical particle of diameter D_p, the force balance is:

$$F_{D\infty} = \frac{\pi}{6} D_p^3 (\rho_s - \rho_g) g \tag{1.3}$$

where

$F_{D\infty}$ is the Fluid drag

D_p is the Particle diameter

ρ_s is the Particle density

ρ_g is the Fluid density

g is the Acceleration due to gravity

The hydrodynamic drag experienced by such a particle was first derived theoretically by Stokes (1891), for creeping flow conditions:

$$F_{D\infty} = 3\pi \mu_g V_t D_p \tag{1.4}$$

where

μ_g is the Fluid viscosity

However, it is the turbulent flow case that is of practical interest, and no satisfactory theoretical treatment has been developed because of the complexity of representing the turbulent flow field mathematically; and as a consequence, empirical methods have been resorted to. Following the dimensional analysis approach, it is established experimentally that the drag coefficient, which is defined as the ratio of drag force per unit projected area to velocity head, is a unique function of the particle Reynolds number which characterises the flow field around the particle. Therefore:

$$C_{D\infty} = \frac{F_{D\infty}/A_p}{\frac{1}{2}\rho_g V_t^2} = f(Re_p) \tag{1.5}$$

where

$C_{D\infty}$	is the Drag coefficient in an infinite medium
Re_p	is the Particle Reynolds number
A_p	is the Surface area of the particle normal to the direction of flow

The above functional relationship is very well established and is presented in graphical form, tables, or in the form of empirical equations. The terminal velocity of a spherical particle can now be expressed as follows (from equations 1.3 and 1.5).

$$V_t = \sqrt{\frac{4gD_p(\rho_s - \rho_g)}{3C_{D\infty}\rho_g}} \tag{1.6}$$

From the above expression the significance of drag coefficient in determining the relative motion can be easily seen.

1.4.1.1 Effect of Free Stream Turbulence

The standard drag coefficient-particle Reynolds number relationship (Fig. 1.1) is based on the experiments with particles in a quiescent fluid medium. It has been accepted practice, in pneumatic transport work, to estimate terminal velocities of particles using the standard drag curve.

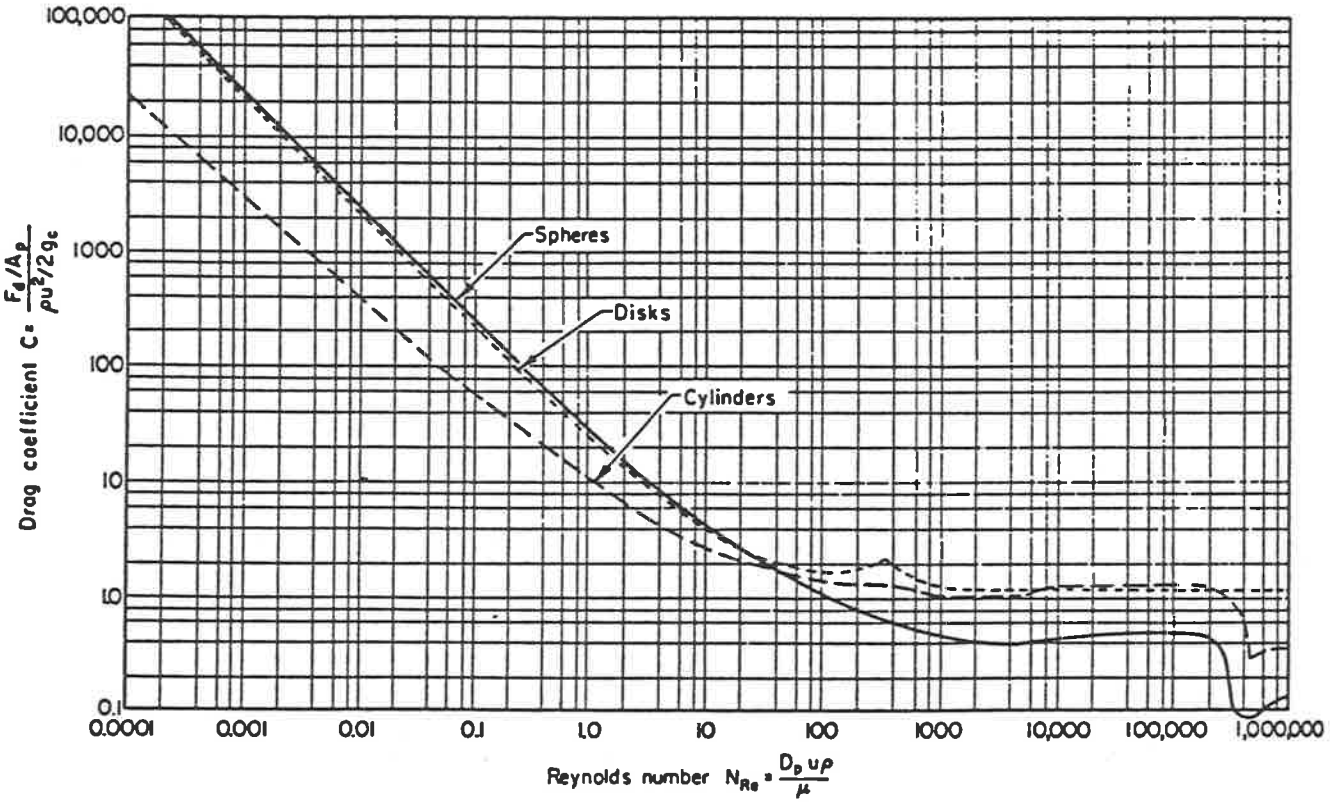

Fig. 1.1 Drag coefficient for spheres, disks and cylinders.
From Lappel and Shepherd (1940).

However, it was suggested by some workers (Dryden et al 1937, Clamen & Gauvin 1969, Torobin & Gauvin 1961, Clift & Gauvin 1970, Uhlherr & Sinclair 1970) that the free stream turbulence influences the boundary layer around the sphere, thus affecting the drag coefficient. Consequently, the drag coefficient is a function of not only the particle Reynolds number but also of the intensity of turbulence. Thus:

$$C_{D\infty} = f\,(Re_p, T) \qquad [Uhlherr]$$

$$T = \frac{\sqrt{\overline{u^2}}}{V_t}$$

where

T is the Turbulent intensity

$\overline{u^2}$ is the Mean square fluctuation velocity of gas

Based on experimental results with spheres of diameter ranging from 1.6mm to 19mm and densities ranging from 1.0 to 8.0 gm/cc, in water and glycerol solutions of viscosities up to 4cp, Uhlherr & Sinclair (1970) proposed the following correlations (Fig. 1.2).

$$C_{D\infty} = \begin{cases} 162\frac{\sqrt[3]{T}}{Re_p} & \text{for} \quad Re_p < 50 \ \text{ and } \ .05 \le T \le 0.5 \\ 0.133\left(1 + \frac{150}{Re_p}\right)^{1.565} + 4T & \text{for} \quad 50 < Re_p < 700 \ \text{ and } \ .05 \le T \le 0.5 \end{cases} \qquad [Uhlherr]$$

In summary, they conclude that the drag coefficient increases with increasing free stream turbulence at higher levels of intensity, while its value is less than the value given by the standard drag curve at lower levels of intensity. The qualitative explanation of this behaviour was also presented.

Clift & Gauvin (1970) calculated terminal velocities of silica and steel spheres in air for different levels of free stream turbulence, making use of correlations presented by Dryden et al (1937), Torobin & Gauvin (1961), and Clamen & Gauvin (1969). The plot (Fig. 1.3) of terminal velocity versus particle diameter as a function of the relative turbulent intensity, suggests that the effect of free stream turbulence is predominant

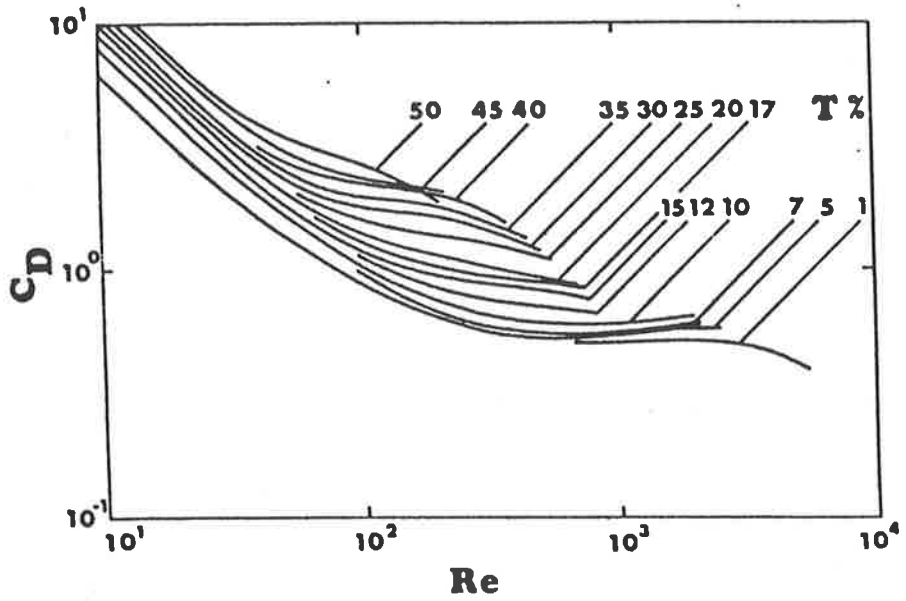

Fig. 1.2 Effect of relative turbulence intensity on the drag coefficient of spheres.
From Uhlherr and Sinclair (1970).

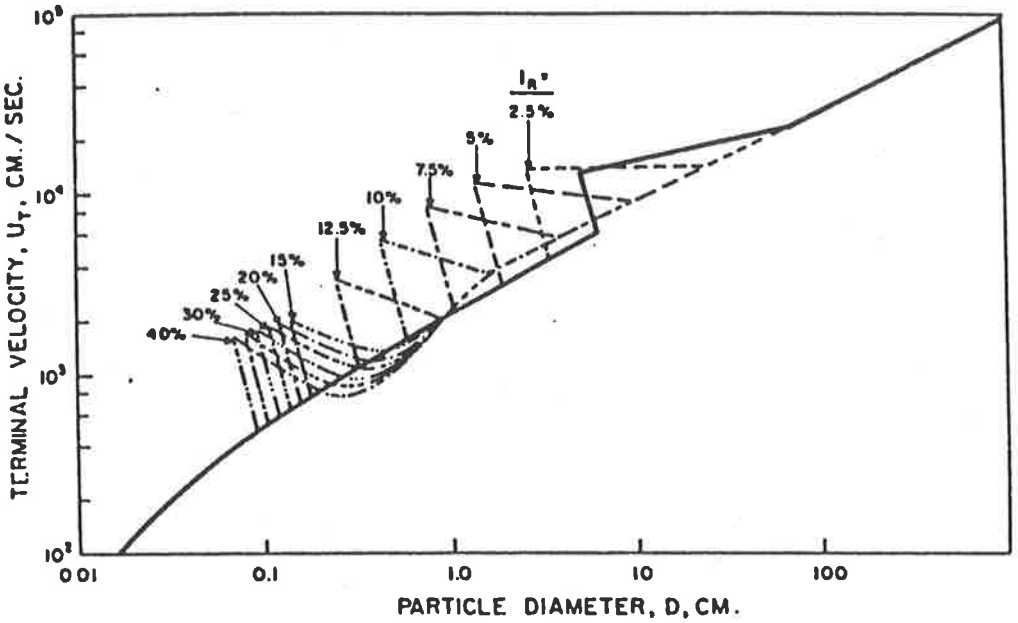

Fig. 1.3 Terminal velocity of silica spheres, as a function of relative intensity of turbulence.
From Clift and Gauvin (1970).

for larger particles. The smallest particle size affected at largest turbulent intensities (40%) is about 1000 microns. Consequently, the effect of the free stream turbulence may safely be ignored for systems with particle size less than 1000 microns. However, it should be borne in mind that the effect of increasing levels of turbulence results in a reduction in the above critical particle size.

From the foregoing discussion, it is clear that the slip velocity between the gas and solid is the terminal velocity of the particle, the value of which depends on the properties of the particle and the fluid medium. The slip velocity can therefore be expressed as follows.

$$V_r = V_t = f(\rho_g, \mu_g, \rho_s, D_p) \tag{1.7}$$

1.4.2 Solid Volumetric Concentration

So far the influence of neighbouring particles on the flow field around a particle has been ignored. There is ample evidence in the literature to show that such an influence is significant. It is very well established for liquid-solid systems that the slip velocity is a strong function of solid volumetric concentration which reflects the degree of proximity of neighbours and their influence on the flow field. Barnea & Mizrahi (1973) presented an excellent review of the literature on this aspect, for liquid-solid systems.

1.4.2.1 Theoretical Solutions

Theoretical solutions describing the effect of concentration on slip velocity are summarized in Table 1.1. These solutions are based on the assumptions:

1. creeping flow conditions prevail
2. there is no slip on the solid surface
3. there are no collisions between particles or formation of clusters
4. a convenient spatial organisation of the particles may be chosen

Table (1.1)

Comparison of the asymptotic solutions for very dilute suspensions in creeping flow region

(after Barnea et. al.,)

Author	Method	Equation
Uchida (1949)	Cell model, cubic cell	$\frac{V_f}{V_t} = \frac{1}{1+2.1C^{\frac{1}{3}}}$
Happel (1958)	Cell model, spherical cell, free surface boundary conditions	$\frac{V_f}{V_t} = \frac{1}{1+1.5C^{\frac{1}{3}}}$
Leclair and Hamielee (1968) Gal-Or (1970)	Cell model, spherical cell, zero vorticity boundary condition	$\frac{V_f}{V_t} = \frac{1}{1+1.8C^{\frac{1}{3}}}$
Hasimoto (1959)	Point force technique, cubic arrangement	$\frac{V_f}{V_t} = \frac{1}{1+1.76C^{\frac{1}{3}}}$
McNown and Lin (1952)	Point force technique	$\frac{V_f}{V_t} = \frac{1}{1+1.6C^{\frac{1}{3}}}$
Smoluchowski (1911) McNown and Lin (1952) Famularo and Happel (1965)	Reflections, cubic arrangements	$\frac{V_f}{V_t} = \frac{1}{1+1.92C^{\frac{1}{3}}}$
Famularo and Happel (1965)	Reflections, rhombohedral arrangements	$\frac{V_f}{V_t} = \frac{1}{1+1.79C^{\frac{1}{3}}}$
Famularo and Happel (1965)	Reflections, random arrangement	$\frac{V_f}{V_t} = \frac{1}{1+1.3C^{\frac{1}{3}}}$
Burgers (1942)	Random arrangement	$\frac{V_f}{V_t} = \frac{1}{1+6.88C}$
*Bachleor (1972)	Random allocation	$\frac{V_f}{V_t} = 1 - 6.5C$

** (added reference)*

Although almost all the works cited in the Table 1.1 adhered to the hypothesis of regular arrangement of particles as they settle through the fluid medium, Burgers (1942) and Batchelor (1972) deduced the effect of concentration on slip velocity assuming random spatial distribution of settling particles. In this context it should be mentioned that the fluidization experiments with 4mm acrylic spheres in silicone liquid by Smith (1968), suggest that the spatial distribution of settling spheres in a viscous liquid agrees with a random distribution based on allocation of spheres to space according to binomial probability distribution at 0.025 concentration level.

However, it is interesting to note that all these solutions indicate that the slip velocity decreases with increasing solid volumetric concentration. The predicted trend was confirmed by batch fluidization and sedimentation experiments carried out by several workers. These works were extensively reviewed by Garside & Al-Dibouni (1977) and Barnea & Mizrahi (1973), for liquid-solid systems. Similar trends were also reported for gas-solid systems (Mogan et al 1969 & 1971, Rowe et al 1982, Capes & McIlhinney 1968, Richardson & Davies 1966, Godard & Richardson 1968).

1.4.2.2 Semi Theoretical Solutions

Ishii & Zuber (1979) and Barnea & Mizrahi (1973) proposed drag similarity criteria based on a mixture viscosity concept, to explain decreasing slip velocity with the increase in solid volumetric concentration. It was postulated that a particle settling in a suspension, experiences an increase in effective viscosity of the medium, due to the interacting momentum exchange mechanism between neighbouring particles. Redefining drag coefficient and particle Reynolds number based on mixture viscosity, it was postulated that the standard drag-Reynolds number relationship could be extended to suspensions using a redefined mixture drag co-efficient as a function of the particle Reynolds number. Barnea & Mizrahi (1973) and Ishii & Zuber (1979) report that experimental results from various sources could be represented successfully by this model, although different expressions for mixture viscosity were used. The uncertainty in de-

termining the mixture viscosity, renders this approach unattractive. Moreover, viscosity of a suspension is a useful idea only if objects are settling through it in relative motion to the body of particles forming the suspension. If all particles are settling together, they are moving through the simple fluid.

1.4.2.3 Empirical Solutions

The most widely accepted correlation is that due to Richardson and Zaki (1954), based on liquid-solid sedimentation and fluidization experiments.

Based on a dimensional analysis, Richardson & Zaki (1954) conclude that the ratio of slip velocity to single particle terminal velocity is a function of particle Reynolds number, particle to tube diameter ratio, and solid volumetric concentration.

$$V_r = V_0 (1 - C)^n$$
$$V_0 = V_t (10)^{-\frac{D_p}{D_t}} \qquad [Richardson]$$
$$n = f\left(Re_p, \frac{D_p}{D_t}\right)$$

where

C is the Volumetric concentration of solids

D_t is the Tube diameter

D_p is the Particle diameter

V_0 is the Slip velocity corresponding to zero concentration

The above correlation was reported to be applicable to particulate gas-solid systems by several authors (Capes & McIlhinney 1968, Richardson & Davies 1966, Godard & Richardson 1968, Mogan et al 1969), based on fluidization experiments.

1.4.2.4 Deviations from Zaki's Correlation

However, Garside & Al-Dibouni (1977), Addler & Happel (1962), and Capes (1971) report that the Zaki's correlation overestimates the slip velocity at solid volumetric concentrations less than 1%.

Rowe et al (1982) and Mogan et al (1971) report larger values of exponent (n), for gas fluidization of fine solids, which do not give particulate fluidization. Capes (1974) attributes these larger values of exponents to particle agglomeration, which reduces the effective voidage and increases the effective particle size. Following the above postulation, and fitting Richardson & Zaki's correlation to Mogan's (1967,1971) data, the deviations from the calculated and experimental results were reduced.

All the works cited so far report that the slip velocity decreases with increasing concentration while its value is always less than the corresponding single particle terminal velocity. This conforms to the theoretical predictions based on the assumption that particulate conditions prevail.

Barfod (1972), based on sedimentation of fine powders (15-30μ range) in water, reports an increase in slip velocity with increasing concentration up to 0.1%. Matsen (1982) and Barfod (1972) quote the works of Jayaweera et al (1964), Jovanovic (1965), Johne (1966) and Kaye et al (1962) on sedimentation of solids in liquids reporting an increase in slip velocity with increasing concentration (up to 1%). The slip velocities were larger than the single particle terminal velocity by a factor of 1.1 to 2.4. The higher slip velocities are attributed to formation of clouds or clusters of particles whose effective terminal velocity is higher than the single particle terminal velocity. The growth of such clusters is said to increase with increasing concentration thereby increasing the slip velocity.

Similar trends were reported by Yerushalmi & Cankurt (1979) based on fast fluidization experiments with fine particles (33μ, 49μ), in 152mm (ϕ) test section. The concentration versus slip velocity plot presented in their work indicates that the slip velocity is larger than the terminal velocity, and its value increases with increasing concentration up to 10%. However, the concentration-slip velocity relationship was not unique, and dependent on the solid flow rate as well. This could be due to non-ideal effects such as solid-wall friction and incomplete acceleration of solids.

Yousfi & Gau (1974) reported slip velocities several times larger than the single particle terminal velocity, while transporting fine catalyst particles (20μ, 183μ). It was observed that large clusters of particles were formed near the walls. The range of concentrations studied was as high as 22%. Although the concentration and slip velocity were not presented explicitly, the correlation presented indicates that slip velocity increases with increasing concentration.

Capes & Nakamura (1973) also report slip velocities larger than the single particle terminal velocity at low gas velocities. They attribute this to a particle recirculation phenomenon, which is characterised by solid particles sliding down the wall, then subsequently picked up by the upward moving gas in the core of a transport tube. Unfortunately, the dependence of slip velocity on concentration was not presented.

Matsen (1982) proposed the following correlation, based on the entrainment data of Wen & Hashinger (1960), and the sedimentation data of Koglin(1971).

$$\frac{V_r}{V_t} = \begin{cases} 1 & \text{for} \quad C < 0.0003 \\ 10.8C^{0.293} & \text{for} \quad 0.0003 < C < 0.1 \end{cases} \qquad [Matsen]$$

Their work is significant, as they show that flow maps constructed from the correlations predicting a decrease in slip velocity with increasing concentration (eg. Richardson & Zaki's correlation), do not predict the experimentally observed voidage discontinuity at "choking". Their work suggests such a discontinuity would be possible, only if the slip velocity increases with an increase in the concentration. Fig. 1.4 and Fig. 1.5 are presented to illustrate this point. Unlike Fig. 1.4, Fig. 1.5 exhibits an envelope which limits the possible solid rate at any given gas velocity. Below this envelope a slight change in either gas velocity or solid rate results in a corresponding slight change in voidage. However, as the envelope is reached, in order to accommodate any further decrease in gas velocity or increase in solid feed rate, the system should change to a totally different voidage-slip line. This results in a sudden increase in volume fraction of solid which is called "choking".

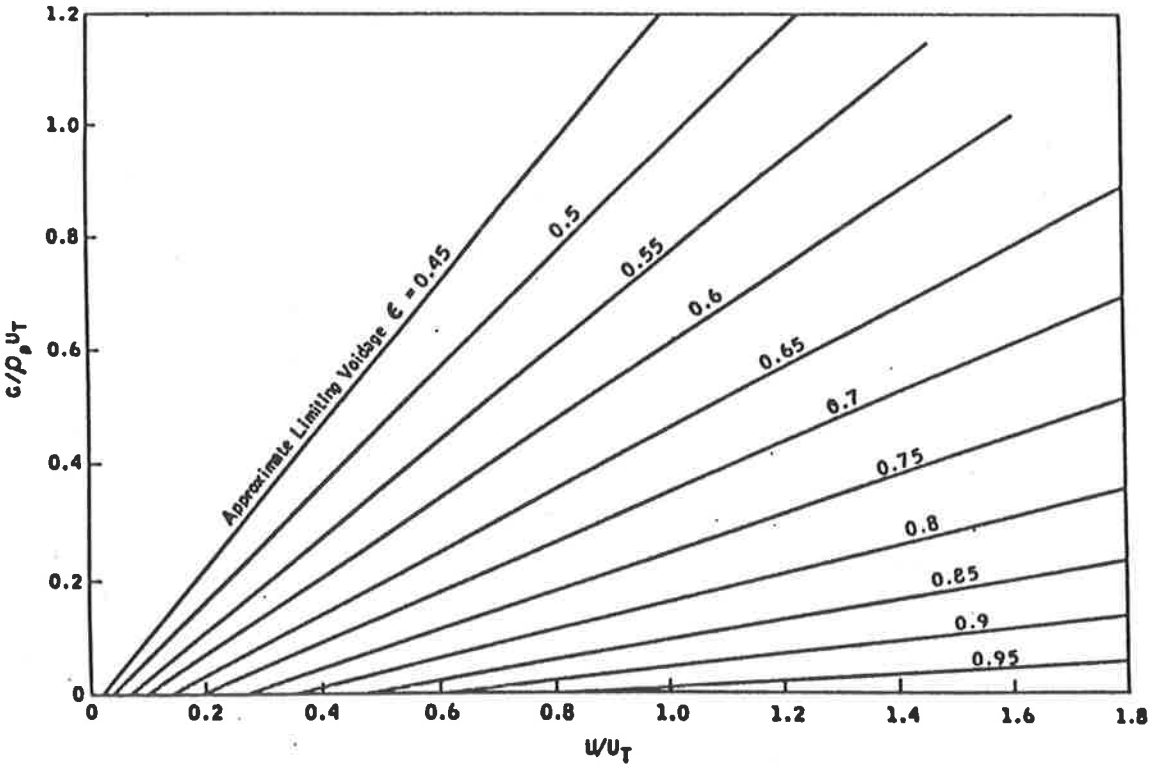

Fig. 1.4 Gas-solid flow map. Richardson-Zaki slip velocity. *From Matsen (1982).*

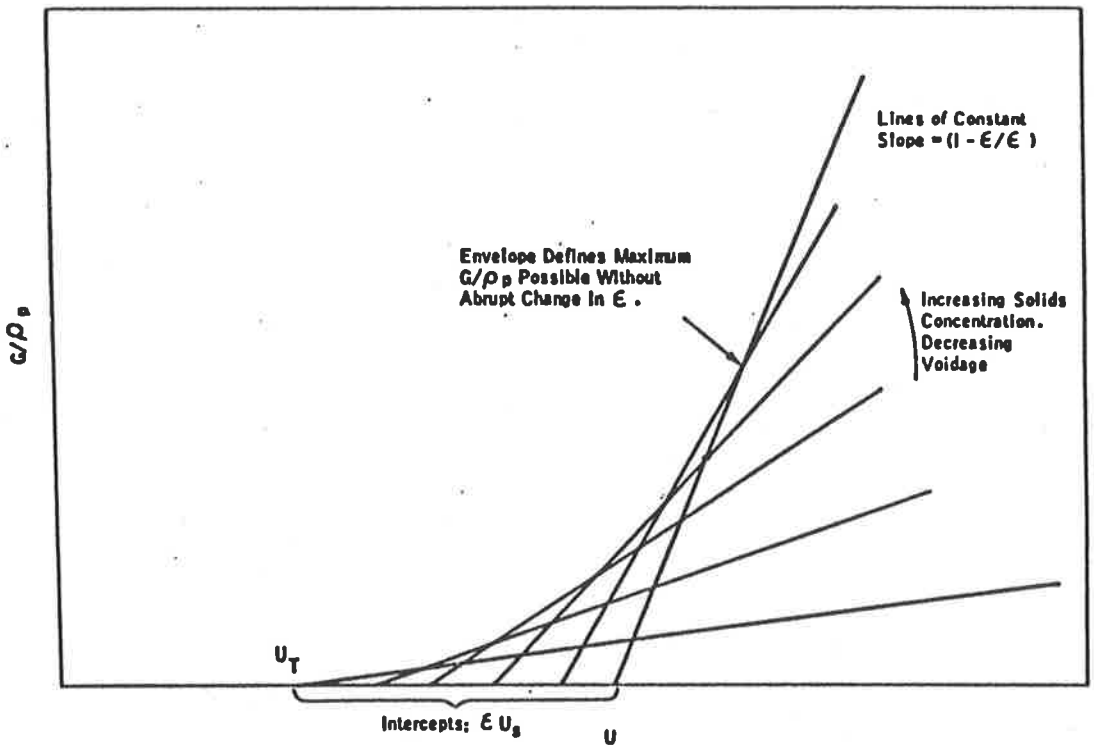

Fig. 1.5 Gas-solid flow map. Schematic behaviour for dilute phase flow when slip velocity increases with particle concentration. *From Matsen (1982).*

In summary, the effect of concentration on slip velocity should be considered with caution. While for particulate conditions in both gas-solid and liquid-solid systems slip velocity is less than the single particle terminal velocity, and its value decreases with increasing concentration, in aggregative conditions where formation of clusters is possible, slip velocity exceeds terminal velocity and its value increases with increase in concentration.

At this point, it should be noted that the majority of works (Leung 1971, Yang 1973, Capes & Nakamura 1973, Dixon 1976, Arastoopour & Gidaspow 1979) on vertical pneumatic transport assume that Richardson & Zaki's correlation can be used to represent the effect of concentration on the slip velocity. Although extension of batch fluidization results to transport systems, with the assumption that actual transport can be represented by moving fluidized bed, was experimentally verified for liquid-solid systems, so far no such direct verification is presented for gas-solid systems to the author's knowledge. Richardson & Zaki (1954), while discussing the extension of their correlation to vertical hydraulic transport, suggest that the fluid velocity gradient and turbulence could be of considerable importance.

In conclusion, slip velocity is a strong function of concentration. The functional relationship between these two quantities depends on the flow regime. The above relationship is yet to be established for pneumatic transport of solids. The majority of studies on pneumatic transport have been done at very low concentrations and high transport velocities where solid-wall friction governs the slip velocity. Very few studies (Yerushalmi 1976, Yerushalmi & Cankurt 1979, Yerushalmi et al 1978, Yousfi & Gau 1974) have extended the results to the situation of low transport velocities and high solid concentrations. No attempt has been made to correlate concentration to slip velocity.

Clearly, there remains a need to establish this relationship, at low transport velocities where influence of solid-wall friction on slip velocity is negligible, and the

influence of concentration alone is determined.

$$V_r = f(V_t, C) \tag{1.8}$$

1.4.3 Effect of Tube Wall

1.4.3.1 Hydrodynamic Influence

The effect of the tube wall on the single particle terminal velocity was discussed by Garside & Al-Dibouni (1977) and Barnea & Mizrahi (1973). Theoretical and empirical solutions quoted by these authors are summarised in Table 1.2. These solutions indicate that the presence of the wall increases the drag on the particle, thereby reducing the terminal velocity. The correlation presented by Richardson & Zaki (1954) was derived from extrapolation of slip velocities to zero volumetric concentration of solids. Richardson & Zaki's correlation suggests that at any particular solid concentration, the slip velocity decreases with decreasing tube diameter.

Capes & Nakamura (1973) report that the particle terminal velocities determined from the intercepts of gas-solid velocity plots are less than the calculated terminal velocity of the particle. The ratio of intercept value to the calculated value decreased with increasing particle size. This was attributed to a solid-wall effect, and disputed by Wheeldon & Williams (1980) who maintained that the effect of tube diameter on terminal velocity was insignificant. They attribute this lower value derived from the intercept to a failure to use correct gas density in the terminal velocity calculations.

Yousfi & Gau (1974), based on their investigations with fine catalyst particles (20μ) in 38mm and 50mm diameter tubes, proposed a correlation which indicates that the slip velocity decreases with increasing D_p/D_t ratio.

$$\frac{V_r}{V_t} = 1 + 3.2 \times 10^{-3} (Re_g)^{0.5} (C)^{0.25} \left(\frac{D_p}{D_t}\right)^{-1.8} \left(\frac{\rho_g}{\rho_s}\right) \qquad [Yousfi]$$

Table (1.2) WALL EFFECT ON TERMINAL VELOCITY

Author	Correlation	Comments
Happel and Brenner (1965)	$\frac{V_0}{V_t} = 1 - 2.1\left(\frac{D_p}{D_t}\right) + 2.19\left(\frac{D_p}{D_t}\right)^3 - 0.95\left(\frac{D_p}{D_t}\right)^5 \cdots$	Theoretical solution (creeping flow)
Ladenburg (1907)	$\frac{V_0}{V_t} = \left(1 + 2.4\frac{D_p}{D_t}\right)^{-1}$	Theoretical solution (creeping flow)
Francis (1933)	$\frac{V_0}{V_t} = \left(\frac{1-\frac{D_p}{D_t}}{1-.475\frac{D_p}{D_t}}\right)^4$	Theoretical solution (creeping flow)
Munroe (1888)	$\frac{V_0}{V_t} = 1 - \left(\frac{D_p}{D_t}\right)^{3/2}$	Turbulent flow $10^3 < Re_p < 3 \times 10^3$
Garside and Al-Dibouni (1977)	$\frac{V_0}{V_t} = \left(1 + 2.35\frac{D_p}{D_t}\right)^{-1}$	$3 < Re_p < 120$ Experimental
Richardson and Zaki (1954)	$\frac{V_0}{V_t} = 10^{-\frac{D_p}{D_t}}$	$0.2 < Re_p < 10^3$ From extrapolation of results to zero concentration

where

Re_g is the Tube Reynolds number

Van Zuilichem et al (1973) reported that the calculated slip velocities were less than measured values for wheat particles of 4mm size in tubes of diameters 53, 81 and 130mm. However, this deviation was reported to increase with increasing tube size, contradicting the previously reported trend. Unfortunately the method of determining the experimental terminal velocities was not presented. It is thus not possible to comment on the accuracy of their observations.

1.4.3.2 Boundary Influence

Apart from the indirect influence of the tube wall on the motion of particles, it is possible that the effect of actual contact of particles with the tube wall is significant. If the solid wall friction is significant, and the frequency of contact of the solid particle with the wall is substantial, then the presence of the wall should result in large slip velocities in vertical transport. In other words, given that the solid friction is significant, at a given solid velocity the frequency of contact between the solid and the tube wall would be expected to increase with decrease in tube size, resulting in greater momentum loss, thus increasing the slip velocity.

Van Zuilichem et al (1973), from their experiments with wheat particles, in tubes of 51, 80 and 130mm diameters, quoted increasing slip velocities with decreasing tube diameter.

Maeda et al (1974), from their experiments with tube diameters ranging from 8mm to 20mm, found that the slip velocity increased with decreasing tube diameter.

Klinzing & Mathur (1981) quoted the following correlation given by Hinkle (1953), based on high transport velocity experiments.

$$V_r = 0.68\,(\rho_s)^{0.5}\,(\rho_g)^{-0.2}\,(D_p)^{0.93}\,(D_t)^{-0.54} \qquad [Klinzing]$$

The above correlation also suggests that the slip velocity increases with decreasing tube diameter.

Konno & Satio (1969) maintained that the slip velocity can be approximated to terminal velocity, based on their experiments with various particle sizes (120-1440μ) in 26.5 and 46.8mm tubes. However, closer examination of their results reveals that for a particular particle size slip velocities in a 26.5mm tube were larger than the slip velocities in a 46.8mm tube.

Jotaki et al (1978) observed that the influence of tube diameter on slip velocity was not significant, in their experiments with polyethylene pellets (4mm in diameter and 2.4mm thick) in P.V.C. tubes of diameters 41.2, 52.6, 66.8, 78.3 and 100mm. It is possible that this is due to large tube sizes involved in their investigations. Van Zuilichem et al (1973) also reported significantly smaller changes at large tube sizes.

In conclusion, tube diameter appears to be a significant factor in determining slip velocities. Its influence is two fold. Firstly when the solid-wall friction is significant its influence is to increase the slip velocity. Secondly the indirect influence of the tube wall, which is imparted through the fluid medium, is to decrease the slip velocity by increasing the hydrodynamic drag on the solid. In batch settling, the particles go down and the fluid goes up. Drag on the particle is increased by the influence of the wall on the fluid which is impeding its upward flow and tending to impart a greater pressure gradient. A similar increase in the fluid-solid drag can be expected in the case of cocurrent transport of solids. However, there is a fundamental difference between these two processes. In batch settling solids move up the pressure gradient, while in forward transport they move down the pressure gradient. It is interesting to note that Richardson & Zaki (1954) reported that the terminal velocities derived from extrapolation to zero concentrations agreed well with calculated terminal velocities in the case of sedimentation experiments, while lesser values were obtained for fluidization experiments. In this context, Richardson & Zaki (1954) suggested that the velocity gradient near

the wall could be the cause of this difference. Considering the above observations, the influence of the transport wall on the slip velocity needs to be investigated for transport systems.

$$V_r = f(V_t, C, D_t) \tag{1.9}$$

1.4.4 Effect of Transport Velocity

There is no doubt that slip velocity increases with transport velocity of the solids. Fig. 1.6 and Fig. 1.7 present the data published by Birchenough & Mason (1976), but in a different form. They have plotted the slip velocity against loading ratio with gas velocity as a parameter. From their data, the concentration-slip velocity (Fig. 1.6) and gas-solid velocity (Fig. 1.7) plots were derived, which helped determine the effect of transport velocity. Their data suggests that at a given volumetric concentration, slip velocity increases with increasing mass flow rate of solid. In other words, slip velocity increases with increasing solid velocity. The data further indicates that for a given mass flow rate, an increase in solid concentration (thus decreasing the solid velocity) results in a decrease in the slip velocity. Considering these trends, and the fact that solid velocities are as high as 40 m/sec, the influence of solid velocity on solid-wall friction is quite clear. The high transport velocity data of Stemerding (1962), Ottjes (1976), Maeda et al (1974), Mehta et al (1957), Capes & Nakamura (1973) and Reddy & Pei (1969) suggest a linear relationship between the slip velocity and the transport velocity.

This trend is explained simply by greater friction between particles and the wall with increasing solid velocity. With neglect of any complication by volume fraction, the balance of forces on a transporting particle may be written as follows.

$$\frac{1}{2} C_D \rho_g (V_g - V_s)^2 = \frac{1}{2} f_s \rho_s V_s^2 + \frac{2}{3} \rho_s g D_p \tag{1.10}$$

where

f_s is the Solid-wall friction factor

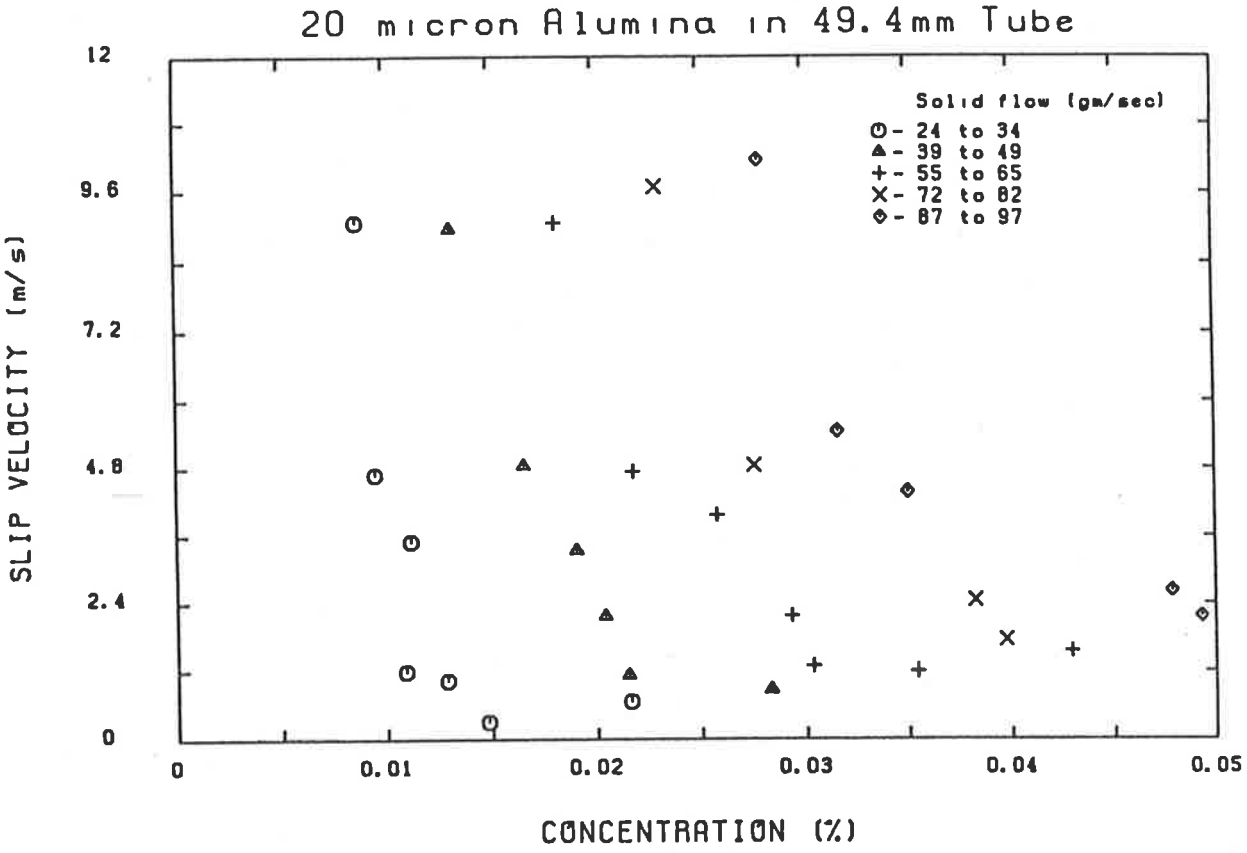

Fig. 1.6 Concentration-slip velocity map. *(Birchenough's data)*

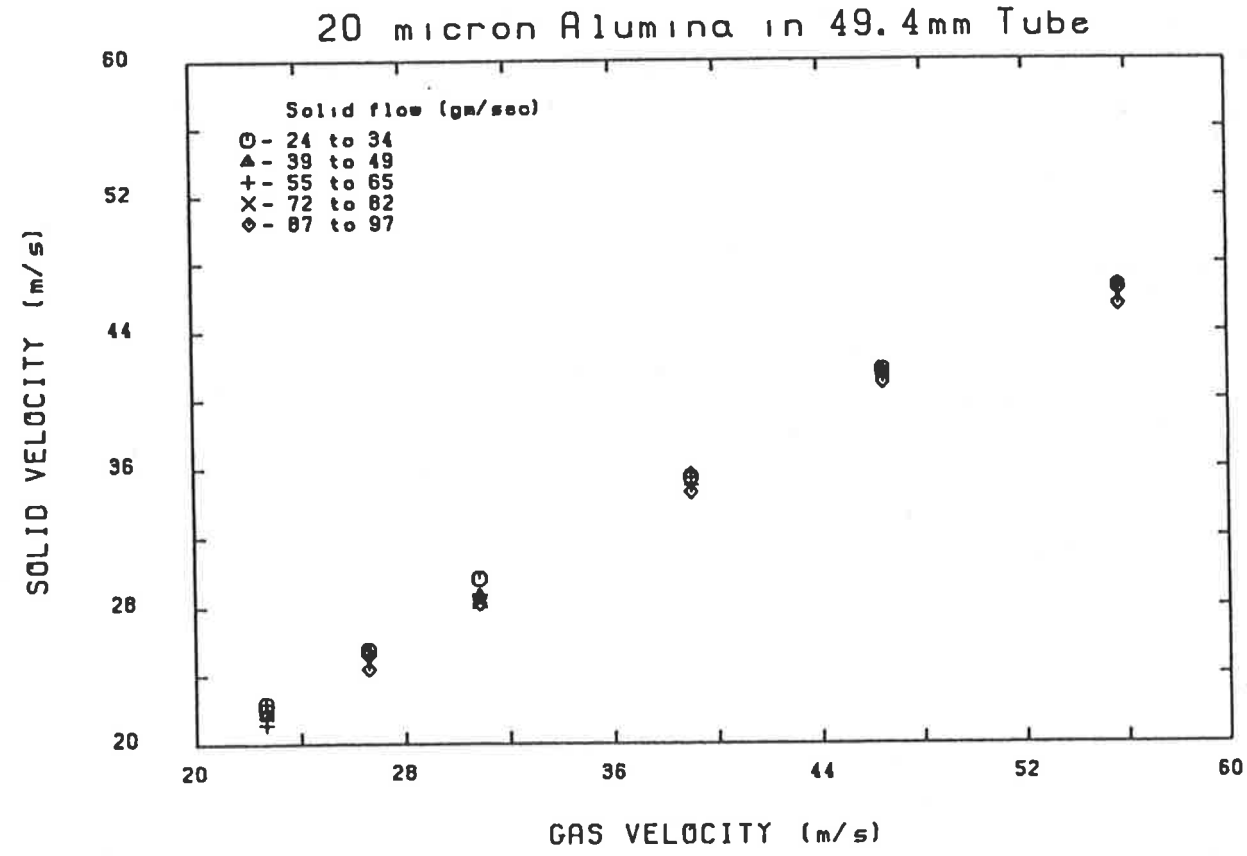

Fig. 1.7 Gas-solid velocity map. *(Birchenough's data)*

As the transport velocity becomes greater, the contribution of the wall friction term on right hand side of the equation increases. When it predominates the relationship between the slip velocity and transport velocity approach direct proportionality. What interaction there may be between transport velocity and volume fraction cannot be inferred from published data. The difficulty is that small transport velocities are usually associated with small volume fractions. This is an inevitable result of tests with fixed solid feed rate and variable air flow rate.

1.4.4.1 Solid-wall Friction Factor

The frictional loss term in equation (1.10) needs some explanation. The great majority of workers in the transport field have investigated the energy loss due to the solid-wall friction. The most common approach to the problem has been to determine this loss by subtracting the contributions due to hold up and gas-wall friction from the total measured pressure loss.

The frictional loss due to gas phase is generally approximated to that of the value when gas alone was flowing in the tube. However, Doig & Roper (1967) report that at low loading ratios the solid phase causes the air velocities relative to the single phase profiles to increase in the core and decrease at the wall; while at higher loading ratios the effect is just the opposite.

Where as, Birchenough & Mason (1976) and Reddy & Pei (1969) report that the effect of particles on the air velocity profile is not significant. Reddy & Pei (1969), quote the works of Soo et al (1964) who also reported similar trends. The influence of solids on velocity profiles is not very well understood. But the dominant influence of solid-wall frictional losses at high transport velocities and hold up losses at low velocities appear to justify the approximation mentioned earlier. Having determined the pressure loss contribution from solid-wall friction, a solid-wall friction factor (f_s) is defined analogous to the Fanning friction factor. The solid phase is approximated to a continuous phase of density ($C\rho_s$), moving at a velocity (V_s) relative to the solid wall

(D_t), where the frictional loss is given by

$$(\Delta P)_{f_s} = 2 f_s L C \rho_s \frac{V_s^2}{D_t} \tag{1.11}$$

where

$(\Delta P)_{f_s}$ is the Pressure drop due to solid-wall friction

The solid-wall friction factor (f_s) defined above is generally correlated to either gas Froude number or solid Froude number. While Maeda et al (1974), Jotaki et al (1978) and Stemerding (1962) report constant values of friction factor, Reddy & Pei (1969), Konno & Satio (1969), Swaaij (1970) and Capes & Nakamura (1973) report decreasing friction factors with increasing particle Froude number. While Maeda et al (1974) report decreasing values of friction factor with increasing tube diameter, Jotaki et al (1978) report quite opposite trends.

Negative friction factors were also reported, especially at gas velocities approaching solid terminal velocity, by Yousfi & Gau (1974), Swaaij (1970) and Capes & Nakamura (1973). An explanation was proposed based on the observed phenomenon of solid particles moving downwards along the walls, thus resulting in a negative particle-wall shear.

There are also reports of negative friction factors (Soo 1967) with transport of fine particles at higher velocities, owing to the damping of the fluid turbulence by the solids.

1.4.4.2 Some other Definitions of Friction Factor

Jodlowski (1976) and Mehta et al (1957) propose the concept of a combined friction factor (f_m) including gas- wall frictional losses, with some variations.

$$(\Delta P)_{fg} + (\Delta P)_{f_s} = 2 f_m \rho_g L \frac{V_g^2}{D_t} \qquad [Jodlowski]$$

$$=2f_m\rho_g L\frac{V_g^2}{D_t}\left(1+\left(\frac{CV_s^2\rho_s}{V_g^2\rho_g}\right)^a\right) \qquad [Mehta]$$

where

$(\Delta P)_{fg}$	is the Pressure drop due to gas-wall friction
$(\Delta P)_{fs}$	is the Pressure drop due to solid-wall friction
f_m	is the Combined friction factor
a	is the Correlation constant

The combined friction factor was correlated to the gas Froude number and volumetric concentration by Jodlowski, and was found to increase with increasing Froude number and solid concentration. Alternately, Mehta et al (1957), attempted to correlate f_m to the gas Reynolds number.

Although introduction of a combined friction factor eliminates the necessity of estimating gas- wall frictional loss in the presence of solids, the delineation of the magnitude of individual contributions is lost.

Barth (1962) introduced another friction factor for solid-wall friction alone.

$$(\Delta P)_{fs} = 2f_s LC\rho_s\left(\frac{V_s V_g}{D_t}\right) \qquad [Barth]$$

His definition is almost similar to the generally accepted definition mentioned earlier (1.10), except that instead of using the square of solid velocity, the product of gas and solid velocities was used.

The varied definitions of friction factors, range of parameters studied, and the different dimensionless groups employed to correlate friction factor, make the task of comparison difficult.

In conclusion, the solid-wall friction is a principal factor in determining the slip velocity at high transport velocities. Clearly, there is a need to investigate the effect of transport velocity at high solid concentrations, and the interaction between these two

quantities in determining the slip velocity.

$$V_r = f(V_t, C, D_t, V_s) \tag{1.12}$$

1.4.5 *Effect of Particle Size and Density*

The combined effect of particle size and density is indirectly represented through particle terminal velocity. Maeda et al (1974), Capes & Nakamura (1973), and Mehta et al (1957) report higher slip velocities for particles with high terminal velocities. Although one could investigate particles of the same density and of different diameters or vice versa, it will be impossible to identify the individual influences, as the terminal velocities and, therefore, transport velocities will be different as well.

However, the tendency of particles to agglomerate has generally been reported to increase with decreasing particle size. Consequently, the effect of the size of the particle on the degree of dependence of slip velocity on volume fraction could be significant.

Yousfi & Gau (1974) report ratios of slip velocity to terminal velocity of up to 4 for 138μ glass, up to 40 for 55μ catalyst and up to 300 for 20μ catalyst in the effects of increasing volume fraction. Similar trends have been reported by Decamps et al (1972), from their experiments with 55μ Uranium oxide spheres and 165μ Aluminium oxide particles in 10mm glass tube. However, the densities of these particles were slightly different.

The size and density of particle could be of significance if the number concentration of particle is a governing factor. The effect of particle size could also be through the wall effect (D_p/D_t *ratio*) mentioned earlier.

$$V_r = f\,(V_t, C, D_t, V_s, D_p, \rho_s) \tag{1.13}$$

Although the above expression includes particle size and density along with the terminal velocity as parameters for the reasons mentioned earlier, it should be pointed

out that the terminal velocity is in fact an expression of the effect of both the size and density of the particle on slip velocity. In a given fluid medium heavier and larger particles have higher terminal velocities, thus resulting in larger slip velocities. Not withstanding any complications due to agglomeration, concentration and wall effects terminal velocity of single particle and hence the slip velocity can be functionally related to the particle size and density depending on the flow regime.

1.5 Conclusions

From the foregoing discussion, it is clear that there is a need to

1. investigate the dependence of slip velocity on solid volumetric concentration for pneumatic transport conditions, especially at large concentrations.
2. investigate the effect of key parameters such as tube diameter, particle size and density, on the above relationship.
3. investigate the significance of transport velocity on solid-wall friction, and the interaction between transport velocity and concentration in influencing the slip velocity.

CHAPTER 2

COUNTERCURRENT EXPERIMENTS

2.1 Introduction

Following the conclusions of the previous discussion it was proposed to design experiments to investigate the effect of concentration on the slip velocity and also to study the influence of pertinent variables such as the tube diameter particle size and density and transport velocity.

The first phase of experimental programme whose prime objective is to determine slip velocities at large concentrations and low transport velocities is presented in this chapter.

2.2 Countercurrent Experiments

Briefly, experiments were carried out using an apparatus in which solid flows downward against a rising stream of air. Although this type of arrangement does not represent actual transport conditions, it corresponds to the region between batch fluidization and cocurrent transport. The following factors prompted the choice of such an arrangement.

1. It is of direct interest for some operations such as heat transfer,drying and reaction.

2. It facilitates investigation of lower limit to transport velocity.

3. It allows accurate and easy determination of slip velocities, especially at large solid loadings, which would otherwise be difficult with cocurrent transport.

2.2.1 Apparatus

The apparatus used in the countercurrent experiments is depicted in Fig. 2.1.

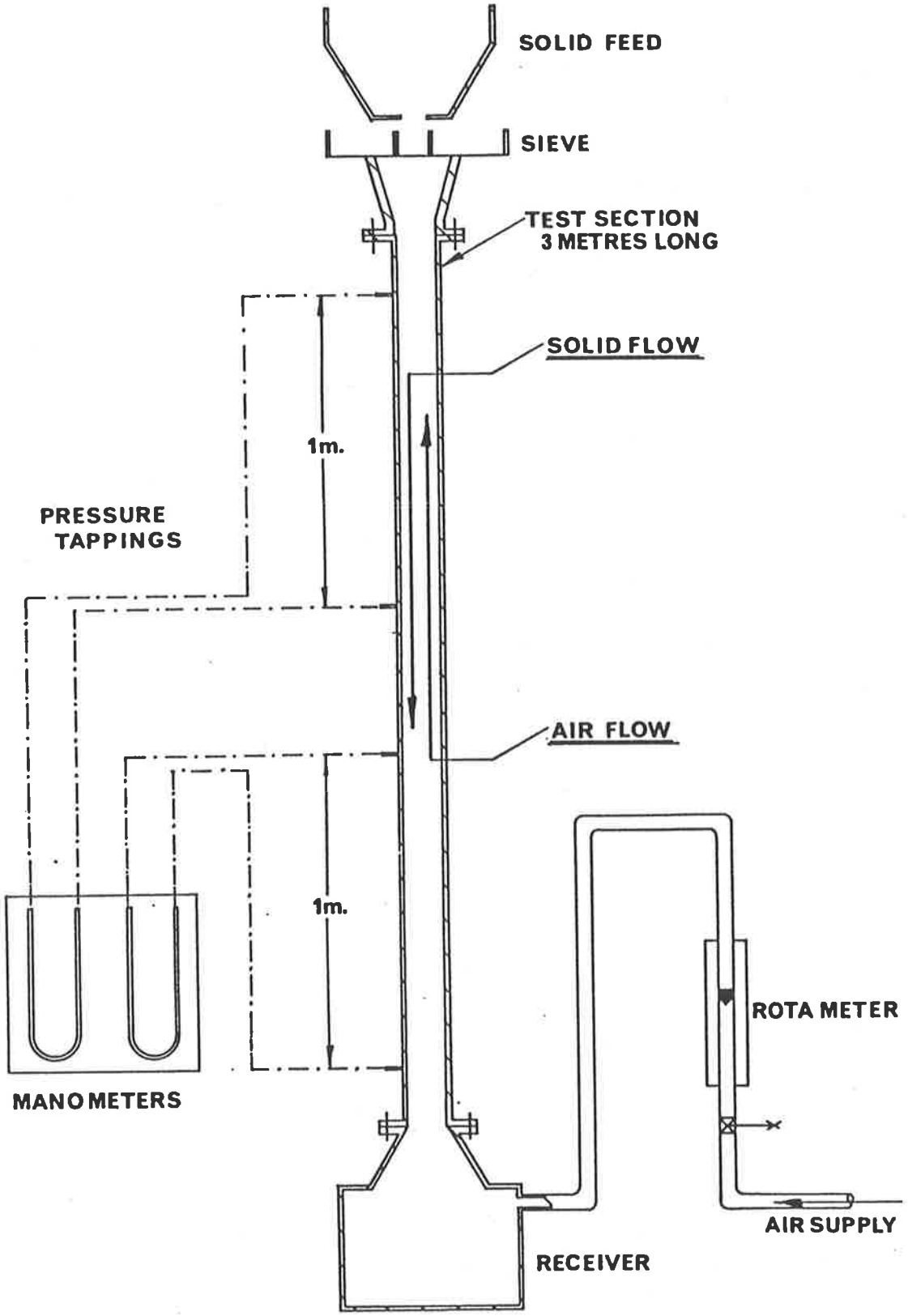

Fig. 2.1 COUNTER CURRENT FLOW APPARATUS

Solids fall from an open container at a rate fixed by the size of the orifice selected for the test. To ensure even distribution of solids, arrangement shown in Fig. 2.2 was used. The stream of solids was distributed to a width corresponding to that of test conduit by a sieve with appropriately chosen mesh. From the sieve the solids fall through a distance calculated to allow them to accelerate to near equilibrium transport velocity before they pass into the test conduit.

Air from the blower, metered through a rotameter, enters the closed receiving vessel at the bottom of the tube and passes through a converging section into the tube. From the top of the tube the air flow is diffused to the atmosphere through a diverging section. The test conduit was 3 meters long and was provided with pressure tappings at half a meter intervals. Two "U" tube manometers were connected to pressure tappings one meter apart, at top and bottom ends of the test section. Butanol (0.808 gm/cc density) was used as the manometric fluid for good sensitivity. The leads of the manometer were provided with needle valves to dampen any high frequency oscillations in pressure differential which are characteristic of two phase flows.

2.2.2 Experimental Procedure

With a fixed flow of solid through the tube, pressure drop readings at top and bottom ends of the tube were recorded at several gas flow rates. The air flow was raised in increments from zero to the point at which solid flow becomes unstable or is arrested, which is characterised by large fluctuations in pressure drop readings. The procedure was repeated with different solid flow rates fixed by selected orifice sizes at solid feed container.

2.2.3 Range of Variables Investigated

Six different materials with mean particle sizes ranging from 96μ to 644μ and densities ranging from 2.5 gm/cc to 7.6 gm/cc were investigated in four test conduits with diameters ranging from 12.7mm to 38.1mm. Details of these variables are presented

Fig. 2.2 ARRANGEMENT FOR EVEN DISTRIBUTION OF SOLIDS

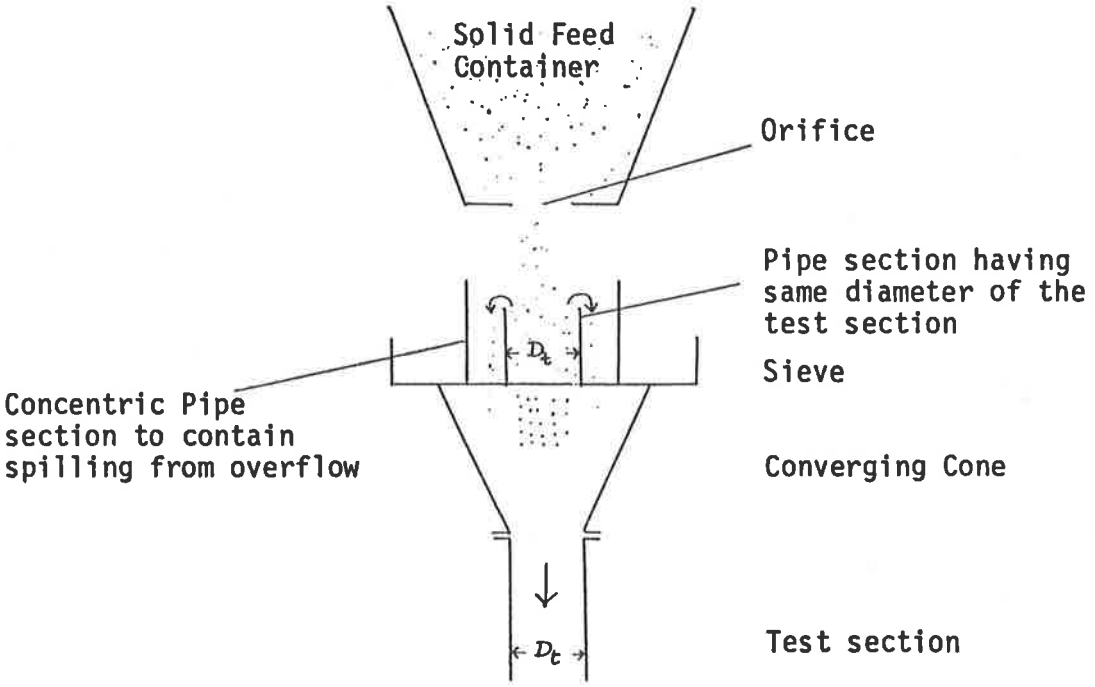

in Table (2.1) and Table (2.2). The volume to surface mean diameter of particles presented in the above tables were obtained from the sieve analysis of materials using standard BSI sieves. Details of the analysis of each material are given in Appendix (A). The materials chosen were found to be closely sized.

Experiments were conducted at several solid flow rates fixed by the feed container orifice diameter, which varied from 6mm to 25mm. Calibration of the solid flow rate with different orifice sizes for all types of solid material used is presented in Table (2.3). The feed rate from the container was found to be constant over the period of the test.

2.2.4 Analysis of Data

It is desired that solids reach equilibrium velocity by the time they enter the test section, as steady state conditions are of interest. Details of the minimum fall distance required to reach equilibrium velocity in still air, for all particles investigated are presented in Table (2.4). The calculated dropping distance for the heaviest and largest particle, used in the tests, to reach its terminal velocity in still air was calculated to be 9.4 meters. This requirement is further reduced with increasing upward gas velocity. Furthermore, the distances calculated are overestimated in the sense that it is impossible to achieve a distribution of particles where particles are dropped individually. In reality a maximum dropping distance of about one meter was found to be quite adequate in the majority of the runs.

The above-mentioned steady state condition is represented by correspondence of pressure gradients at the top and bottom ends of the test conduit. This was realised in substantial number of observations. However, at large solid feed rates corresponding to low gas flows, the pressure drop at the bottom end of the tube was found to be higher than the pressure drop at the top end of the tube indicating incomplete acceleration of solids. This results from the fall of a group of particles whose dropping distance is larger than that of an individual particle. However, such observations with large differences in pressure gradients at the top and bottom ends of the tube were excluded from the

Table (2.1) DETAILS OF MATERIALS USED

No.	Material	Density (gm/sec)	Particle Diameter (microns)	Shape	Terminal Velocity (m/s)
1	Glass beads	2.47	96	Spherical	0.522
2	Sand	2.63	173	-	1.230
3	Glass beads	2.47	644	Spherical	4.740
4	Steel shot	7.62	179	Spherical	2.785
5	Steel shot	7.62	375	Spherical	5.945
6	Steel shot	7.62	637	Spherical	9.379

Table (2.2) TEST SECTION DETAILS

No.	Tube Diameter (mm)	Tube Material
1	12.7	Steel
2	19.1	Steel
3	25.4	Steel
4	38.1	Steel

Table (2.3) CALIBRATION OF MASS FLOW RATE OF SOLIDS

No.	Solid Material	Mass Flow Rate (gm/sec) *Orifice Size (mm)*						
		6	8	10	12	15	19	25
1	96μ Glass	8.74	16.9	27.66	49.39	83.77	139.9	290.47
2	173μ Sand	7.71	15.21	24.53	46.6	77.54	133.4	284.0
3	644μ Glass	4.76	10.71	18.33	33.87	61.83	104.2	227.8
4	179μ Steel	26.63	53.1	84.47	158.9	271.4	464.2	974.3
5	375μ Steel	21.97	45.44	73.46	140.7	245.8	425.5	919.3
6	637μ Steel	18.07	39.18	64.58	127.1	226.3	386.8	854.7

Table (2.4) DROPPING DISTANCES IN AIR

No.	Particle Size (μm)	Density (gm/cm^3)	Terminal Velocity (m/s)	Dropping Distance (m)
1	96	2.47	0.52	0.05
2	173	2.63	1.23	0.21
3	644	2.47	4.74	2.81
4	179	7.62	2.79	1.03
5	375	7.62	5.95	4.64
6	637	7.62	9.38	10.01

NB: ***Dropping distance*** is the distance travelled by the particle before reaching 95% of it's equilibrium velocity, while moving under gravity with zero initial velocity

analysis. Observations with pressure drop readings differing by more than 10% at both ends of the tube were not recorded. A pair of solid volumetric concentration and slip velocity was obtained at each observation.

2.2.4.1 Concentration - Slip Velocity Calculations:

Solid volumetric concentration was derived from the measured pressure drop. For steady state conditions the total pressure drop (ΔP_t) can be expressed as follows.

$$(\Delta P)_t = (\Delta P)_{gs} + (\Delta P)_{ss} + (\Delta P)_{fs} + (\Delta P)_{fg} \tag{2.1}$$

where

$(\Delta P)_t$ is the Total pressure drop

$(\Delta P)_{gs}$ is the Pressure drop due to static head of gas

$(\Delta P)_{ss}$ is the Pressure drop due to static head of solid

$(\Delta P)_{fg}$ is the Pressure drop due to gas-wall friction

$(\Delta P)_{fs}$ is the Pressure drop due to solid-wall friction

Since the density of solid is quite large (by a factor of 1000) in comparison with the density of air, the static head of air $(\Delta P)_{gs}$ can be ignored. The solid-wall friction component $(\Delta P)_{fs}$ can also be ignored as its magnitude is insignificant in comparison with the solid static head $(\Delta P)_{ss}$, especially at larger volumetric concentrations. In addition, solid velocities are always much less than particle terminal velocity due to countercurrent arrangement. The maximum solid velocity encountered was about 10m/s. Such low solid velocities justify neglect of solid-wall friction component. The gas-wall friction component was experimentally determined with only air flowing through the test section and was found to be negligible in comparison with the solid static head term.

Following the above arguments the total pressure drop can be approximated to solid static head component without incurring much error.

$$(\Delta P)_t = (\Delta P)_{ss} \tag{2.2}$$

The pressure drop due to the solid hold up is expressed as follows.

$$(\Delta P)_{ss} = C\rho_s gL \tag{2.3}$$

where

C is the Volumetric concentration of solids

ρ_s is the Solid density

L is the Length of test section between pressure taps

From equations (2.2) and (2.3), the solid volumetric concentration can now be derived from the pressure drop as follows.

$$C = \frac{(\Delta P)_l}{\rho_s gL} \tag{2.4}$$

From known quantities of solid and air volumetric fluxes through the tube solid and air velocities were derived as follows.

$$V_g = \frac{\Phi_g}{1 - C} \tag{2.5}$$

$$V_s = \frac{\Phi_s}{C} \tag{2.6}$$

where

Φ_g is the Volumetric flux of air

Φ_s is the Volumetric flux of solid

The total upward volumetric flux of air (Φ_g) through the test section was derived from the volumetric flow introduced through the blower plus the rate of volume displaced by the solids collected in the receiving container.

Knowing air and solid velocities, the slip velocity (V_r) was derived as follows.

$$V_r = V_g + V_s \tag{2.7}$$

The positive sign on the solid velocity is appropriate, since the solids are flowing in a direction opposite to the air flow.

2.2.5 Results

2.2.5.1 Effect of Concentration

The concentration and slip velocity values derived from the above mentioned procedure were analysed for a solid material in a test conduit. Slip velocity normalised with respect to particle terminal velocity was plotted against solid volumetric concentration to determine the relationship between them. Results of 96μ glass beads in 12.7mm tube are presented in Fig. 2.3. The following observations can be made from this plot.

1. Slip velocity is a unique function of solid volumetric concentration. Higher mass flow rates of solids result in extension of concentration range.

2. While at very low concentrations slip velocity is almost equal to calculated particle terminal velocity, its value is larger than the terminal velocity at higher concentrations.

3. The rate of change of slip velocity with concentration decreases with increasing concentration.

The above trends are typical of the results obtained with other particles in all the tubes investigated. These results are presented in Appendix (B).

2.2.5.2 Effect of Particle Properties

In order to assess the influence of particle properties such as density and size on the slip velocity-concentration relationship, slip velocities normalised with respect to the corresponding particle terminal velocities were plotted against solid volumetric concentration. The results of six different solid materials in 12.7mm diameter tube are presented in Fig. 2.4. The following observations can be made from this graph.

1. At a given concentration smaller particles have larger dimensionless slip velocities.

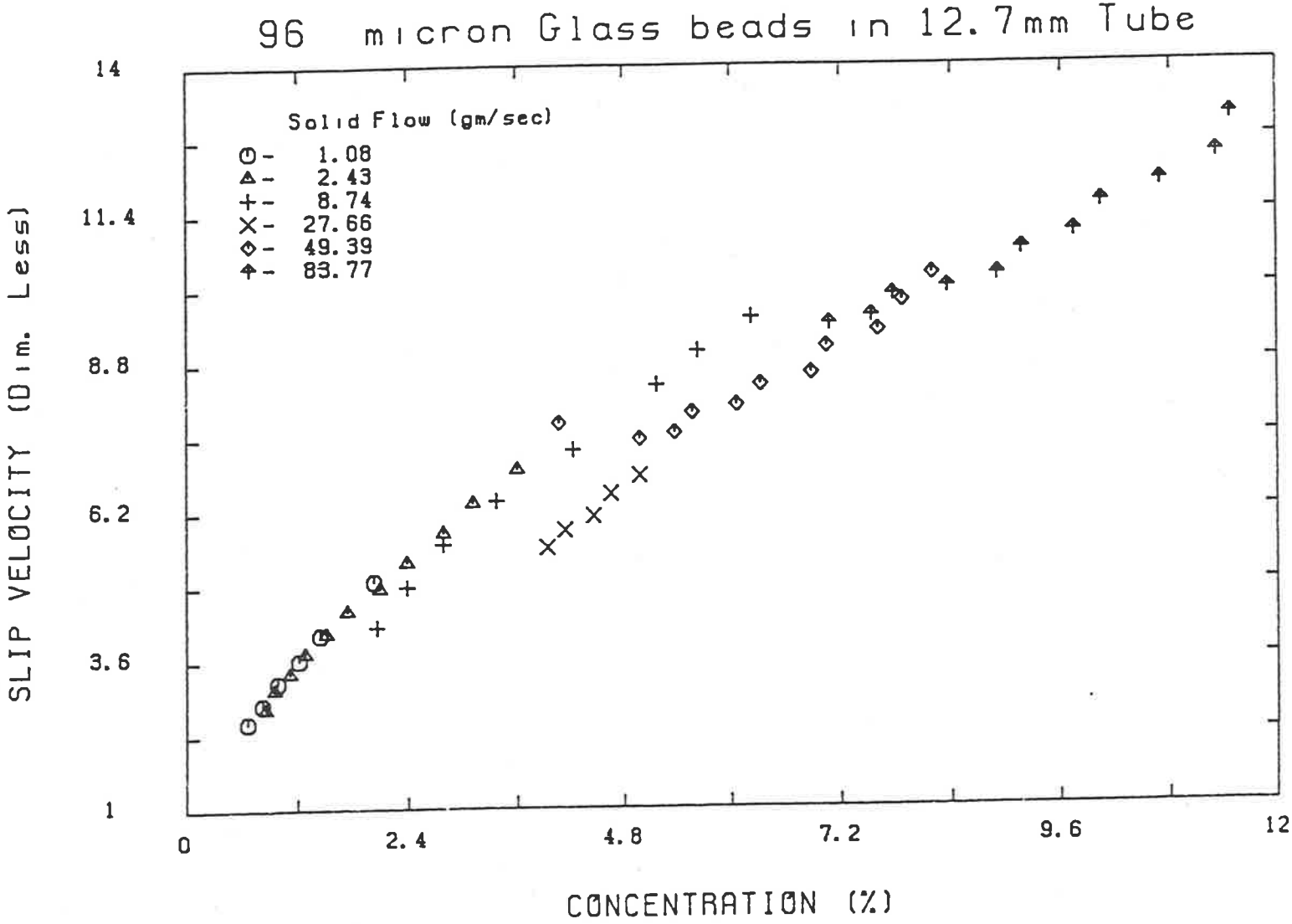

Fig. 2.3 Effect of concentration

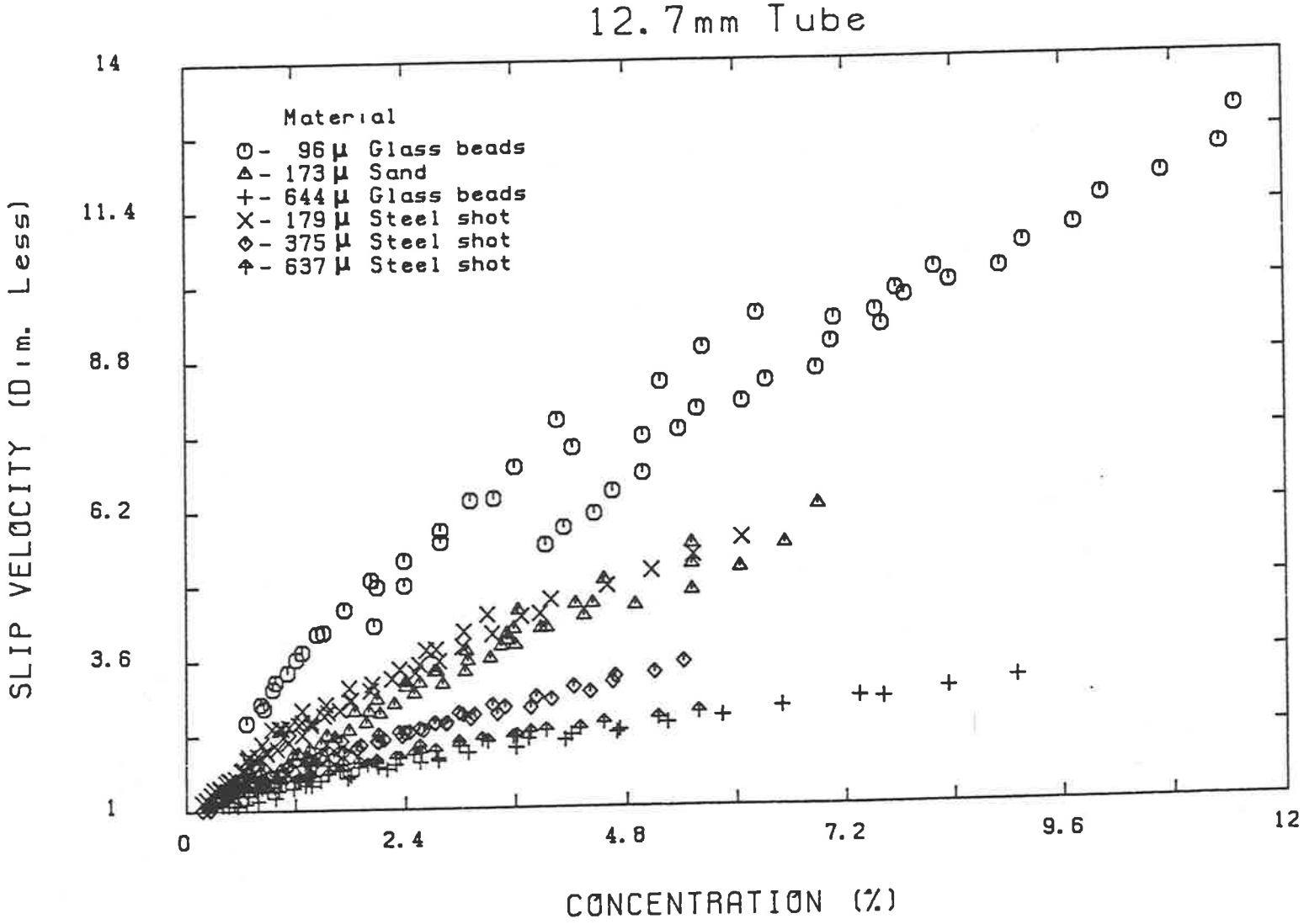

Fig. 2.4 Effect of particle properties

2. The degree of dependence of slip velocity decreases with increasing particle size.

3. The effect of particle density appears to be of little significance in comparison with the effect of particle size. This was concluded from the observation that the results of 173μ sand ($\rho_s = 2.6gm/cc$) and 179μ steel shot ($\rho_s = 7.6gm/cc$) tend to fall on the same line. Similar observations can be made with 644μ glass beads and 637μ steel shot.

Plots with other tube sizes are presented in Appendix (C). All these plots show similar trends.

2.2.5.3 Effect of Tube Diameter

Plotting dimensionless slip velocity against concentration for a given material in different tube sizes, the following observations can be made. Results of 96μ glass beads in four different tubes are presented in Fig. 2.5.

1. At a given solids concentration dimensionless slip velocity increases with decreasing tube size.

2. The degree of dependence of slip velocity on concentration decreases with increasing tube diameter.

Similar trends were observed with other particles. These plots are presented in Appendix (D).

2.2.6 Summary of Results

The trend of entire experimental data from the tests with six different particles in four different tubes can be summarised as follows.

1. Dimensionless slip velocity is a unique function of concentration for a given solid material and tube size.

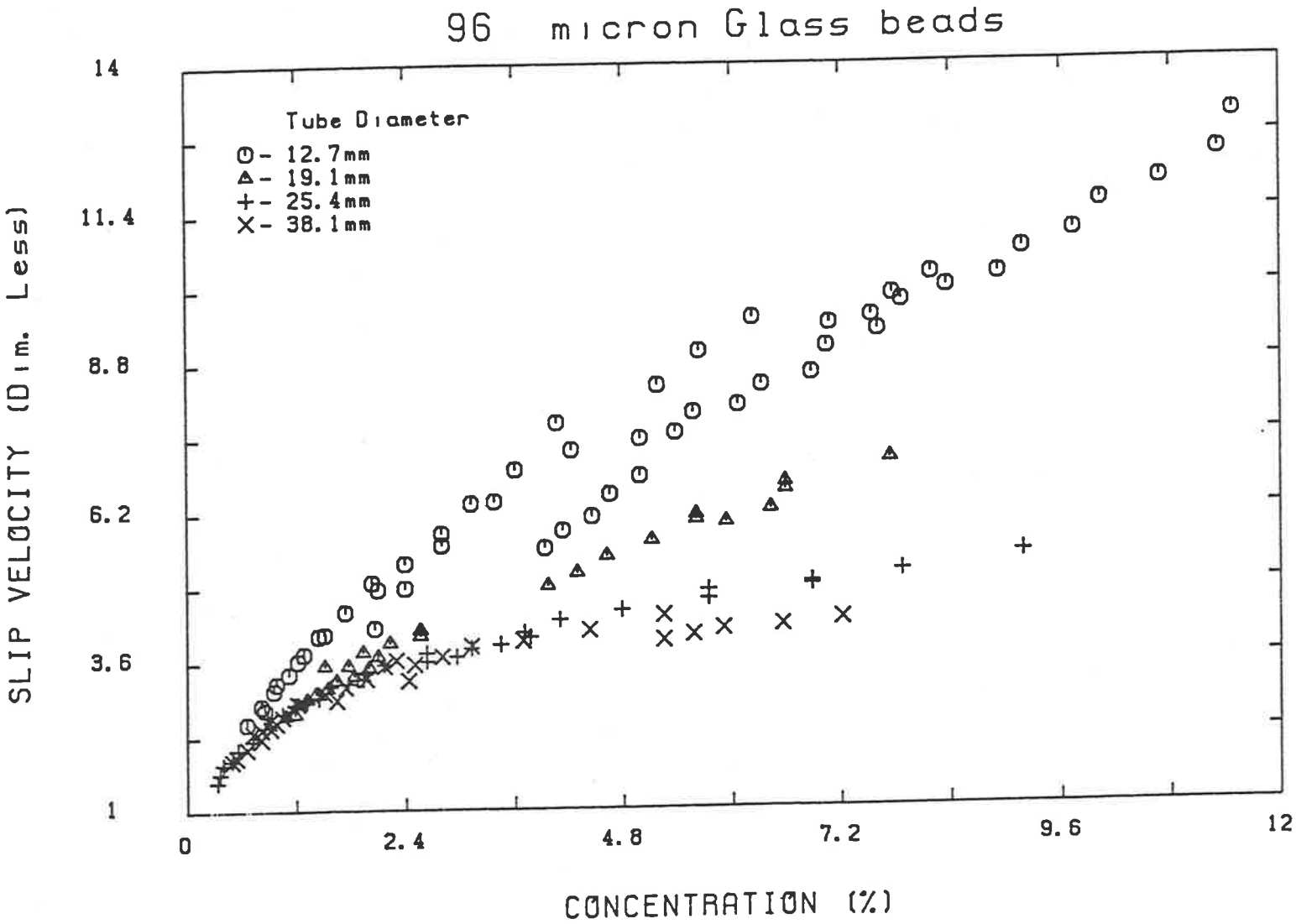

Fig. 2.5 Effect of tube diameter

2. Slip velocity increases with increasing concentration and its magnitude is larger than the corresponding single particle terminal velocity.

3. The degree of dependence of slip velocity on concentration decreases with increasing tube size and particle size.

4. The influence of particle density on slip velocity-concentration relationship is less significant than that of particle size.

2.2.7 Comparison with Existing Data:

Slip velocities related explicitly to volume fraction are rarely reported in literature. In general data are presented in terms of loading ratio or gas to solid velocity ratio. Lack of information about the corresponding solid and gas mass flow rates limits the derivation of the variables of interest. In addition, the majority of the data published are confined to very low concentrations at high transport velocities, where solid-wall friction effects dominate.

Matsen (1982) presents the following correlation based on the elutriation data of Wen & Hashinger (1960), with 70μ glass beads in 100mm diameter bed.

$$\frac{V_r}{V_t} = \begin{cases} 1 & \text{for} \quad C < 0.0003 \\ 10.8C^{0.293} & \text{for} \quad C > 0.0003 \end{cases} \qquad [Matsen]$$

The above correlation suggests a linear relationship between the logarithmic values of volumetric concentration of solids and the dimensionless slip velocity. Analysis of the present experimental data suggests that such a linear relationship does indeed exist. Fig. 2.6 represents the data obtained with 96μ glass beads in 12.7mm tube. Observations with other particles in all the tubes investigated gave similar results. The values of "A" and "B" obtained by linear regression are presented in Table (2.5) for all the experiments. The correlation coefficients are also presented. These values are greater than 0.95 for majority of the data indicating a good fit. However, it is interesting to note that the values of "A" and "B" varied depending on the system properties; that

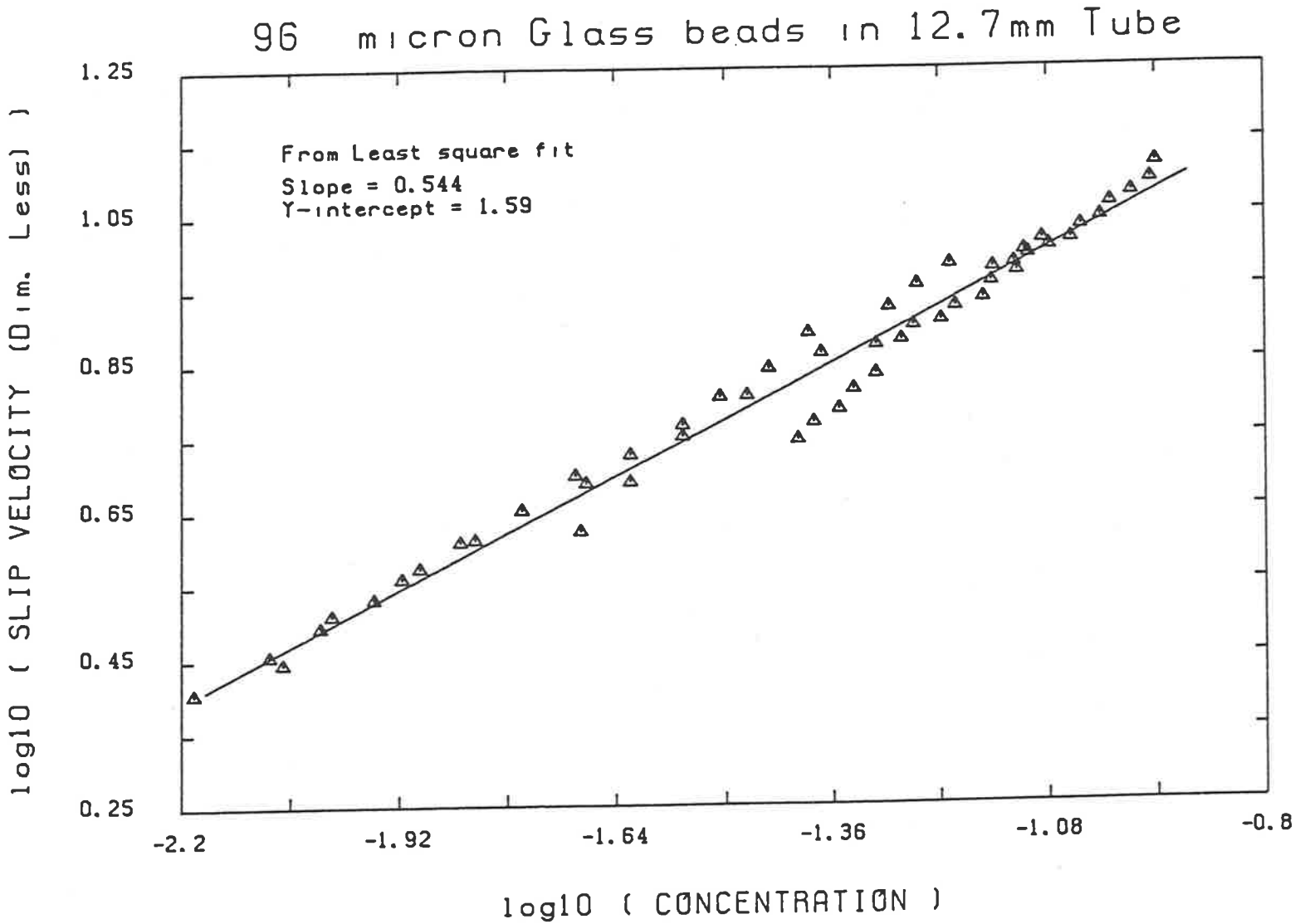

Fig. 2.6 Concentration-slip velocity map on log-log scale

Table (2.5) PARAMETER ESTIMATES OF CORRELATION

$$\frac{V_f}{V_t} = AC^B$$

No.	Tube Size (mm)	Particle Size (μ)	Particle Density gm/cm^3	A	B	Regression Coefficient
1	12.7	96	2.47	39.00	0.544	0.988
2	19.1	96	2.47	24.05	0.482	0.995
3	25.4	96	2.47	13.28	0.356	0.992
4	38.1	96	2.47	10.45	0.305	0.974
5	12.7	173	2.63	33.37	0.642	0.992
6	19.1	173	2.63	12.64	0.426	0.977
7	25.4	173	2.63	6.81	0.297	0.989
8	38.1	173	2.63	7.55	0.320	0.987
9	12.7	644	2.47	7.38	0.374	0.993
10	19.1	644	2.47	3.23	0.232	0.967
11	25.4	644	2.47	1.88	0.160	0.918
12	38.1	644	2.47	1.29	0.058	0.622
13	12.7	179	7.62	20.31	0.476	0.992
14	19.1	179	7.62	14.60	0.467	0.991
15	25.4	179	7.62	7.43	0.349	0.971
16	38.1	179	7.62	5.82	0.286	0.980
17	12.7	375	7.62	9.07	0.359	0.989
18	19.1	375	7.62	3.40	0.212	0.964
19	25.4	375	7.62	3.20	0.215	0.959
20	38.1	375	7.62	3.31	0.231	0.960
21	12.7	637	7.62	5.60	0.281	0.963
22	19.1	637	7.62	2.48	0.164	0.953
23	25.4	637	7.62	1.76	0.113	0.925
24	38.1	637	7.62	1.79	0.126	0.881

is tube diameter and particle properties. These two parameters are correlated to three dimensionless groups which characterise the system namely, particle Reynolds number (Re_p) particle to tube diameter ratio (D_p/D_t), particle to air density ratio (ρ_s/ρ_g).

The entire data of countercurrent experiments can be represented by the following correlation.

$$\frac{V_r}{V_t} = AC^B \tag{2.8}$$

$$A = 93.67\,(Re_p)^{-0.994}\left(\frac{D_p}{D_t}\right)^{1.014}\left(\frac{\rho_s}{\rho_g}\right)^{0.706}$$

$$B = 1.075\,(Re_p)^{-0.445}\left(\frac{D_p}{D_t}\right)^{0.476}\left(\frac{\rho_s}{\rho_g}\right)^{0.313}$$

$$Re_p = \frac{D_p V_t \rho_g}{\mu_g}$$

The values of the parameters " A" and "B" predicted by the above correlation are plotted against the observed values (Fig. 2.7 and Fig. 2.8), and the correspondence is reasonably good. For comparison the values of "A" and "B" reported by Matsen (1982) are also presented. Since Matsen's correlation was based on Wen's experiments with 71μ glass spheres in 101.1mm tube, the parameters "A" and "B" were estimated from these system properties using the above correlation. The agreement between the estimated and reported values is good, considering the fact that the tube size used in Wen et al's work was larger than the tube diameters used in the present study by at least a factor of three.

Yerushalmi & Cankurt (1979), report increasing slip velocities with increasing concentration, based on their experiments with 50μ spherical catalyst particles in 152mm tube. However, the concentration-slip velocity relationship was not unique, but depended on the mass flow rate of solids. The solid volumetric concentration and slip velocity were inferred from the pressure gradient measured over the middle of the test section. Unfortunately, no mention was made as to whether steady state conditions prevailed in such measurements. If the acceleration of solids in the test section is in-

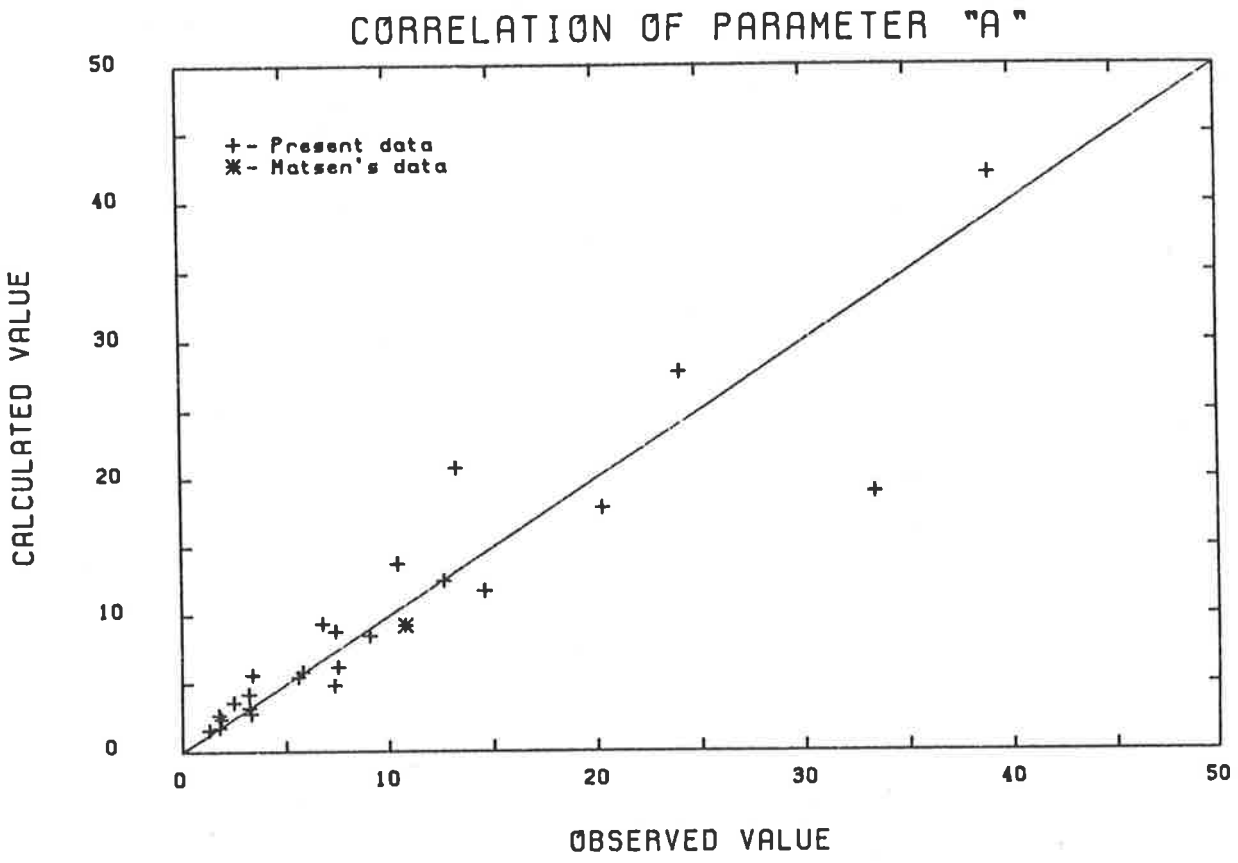
CORRELATION OF PARAMETER "A"
+- Present data
*- Matsen's data
CALCULATED VALUE
OBSERVED VALUE
0
10
20
30
40
50

Fig. 2.7

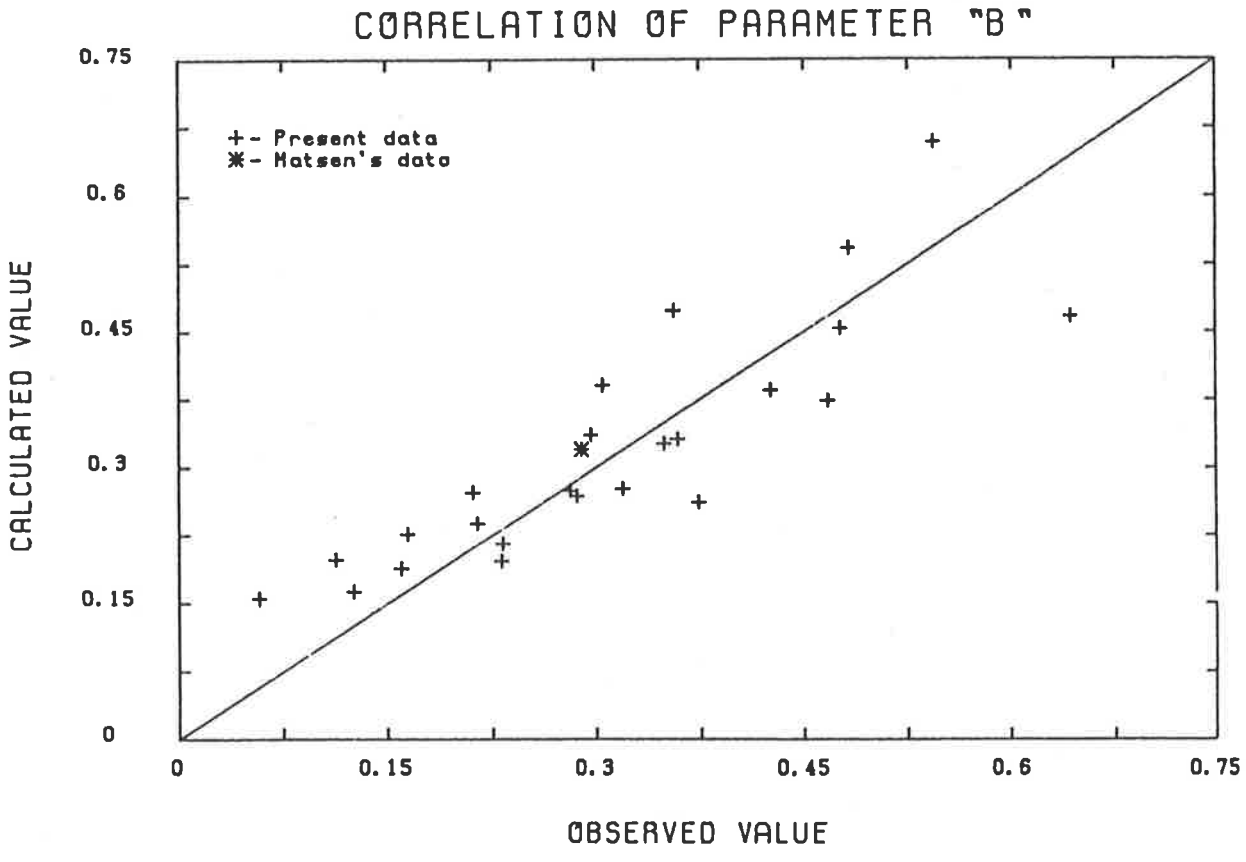
CORRELATION OF PARAMETER "B"
+- Present data
*- Matsen's data
CALCULATED VALUE
OBSERVED VALUE
0
0.15
0.3
0.45
0.6
0.75

Fig. 2.8

complete, the concentrations and slip velocities may have been overestimated. This in turn explains the introduction of solid flux as a parameter in concentration-slip velocity relationship. Also, the size range of catalyst particles used in their tests was reported to be 0-130μ. Information on the distribution of the particle size was not presented except for the mean particle size. The reported slip velocity at negligible solid volumetric concentration ($C < 0.1\%$) is about 13 times larger than single particle terminal velocity, when a correspondence is expected instead.

Yousfi & Gau (1974), present the following correlation for slip velocity, based on their experiments with 20μ and 183μ particles in 38mm and 50mm diameter tubes. The range of solid volumetric concentrations reported is 0.5% to 22% .

$$\frac{V_r}{V_t} = 1 + 3.2 \times 10^{-3} (Re_g)^{0.5} C^{0.25} \left(\frac{D_p}{D_t}\right)^{-1.8} \left(\frac{\rho_g}{\rho_e}\right) \qquad [Yousfi]$$

The above expression suggests that slip velocity is a strong function of concentration and it increases with increasing concentration. Since this correlation involves gas Reynolds number as a parameter, comparison with the correlation proposed (2.8) is not feasible. However, the following observations reported by Yousfi & Gau (1974), agree with the trends observed in the present work.

1. While the dimensionless slip velocity ranged from 8 to 40 in the case of 55μ catalyst particles, its value varied from 40 to 300 in the case of 20μ particles.

2. For large 290μ Polystyrene particles dimensionless slip velocity was much smaller than that observed with fine particles. Its value ranged from 1 to 4.

3. The effect of concentration on slip velocity was less significant in the case of large particles.

The large magnitudes of dimensionless slip velocity reported in the case of fine particles need some attention. In fact, dimensionless slip velocities as high as 300 were reported while the value predicted by the correlation (2.8) is only about 37 at the maxi-

mum solid concentration studied (22%). This discrepancy is possibly due to electrostatic charging and adhesion of particles. These effects are known to be enhanced with decreasing particle size. Nevertheless, the correlation proposed [2.8] is not recommended for such fine particle systems until additional data are available in support of it.

2.2.7.1 Some Remarks on the Correlation

On closer examination of the correlation (2.8) the powers on particle Reynolds number and diameter ratio groups are almost same in magnitude, but opposite in sign. Approximating the magnitudes of the powers to the same value, a new dimensionless group is realised.

$$(Re_p)\left(\frac{D_t}{D_p}\right) = \frac{D_t V_t \rho_g}{\mu_g}$$

This new dimensionless group is the tube Reynolds number corresponding to particle terminal velocity. The significance of this group is that it represents ideal choking flow gas Reynolds number. The correlation presented earlier can be rewritten in terms of this new group as follows.

$$\frac{V_r}{V_t} = AC^B \tag{2.9}$$

$$A = 93.7\,(Re_t)^{-1}\left(\frac{\rho_s}{\rho_g}\right)^{0.71}$$

$$B = 1.075\,(Re_t)^{-0.445}\left(\frac{\rho_s}{\rho_g}\right)^{0.313}$$

$$Re_t = \frac{D_t V_t \rho_g}{\mu_g}$$

The above correlation suggests that higher the choking Reynolds number smaller is the magnitude of dimensionless slip velocity (A) and the degree of dependence on concentration (B). The contribution of density ratio is also significant. This might appear to contradict the observed correspondence of slip velocity-concentration relationship between particles of almost same size with large differences in densities . The following reasoning should clarify the matter.

Particle Reynolds numbers of the materials used in this study range from 3 to 400 . In this intermediate region the experimental study of Jones et al (1966), suggests that the terminal velocity of a particle is proportional to

$$V_t \propto \frac{D_p \left(\frac{\rho_s}{\rho_g} - 1\right)^{0.66}}{\rho_g \mu_g^{0.33}} \qquad [Jones]$$

Since density ratio for gas solid systems is very large the above expression can be approximated to

$$V_t \propto \frac{D_p \left(\frac{\rho_s}{\rho_g}\right)^{0.66}}{\rho_g \mu_g^{0.33}} \qquad (2.10)$$

Examining the expressions (2.10) and (2.9), the effect of particle density on parameters "A" and "B" is made clear. Although higher particle density results in larger values of density ratio term, a corresponding increase in particle terminal velocity results in little change in the value of parameter "A". Similarly parameter "B" suffers little change.

Although correlation (2.9) is attractive in terms of fewer dimensionless groups, correlation (2.8) should be preferred, until additional data are acquired to establish that the correspondence of powers on particle Reynolds number and tube to particle size ratio is not fortuitous.

2.2.7.2 Proposed Correlation

The form of the correlation (2.8) to predict slip velocity at any particular solid concentration, is not completely satisfactory in the sense that it can not be extended to very low concentrations, and requires the specification of a lower limit to concentration below which slip velocity is approximately equal to particle terminal velocity. Therefore other forms of correlations which extend to zero concentration are considered. One of such forms is as follows.

$$\frac{V_r}{V_t} - 1 = AC^B \qquad (2.11)$$

Unfortunately, the degree of fit for the above type of correlation is very poor. The left hand term in the above expression is very sensitive at low concentrations and for large particles where V_r/V_t term is closer to unity. As a consequence, the correlation (2.8) presented earlier is preferred but with the following modification.

$$\frac{V_r}{V_t} = \begin{cases} 1 & \text{for} \quad C < C_{min} \\ AC^B & \text{for} \quad C > C_{min} \end{cases} \tag{2.12}$$

$$\text{where} \qquad C_{min} = (A)^{-1/B}$$

The above correlation suggests that the lower limit of concentration (C_{min}) depends upon the values of parameters "A" and "B" which in turn depend on the system properties. The expressions for these parameters suggest that their values decrease with increasing particle size and tube diameter. In other words, for large particles the value of minimum concentration (C_{min}) is larger than for small particles. This, indeed, is experimentally observed fact. While for 96μ glass spheres in 12.7mm tube slip velocity started to increase even from concentrations as low as 0.1%, its value remained approximately equal to terminal velocity even up to 1% concentration in the case of 644μ glass beads in 38.1mm tube.

Although the above correlation adequately represents the data of the present experimental programme as well as some of the data reported in literature, correlations with some theoretical background need to be explored. Some of these aspects will be discussed in the following section.

2.2.8 Theoretical Approach

The significance of the above results, is that it is clearly demonstrated that slip velocity increases with increasing concentration for gas-solid flows in tubes. Remarkably, in batch fluidization and sedimentation phenomena it is very well established that slip velocity decreases with increasing concentration. This in turn suggests, a fundamental

difference between batch fluidization where there is no net movement of solid phase, and the flow of gas solid suspensions in tubes.

In order to gain some qualitative understanding of gas-solid flow through tubes, a section of transparent transport tube of 25.4mm diameter was filmed with 173μ sand flowing in it against upward moving air (Fig. 2.9). The photographic study revealed formation of large clouds of particles which moved downward faster than the individual particles. Collision and break up of large and fast moving clouds with slow moving clouds was also observed. This phenomenon was much more pronounced at higher concentrations corresponding to larger upward gas velocities. When the gas velocity was sufficiently high, reverse flow of solid was observed along with extensive backmixing. Overall the coalescence of particles into clouds appeared to be more pronounced near the wall of the tube. These observations were limited due to the two dimensional nature of the pictures and are likely to be subjective. Nevertheless, based on the above observations, the results obtained in the counter current experiments can be given some physical basis.

The terminal velocity of a cluster of particles is larger than that of a single particle. This accounts for the observed slip velocities being larger than corresponding particle terminal velocities. The formation of such clusters especially near the walls of the tube suggests that the velocity gradient might be a governing factor. In other words, layers of gas moving at different velocities tend to bring the particles in them together at least momentarily to form a cluster. This phenomenon, usually known as gradient coagulation is the basis of the model that will be presented in the following section, in an attempt to explain the observed trends in slip velocity.

2.2.8.1 Gradient Coagulation Model

Fuchs (1964) presents the gradient coagulation theory proposed by Smolchowski (1911). According to this theory, the frequency of contact (f) of a particle by other particles, moving in a fluid with a velocity gradient transverse to the direction of flow

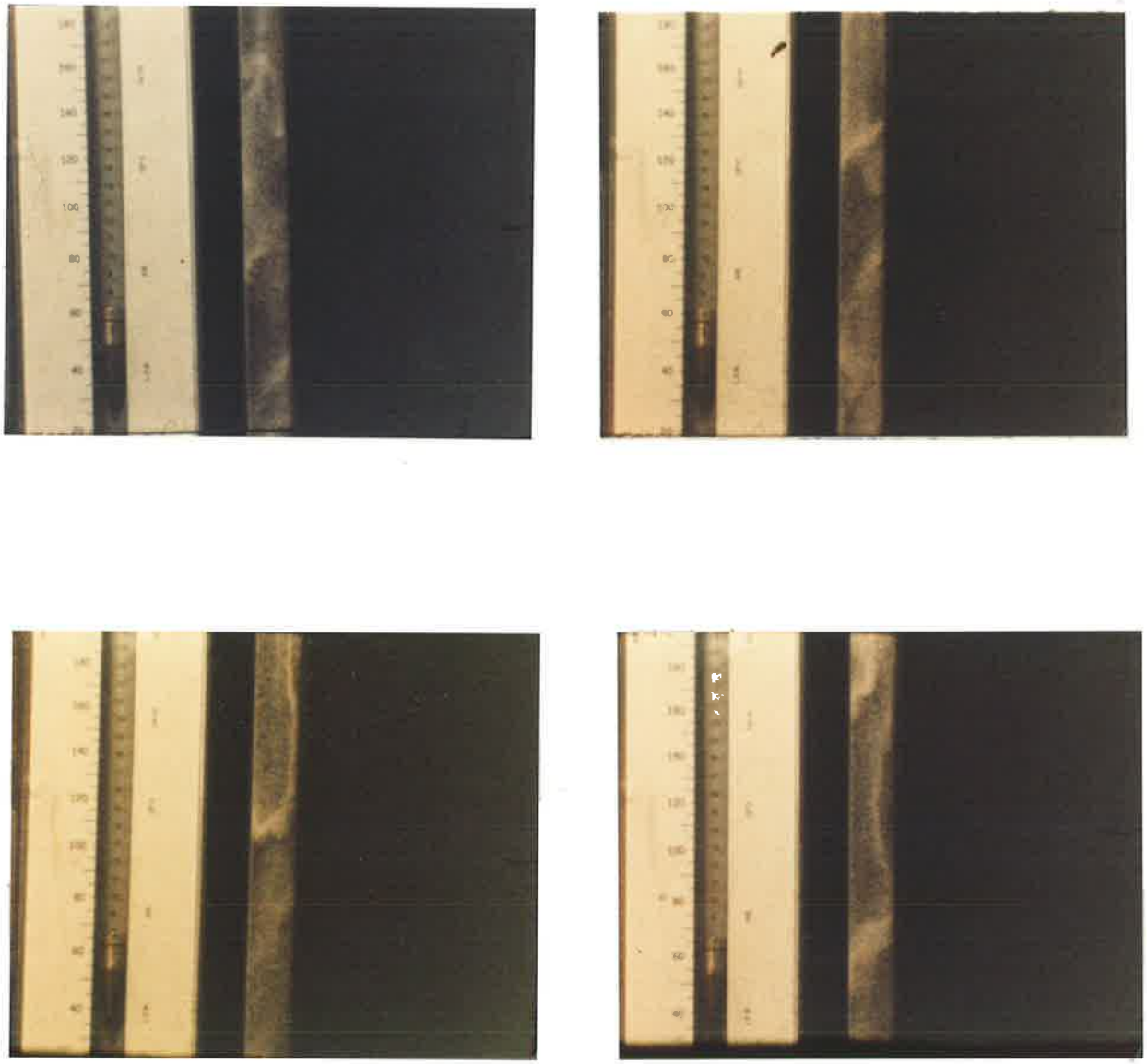

Fig. 2.9 Pictures of 25.4mm test section with sand flowing against rising air stream.

is given by

$$f = \frac{4}{3} n D_p^3 \tau \tag{2.13}$$

where

n is the Number concentration of particles

D_p is the Particle diameter

τ is the Fluid velocity gradient

The above result has been confirmed by Manley & Mason (1952), based on their experiments with 173μ glass spheres in high viscosity corn syrup, at concentrations ranging from 0.3 to 2.3% and velocity gradients ranging from 0.4 to 2 sec^{-1}.

Extending the above theory, for gas-solid flow through the tubes, the frequency of collisions between the clusters having "N" particles is

$$f_{2N} \propto n_N \tau \tag{2.14}$$

where n_N is the Number concentration of clusters of size "N"

f_{2N} is the Frequency of collisions between clusters

If the total volumetric concentration of solids is C

$$n_N = \frac{C}{N v_p}$$

where

v_p is the Volume of a particle

N is the Number of particles in a cluster

$$f_{2N} \propto n_N \frac{V_g}{D_t} \tag{2.15}$$

The velocity gradient (τ) for pipe flow is V_g/D_t, where V_g and D_t are gas velocity and tube diameter respectively.

If it is postulated that the frequency of collision of these clusters to form a doublet is in equilibrium with the frequency at which these doublets break up into singlets owing

to what ever destructive forces there are, then the following expression results.

$$N = \frac{1}{K_{2N}} C \frac{V_g}{D_t} \tag{2.16}$$

where

K_{2N} is the Equilibrium constant

This model is extremely simplistic because clusters of all sizes will be forming from collisions of all kinds of groups of particles and there will be some kind of complex equilibrium. However, the simplified model suggests that the average size of a cluster (N) is a function of concentration of solids in the tube and the velocity gradient (V_g/D_t). If the above model adequately describes the gas-solid flow in tubes, the trend of increasing slip velocity with decreasing tube size at a given volumetric concentration, can be attributed to higher velocity gradients in smaller tubes. Since slip velocity of a cluster is a function of the size of the cluster(N), plotting slip velocity against product of solid volumetric concentration and velocity gradient should bring the results of a solid material in different tubes together.

Plots of dimensionless slip velocity versus product of concentration and velocity gradient are presented for six different solid materials in Appendix (E). For a quick reference, Fig. 2.10 represents the results of 179μ steel shot in tubes of diameter ranging from 12.7mm to 38.1mm. Although, the correspondence of slip velocities between different tube sizes is not exact, the general trend is to bring the results of different tube sizes together.

Some deviations from the general trend were noticed, especially with the data corresponding to low gas velocities in small tubes. These deviations are larger for heavy and large particles (637μ steel shot). One possible explanation for the deviations at low gas velocities is that the gradients are not large enough to bring about substantial coagulation. The large deviations for large and heavy particles can be attributed to the large relaxation times of the particles. In other words, large particles are less influenced

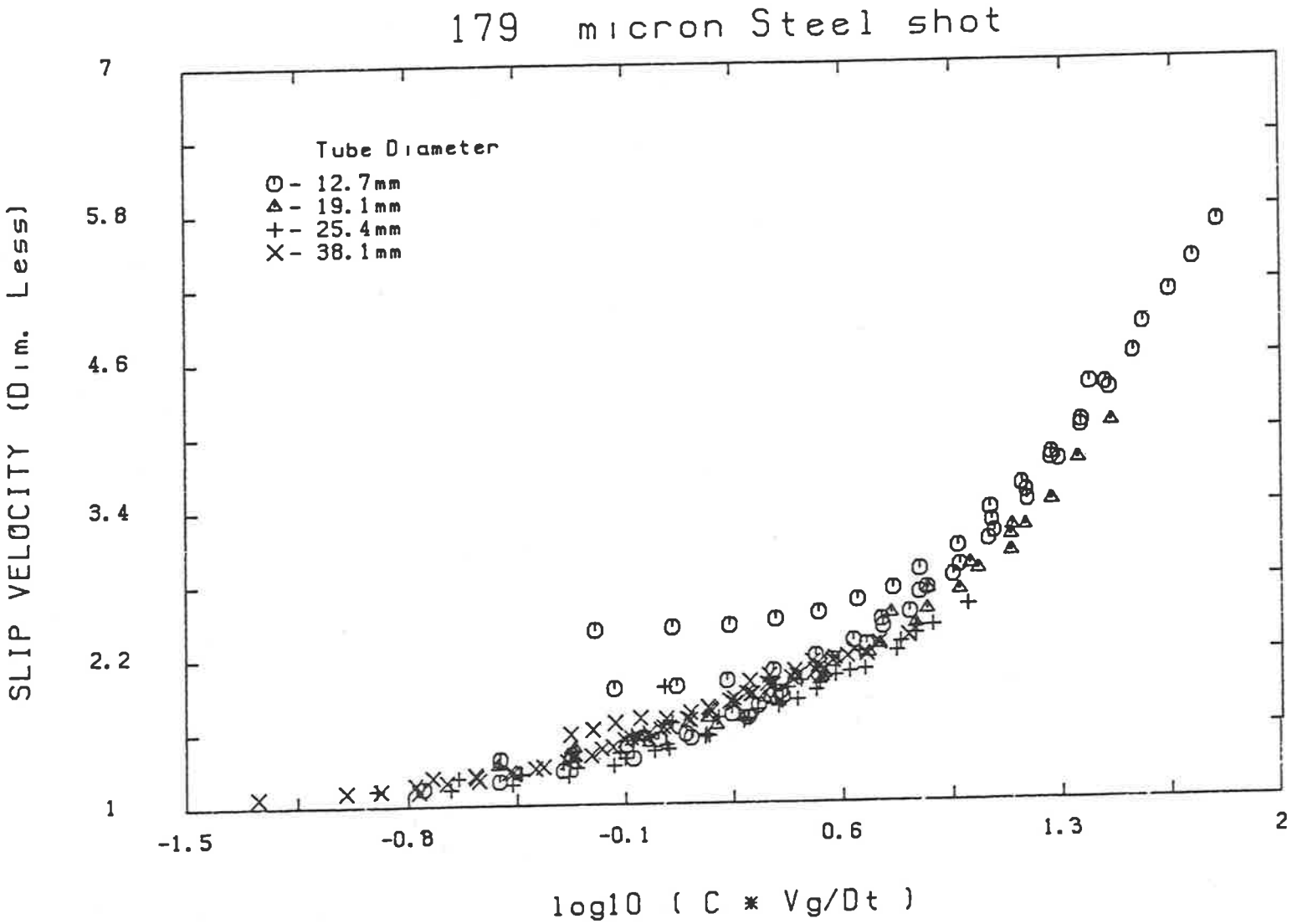

Fig. 2.10 Test of gradient coagulation model

by intermixing layer of gas. As a result these particles have lesser tendency to come into contact with each other, than the light and small particles which follow the fluid stream at a given velocity gradient and particle concentration.

The limitations of the proposed model can possibly be overcome by mathematical representation of the phenomena of coalescence and break up of clusters due to collisions with each other and the transport tube wall. Lack of understanding of these complex mechanisms limits any further analysis. Some quantitative information about the size distribution of clusters and their densities (solid content) is necessary before contemplating models with further complications.

2.3 Significance of Concentration-Slip Velocity Relationship

Having determined the slip velocity and its dependence on concentration, the significance of such a relationship to the design of forward transport systems will be considered here.

If it is presumed that the above relationship obtained from the countercurrent apparatus, can be applied to forward transport at velocities which are not too high (where solid-wall friction component is negligible) the dependence of solid volumetric concentration on air flow at a fixed solid throughput may be derived from the continuity and slip velocity statements.

From the experimentally determined slip velocity-concentration relationship (equation 2.8), the solid concentration (C) at a given superficial gas velocity (Φ_g) for a fixed solid flux (Φ_s) can be calculated by trial and error procedure using the following equalities.

$$\Phi_g = (1 - C)\, V_g \tag{2.17}$$

$$\Phi_s = C V_s \tag{2.18}$$

$$V_r = V_g - V_s \tag{2.19}$$

(for cocurrent transport)

The result of such a calculation using a value of solid flux (Φ_s), of 0.1m/s is given in Fig. 2.11. What it shows is best appreciated by considering a progressive reduction in air flow (Φ_g) from an initially large value. The concentration of solid increases slowly at first in accordance with a value of relative velocity not very different from the terminal velocity of a single sand particle. As this concentration rises, however, its effect on slip velocity becomes significant. The concentration then rises more steeply with falling air velocity. The steeper rate of increase leads to a more rapid rate of rise of slip velocity and the process accelerates. Eventually there is a dramatic increase in concentration at a particular air velocity. This may be regarded as the "choking" velocity. The large concentration of solid presents a correspondingly large pressure gradient to impede transport.

Other solid loadings produce different curves of concentration against air velocity and, indeed, different values for the choking velocity. Results for solid fluxes of 0.02 and 0.5m/s are also shown on the Fig. 2.11. At the greater flux the choking velocity is higher and the rate of onset is more gradual. At the lesser flux the choking velocity is somewhat lower than for 0.1m/s but the event is catastrophic. The increase in choking velocity with solid loading is simply a reflection of the variation of slip velocity with volume fraction. The different rates of approach to choking can be explained in terms of the ranges of slip velocity within each of the solid loadings. At the lower solid flux the range of slip velocity is from the particle terminal velocity to the high value near the volume fraction of 0.15. For the higher solid flux, range of slip velocity is shorter because volume fraction is already considerable, so that the slip velocity is substantially greater than terminal velocity, before the air flow is reduced.

Alternatively, similar remarks about the family of curves of the concentration versus gas velocity profiles can be made on the basis of the following mathematical approach. From equation (2.19)

$$\frac{\partial V_r}{\partial V_g} = 1 - \frac{\partial V_s}{\partial V_g}$$

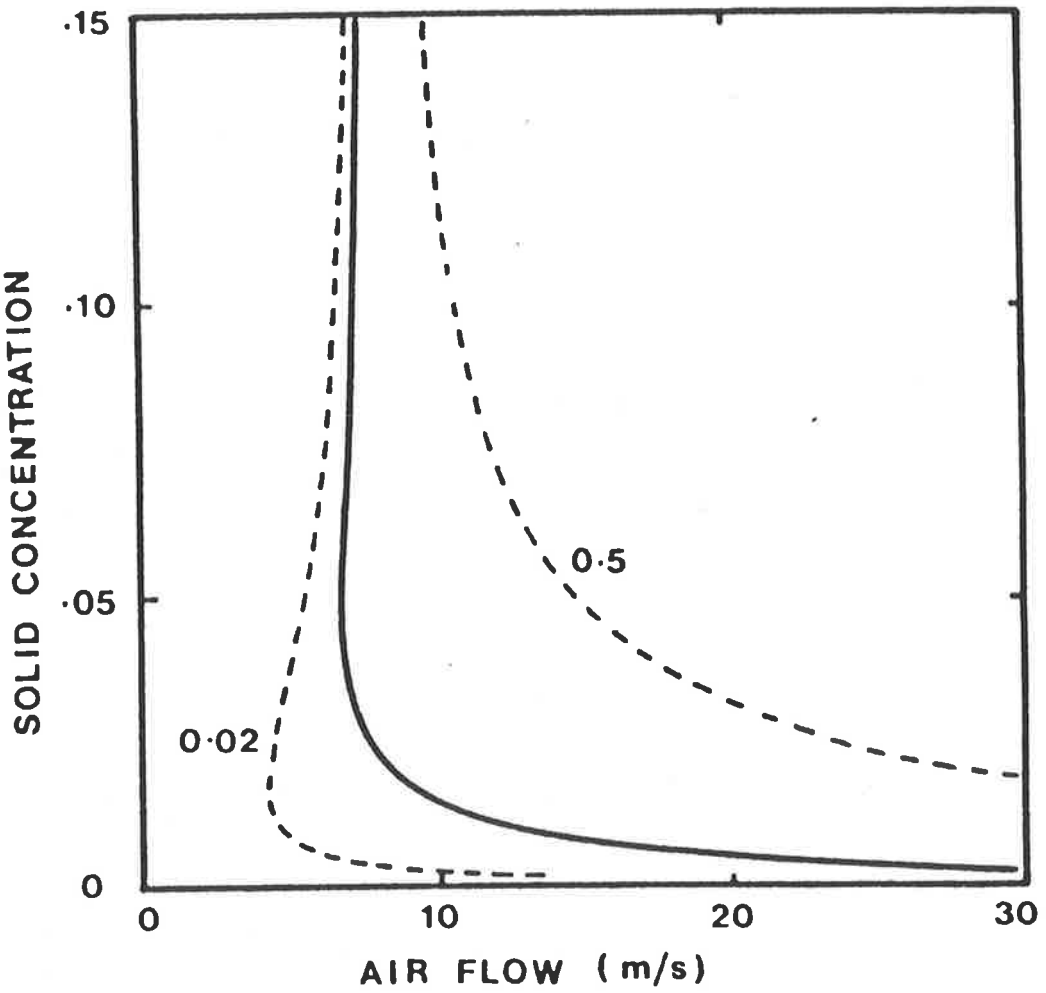

Fig. 2.11 Calculated variation of solid volume fraction with air flow in cocurrent vertical flow at a fixed solid flux of 0.1 m/s.

For constant solid flux (Φ_s)

$$\frac{\partial V_s}{\partial V_g} = -\frac{\Phi_s}{C^2} \cdot \frac{\partial C}{\partial V_g}$$

and

$$\frac{\partial V_r}{\partial V_g} = \frac{\partial V_r}{\partial C} \cdot \frac{\partial C}{\partial V_g}$$

Therefore,

$$-\frac{\partial C}{\partial V_g} = \frac{1}{\frac{\Phi_s}{C^2} - \frac{\partial V_r}{\partial C}} \tag{2.20}$$

The equation (2.20) suggests that the rate of approach of choking ($\partial C/\partial V_g$) depends on the solid flux, concentration and the rate of change of slip velocity with concentration. What it shows is that the slip velocity concentration relationship governs the choking phenomenon. At a given concentration ($\partial V_r/\partial C$) is fixed. Consequently, the rate of change of concentration with gas flow rate increases with decreasing solid volumetric flux. This explains the catastrophic event mentioned earlier at low flux values. In addition the term ($\partial V_r/\partial C$) decreases with increasing concentration.

2.4 Conclusions

1. The influence of solid volumetric concentration on slip velocity in the case of gas-solid flows in pipes is different from that of fluidization and sedimentation phenomena. Use of Zaki's correlation which predicts decreasing slip velocity with concentration is inappropriate for gas-solid flows in pipes.

2. The experiments carried out covering a wide range of particle and tube sizes, confirm the conclusion of Matsen (1982) that slip velocity should increase with increasing concentration in order to explain the choking phenomenon observed in gas-solid flows.

3. An attempt is made to give some physical basis for the observed trends in slip velocity. The large values of slip velocities are due to the formation of clouds of particles whose terminal velocities exceed corresponding particle terminal velocity. A plausible mechanism by which these clouds are formed is gradient coagulation.

4. The usefulness of the slip velocity-concentration relationship which was determined with ease and accuracy, in predicting choking flow rates is demonstrated. Although this was based on the presumption that the above relationship holds good for forward transport at low transport velocities, the results of subsequent experiments which will be discussed in the following chapter validate the assumption.

CHAPTER 3

COCURRENT EXPERIMENTS

3.1 Introduction

Having determined the effect of concentration, tube diameter and particle properties on slip velocity, the effect of transport velocity remains to be investigated. The cocurrent transport experiments designed with the following objectives are described in this chapter.

3.2 Objectives

1. Investigate the effect of transport velocity on slip velocity.
2. Determine the significance of solid-wall friction at high transport velocities.
3. Investigate the applicability of the concentration-slip velocity relationship obtained from cocurrent experiments to forward transport situations.
4. Determine slip velocity with ease and accuracy.

3.3 Review of Measurement Techniques

To study the effect of transport velocity, accurate determination of the same is essential. Although solid velocity and concentration values were derived from the pressure drop measurements in the countercurrent experiments, similar technique can not be adopted in the cocurrent transport arrangement since the role of solid-wall friction can not be ignored, especially at large transport velocities.

Before going into details of the experimental programme, it is worthwhile reviewing the various solid velocity measurement techniques. Boothroyd (1971) presented a good review of instrumentation for use in gas-solid systems. Some of the measure-

ment techniques used by several investigators in the flow of gas-solid suspensions will be reviewed here.

Usually, measurements of mass flow rates of gas and solid are simple and accurate, however determination of solid velocity poses some problems. Basically the measurement techniques for solid velocity can be classified as direct and indirect measurements.

3.3.1 Direct Measurements

3.3.1.1 Radioactive Tracer Method

Solid velocity is determined by measuring the time required for the radioactively tagged particles to move from one point to another. This technique was employed by Hours & Chen (1976), Van zuilichem (1973) and Jodlowski (1976). The problem of contamination of test material by the tagged particles was overcome by making use of short lived radioactive tracer material for tagging process. The advantages of the method are as follows.

1. The detectors are external, readily moved to a desired location and do not induce flow disturbances.

2. The instrument does not require calibration as the particle velocity is measured directly.

However, this method is expensive. Brewster & Seader (1980) reported that by using a phosphorescent material for tagging and photomultiplier detectors for signal processing the above technique can be made much cheaper. They maintain that the photomultiplier detectors are far cheaper than the gamma radiation detectors. Except for the disadvantage of having to have windows at the detector locations their method offers all the advantages of the radioactive tracer technique.

3.3.1.2 Electrical Capacity Method

This method was developed by Beck et al (1969,1971) and found its application in industry as a means of mass flow measurement and detection of solids. The velocity of solid is derived from the transit time of the naturally occurring flow noise pattern between capacitance transducers at two positions along the transport line. The transit time is determined by cross correlating the transducer outputs either with an on-line computer or by collecting the data to be processed later. The advantage of such a system is that it does not disturb the flow as the capacitors are fixed on the transport line and the instrumentation is less involving. Ottjes (1976) used this method to measure the velocity of solids in vertical transport. However, one criticism of this technique is that it assumes that the noise or disturbance travels at the same velocity as that of the medium without being attenuated.

3.3.1.3 Photographic Stroboscopic Method

In this method, two photographs of the gas-solid stream are superimposed on the same photographic negative. The velocity of a particle is derived from the displacement of the particle in the negative. The light source is a stroboscope, the interval being predetermined by a multivibrator. The distance travelled between the flashes should not coincide with the actual distance between the particles for better contrast. This method was employed by Hitchcock & Jones (1958), Reddy & Pei (1969) and McCarthy & Olson (1968). Hitchcock & Jones (1958) in their work with particles of size range 2 to 7mm reported difficulty in measurements with smaller particle sizes due to double images on the photographs. They also observed that the method failed for rotating particles and dense medium in which resolution was poor. Later works of Reddy & Pei (1969) and McCarthy & Olson (1968) did not have these difficulties even with particles as small as 100μ, probably due to improved techniques such as the use of a narrow depth of field camera. Although this technique provides the means of obtaining the local solid velocity, the average solid velocity which is often of interest can not be

directly determined. Also continuous measurement of solid velocity is not possible.

3.3.1.4 Cine Camera Method

Particle velocity is determined by comparing the progress of the coloured granules, frame by frame against a metered scale. Though the technique is simple it could not be used for smaller particles owing to rapid dispersion of coloured particles. Jodlowski (1976) employed this technique successfully with large particles (about 3mm in diameter) and the results were found to be in good agreement with those obtained from the radioactive tracer technique.

3.3.1.5 Laser Doppler Velocimetry (LDV)

This technique was first introduced in 1964 and was applied to single phase flows. It is based on the principle that when a particle with some velocity is intercepted by a laser beam, the scattered beam experiences a shift in its frequency. This frequency shift is then related to particle velocity. Briefly, the relationship is given as follows.

$$f_D = \vec{V}_s \frac{\left(\vec{l}_s - \vec{l}_i\right)}{\lambda_0}$$

where

f_D is the Doppler shift

V_s is the Velocity of particle

$\vec{l}_s$ is the Unit vector along scattered direction

$\vec{l}_i$ is the Unit vector along incident direction

There are three different modes of operation of LDV, details of which are given by Durst et al (1972). The advantages of LDV are as follows.

1. The instrument is linear

2. It does not require calibration as all parameters are easily determined

3. Using the dual beam method, a control volume of any dimension can be chosen. This enables the measurement of local velocities without disturbance to the flow, which occurs in probe type instruments.

Studies by Riethmuller & Ginoux (1973) with particles from 100 to 500μ in diameter transported at velocities between 2 and 100m/s showed that LDV can be successfully used for velocity measurements. Birchenough & Mason (1976) encountered difficulties at higher solid loading ratios due to a decrease in the signal to noise ratio. It was reported that the maximum loading that allows measurement is determined by the point at which processing electronics can no longer deal with the inadequate frequency information. However, this difficulty was overcome by increasing the intensity of laser beam. Disadvantages of this technique are that it is expensive and sophisticated.

3.3.2 Indirect Measurements

The velocity of solids can be derived from the knowledge of volumetric concentration of solids in the pipe, and volumetric flux of the solids. The later quantity is usually easily determined. Some techniques used to determine solid concentration are described here.

3.3.2.1 Isolation Method

The average concentration of solids in a pipe is determined by trapping the solids in a section of the pipe by simultaneous quick closing valves. Hariu & Molstad (1949), Gopichand et al (1959) and Capes & Nakamura (1973) used this technique in their studies. Although this method is simple, its major disadvantage is that it is very time consuming as the flow needs to be interrupted for each measurement. Another draw back with this method is the effect of time delay in closing the valves. Although it is argued that by synchronizing the two valves the effect of time delay is nullified since in that time the same amount of solids escape from the downstream valve as the amount of solids that enter through upstream valve, it is hard to account for any disturbances

created in the flow by the closing valves. The results of Capes & Nakamura (1973) are more reliable than other workers as the hand operated valves were replaced by electrically controlled, pneumatically operated valves.

3.3.2.2 Attenuation Of Nuclear Radiation

A flux of beta particles from a radioactive source can often be attenuated to a suitably measurable extent by gas-solid suspensions. The degree of attenuation is a function of the concentration of solids. The beta ray source is of interest because the attenuation of rays is independent of the atomic number of the material used for calibration and tests. This method gives only average values of concentration and was used by Jodlowski (1976) in his studies.

3.3.2.3 Optical Method

Arundel et al (1971) used this method to measure the density of suspensions. The instrument used operates on the following principle. Light from a bulb travels along two identical paths, one beam passes through the suspension while the other passes through an optical wedge to simulate the suspension. Fiber optic guides allow the instrument to traverse without causing the light signal to change. Both the light signals pass alternately through a chopper to a photo-multiplier. Any fluctuations from the amplified signal are eliminated by adjusting the optical wedge, the position of which is calibrated to give suspension density. Unfortunately, this technique requires calibration prior to use, and may cause damage to the optical surfaces due to particles in the suspension.

In summary, techniques such as Laser Doppler Velocimetry, Capacitance method and beta ray adsorption are attractive in the sense that they enable continuous measurement of solid velocity without disturbing the flow. However, they suffer from the disadvantage of being sophisticated and expensive.

Consequently, it is felt that the development of a simple technique to measure solid velocity is necessary. Measurement of the momentum of solid material by impact on a plate is considered. This technique although not entirely new, has never been used for solid velocity measurement. Boothroyd (1971) reviewd some of the impact meters used for mass flow rate measurements.

3.4 Impact Meter

3.4.1 Principle of Operation

The total axial momentum of solids moving in a transport line at a certain velocity (V_s) can be expressed as follows.

$$\text{Solid phase axial momentum} = \Phi_s \rho_s A_c V_s \tag{3.1}$$

If this momentum can be accurately measured, then solid velocity (V_s) and concentration (C) can be inferred from the knowledge of total volumetric flux of solids (Φ_s), which is usually determined with ease.

The principle of operation of the impact meter is conversion of the axial momentum to a measurable force. This is achieved by deflecting the solid material at right angles to their mean travel direction. Ideally, if all the particles lose their axial momentum on impact, the force experienced by the impact plate can be derived from Newton's second law as follows.

$$\begin{aligned} Force &= \text{Rate of change of axial momentum} \\ &= \Phi_s \rho_s A_c V_s - \Phi_s \rho_s A_c (0) \\ &= \Phi_s \rho_s A_c V_s \end{aligned} \tag{3.2}$$

This force is easily measured with the aid of a load cell. The advantages of such a system are as follows.

1. Measurement of force is simple and accurate

2. Does not disturb the flow, as the impact plate is placed at the exit of the transport tube.

3. Allows continuous measurement without any interruptions.

3.4.2 Description of Impact Meter

The objective in the design of the impact plate is to ensure that the solids lose all their axial momentum on impact. In order to achieve this, the circular impact plate of 150mm diameter, was machined to have a central cone with a 50mm base radius (Fig. 3.1). The cone was machined to have curvature of 25mm radius. The tip of the cone was positioned at the exit of the transport line, on the central axis of the test section. The purpose of the curvature on the conical tip is to guide the deflecting solid particles with successive collisions to a direction normal to their flight path. It is essential that particles have no vertical velocity component as they leave the impact plate. If the particles bounce with a velocity component opposite to the general direction of flow, the measured thrust will be higher and as a consequence solid velocity is overestimated. On the other hand if the particles leave with some velocity component in the direction of flow, the thrust will be lower, resulting in underestimation of solid velocity.

In order to ensure proper functioning of the impact plate, flight path of 644u glass beads travelling at an estimated speed of 20m/s in 25.4mm (ϕ) tube, was filmed while they were bouncing off the impact plate situated at the exit of the transport line. Pictures taken at 250 frames per second indicate that the majority of particles are being deflected by the impact plate normal to the direction of travel. Some of the frames selected at random are presented (Fig. 3.2). The blurred streaks are the fast moving glass beads. In general it was observed that the direction of these streaks is at right angles to the direction of the impinging solid stream.

Fig. 3.1 Impact Plate (side view)

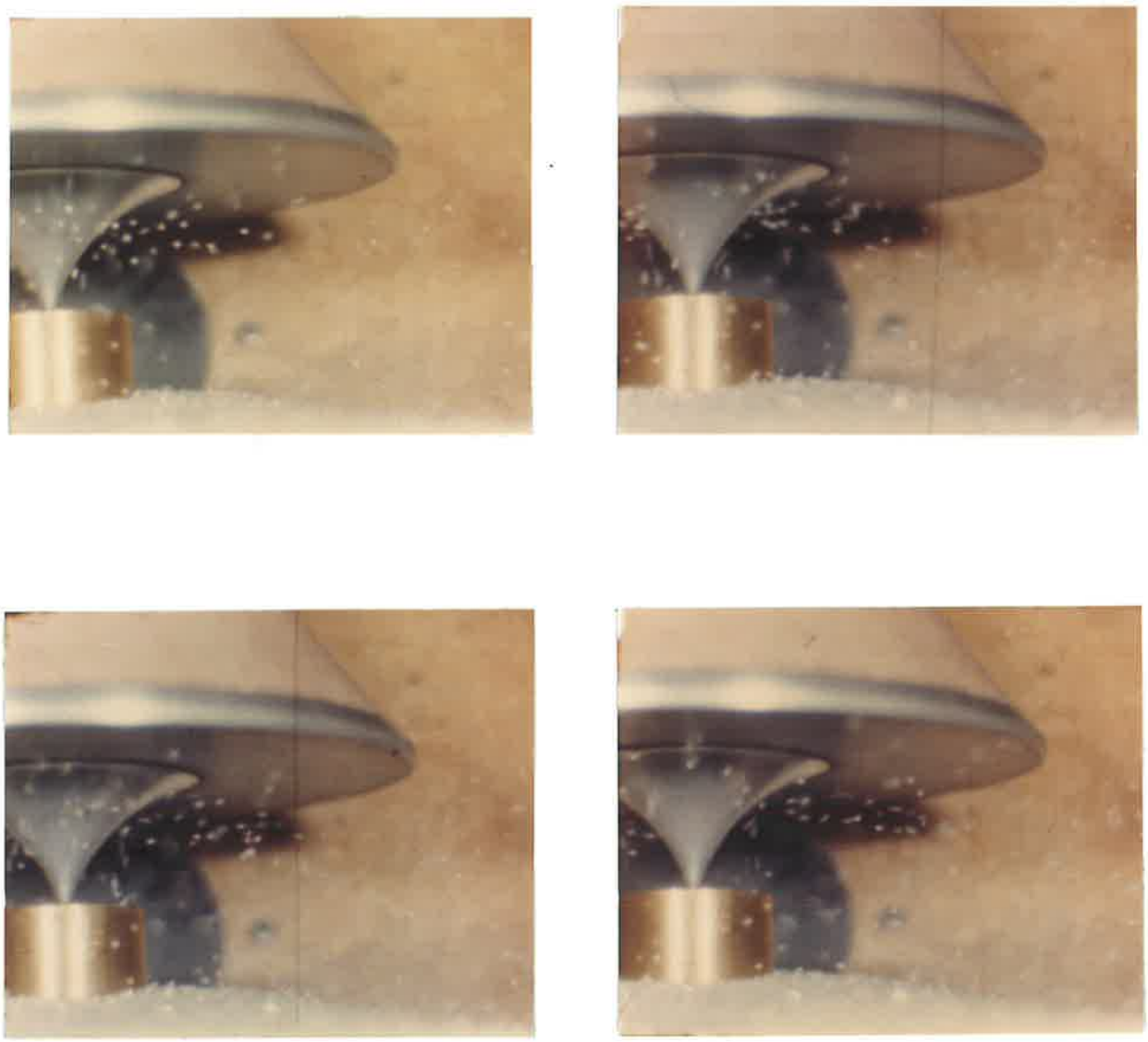

Fig. 3.2 Pictures of impact plate with 644 micron glass beads hitting it at an estimated speed of 20 m/s.

3.4.3 Measurement of Thrust on the Impact Plate

The thrust on the impact plate was measured with a "Mini Beam" load cell. The actual load on the load cell was read with the help of a VIP504 Strain-Gauge input digital process indicator. This device provides the DC excitation necessary for a four wire strain gauge load cell and gives an easy-to-read display of the transducer output. The meter also provides an analogue DC signal of one volt corresponding to the maximum load specification. This DC signal was fed to a continuous running "Rekidenki" chart recorder. The signal from the transmitter, corresponding to the weight of the impact plate experienced by the load cell was biased with a variable DC voltage source. When the impact plate experiences upward thrust due to the impinging flow of gas-solid suspension, the resulting change in the net force on the load cell beam is measured by the corresponding change in transmitter output. The transmitter output was calibrated against the force experienced by the load cell with the help of standard weights. The response is linear. The gain of the system is 0.485mv/gmf. Fig. 3.3 presents the calibration of the load cell response. In order to dampen the high frequency fluctuations of the impact due to gas-solid suspension, the signal from the transmitter was filtered with an RC circuit before feeding it to the chart recorder.

3.4.4 Calibration of Thrust due to Air

In order to determine the thrust due to the solid phase the contribution of thrust due to air alone should be determined. It is therefore necessary to calibrate the actual thrust imparted by air, against the theoretical value obtained by assuming that the air gives up all of its axial momentum on impact with the plate. The thrust experienced by the impact plate was measured at several gas flow rates through all the tubes investigated. The calculated value was plotted against the observed thrust(Fig. 3.4). A linear relationship is obtained in all experiments. The observed thrusts are in close agreement with the calculated values in the case of 12.7mm and 19.1mm diameter tubes. However, with larger tubes, observed thrust is higher than the calculated value

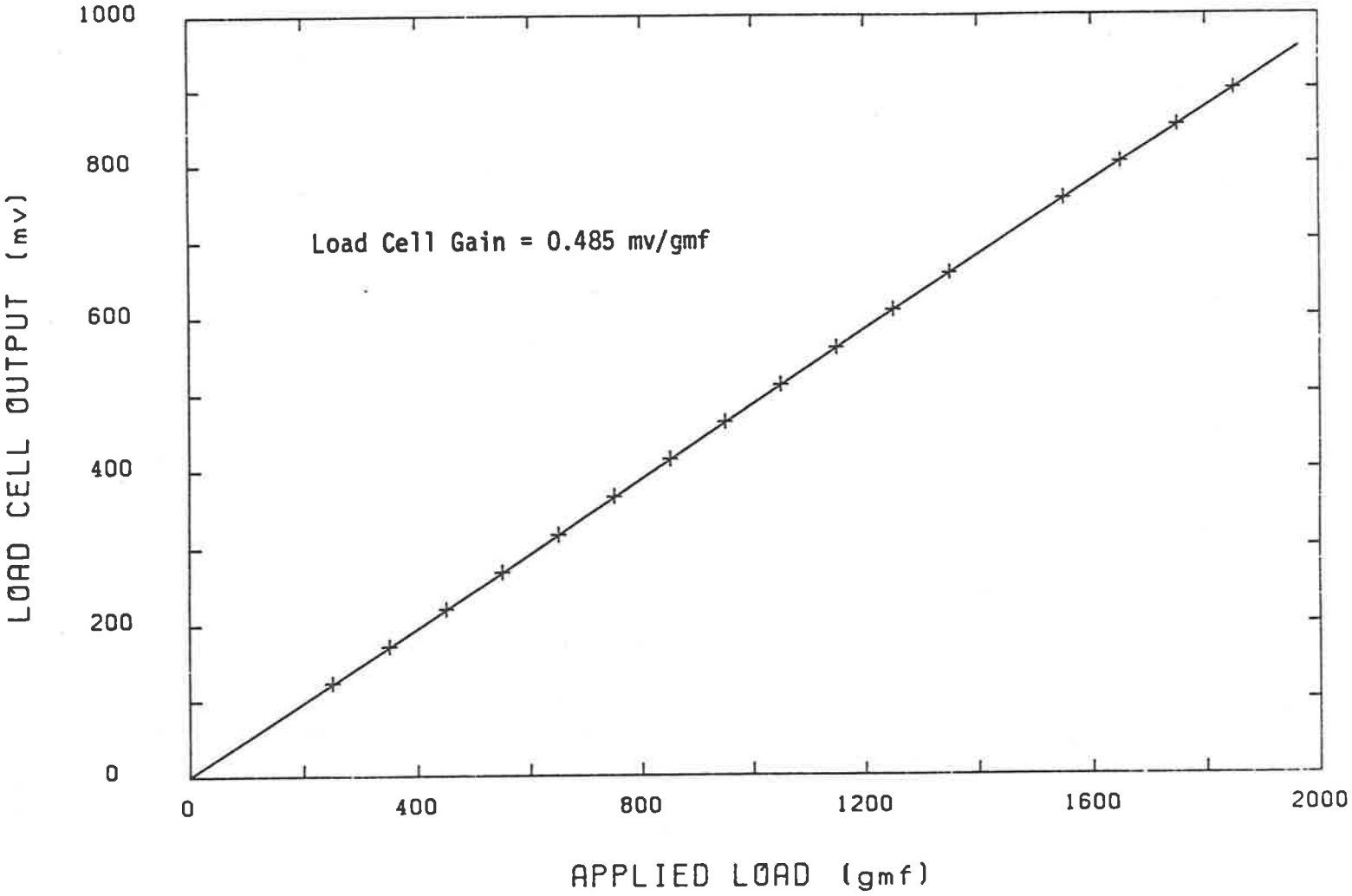

Fig. 3.3 Calibration of load cell response

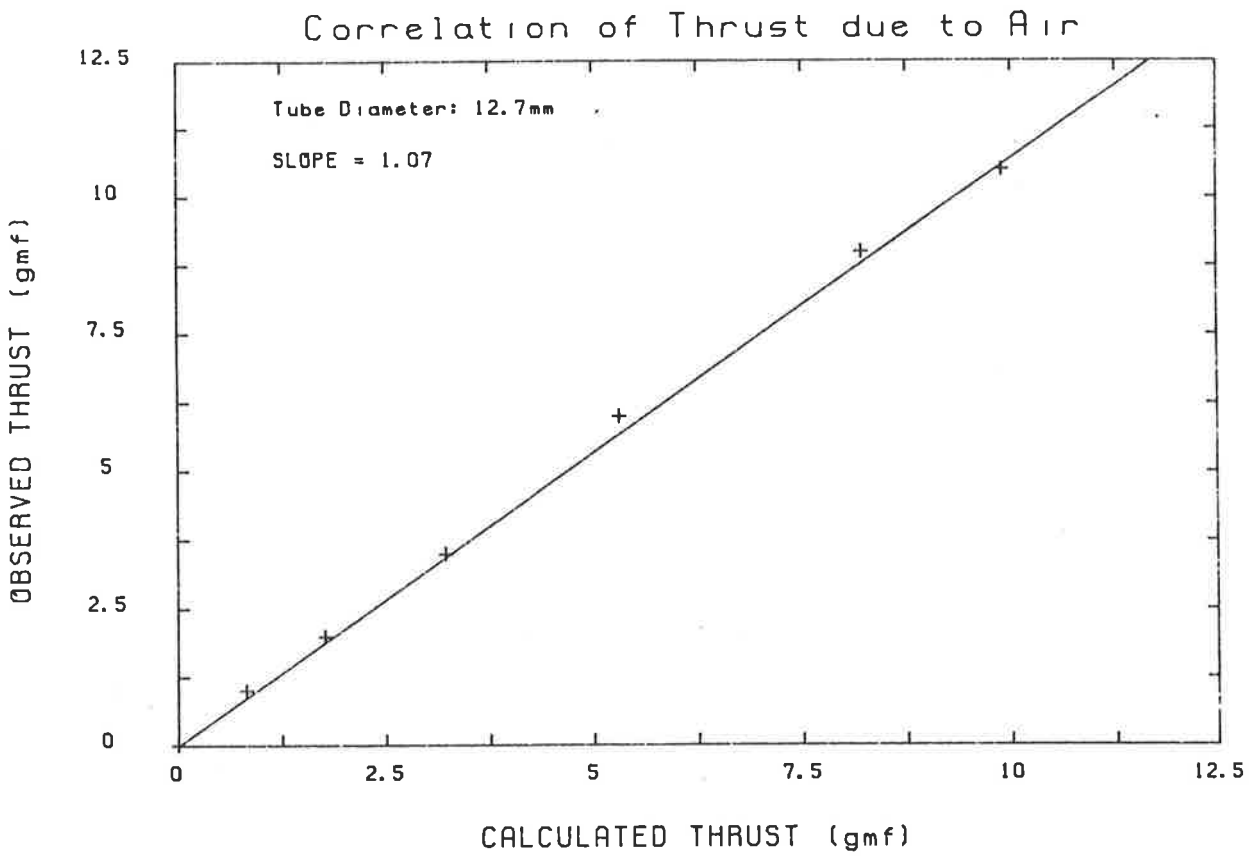

Fig. 3.4(a)

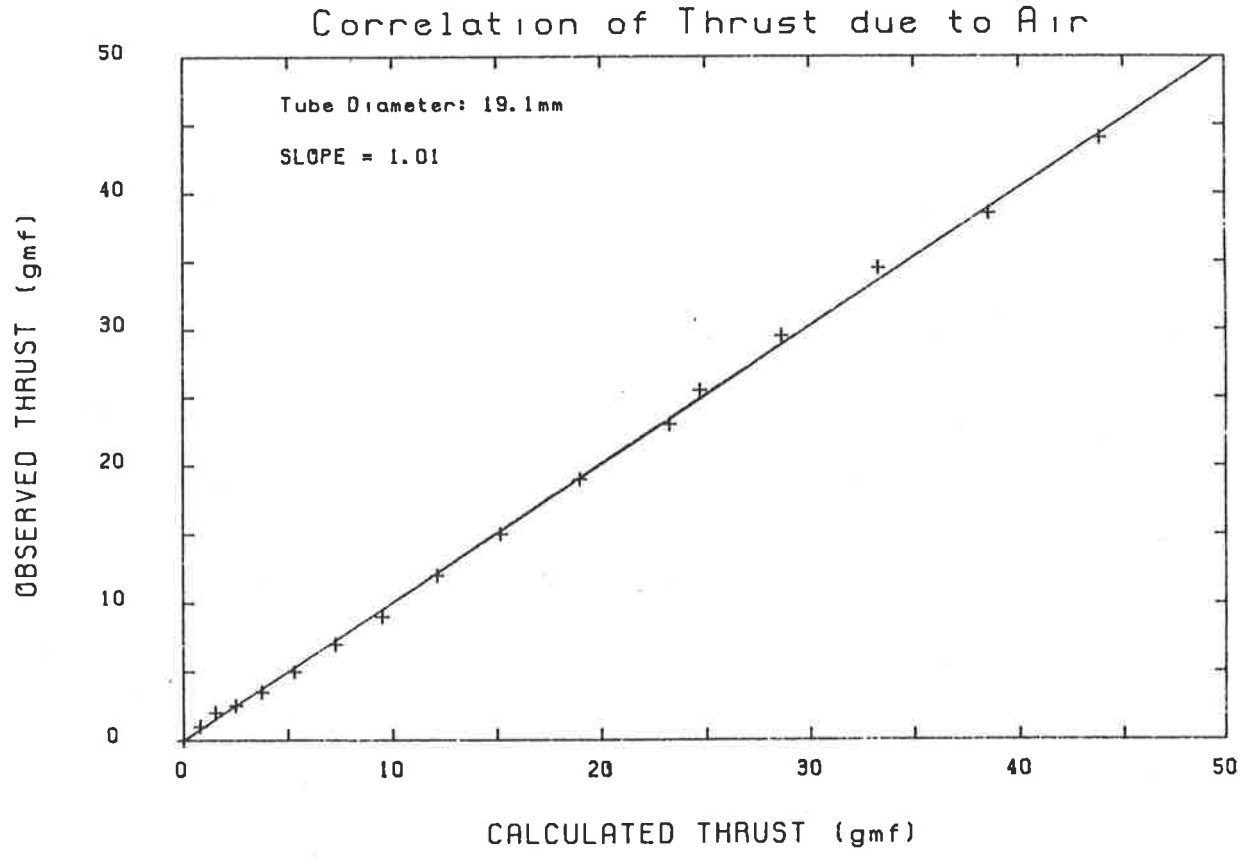

Fig. 3.4(b)

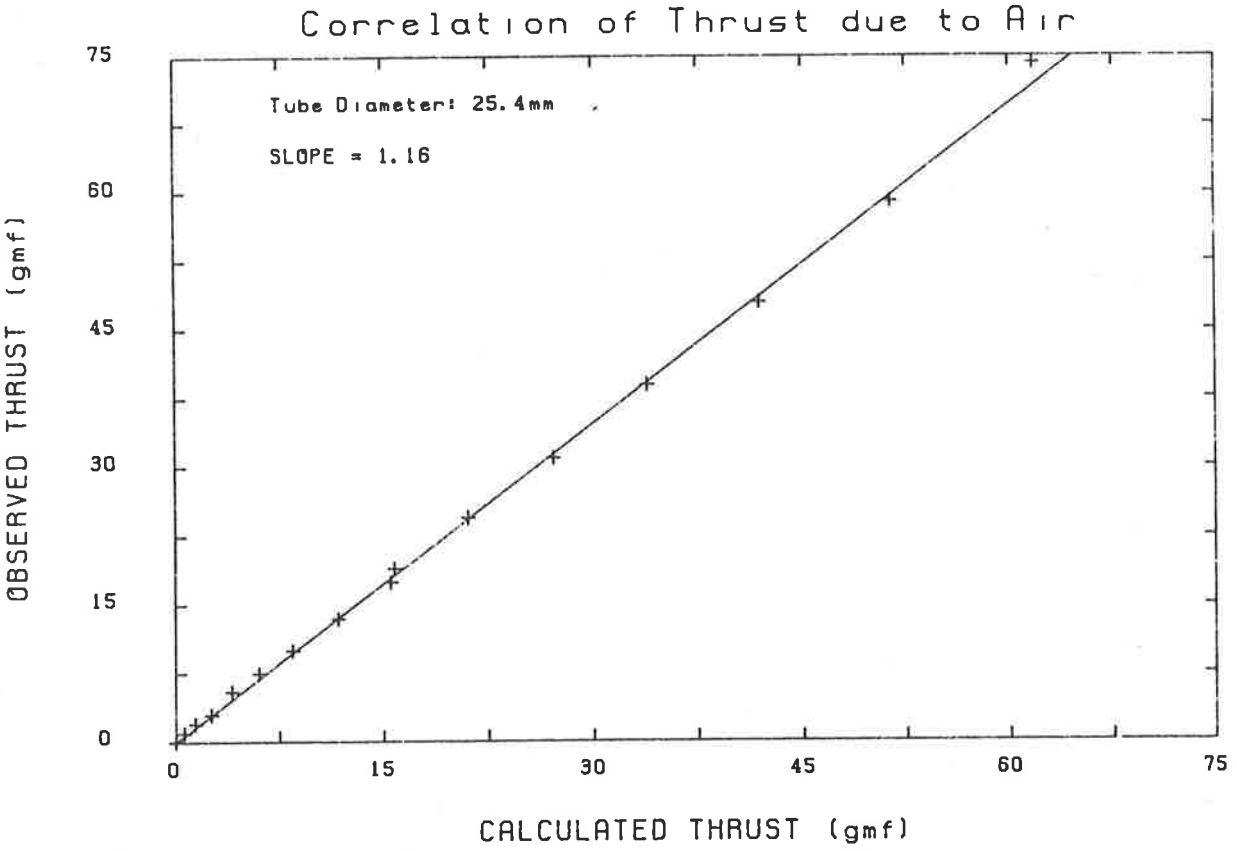

Fig. 3.4(c)

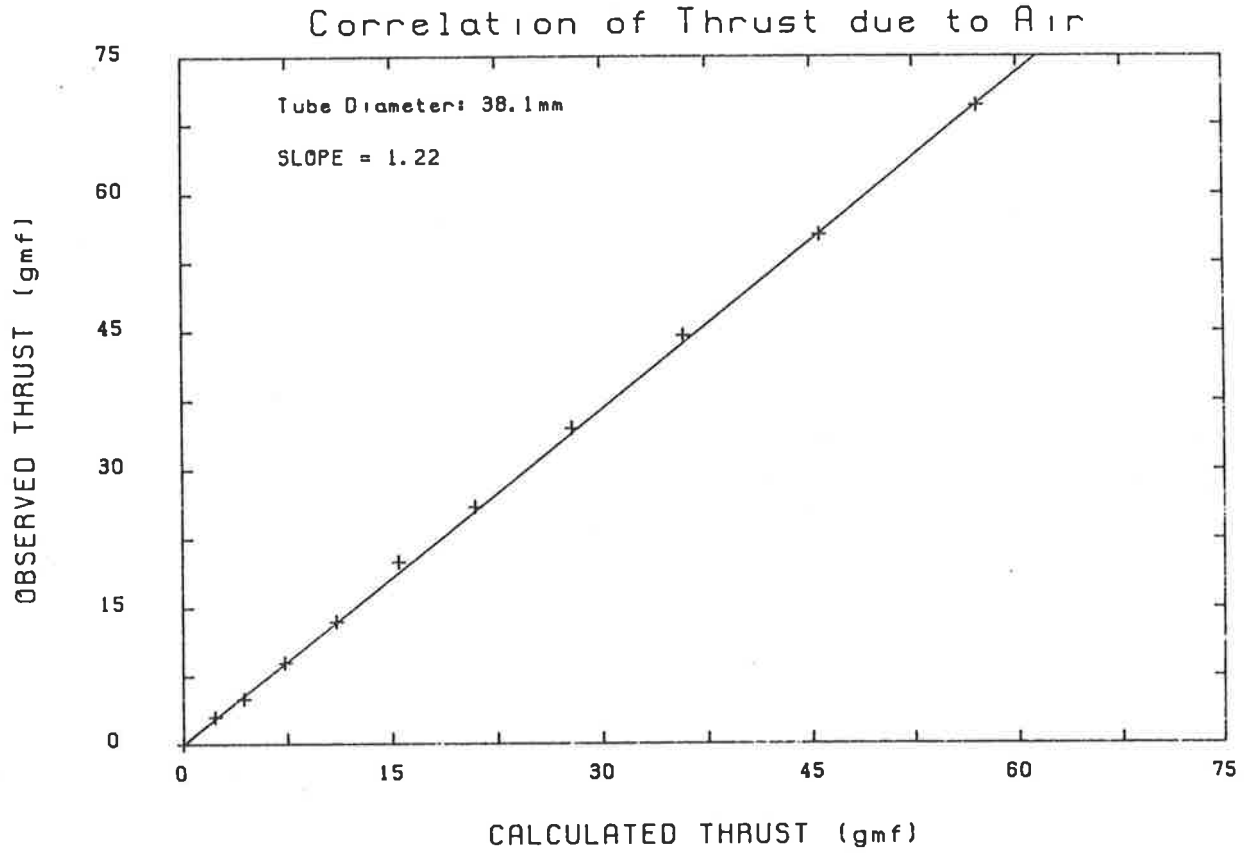

Fig. 3.4(d)

by about 20%. This suggests that in the case of large diameter tubes where turbulent conditions prevail, the air stream is leaving the plate with some negative component of its axial velocity. Another possible explanation is that the air stream might be flowing around the edges of the plate resulting in fluid drag. Additional thrust could also have been induced due the pressure difference between the front and rear of the impact plate. All these non-idealities could possibly be associated with a drag coefficient. However, this factor should not affect the accuracy of the measurement of slip velocity, since air velocity is inferred from total volumetric flow of air and the solid velocity is calculated from the thrust due to solid phase alone. The thrust due to solid phase is determined by subtracting the thrust due to air from the total thrust. The underlying assumption in such a procedure is that the thrust due to air in the presence of solid is same as the thrust when air alone was flowing at the same velocity.

3.5 Apparatus

The apparatus for cocurrent transport experiments is schematically represented in Fig. 3.5.

3.5.1 Solid Feed Mechanism

The solid feed mechanism consists of a solid feed tank with provision for interchanging orifices at the bottom of the tank. Solid flow through the orifice is controlled by a tapered plug valve designed to allow gradual opening of the orifice aperture. The solids leaving the feed tank are introduced into the transport line . The pressure at this point and the pressure in the feed tank are equalised by a connecting line between them. This allows smooth flow of solids through the orifice irrespective of the pressure fluctuations in the system.

The advantages of such a system over the conventional screw feeders, fluidized stand pipes and venturi feeders (which suffer from the fluctuations in solid feed rate or limited control over the solid feed rate) are as follows.

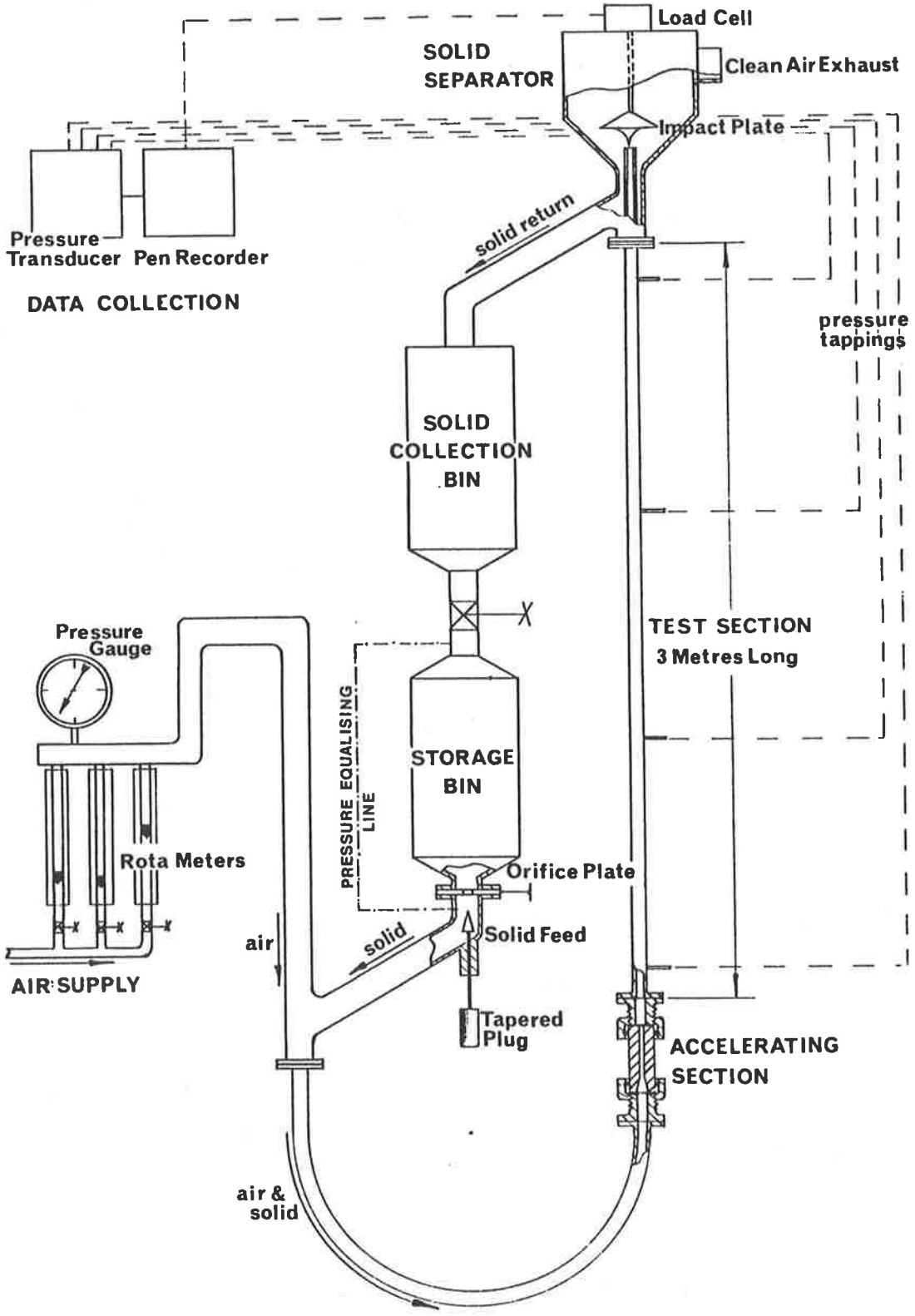

Fig.3.5 COCURRENT FLOW APPARATUS

1. Any solid feed rate can be selected simply by choosing corresponding aperture size.

2. Solid feed rate can be accurately predetermined for a given orifice size thus avoiding insitu arrangements for solid feed rate measurement such as continuous monitoring of weight of the storage vessel or collection vessel.

3. Does not suffer from fluctuations in solid feed rate.

4. Simple and trouble free operation.

3.5.1.1 Drawback with the Solid Feed Mechanism

Although the solid feed mechanism worked well for coarse particles, runs with very fine glass beads (96μ) proved to be problematical. While transporting 96μ glass beads the flow of solids through the orifice was found to be oscillatory (stop-start flow). This behaviour was pronounced when the solid bed height above the orifice in the storage tank was large. This was due to time lag in the pressure equalisation at the orifice. However, once a certain minimum bed level was reached steady solid flow was realised. When solids are introduced into the transport line, the system pressure increases. For solids to flow through the orifice uninterrupted, a corresponding increase in pressure above the orifice at the storage vessel should occur. Although the equalising line ensures that there is a corresponding increase in pressure above the solid bed in the storage vessel, in the case of fine solids the bed resistance is so large, that there is a time delay in equalising the pressure just above the orifice. As a result solid flow through the orifice stops. Thus the time delay in pressure equalisation results in stop-start flow. Once the bed height is sufficiently low, thus reducing the resistance, smooth flow is established. No such problem is encountered with a coarse solid bed, since the resistance offered by a coarse solid bed is small compared with that offered by a fine solid bed of the same height.

In view of the above difficulty with fine solids, experimental runs with 96μ glass

beads were carried out with some modifications to the apparatus. Instead of using a compressor to drive the air through the system, two vacuum cleaners were used down stream at the solid separator outlet. Thus, air was drawn into the system at atmospheric conditions, and solids were fed from the feed tank which was open to atmospheric pressure. This arrangement ensured smooth flow of solids without any pressure equalising problems. The air flow was monitored down stream of the apparatus with rotameters connected at the vacuum cleaner inlet.

3.5.2 Driving Air Supply

Air from the screw compressor was freed from oil and moisture by a freeze dryer. The dew point of air leaving the compressor was reduced to $4°C$. The oil and moisture free air metered through one of the four rotameters depending on the range of flow investigated, was fed to the point at which solids are introduced into the transport line. Air pressure at the rotameter was measured by a Bourdon type pressure gauge (0 to 100Kpa) situated downstream.

3.5.3 Acceleration Section

The solids fed from the storage vessel are picked up by the driving air and the suspension travels along the gradual 360 degrees bend before commencing its upward journey through the test section of 3.5meters length. In order to facilitate acceleration of solids to the equilibrium velocity, an acceleration section was provided at the entrance of the test conduit.

The principle of operation of acceleration section is to reduce the cross sectional area of the transport line to provide larger air velocities thus increasing the speed of the solids, over a short distance. The acceleration section is shown schematically in Fig. 3.5. It is designed to facilitate the selection of the desired cross sectional area corresponding to the degree of acceleration required. The advantage of such a system is that it is not necessary to provide long test sections in order to realise equilibrium conditions.

3.5.4 Solid Separator

The solids traversing the test conduit hit the impact plate positioned near the exit of the conduit, which is situated in the solid separator. The purpose of the solid separator is two fold. (i) To reduce the air velocity so that solids can be collected from the gas-solid suspension after impact with the plate. (ii) To provide the housing for the impact plate and load cell. The solid separator is a cylindrical construction whose cross sectional area is such that the air velocity in it corresponding to highest volumetric flow rate anticipated, is less than the terminal velocity of smallest particle used in the tests. This ensured complete separation of solids. The clean air leaves through the two outlets provided at the sides of the separator. The separated solids are then collected in the closed collection vessel situated on the top of the feed tank.

3.5.5 Impact Plate & Load Cell Housing

The load cell was mounted on the top of the solid separator. The extended stem from the impact plate hung from the beam of the load cell. The beam of the load cell was provided with an overload protection spring.

The tip of the impact plate was positioned exactly at the centre of the exit of the test conduit by an air bearing. This prevented displacement of the impact plate in the lateral direction due to the impinging gas-solid stream, while transmitting the axial thrust without frictional loss.

3.5.6 Differential Pressure Transducer

Pressure drop along the transport line was measured using a high precision MKS Baratron Type 220B differential pressure transducer. The transducer is a self contained unit with the sensor, associated electronics and power supply mounted in a dust proof box. The sensor is made up of 3 parts: (1) a taut metal diaphragm welded to support rings, (2) a single ceramic-based electrode, and (3) a reference side cover through which

feedthrough terminals make connections to the electrode within the reference cavity. The P.C. mounted electronic circuitry contains those components necessary to convert a change in capacitance caused by diaphragm deflection to a linear +10 V DC signal.

The gain of the pressure transducer is 10Volts/100Torr. The signal from the transducer was fed to a "Rekidenki" chart recorder. The manometer leads from the pressure tappings were provided with needle valves which introduce adequate damping of the pressure signal and provide a steady state average value. Pressure drops along two sections, each one meter long, downstream of the transport line were measured with the help of the pressure transducer and a switching station making use of a two way valves.

3.6 Procedure

The solid material being investigated was loaded into the solid feed tank, after placing the appropriate orifice selected for a desired solid flow rate. Initially, the diameter of the insert in the acceleration section was the same as that of the test conduit. Air flow from the compressor was established by opening the inlet valve at the rotameters. Air flow was routed through one of the four rotameters appropriate to the range of air flows being investigated. With a sufficiently large air velocity established through the transport line, solids were introduced gradually by withdrawing the tapered plug from the orifice. Once a solid flow was established, pressure drops at two sections downstream of the transport line were recorded. If the pressure drop in the upstream section was higher than the pressure drop in the downstream section, indicating incomplete acceleration of solids, then the procedure was repeated (with a smaller insert in the acceleration section), until the correspondence between the pressure drops was satisfactory. Once this was realised, air pressures at the rotameter and the impact plate in the solid separator were recorded using Bourdon type pressure gauges. The pressure transducer signals from the two sections of the tube and the signal from the impact meter were recorded on the chart recorder. The above procedure was repeated at several gas

velocities by reducing the air flow rate progressively until the gas-solid suspension flow was erratic characterised by large fluctuations in the pressure drop readings. Once all the material in the feed tank was transported up, the air flow was shut off. Another solid flow rate was selected by using the appropriate orifice. With the tapered plug in place the solids in the collection bin were drained back into the solid feed tank by opening the isolation valve. The procedure was repeated at several solid flow rates.

The experiment was repeated with different solid materials in transport tubes of different diameters.

3.7 Range of Variables Studied

Six different solid materials were studied in four different test sections. The solid materials and the transport tubes used in the study were the same as those used in the countercurrent experiments. Details of these materials are provided in Chapter 2 [page 3].

The maximum air velocity studied in these experiments was about 20m/sec. The range of loading ratios used was about 0 to 60.

3.8 Analysis of Data

3.8.1 Thrust Due To Air

From the rotameter reading and corresponding air pressure at the rotameter, inlet mass flow rate of air was determined. The net volumetric flow rate of air introduced into the test section was then equal to the total volumetric flow rate less the volume flow rate of solids introduced into the transport line. With the knowledge of inlet flow conditions, mass flow rate of air through the conduit was determined.

Knowing the exit conditions at which the solid velocity was being measured,

contribution of thrust due to air to the total thrust was calculated as follows.

$$F_g = K_f\,(M_g)\,(V_g)_{exit}$$

$$= \frac{K_f M_g^2}{(\rho_g)_{exit}\,A_c\,(1-C)} \tag{3.3}$$

where

F_g is the Thrust due to air alone

M_g is the Mass flow rate of air

C is the Volume fraction of solids

K_f is the Ratio of observed thrust to theoretical thrust

3.8.2 Thrust Due To Solids

The total thrust due to the suspension impinging on the impact plate was derived from the load transducer voltage signal. The thrust due to solid phase was calculated as follows.

$$F_s = F_t - F_g \tag{3.4}$$

where

F_g is the Thrust due to air alone

F_s is the Thrust due to solid phase

3.8.3 Solid Velocity And Concentration

Knowing that solids loose all their axial momentum on impact with the plate, thrust due to the solid phase can be expressed as follows.

$$F_s = \Phi_s \rho_s V_s A_c \tag{3.5}$$

Combining (3.3), (3.4) and (3.5)

$$V_s = \frac{F_t A_c\,(1-C)\,(\rho_g)_{exit} - K_f M_g^2}{(\rho_g)_{exit}\,\rho_s A_c^2 \Phi_s\,(1-C)} \tag{3.6}$$

and

$$\Phi_s = CV_s \tag{3.7}$$

From equations (3.6) and (3.7) solid velocity and concentration were derived from the knowledge of the remaining quantities. The above two quantities can be evaluated either by direct substitution of equation (3.7) in equation (3.6) to yield a quadratic equation in terms of concentration or solid velocity, or by iterative substitution starting from an initial guess value.

3.8.4 Slip Velocity

Air velocity was determined from the knowledge of volume flux of gas at exit conditions and corresponding voidage. Having determined gas and solid velocities slip velocity, was calculated as follows.

$$V_r = V_g - V_s \tag{3.8}$$

The negative sign on solid velocity is appropriate since solids are travelling in the same direction as air flow.

3.8.5 Pressure Drop Calculations

3.8.5.1 Total Pressure Drop

From the pressure transducer voltage signal and the transducer gain, the pressure drop across one meter length of the test section was derived.

3.8.5.2 Gas-wall Frictional Loss

Pressure drop due to air was determined experimentally with only air flowing through the test section. The correspondence between experimental values and the

theoretical values obtained from friction factor-Reynolds number correlation is reasonably good. Plots of experimental pressure drop versus calculated values at several air velocities, for all four test sections used in the study are presented in Fig. 3.6.

The pressure drop due to gas-wall friction in the presence of solids was assumed to be the same as when air alone was flowing at the same velocity.

3.8.5.3 Pressure Drop Due To Solid Holdup

Pressure drop due to static head of solids was derived from the knowledge of solid volumetric concentration.

$$(\Delta P)_{ss} = C\rho_s gL \tag{3.9}$$

3.8.5.4 Solid-wall Frictional Loss

Pressure drop due to solid-wall frictional loss was determined by subtracting the contributions of gas-wall friction and solid static head components from the measured total pressure drop.

$$(\Delta P)_{fs} = (\Delta P)_t - (\Delta P)_{ss} - (\Delta P)_{fg} \tag{3.10}$$

3.8.6 Calculation Of Solid-wall Friction Factor

Analogous to the Fanning friction factor definition for single phase flow, solid-wall friction factor defined as follows was calculated from the solid-wall frictional pressure drop.

$$(\Delta P)_{fs} = 2f_s LC\rho_s \left(\frac{V_s^2}{D_t}\right) \tag{3.11}$$

3.9 Results and Discussion

As the objective of the cocurrent experiments was to investigate the effect of transport velocity on slip velocity, and its influence on concentration slip velocity rela-

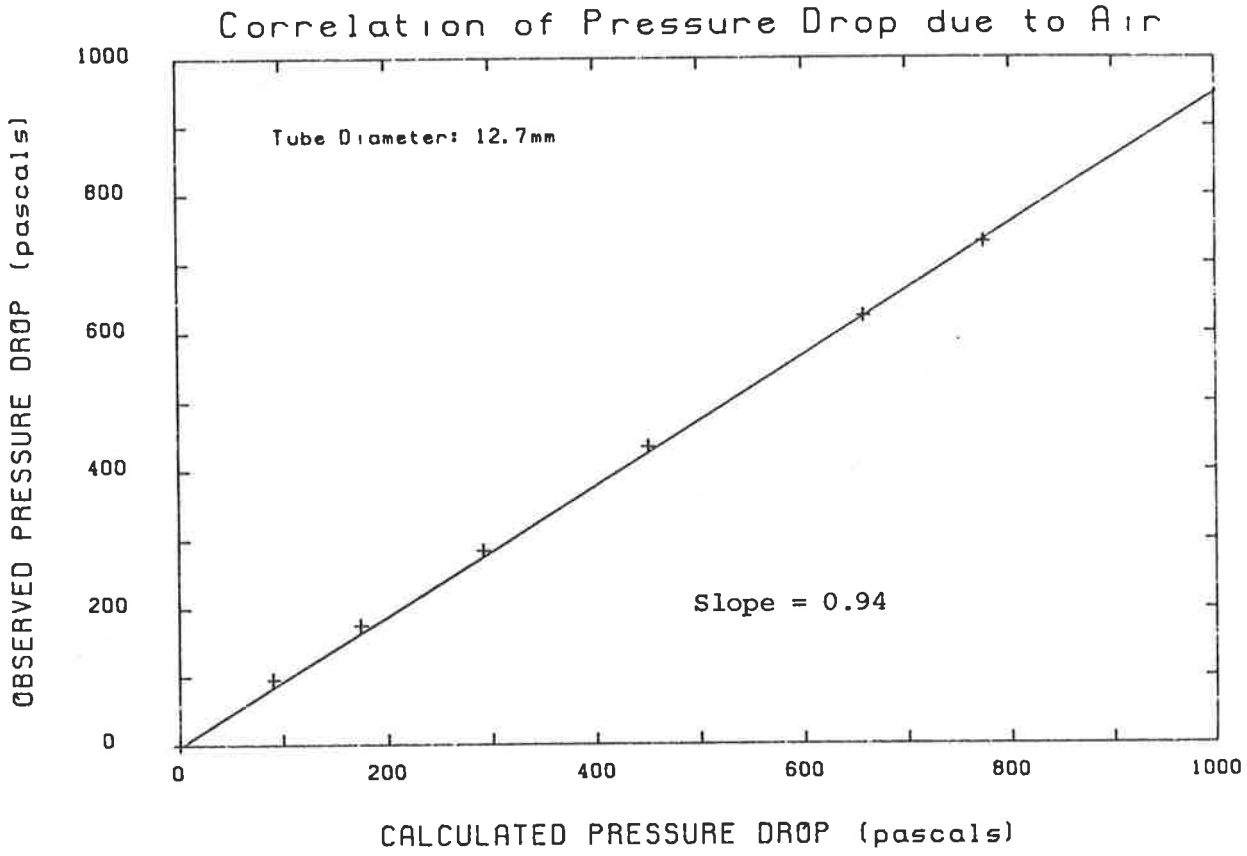

Fig. 3.6(a)

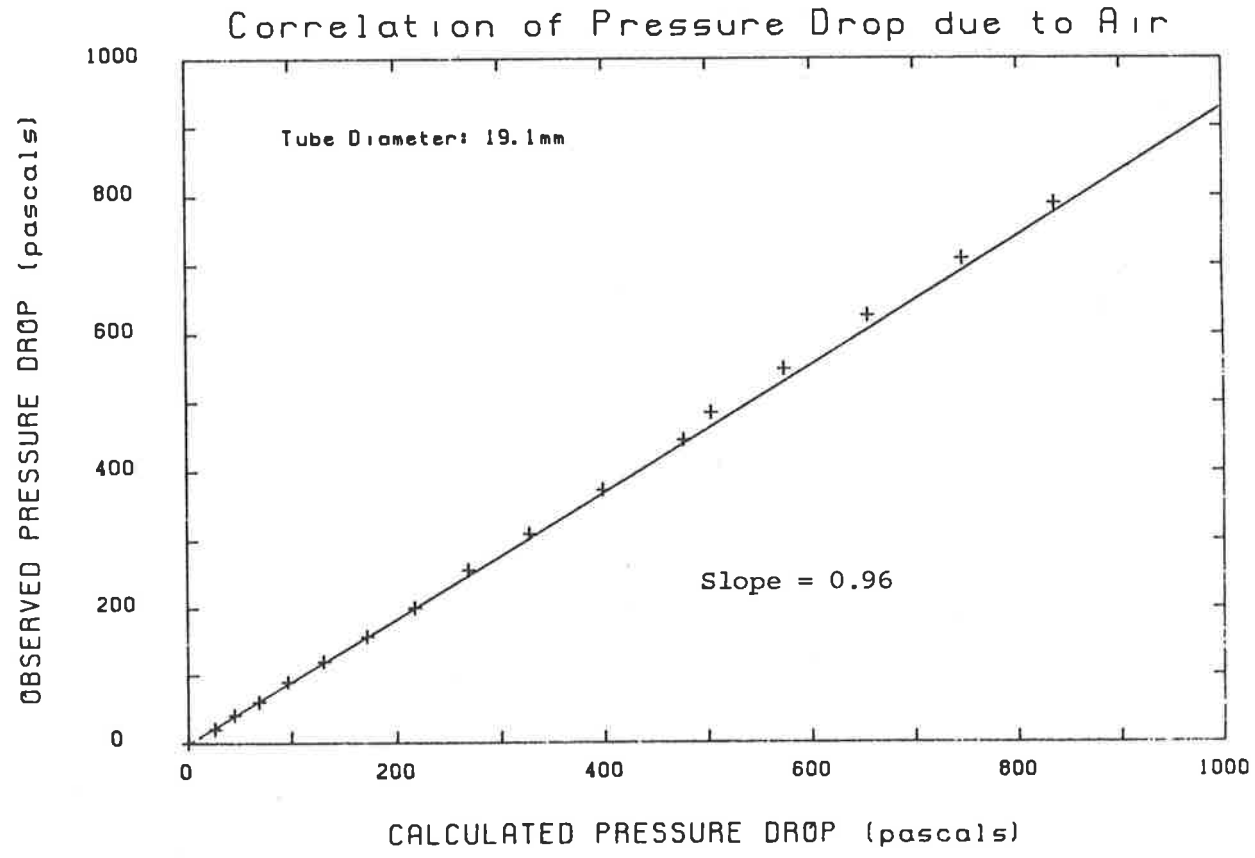

Fig. 3.6(b)

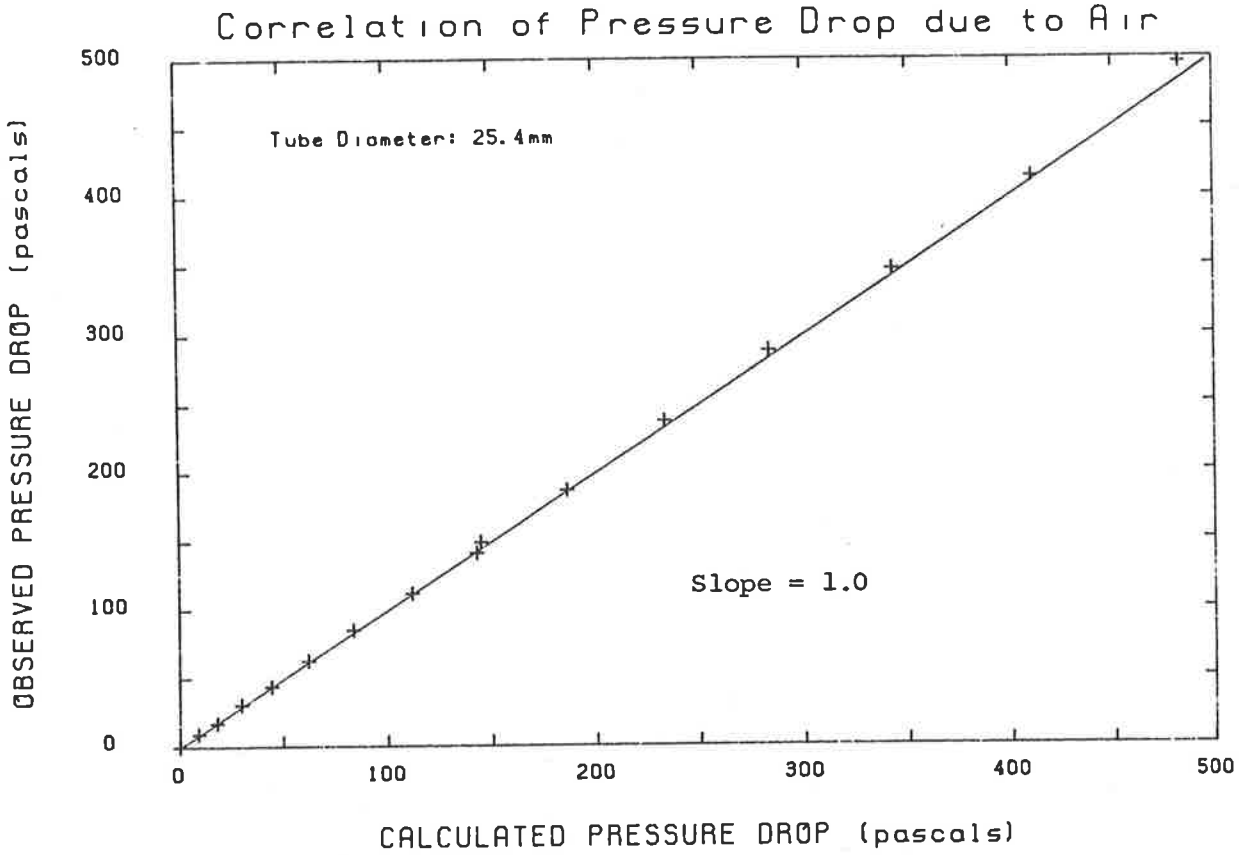

Fig. 3.6(c)

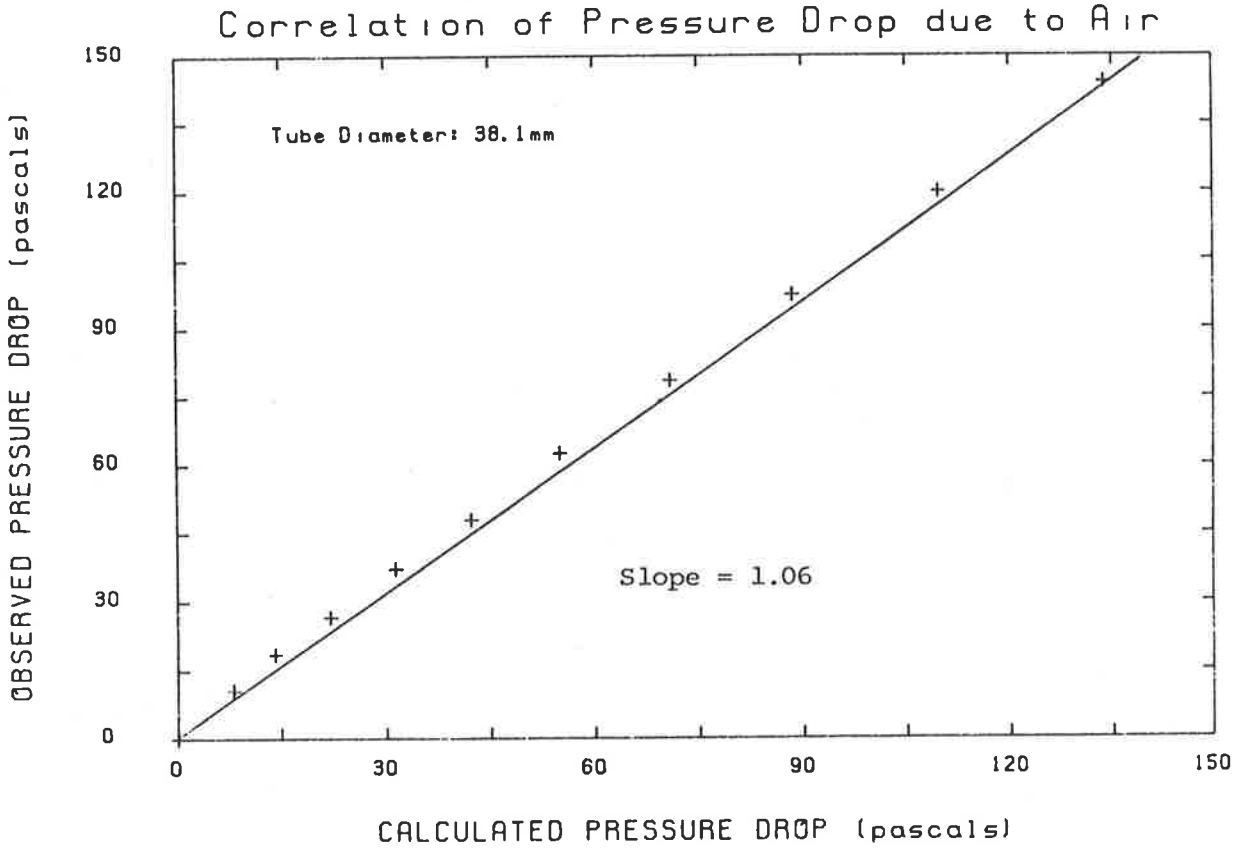

Fig. 3.6(d)

tionship obtained from countercurrent experiments, data of both the experiments were analysed simultaneously.

3.9.1 Concentration - Slip Velocity Relationship

From the procedure presented in the earlier section, slip velocity and concentration values were derived for all the tests with six different particles in four different transport tubes. Data in which the pressure drops at the top and bottom sections differed by more than 10% were discarded to ensure that only steady state conditions were analysed. This criterion should ensure that the error in evaluation of solid velocity is much less than 10%. From momentum balance the pressure gradient due to the acceleration effect is proportional to the velocity gradient. Even if one assumes that the pressure gradient is solely due to acceleration of solids, the corresponding change in velocity gradient is only 10%. The change in solid velocity should be much less. Moreover, the additional contributions of solid weight and solid-wall friction should further reduce these errors. Slip velocity normalised with particle terminal velocity, was plotted against solid volumetric concentration for all test runs. For comparison corresponding results from countercurrent experiments are also presented on the same plots. These plots are presented in Appendix (F). For quick reference, results with 375μ steel shot in 12.7mm tube are presented in Fig. 3.7. The following observations can be made from these plots.

1. Slip velocity is not a unique function of concentration, but also depends on solid flow rate.

2. At a constant mass flow rate of solids, slip velocity decreases with increasing concentration.

3. At a given concentration of solids, slip velocity increases with increasing solid mass flow rate.

4. At low mass flow rates of solids a large reduction in slip velocity results over a

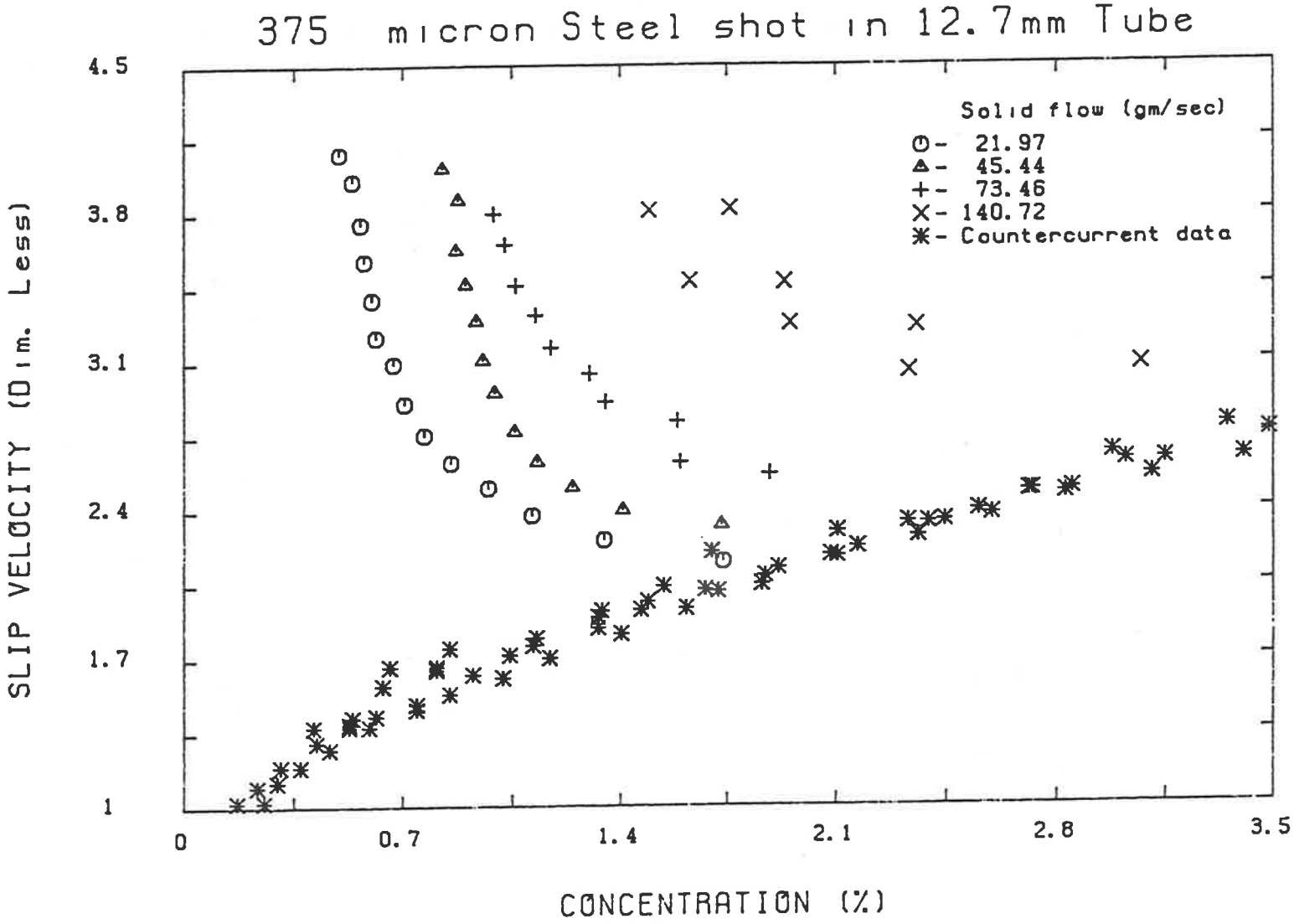

Fig. 3.7 Concentration-slip velocity map for cocurrent transport. Countercurrent data is included for comparison.

small increase in concentration, while at larger mass flow rates the change in slip velocity with concentration is gradual.

5. For a fixed solid flow rate, slip velocity decreases as the gas velocity decreases, and approaches countercurrent experimental data as the lower limit to transport approaches.

6. At large transport velocities slip velocities are much higher than the corresponding values obtained with countercurrent experiments at the same concentration.

From the above observations the significance of transport velocity is quite clear. At large transport velocities solid-wall friction is dominant. Due to this solid-wall friction, solid particles hitting the transport line walls loose some of their momentum. This additional loss in energy should be compensated by larger hydrodynamic drag, in order to sustain transport. Hence larger slip velocities.

At a given concentration solid velocity increases with increasing solid flow rate, which results in larger solid-wall friction. At a fixed solid flow rate solid velocity decreases with increasing concentration. This explains the trends (2) and (3) mentioned above.

3.9.2 Slip Velocity Due To Solid-Wall Friction

At large transport velocities, which often are associated with lower volumetric concentrations, the slip velocity is mainly due to solid-wall frictional loss. In such a situation momentum balance on solid phase results in the following expression.

$$\frac{1}{2}C_D\rho_g V_r^2\left(\frac{\pi D_p^2}{4}\right)\left(\frac{6C}{\pi D_p^3}\right) = 2f_s C\rho_s\left(\frac{V_s^2}{D_t}\right)$$

Then

$$V_r = kV_s \tag{3.12}$$

where $$k = \sqrt{\frac{8}{3}\ \frac{f_s}{C_D}\ \frac{D_p}{D_t}\ \frac{\rho_s}{\rho_g}}$$

Barring any variations in "k" due to other factors, equation (3.12) suggests that slip velocity is directly proportional to solid velocity at large transport velocities and low concentrations.

With the above arguments in mind the observed trends in the concentration-slip velocity diagrams can be explained mathematically as follows.

At constant solid flux (Φ_s) the rate of change of solid velocity with concentration is given by

$$\frac{\partial V_s}{\partial C} = -\frac{\Phi_s}{C^2} \tag{3.13}$$

writing

$$\frac{\partial V_r}{\partial C} = \frac{\partial V_r}{\partial V_s} \cdot \frac{\partial V_s}{\partial C}$$

and from eqn. (3.12)

$$\frac{\partial V_r}{\partial C} = -k\frac{\Phi_s}{C^2} \tag{3.14}$$

From equation (3.14) it is clear that at a constant solid flux, the rate of decrease in slip velocity with concentration, increases with decreasing concentration or increase in solid velocity. This should explain the observation (4) mentioned earlier.

As the transport velocity is reduced, the solid-wall friction becomes less significant. When the transport velocity approaches almost lower limit, slip velocity is governed solely by the effect of concentration. This explains the observation (6) mentioned earlier.

Having determined the effect of transport velocity on slip velocity due to solid-wall friction qualitatively, it is proposed to investigate the quantitative relationship between them. Equation (3.12) suggests that slip velocity due to solid-wall friction is directly proportional to solid velocity. The measured slip velocity in cocurrent transport experiments includes the sum total of the effects of concentration and transport velocity. Based on momentum balance, if the total energy loss is broken into energy loss due to effect of transport velocity (wall friction), and effect of concentration (solid

weight), then the associated squares of slip velocities are additive. This procedure however, is not rigorous in the sense that even though the energy loss is proportional to the square of slip velocity the corresponding proportionality constants need not necessarily be the same for all the terms. A rigorous method of determining the individual effects of transport velocity and concentration involves solving the solid phase momentum equation after substitution of the concentration-slip velocity relationship from the countercurrent experiments. Unfortunately, lack of knowledge of drag coefficient and solid-wall friction factor values makes the task difficult.

$$(V_r^2)_{friction} = V_r^2 - (V_r^2)_{concentration} \tag{3.15}$$

The contribution of effect of concentration is already known from the countercurrent low transport velocity data.

Following the above procedure the slip velocity due to solid-wall friction was plotted against solid velocity for some of the tests (Appendix G). Results with 375μ steel shot in 12.7mm tube are presented in Fig. 3.8. According to equation (3.12) a linear relationship between these two is predicted, provided the parameter "k" remains constant. Fig. 3.8 suggests that the slip velocity due to solid-wall friction indeed increases with solid velocity. Although the dependence is linear at large solid velocities, at lower range of solid velocities, rate of change of slip velocity decreases. Also, data with different mass flow rates, results in different lines. At a given solid velocity slip velocity is smaller at higher solid feed rates. What it suggests is that the parameter "k" which includes drag coefficient and friction factor is not a constant but varies with other factors. From these observations it appears that the value of "k" decreases with increasing concentration. In other words, at the same solid velocity solid-wall friction component decreases with increasing concentration. One possible explanation is that the mean free path of solid particles (which signifies the average distance travelled by a particle before it comes into contact with another particle) decreases with increasing concentration. Consequently the relative magnitudes of inter particle collisions to particle wall collisions

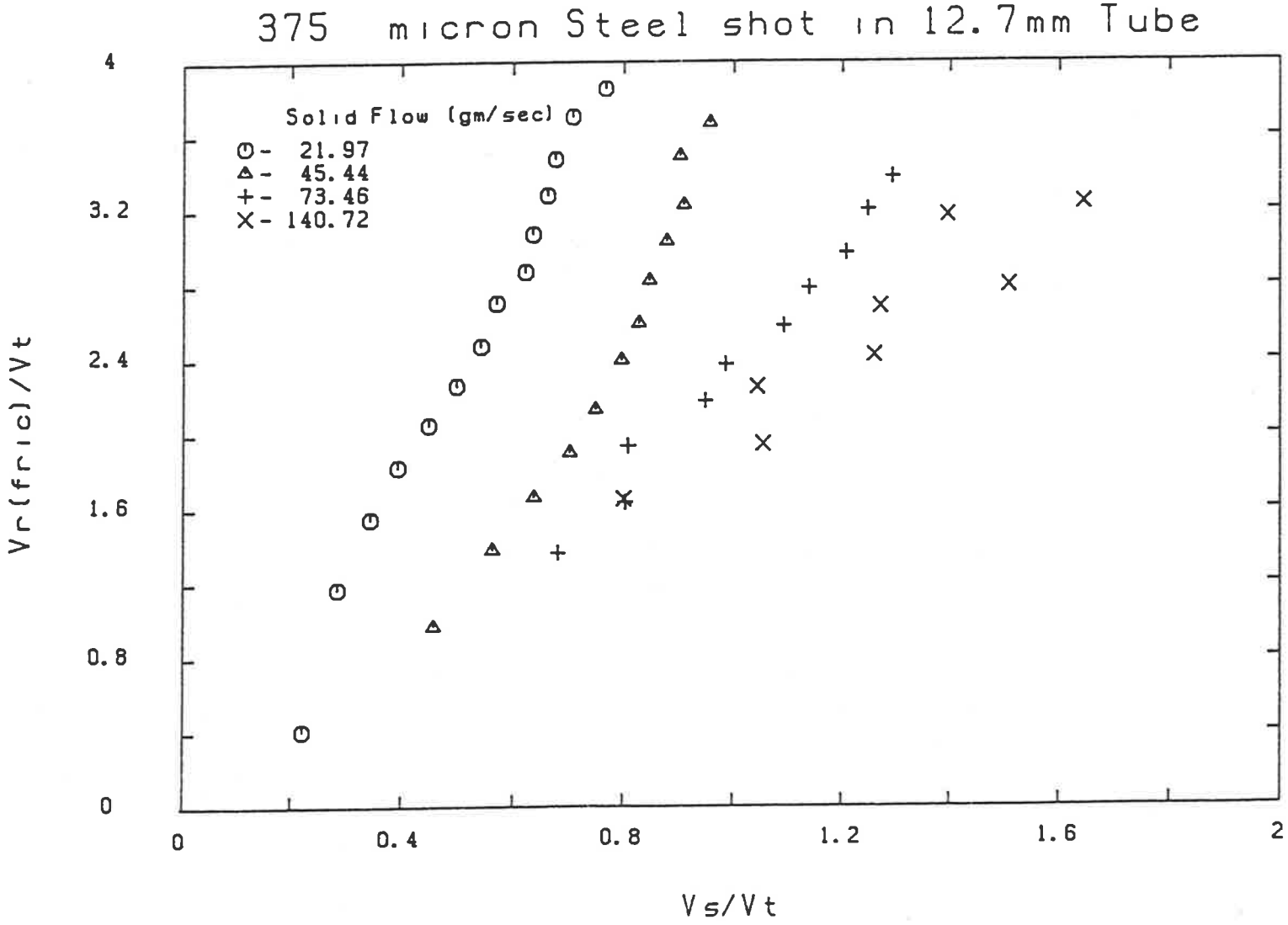

Fig. 3.8 Effect of transport velocity on slip velocity due to solid-wall friction

increases with concentration. Since interparticle collisions merely result in the transfer of momentum from fast moving particles to slow moving particles, the net loss in axial momentum due to such collisions is negligible. On the other hand particles colliding with the stationary transport wall suffer considerable momentum loss due to solid-wall friction. An increase in particle concentration results in fewer solid-wall collisions, hence smaller slip velocities.

The ratio of slip velocity due to solid-wall friction, to solid velocity was plotted against solid volumetric concentration for 375μ steel shot in 12.7mm tube (Fig. 3.9). The trend clearly indicates that the parameter "k" decreases with increasing concentration.

The parameter "k" can be evaluated (equation 3.12) from knowledge of the solid-wall friction factor (f_s), drag coefficient (C_D) and the system properties. The solid-wall friction factor was derived from the pressure drop and solid velocity measurements. The drag coefficient which is a function of particle Reynolds number is derived from the standard drag coefficient-Reynolds number relationship. "k" values calculated from the above procedure were compared with the observed values (Fig. 3.10). The scatter about the correspondence line is large. Of the 900 data points analysed only 300 points are within the $\pm 25\%$ confidence limits. One possible source of error is in the evaluation of drag coefficient. Reddy & Pei (1969), based on the experiments with glass spheres (100 to 300μ size range) in 100mm diameter tube, indicate that the standard drag coefficient is altered by the change in the turbulent flow structure due to the presence of the solids. Also the friction factor term could be another source of error, which is calculated based on the assumption that the frictional loss due to air is unaffected by the presence of the solids.

Considering the above observations, it is felt that the slip velocity due to solid-wall friction is best correlated with the pertinent dimensionless groups such as loading ratio (R), gas velocity to particle terminal velocity ratio (V_g/V_t), particle to tube diam-

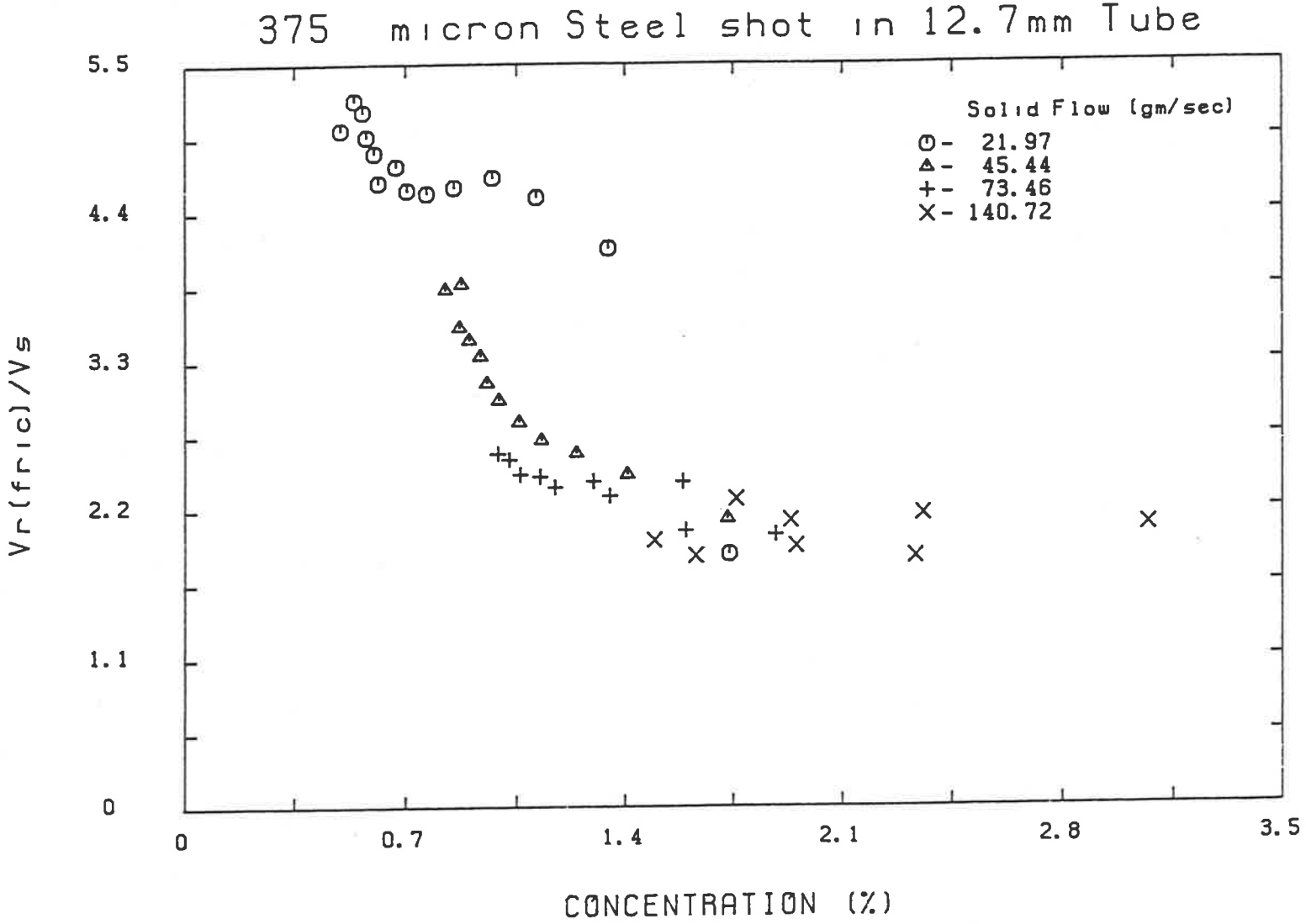

Fig. 3.9 Effect of concentration of parameter "k"

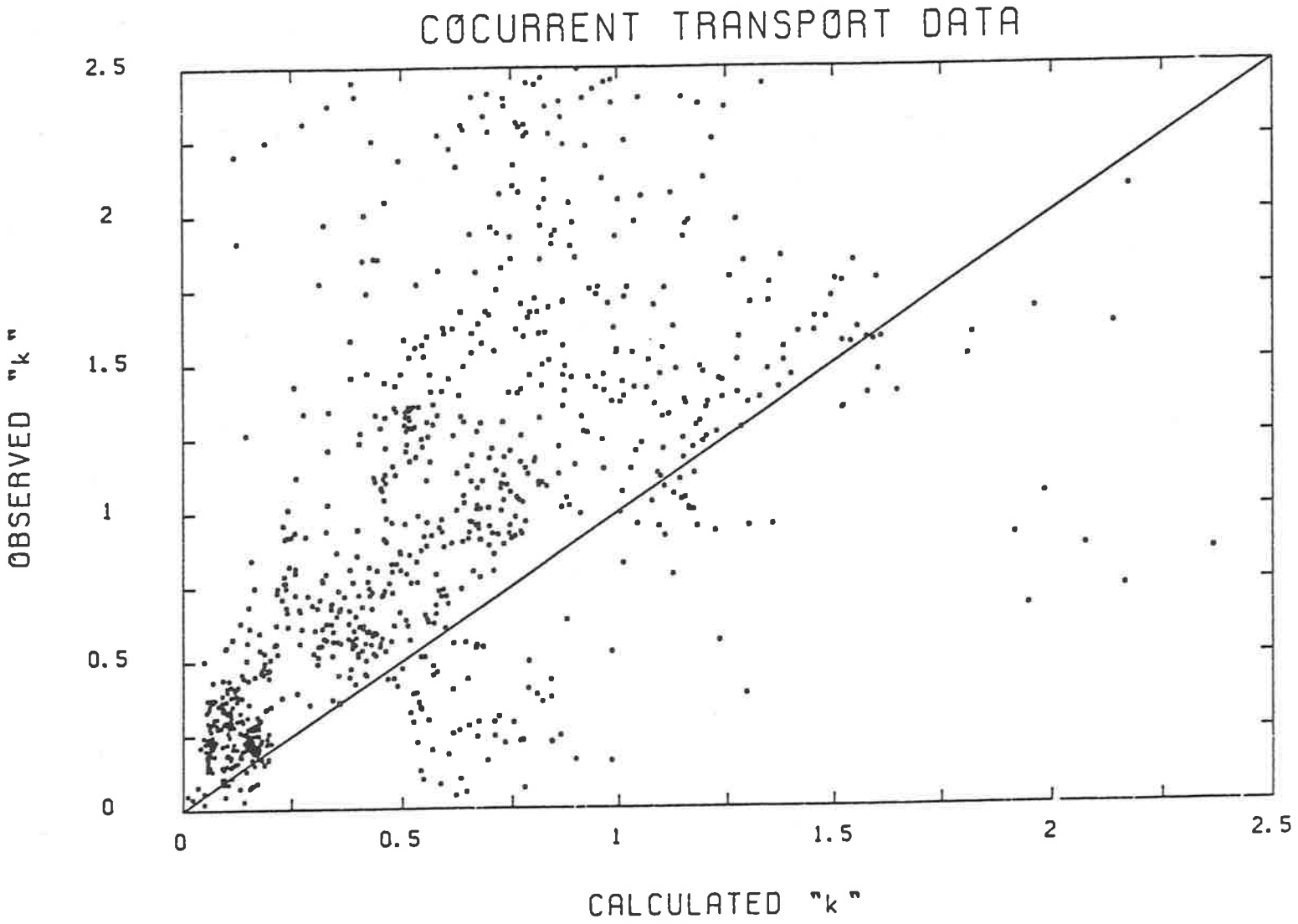

Fig. 3.10 Estimation of parameter "k" from momentum equation

eter ratio (D_p/D_t) and solid to air density ratio (ρ_s/ρ_f). Experimental data consisting of about 1000 observations from 24 tests with six different particles in four test sections were analysed. The following correlation was obtained from the method of multiple regression of the variables.

$$\left(\frac{V_r}{V_t}\right)_{friction} = 0.011\,(R)^{-0.1}\left(\frac{V_g}{V_t}\right)^{1.34}\left(\frac{D_p}{D_t}\right)^{0.56}\left(\frac{\rho_s}{\rho_g}\right)^{0.68} \tag{3.16}$$

where

R is the Loading ratio

The predicted values of slip velocity were plotted against observed values for all tests (Fig. 3.11). The majority of data lies within ±30% confidence limits. Unfortunately test of correlation(3.16) to the systems beyond the range of variables investigated in the present work is not feasible, as reported slip velocities include the effect of concentration. The correlation suggests that the slip velocity due to solid-wall friction decreases with increasing loading ratio and decreasing gas velocity. At large loading ratios solid volumetric concentration is higher. Hence, smaller solid-wall frictional loss. An increase in gas velocity increases solid velocity thus increasing solid-wall frictional loss. The correlation also suggests that solid-wall frictional loss increases with decreasing tube diameter. When the tube diameter is small the number of particle wall collisions increases thus increasing the energy loss due to such collisions.

3.9.3 Comparison with Existing Data

Several investigators have studied the flow of solids in vertical transport lines. A summary of some of the important works is presented in Table (3.1). The varied measurement techniques, system details, and the range of parameters studied make the task of comparison difficult. However, the majority of the works are confined to very low concentrations (less than 1%) and high transport velocities, excepting the works of Yerushalmi & Cankurt (1978, 1979), Yousfi & Gau (1974). While some workers aimed at correlating gas velocity to solid velocity, others have attempted to correlate slip velocity

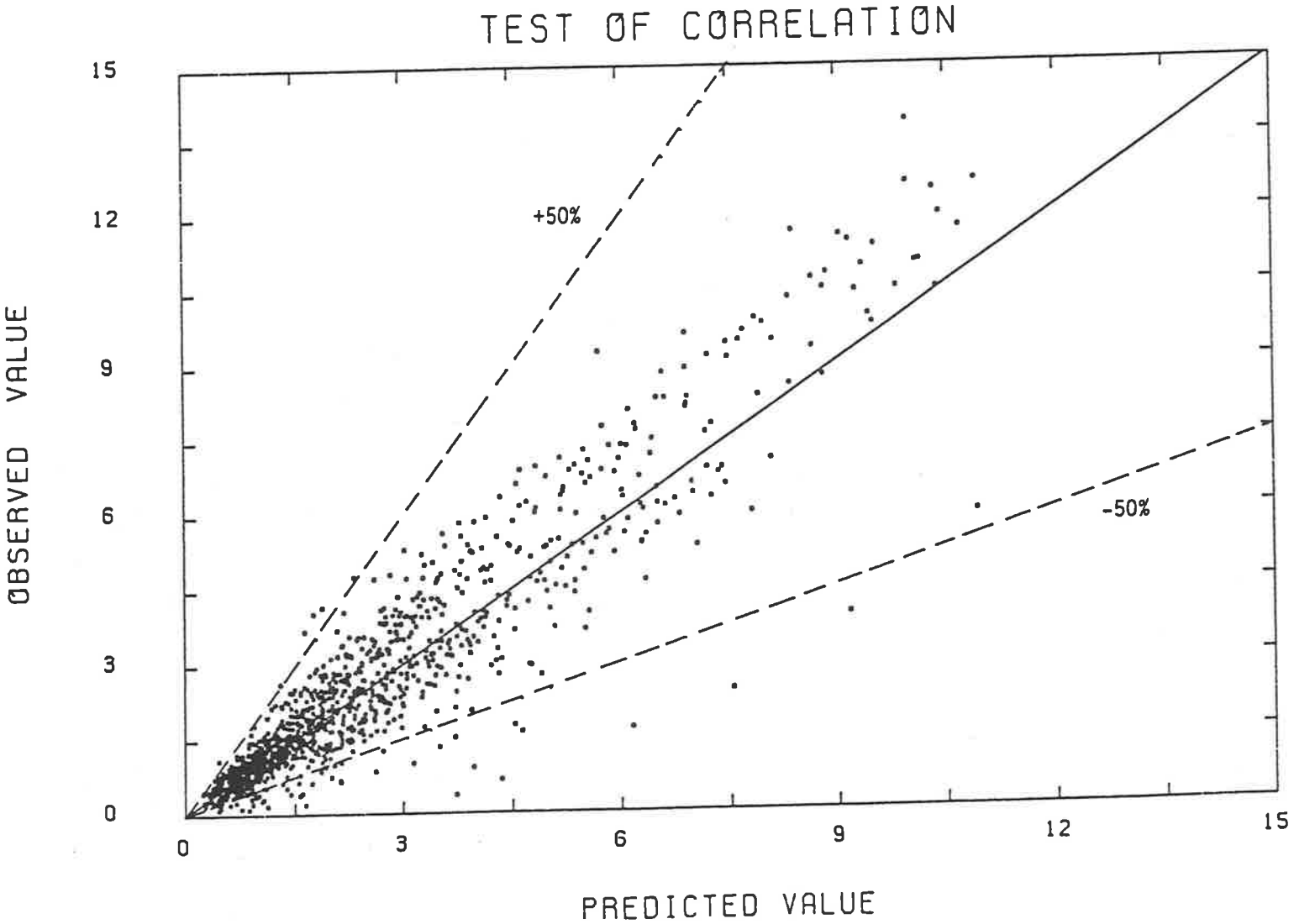

Fig. 3.11 Correlation of slip velocity due to solid-wall friction

TABLE 3.1 SUMMARY OF VERTICAL PNEUMATIC TRANSPORT INVESTIGATIONS

Reference	Materials used	Particle size (u)	Particle density (gm/cc)	Terminal velocity (m/s)	Tube diameter (mm)	Range of gas velocities (m/s)	Max. level of concentration studied (%)	Solid velocity measurement technique	General observations	Friction factor studies
Belden & Kassel (1940)	catalyst	963 1950	0.86 0.98	3.49 6.55	12 26 steel	4-15	1.0*	-	Solid velocity is calculated from particle terminal velocity. No direct measurements were made.	A combined friction factor is correlated to mass velocity ratio term and gas Reynolds number.
Birchenough & Mason (1976)	Alumina powder	20	3.75	.045	49.4 glass	17-56	0.05*	LDV Technique	Slip velocity increases in linearly with loading ratio at a given gas velocity	
Capes & Nakamura (1973)	Glass Steel Rape Seed	470 1080 1780 2900 256 535 1200 2340 1780 3400	2.47 2.9 2.9 2.86 7.51 7.85 7.7 7.7 1.08 0.91	3.54 7.97 11.27 14.94 4.01 8.28 14.93 22.1 6.49 8.98	75 Steel	3-18	3.0	Isolation Technique	Solid velocity increases linearly with gas velocity. $V_g / V_s > 1$ for all the runs. The slope increases with increasing particle terminal velocity.	Negative friction factors are reported. Friction factor is inversely proportional to solid velocity.
Dixon (1976)	Acralyic Alkathene	3280 3600	1.18 0.921	10.1 9.35	47.6	10-30	0.6*	-	Slip velocity at minimum pressure drop point is derived to be 1.41 times particle terminal velocity	Friction-factor is reported to be a constant value (.001)
Doig & Roper (1967)	Glass	300 750	2.5 2.5	2.26 5.45	43 Glass	5.5 - 10.5	0.6*	Pitot tube	Particle and air velocity distributions were measured.	

TABLE 3.1 (CONTD.) SUMMARY OF VERTICAL PNEUMATIC TRANSPORT INVESTIGATIONS

Reference	Materials used	Particle size (u)	Particle density gm/cc	Terminal velocity (m/s)	Tube diameter (mm)	Range of gas velocities (m/s)	Max. level of concentration studied (%)	Solid velocity measurement technique	General observations	Friction factor studies
Gopichand et al (1959)	Catalyst Sand Silica gel Wheat	26 126 196 392 750	0.89 3.1 1.55 1.55* 1.44	.019 0.985 1.0 2.07 3.5	12.7 Steel	6-40	-	Isolation technique	Voidage is correlated to loading ratio and gas velocity normalised with terminal velocity	A friction factor based on total pressure drop and and gas velocity head is correlated to loading ratio, voidage, gas velocity and diameter ratio.
Hariu & Molstad (1949)	Sand Catalyst	213 274 357 503 110	2.64 2.64 2.64 2.74 .977	1.59 2.12 2.82 3.95 0.29	6.78 13.5 Glass	5.5-12.5	3.75	Isolation technique	Observations include acceleration effects Drag co-efficient is correlated to particle Reynolds number.	The order of magnitude of friction factor, after correcting for acceleration is about .001
Jodlowski (1976)	Polyethylene Wheat Sand PVC	3640 4060 105 100	0.96 1.27 2.58 1.4	9.6 11.8 0.62 0.34	31.6 49.5 78.9 Steel	10-25	2.5	Cine Camera and Radio active tracer techniques	Solid velocity is a linear function of gas velocity.	A friction factor based on the combined frictional pressure drop components of gas and solid phases and gas velocity head is defined. This friction factor is correlated to gas Froude number and particle concentration.
Jones et al (1967)	Glass Alumina Zircon Silica Steel Shot	Range 200-765	Range 2.5-7.6	-	7.75 10.21 22.1 Steel	-	0.6	-	A friction factor is defined on the basis of pressure drop due to presence of solids and gas velocity head.	A linear relationship between logarithmic values of friction factor and loading ratio is obtained.

TABLE 3-1 (CONTD.) SUMMARY OF VERTICAL PNEUMATIC TRANSPORT INVESTIGATIONS

Reference	Materials used	Particle size (μ)	Particle density gm/cc	Terminal velocity (m/s)	Tube diameter (mm)	Range of gas velocities (m/s)	Max. level of concentration studied (%)	Solid velocity measurement technique	General observations	Friction factor studies
Jotaki et al (1978)	Polyetnylene pellets	3340	0.57	5.8	41.2 52.6 66.8 78.3 100	8-50	4.3*	Photographic technique	Solid to gas velocity ratio is derived from pressure drop measurements	Friction factor is constant for each tube, and its value increases with increasing tube
Kmiec et al (1978)	Turnip Seed Silica gel	2240 1340 1100 683	0.802 0.802 1.154 1.154	6.44 4.4 4.67 3.08	40 PVC tubes	7-15	-	Isolation Technique	Negative friction factors are reported for Chamber section of the apparatus at low gas velocities	Solid wall friction factor is found to decrease in the increasing solid velocity. size.
Konno & Satio (1969)	Glass Copper HairyVetch Millet	120 320 520 1050 120 270 530 3250 1440	2.5 8.9 1.35 1.44	0.95 2.53 4.10 8.0 2.2 5.0 9.8 10.0 7.13	26.5 46.8	8-20	0.6*	Photographic method	Slip velocities are almost equal to single particle terminal velocities. Concentration and solid velocity distributions are studied.	Solid-wall friction factor is inversely proportional to particle Froude number.
Maeda et al (1974)	Polyethylene Vinyl Chloride Glass Glass	100 150 120 300	0.95 1.42 2.93 2.93	0.25 0.59 0.80 2.60	8 10 12 20 Acralyic	1-40	3.0	Photographic technique	Slip velocity increases linearly with gas velocity at large gas velocities. Slip velocities are higher in smaller tubes.	Friction factor for a given particle and tube is constant and its value decreases with increasing tube diameter.
Mehta et al (1957)	Glass Glass	36 97	2.53 2.53	0.096 0.41	12.7 Iron	3-27	2.5*	Isolation technique	Particle velocity increases linearly with gas velocity. Reproducibility was reported to be poor.	A mixture friction factor is defined based on total pressure drop and mixture velocity. The friction factor is correlated to gas Reynolds number.

TABLE 3-1 (CONTD.) SUMMARY OF VERTICAL PNEUMATIC TRANSPORT INVESTIGATIONS

Reference	Materials used	Particle size (u)	Particle density gm/cc	Terminal velocity (m/s)	Tube diameter (mm)	Range of gas velocities (m/s)	Max. level of concentration studied (%)	Solid velocity measurement technique	General observations	Friction factor studies
Reddy & Pei (1969)	Glass	100 150 200 270	2.59 2.59 2.59 2.59	0.577 1.01 1.45 2.06	100 glass	7-14	0.1*	Photographic technique	Particle and gas velocity profiles were studied. Slip velocity is correlated to loading ratio.	
Shimizu et al (1978)	Copper	174 107 98 92 60 54 46.5	8.92	3.01 1.68 1.5 1.38 0.75 0.64 0.5	28 Acralyic pipe	5-25	0.1	-	The ratio of total pressure drop to gas-wall frictional loss is a linear function of loading ratio	A reduction in frictional pressure drop is observed at lower loading region for small particles.
Stemerding (1962)	Catalyst	65	1.6	0.19	51 Steel	2-20	10*	-	From pressure drop measurements gas to solid velocity ratio is reported to be constant.	Solid-wall friction factor is constant for the system, and is equal to .048.
Tomita et al (1980)	Cement	30	2.56	0.07	41 66.8	10-40	2.3*	-	It is assumed that there is no slip between solid and air. Compressible flow conditions are analysed.	Friction factor based on additional pressure drop and gas velocity head is derived for compressible flow conditions. Friction factor decreases with gas Froude number.
Van Zuilichem et al (1973) & (1980)	Wheat Polypropylene	4600 4000	1.39 0.85	13.2 9.5	53 81 130	10-30	3*	Radio active tracer method	Slip velocity increases linearly in the gas velocity. Slip velocities are larger in smaller tubes.	Friction factor for polypropylene decreases with increasing gas Froude number. Its value tends to be a constant with increasing mass flow rate of solids.

TABLE 3-1 (CONTD.) SUMMARY OF VERTICAL PNEUMATIC TRANSPORT INVESTIGATIONS

Reference	Materials used	Particle size (μ)	Particle density (gm/cc)	Terminal velocity (m/s)	Tube diameter (mm)	Range of gas velocities (m/s)	Max. level of concentration (%)	Solid velocity measurement	General observations	Friction factor studies
Vogt & White (1949)	Sand	203	2.66	1.51	12.7	15-60	4*	0	Ratio of total pressure to pressure drop due to air is correlated to loading ratio, density ratio and diameter ratio.	
		330	2.63	2.59						
		434	2.6	3.39						
		729	2.56	5.4						
	Steel Shot	419	7.21	6.35						
	Clover Seed	1170	1.23	5.1						
	Wheat	4010	1.28	11.77						
Yausfi & Gau (1974)	Glass	118	2.74	0.765	38	2-8	20	Isolation method	Slip velocity is found to be several fold higher than terminal velocity for fine particles. For coarse particles slip velocities are of the order of terminal velocity.	Friction factor is correlated to solid Froude number. Negative friction factors are reported at low Froude numbers. Friction factor is about .0015 at large Froude numbers.
		143	2.74	0.99						
		183	2.74	1.36						
	Polystyrene	290	1.06	1.18	50					
	Catalyst	20	0.868	0.01						
		55	0.85	0.078						
Yerushalmi (1976)	Catalyst	60	0.88	0.076	76	1.7-4.5	25	-	Slip velocities are several fold larger than particle terminal velocities. Solid velocity is derived from pressure drop data.	Large slip velocities are attributed to formation of clusters of particles whose terminal velocity exceeds single particle terminal velocity.
(1978)	FCC	49	1.07	0.078	150	1.7-7.6	10	-	Slip velocity increases with concentration. At large concentrations and low solid velocities solid-wall friction is not significant.	
	Dicalyte	33	1.66	0.055						

* Concentration levels are estimated from loading ratios.

to gas velocity or loading ratio. Very rarely are concentration values reported. Lack of information on corresponding solid flow rates makes the derivation of variables of interest difficult.

3.9.3.1 Concentration-Slip Velocity Maps

Only Birchenough's (1976) data permitted derivation of concentration-slip velocity map, similar to those presented in this work. Their concentration-slip velocity plot (Fig. 1.6) indicates trends similar to those obtained in the present work, significance of which is already explained.

3.9.3.2 Gas-Solid Velocity Relationship

The works of Capes & Nakamura (1973), Jotaki et al (1978), Jodlowski (1976), Mehta et al (1957), Konno & Satio (1969) and Wheeldon et al (1980) indicate a linear relationship between gas and solid velocities. Except Konno & Satio (1969), others report that the rate of change of gas velocity with solid velocity ($\partial V_g/\partial V_s$) is greater than one. This clearly indicates that slip velocity increases with transport velocity. Capes & Nakamura (1973) include data corresponding to very low transport velocities, where the concentration effect dominates. They rightly point out that large slip velocities in this region are due to particle recirculation, whereas solid-wall friction accounts for large slip velocities at higher transport velocities.

In order to compare these trends with the present data, solid velocity was plotted against gas velocity for tests with 644μ glass beads in all the four tubes (Fig. 3.12). From these plots it was observed that in all the four cases the average slope ($\partial V_g/\partial V_s$) is greater than one, and its value decreases with increasing tube diameter.However it should be noted that in the case of small tubes, at large gas velocities, higher solid flow rates result in higher solid velocities. But in the case of large tubes no such dependence on solid flow rate is observed. This could be explained as follows. At a given gas velocity, increasing solid flow rate results in higher concentrations, thus decreasing the solid-wall

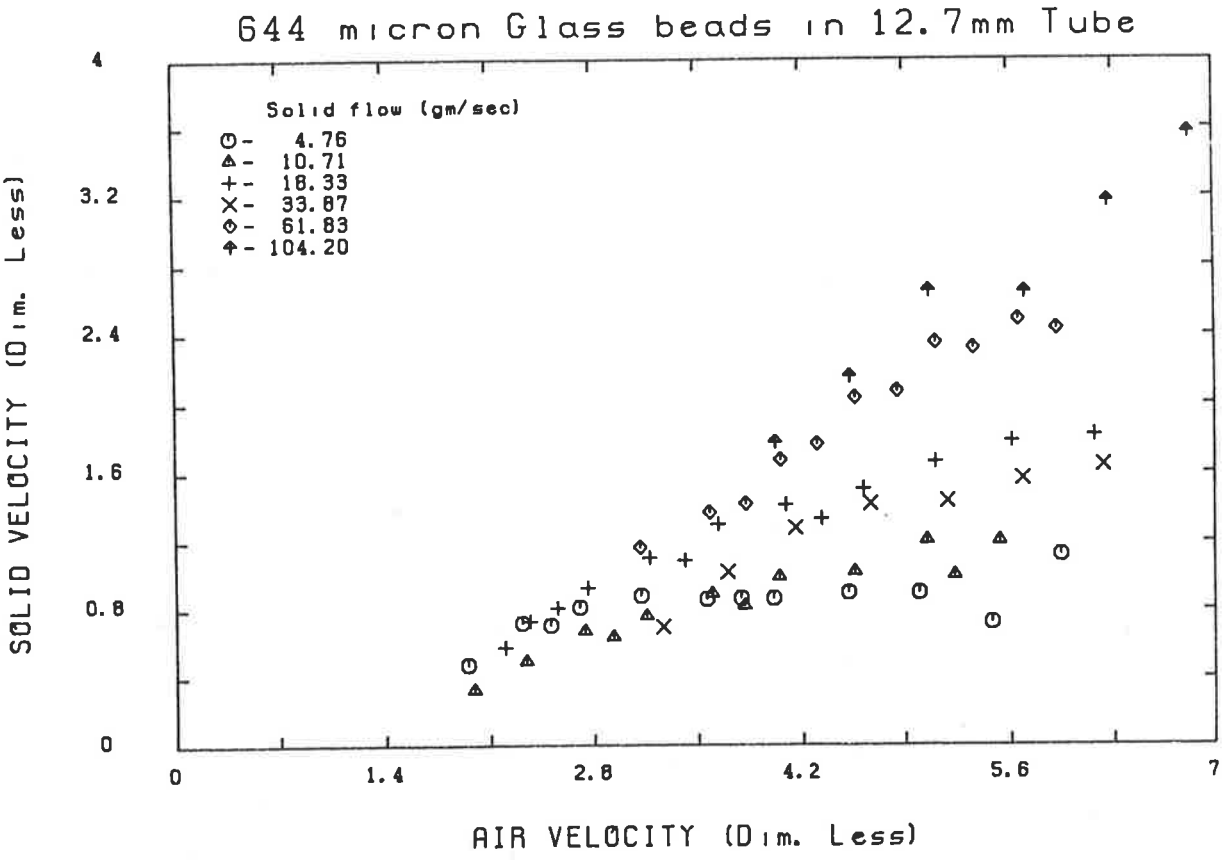

Fig. 3.12(a) Gas-solid velocity map

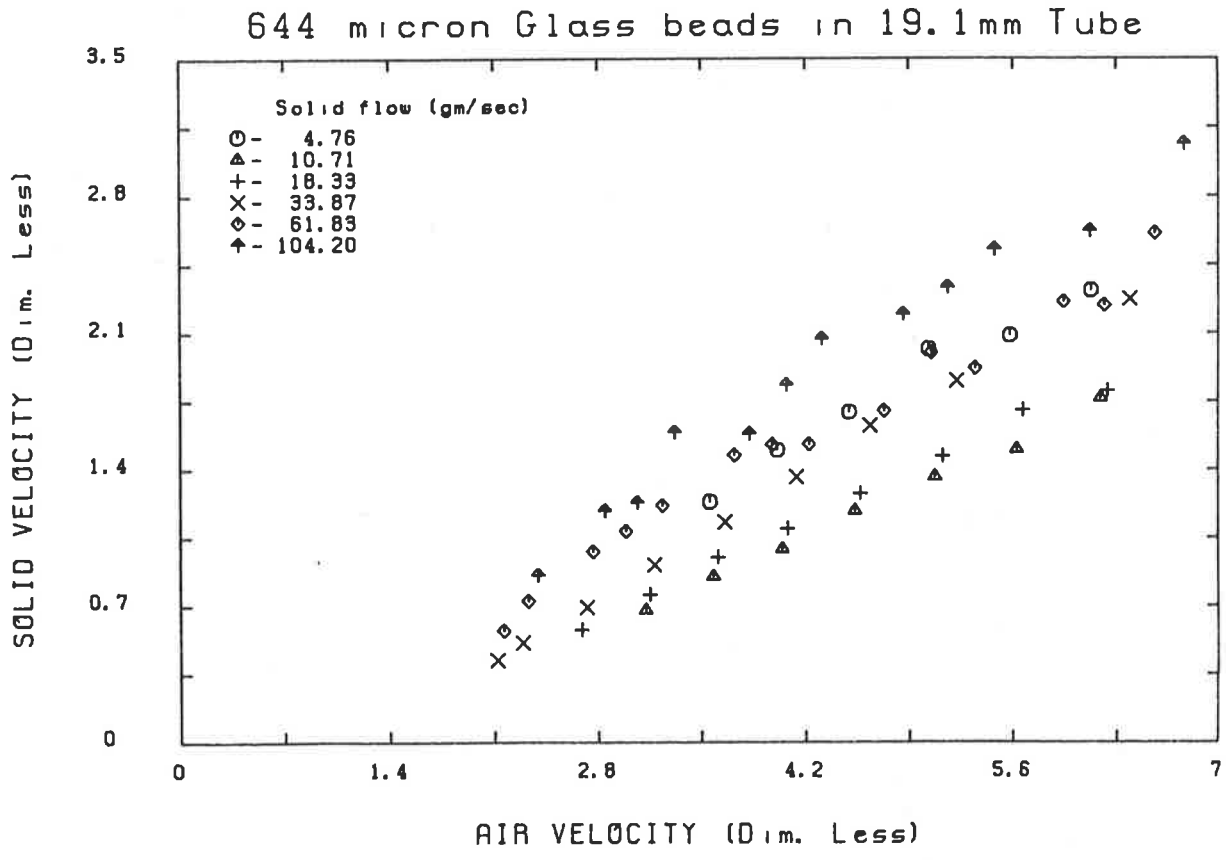

Fig. 3.12(b) Gas-solid velocity map

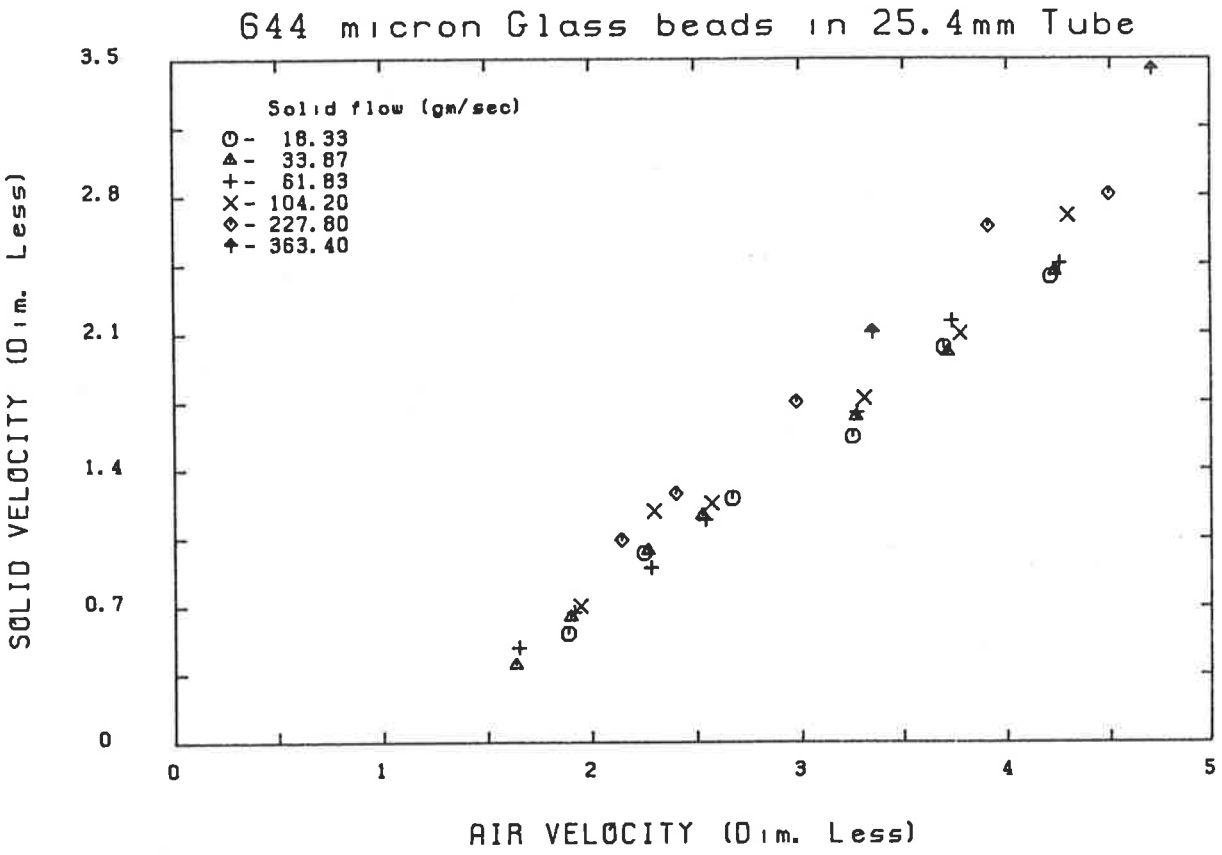

Fig. 3.12(c) Gas-solid velocity map

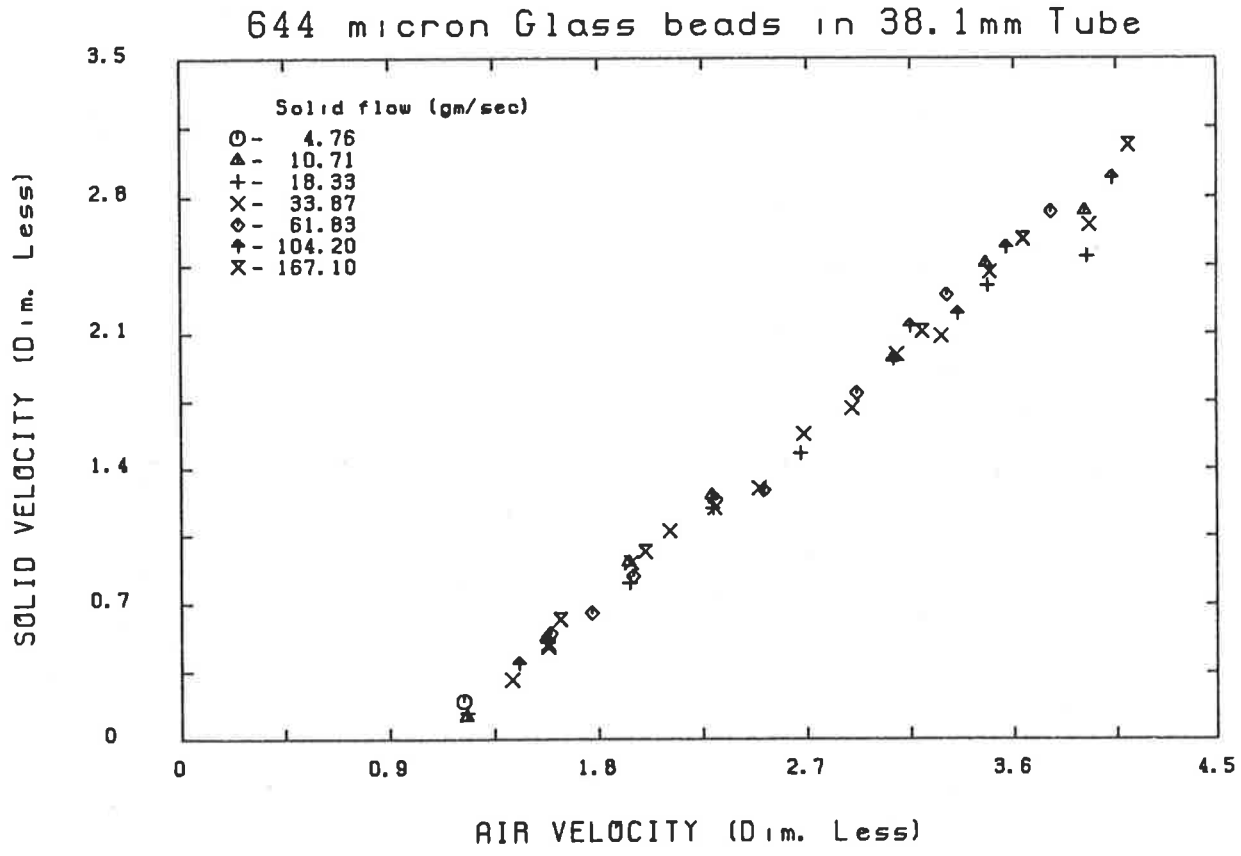

Fig. 3.12(d) Gas-solid velocity map

frictional loss. This in turn results in lower slip velocities, hence solid velocities are higher. This effect is predominant in smaller tubes where solid-wall friction is high. In the case of large tubes this effect is less significant as solid-wall frictional loss is small even at low concentrations. The tube sizes investigated by Capes & Nakamura (1973), Jotaki et al (1978) and Jodlowski (1976) ranged from 40mm to 100mm in diameter. As the effect of concentration on slip velocity in these tubes is weak no noticeable change in solid velocity with mass flow rate is observed. It therefore appears that presentation of data in terms of concentrations and slip velocities can be more meaningful in visualising the individual effects of concentration and transport velocity rather than in terms of gas and solid velocities.

3.9.3.3 Solid-wall Friction Factor

Often, the energy loss due to solid-wall friction is analysed analogous to single phase flow situations. However, the definition of friction factors varied. While some workers defined friction factor based on total pressure drop and mixture velocity head, others used pressure loss due to frictional loss of both the phases and gas velocity head. Recent works define friction factor as follows.

$$4\frac{f_s}{D_t} = \frac{(\Delta P)_{fs}}{\frac{1}{2}C\rho_s V_s^2} \tag{3.17}$$

The above definition is arrived at by treating the two phases separately. The frictional pressure drop due to the solid phase is assumed to be same as when a single phase fluid of density ($C\rho_s$) flows along the tube at mean solid phase velocity. Derivation of the above friction factor requires the knowledge of total pressure loss, pressure loss due to static head of solids and gas-wall friction.

A summary of friction factor correlations based on the above definition is presented in Table (3.2). While the works of Konno & Satio (1969), Capes & Nakamura (1973), Swaaij (9170), Reddy & Pei (1969) indicate that friction factor is an inverse

function of solid velocity, works of Stemerding (1962), Hariu & Molstad (1949), Van Zuilichem (1980) and Yousfi & Gau (1974) suggest that friction factor is almost constant. While Jotaki et al (1978) based on their experiments with tubes ranging from 40mm to 100mm in diameter report that friction factor increases with increasing tube diameter, results of Maeda et al (1974) with tubes ranging from 8mm to 20mm in diameter show quite opposite trend.

Analysis of data of the present work indicated no significant dependence on solid velocity. However, there appears to be some strong dependence on concentration at very low concentrations. Fig. 3.13 indicates that friction factor decreases rapidly with increasing concentration up to about 0.5% and levels off to almost a constant value at larger concentrations. In this region friction factor varied from 0.0005 to 0.0015. These values are of similar magnitude reported in literature (Table 3.2).

Negative friction factors are also obtained especially corresponding to limiting gas velocities where solid velocities are very low. Fig. 3.14 represents friction factor versus particle Froude number data for runs with all the particles investigated in 12.7mm tube. What it shows is that the friction factor is negative at very low Froude numbers and its value increases with increasing Froude number and levels off at a positive value at large Froude numbers. A similar trend was reported by Yousfi & Gau (1974) from their experiments with 20μ and 50μ catalyst particles in 38 and 50mm tubes. Negative friction factors were also reported by Capes & Nakamura (1973), Van Swaaij (1970), and Yousfi & Gau (1974) corresponding to very low solid velocities.

Considering the scatter and uncertainties in determination of friction factor(f_s) reconciliation of the various forms of correlations presented in literature is difficult. Not withstanding possible sources of experimental errors, part of the failure to bring out a unified correlation for solid-wall friction factor similar to single phase flow situations can be attributed to the following uncertainties.

1. Treatment of the solid phase in the transport line as a continuum for the purpose

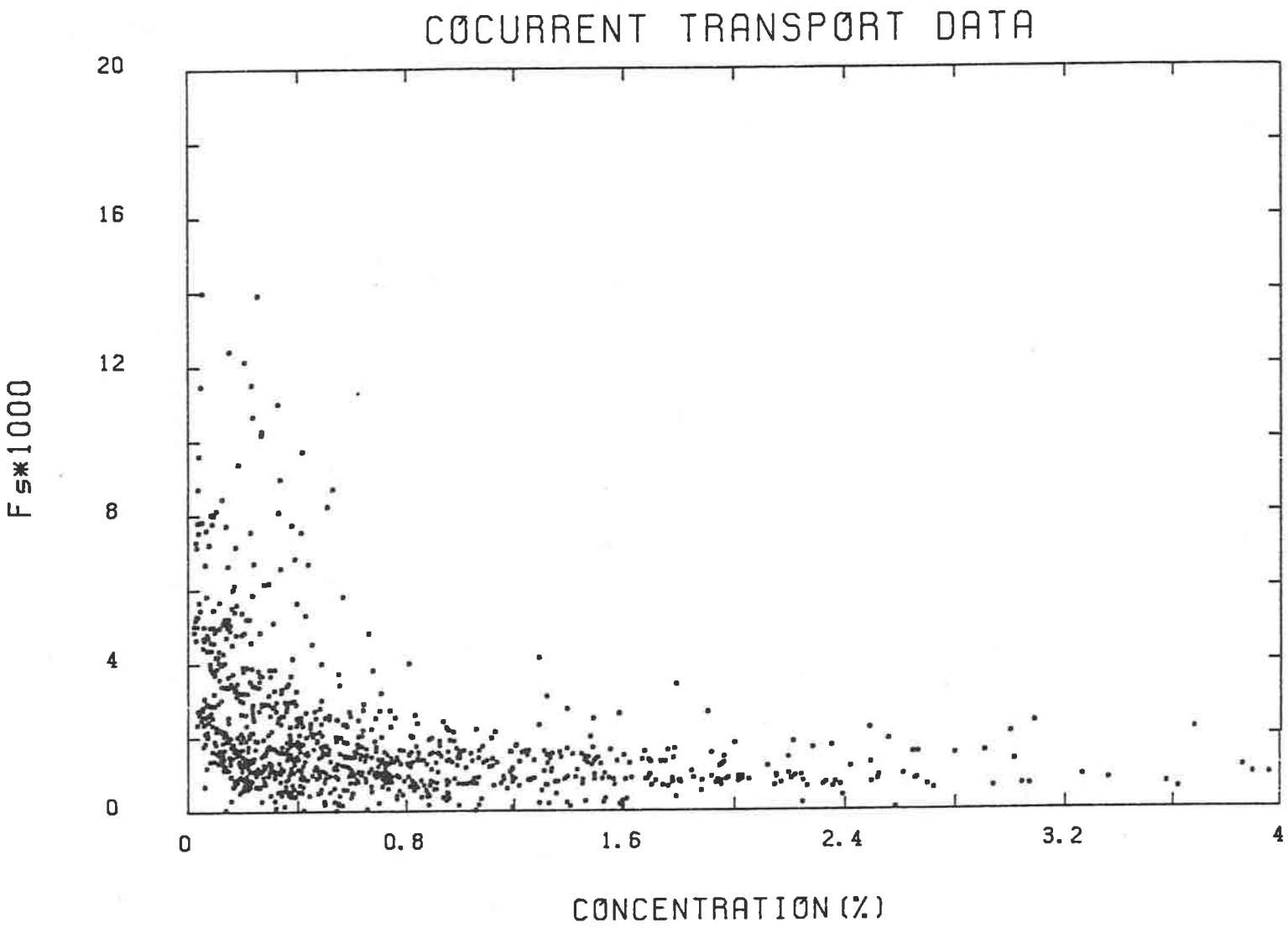

Fig. 3.13 Dependence of solid-wall friction factor on concentration

Table (3.2)

Solid -Wall Friction Factor Correlations

Reference	Correlation
Capes (1974)	$f_s = 0.048 V_s^{-1.22}$
Jotaki (1978)	$f_s = 0.0135\,(D_t - 0.013)$
Khan (1973)	$f_s = 2.66 C_D \left(\frac{V_g}{V_s}\right) \left(\frac{Re}{Fr}\right)_g^{0.5} \left(\frac{D_p}{D_t}\right)^2 \left(\frac{\rho_g}{\rho_s}\right)$
Klinzing (1981)	$f_s = 0.287 U_g^{-1.51} V_t^{0.51} (1 - C)^4 .1$
Kmeic (1978)	$0.0304 V_s^{-0.75}$
Konno (1969)	$f_s = \frac{0.0285}{(Fr^{0.5})_s}$
Maeda (1974)	$f_s = 0.0015$ *to* 0.003
Reddy (1969)	$f_s = 0.046 V_s^{-1}$
Stemerding (1962)	$f_s = 0.003$
Van Swaaij (1970)	$f_s = 0.08 V_s^{-1}$
Van Zuillichem (1980)	$f_s = 0.001$ *to* 0.002
Yousfi (1974)	$f_s = 0.0015$

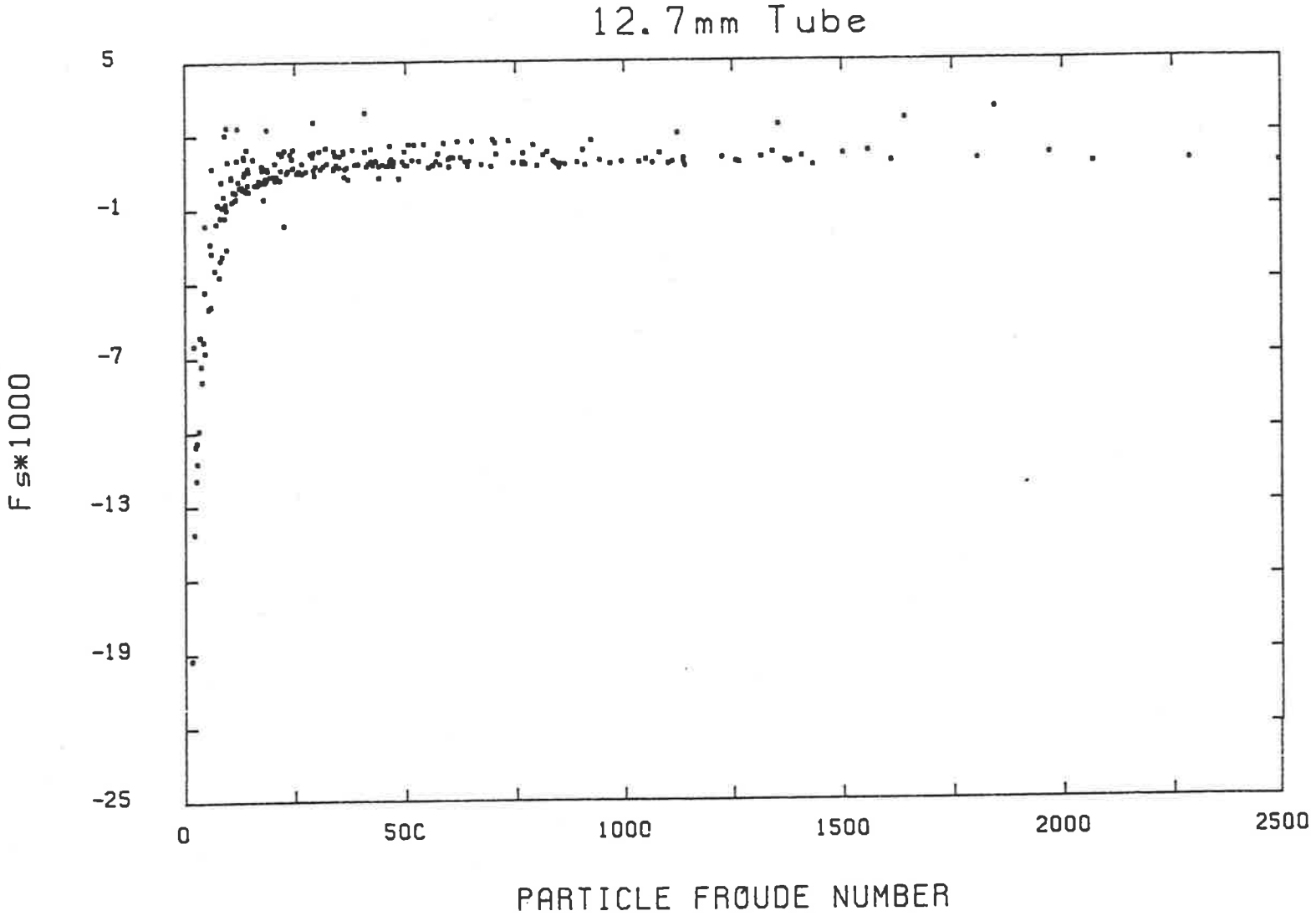

Fig. 3.14 Dependence of solid-wall friction factor on particle Froude number

of determining the frictional losses analogous to gas phase may not be appropriate for all the flow regimes.

2. The solid-wall frictional loss is not determined by direct measurements. Instead, it is inferred from the total frictional loss and gas-wall frictional loss which in itself is not determined with certainty in the presence of solid phase.

Considering the above points it might be worthwhile to investigate the mechanism of solid-wall collisions and the resulting energy losses before attempting to quantify the solid-wall frictional losses. Direct measurement of particle-wall collision flux and radial velocity distributions across the section of the pipe, along with some qualitative observations might be helpful in this regard. Although some preliminary investigations on these aspects were made by Ottjes (1981) and Ribas et al (1980) for horizontal flow situations, no such attempts seem to have been made for vertical transport conditions. These aspects however, are beyond the scope of this work.

3.10 Prediction of Minimum Transport Velocities

In the previous chapter the significance of concentration-slip velocity relationship in explaining choking phenomenon is made clear. It is also mentioned in the introductory remarks of this chapter, that one of the objectives of cocurrent transport experiments is to investigate the extension of countercurrent data to describe forward transport is indeed feasible.

One of the observations from the cocurrent experimental data has been that the concentration-slip velocity relationship at low transport velocities, approach as that of the corresponding countercurrent data, although large deviations occur at high transport velocities. What it suggests is that the information derived from simple countercurrent experimental data is useful in so far as describing the cocurrent transport at very low transport velocities where solid-wall friction is insignificant. Since "choking" is a phenomenon associated with low transport velocities and high concentrations,

the results of countercurrent experiments should prove to be useful in determining the minimum transport velocities for a given system.

In order to substantiate the above arguments, plots of concentration versus superficial air velocity for sand particles in all the four tubes investigated are presented (Fig. 3.15). These plots are similar to the ones predicted from the countercurrent data (Fig. 2.1). The solid lines in Fig. 3.15 correspond to the predicted behaviour based on the concentration-slip velocity relationship derived from countercurrent data. The procedure for calculation of predicted values is already described in the previous chapter. The following observations can be made from these plots.

1. At large gas velocities the predicted values of concentration are lower than the experimental values. This deviation is larger in the case of smaller tubes. This is due to the additional effect of solid–wall friction, which comes into play at large transport velocities.

2. As gas velocity is reduced, the deviation from the predicted curve decreases gradually. At transport velocities approaching the corresponding lower limit, observed values agree well with the predicted values.

3. The predicted curves indicate that choking is characterised by a sudden increase in concentration for small mass flow rates of solids, while at large solid flow rates the process is gradual. This indeed has been confirmed by the experimental results.

4. The limiting gas velocity at which "choking" occurs decreases with decreasing solid flow rate.

From the above observations the significance of countercurrent experiments is established. These simple experiments provide the valuable concentration-slip velocity relationship based on which "choking" velocities can be predicted for a given system. In the design of pneumatic transport equipment specification of minimum transport veloc-

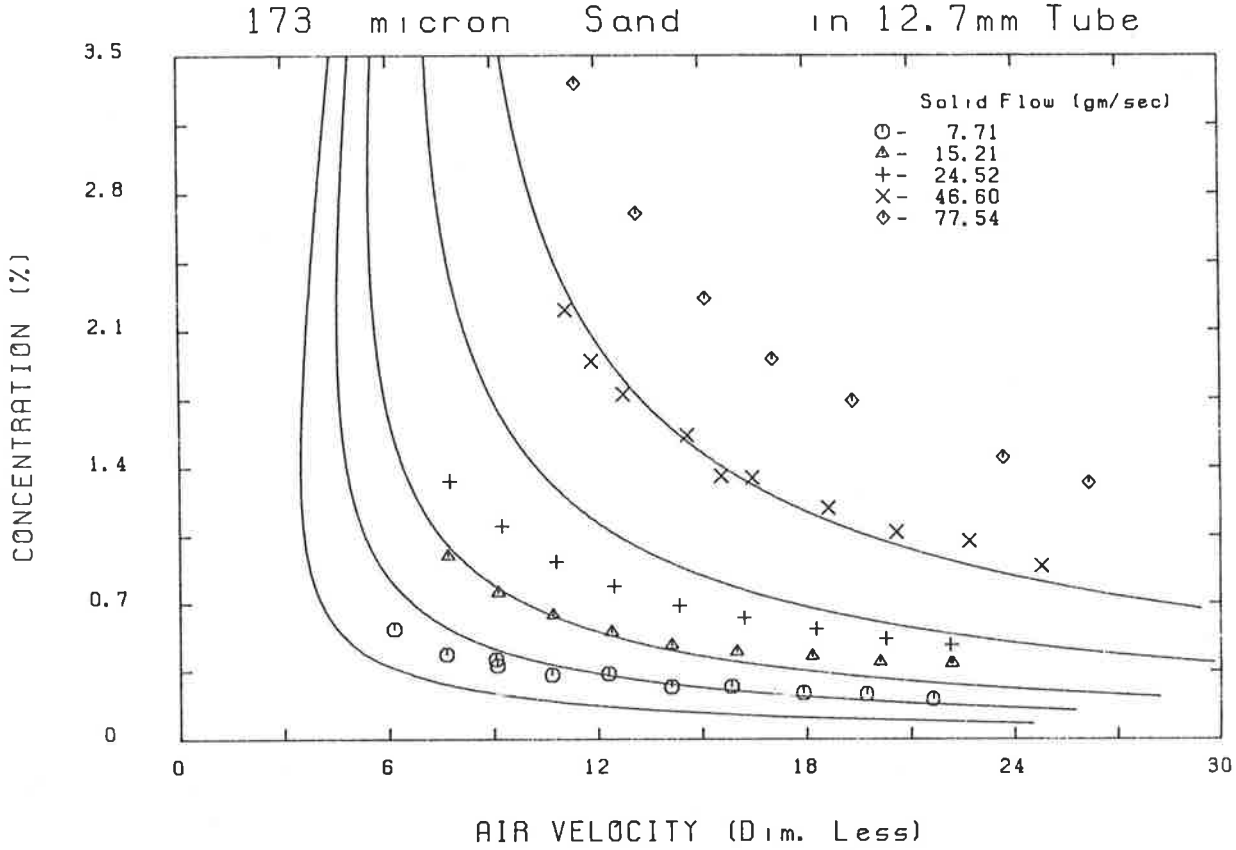

Fig. 3.15(a) Prediction of minimum transport velocity

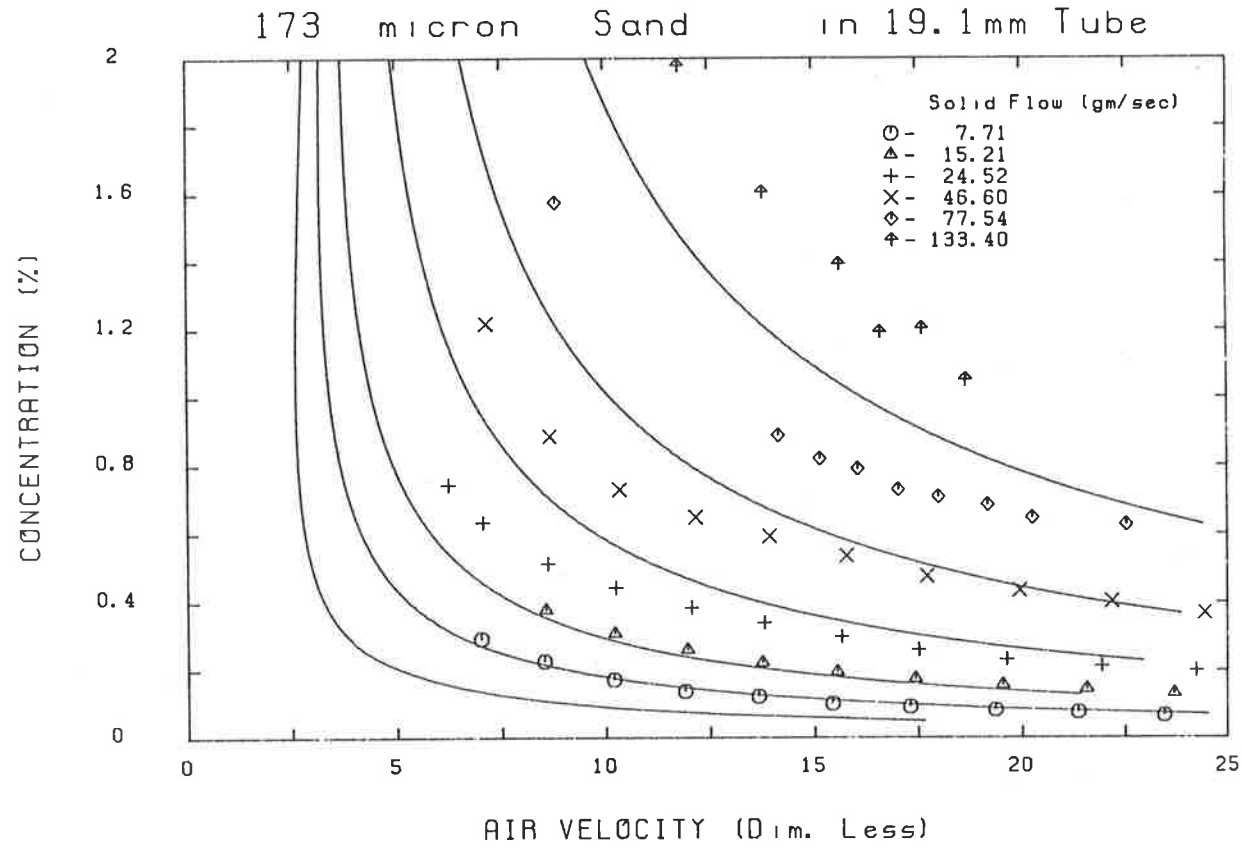

Fig. 3.15(b) Prediction of minimum transport velocity

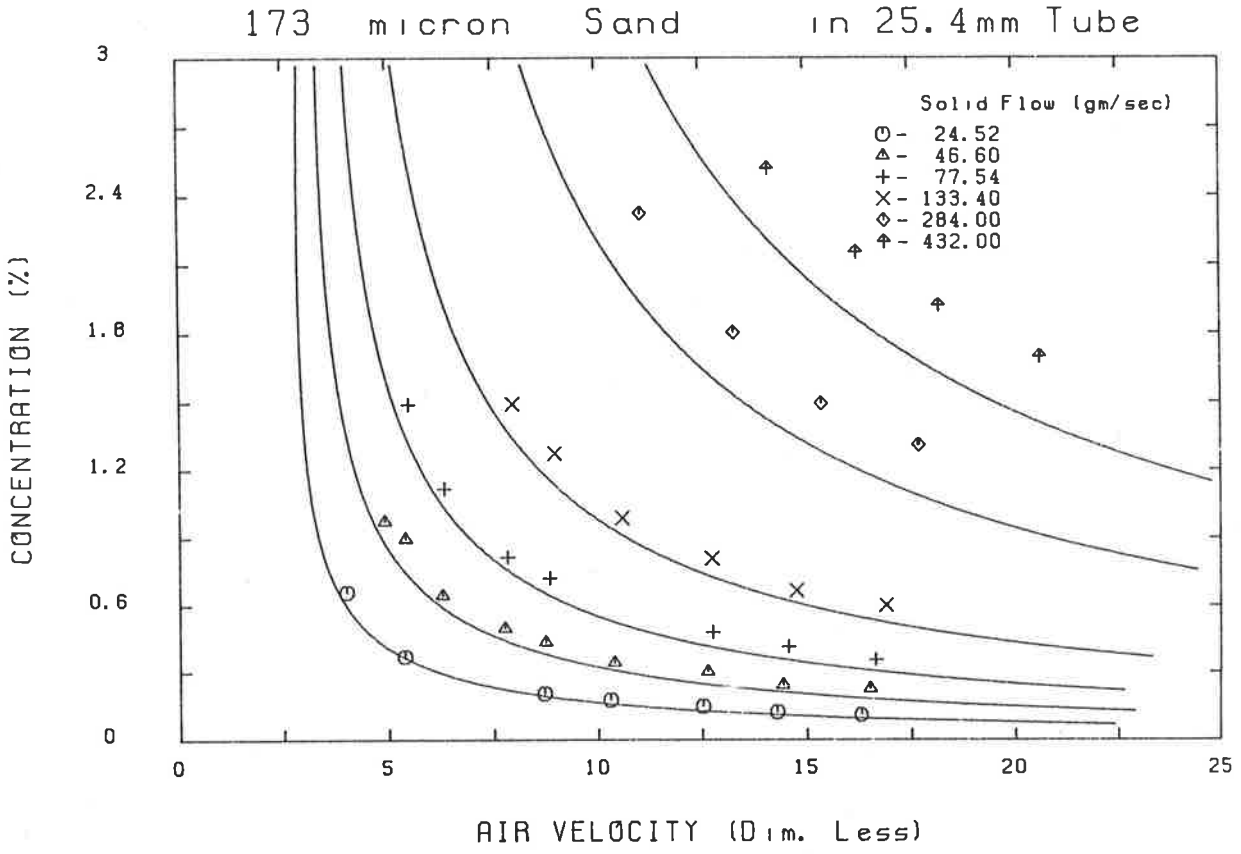

Fig. 3.15(c) Prediction of minimum transport velocity

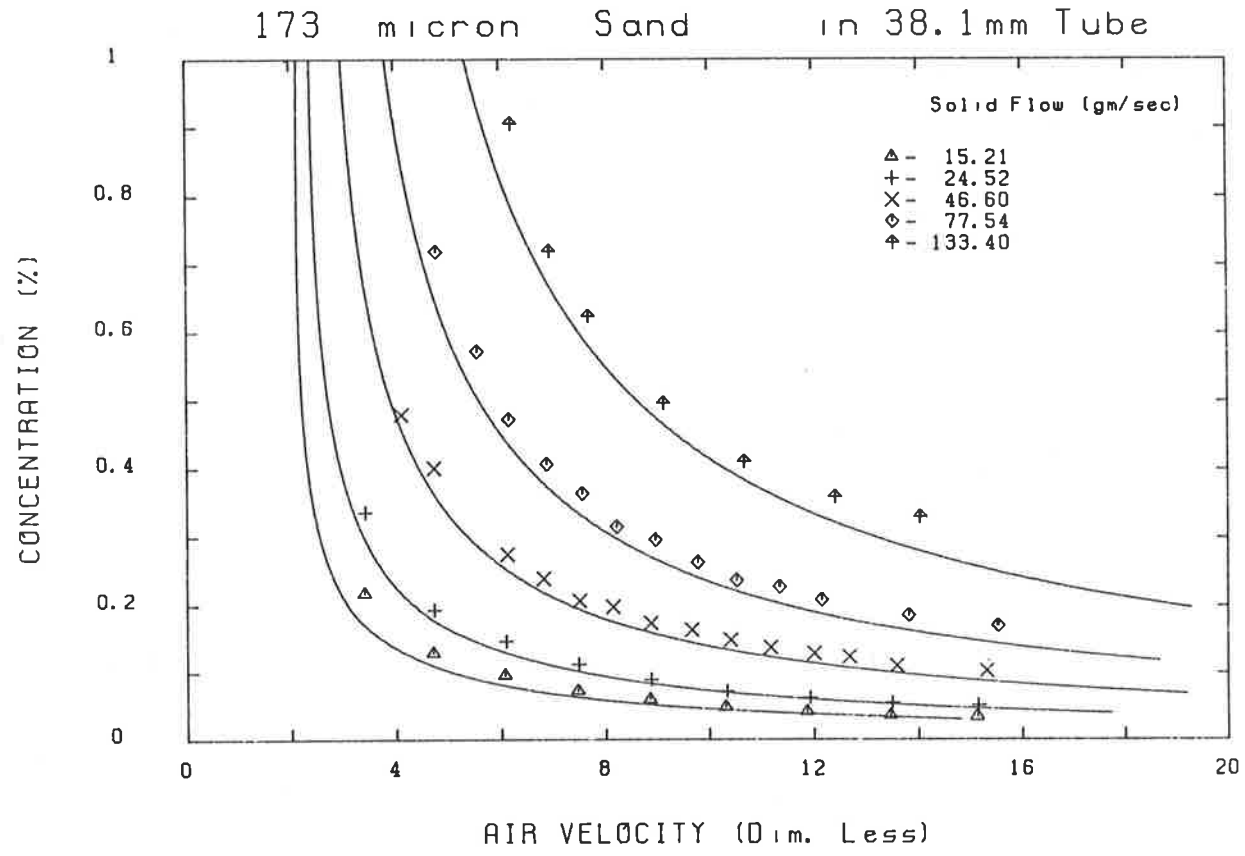

Fig. 3.15(d) Prediction of minimum transprot velocity

ities with confidence is of importance for trouble free operation. Also, at low transport velocities knowledge of volumetric concentration of solids is sufficient for specification of energy requirement, as solid hold up is a dominant factor. At large transport velocities, however, knowledge of the solid-wall friction component is essential in determining the energy requirements.

3.11 Conclusions

1. Derivation of solid velocity from the measured impact of solids on a plate proved to be simple and accurate.

2. At large transport velocities solid-wall friction is significant. In this region higher transport velocities result in higher solid-wall frictional loss, thus increasing the slip velocities.

3. At low transport velocities corresponding to limiting gas velocities, the solid-wall frictional loss is negligible. Slip velocities in this region are governed by solid volumetric concentration.

4. The concentration-slip velocity relationship obtained from the countercurrent experiments can be extended to forward transport conditions, provided the transport velocity is small.

5. Limiting gas velocities predicted from countercurrent experimental data agree with those observed from cocurrent experiments.

6. The additional slip velocity due to solid-wall friction is observed to increase with increasing solid velocity and decreasing concentration. A correlation to account for the additional slip velocity due to the solid-wall friction is proposed.

BIBLIOGRAPHY

1. Addler I.L. and Happel J., Chem. Eng. Prog. Symp. Ser., No.38, Vol.58, pp 98, 1962.

2. Arundel P.A., Bibb S.D. and Boothroyd R.G., "Dispersed Density Distribution and Extent of Agglomeration in a Polydisperse Fine Particle Suspension Flowing Turbulently Upwards in a Duct", Powder Technol., Vol.4, pp 302-312, 1970/71.

3. Batchelor J.K., "Sedimentation in a Dilute Dispersion of Spheres", J. Fluid. Mech., Vol.52, part 2, pp 245-268, 1972.

4. Barfod N., "Concentration Dependance of Sedimentation Rate of Particles in Dilute Suspensions", Powder Technol., Vol.6, pp 39-43, 1972.

5. Barnea E. and Mizrahi J., "A Generalized Approach to the Fluid Dynamics of Particulate Systems Part I. General Correlation for Fluidization and Sedimentation in Solid Multiparticle Systems", The Chem. Eng. Journal, Vol.5, pp 171-189, 1973.

6. Barth W., "Flow Problems with Mixtures of Gases and Entrained Solid Particles", Engineers Digest, Vol.23, pp 81-85, 1962.

7. Beck M.S., Hobson J.H., and Mendies P.J., "Mass Flow and Solid Velocity Measurement in Pneumatic Conveyors", Paper D3, Pneumotransport 1, 1971.

8. Beck M.S., Drane J., Plaskowski A. and Wainwright N., "Particle Velocity and Mass Flow Measurement in Pneumatic Conveyors", Powder Technol., Vol.2, pp 269-277, 1968/69.

9. Belden D.H. and Kassel L.S., "Pressure Drops Encountered in Conveying Particles of Large Diameter in Vertical Transfer Lines", Ind. Eng. Chem., Vol.41, pp 1174-1178, 1949.

10. Birchenough A. and Mason J.S., "Local Particle Velocity Measurements with a Laser Anemometer in an Upward Flowing Gas-Solid Suspension", Powder Technol., Vol.14, pp 139-152, 1976.

11. Birchenough A. and Mason J.S., "Particle Wall Velocity Measurements in a Densely Flowing Gas-Solid Suspension", Pneumotransport 32, Paper B2, pp 9-20, 1976.

12. Boothroyd R.G., "Flowing Gas-solids suspensions", Powder Technology series, Chapman and Hall, London, 1971.

13. Brewster B.S. and Seader J.D., "Nonradioactive Tagging Method of Measuring Particle Velocity in Pneumatic Transport", AIChE Journal, Vol.26, pp 325-327, 1980.

14. Burgers J.M., Proc. Koninkl. Akad. Wetenschap (Amsterdam), Vol.45, pp 9, 1942.

15. Capes C.E., "Dense Phase Vertical Pneumatic Conveying", Can. J. Chem. Eng., Vol.49, pp 182-186, 1971.

16. Capes C.E., "Particle Agglomeration and the Value of the Exponent 'n' in the Richardson-Zaki Equation", Powder Technol., Vol.10, pp 303-306, 1974.

17. Capes C.E. and McIlhinney A.E., "The psuedo-particulate expansion of screen-packed gas-fluidized beds, AIChE Journal, Vol.14, No.6, pp 917, 1968.

18. Capes C.E. and Nakamura K., "Vertical Pneumatic Conveying: An Experimental Study with Particles in the Intermediate and Turbulent Flow Regimes", Can. J. Chem. Eng., Vol.51, pp 31-38, 1973.

19. Clamen A. and Gauvin W.H., AIChE Journal, Vol.15, pp 184, 1969.

20. Clift R. and Gauvin W.H., "The Motion of Particles in Turbulent Gas Streams", Chemeca, pp 14-28, 1970.

21. Decamps F., Dumont G. and Goossens W., "Vertical Pneumatic Conveyer with a Fluidized Bed as Mixing Zone", Powder Technol., Vol.5, pp 299-306, 1971/72.

22. Dixon G., "Particle Velocities in Vertical Pneumatic Conveying Systems", Int. J. Multiphase Flow, Vol.2, pp 465-470, 1976.

23. Doig I.D. and Roper G.H., "Air Velocity Profiles in the Presence of Cocurrently Transported Particles", Ind. Eng. Chem. Fundam., Vol.6, pp 247-256, 1967.

24. Dryden H.L., Schubauer G.B., Mock W.C. and Skramstad H.K., NACA T.R., 581, 1937.

25. Durst F., Melling A. and Whitelaw J.H., "Laser Anemometry - a report on Euromech 36", J. of Fluid Mech., Vol.56, Part 1, pp 143-160, 1972.

26. Famularo J. and Happel J., AIChE Journal, Vol.11, pp 981, 1965.

27. Francis A.W., Physics, Vol.4, pp 403, 1933.

28. Fuchs N.A., "Mechanics of Aerosols", Pergamon, Oxford, 1964.

29. Gal-Or B., Can. J. Chem. Eng., Vol.48, pp 526, 1970.

30. Garside J. and Al-Dibouni M.R., "Velocity-Voidage Relationships for Fluidization and Sedimentation in Solid-Liquid Systems", Ind. Eng. Chem., Process Des. Dev., Vol.16, pp 206-214, 1977.

31. Godard K. and Richardson J.F., "The behaviour of bubble free fluidized beds", Preprints, The Tripartite Chem. Eng. Conf., Montreal, 1968, Symp. on Fluidization II, pp 26.

32. Gopichand T., Sarma K.J.R. and Narasinga Rao M., "Pneumatic Conveyance and Continuous Fluidization of Solids", Ind. Eng. Chem., Vol.51, pp 1449-1452, 1959.

33. Happel J., AIChE Journal, Vol.4, pp 197, 1958.

34. Happel J. and Brenner H., "Low Reynolds Number Hydrodynamics", Prentice-Hall, Englewood-Cliffs N.J., 1965.

35. Hariu O.H. and Molstad M.C., "Pressure Drop in Vertical Tubes in Transport of Solids by Gases", Ind. Eng. Chem., Vol.41, pp 1148-1160, 1949.

36. Hasimoto H., J. Fluid. Mech., Vol.5, pp 317, 1959.

37. Hinkle B.L., Ph.D. Dissertation, Georgia Institute of Technology, 1953.

38. Hitchcock J.A. and Jones C., Brit. J. App. Phys., Vol.9, pp 218, 1958.

39. Hours R.M. and Chen C.P., "Application of Radioactive Tracers and B Rays Absorption Techniques to the Measurement of Solid Particles Velocity and Space Concentration in a Two-phase Air-Solid Flow at High Mass Rate", Pneumotransport 3, Paper B3, pp 21-35, 1976.

40. Irons G.A. and Chang J.S., "Particle Fraction and Velocity Measurement in Gas-Powder Streams by Capacitance Transducers", Int. J. Multiphase Flow, Vol.9, pp 289-297, 1983.

41. Ishii M. and Zuber N., "Drag Coefficient and Relative Velocity in Bubbly, Droplet or Particulate Flows", AIChE Journal, Vol.25, pp 843-855, 1979.

42. Jayaweera K.O.L.F., Mason B.J. and Slack G.W., J. Fluid Mech., Vol.20, pp 121, 1964.

43. Jodlowski C., "Study of Minimum Transport Velocities for Upward Flow in Vertical Pipes", Pneumotransport 3, Paper D2, pp 15-32, 1976.

44. Johne D.P.R., Chem. Ingr. Tech., Vol.38, pp 428-430, 1966.

45. Jones J.H., Braun W.G., Daubert T.E. and Allendorf H.D., "Slip Velocity of Particulate Solids in Vertical Tubes", AIChE Journal, Vol.12, pp 1070-1074, 1966.

46. Jones J.H., Braun W.G., Daubert T.E. and Allendorf H.D., "Estimation of Pressure Drop for Vertical Pneumatic Transport of Solids", AIChE Journal, Vol.13, pp 608-611, 1967.

47. Jotaki T., Tomita Y., Fujimoto K. and Iwasaki M., "Pressure Drop in an Equilibrium Region of Vertical Pneumatic Transport", Bull. JSME, Vol.21, pp 128-133, 1978.

48. Jovanovic D.S., "A quantitative study of Orthokinetic Flocculation in Suspension", Kolloid-Z Polymere, Vol.203, part 1, pp 42-56, 1965.

49. Kaye B.H. and Boardman R.P., "Cluster Formation in Dilute Suspensions", Instn. Chem. Engrs., London, pp 17-21, 1962.

50. Khan J.I. and Pei D.C., "Pressure Drop in Vertical Solid-Gas Suspension Flow", Ind. Eng. Chem. Proc. Des. Develop., Vol.12, pp 428-431, 1973.

51. Klinzing G.E. and Mathur M.P., "The Dense and Extrusion Flow Regime in Gas-Solid Transport", Can. J. Chem. Eng., Vol.59, pp 590-594, 1981.

52. Kmiec A., Mielczarski S. and Pajakowska J., "An Experimental Study on Hydrodynamics of a System in a Pneumatic Flash Dryer", Powder Technol., Vol.20, pp 67-74, 1978.

53. Koglin B., D. Ing. Diss., Univ. of Karlsruhe, 1971.

54. Konno H. and Satio S., "Pneumatic Conveying of Solids Through Straight Pipes", J. Chem. Eng. Japan., Vol.2, pp 211-217, 1969.

55. Ladenburg R., Ann. Physik., Vol.20, pp 287 & Vol.23, pp 447, 1907.

56. Leclair B.P. and Hamielec A.E., Ind. Eng. Chem. Fundm., Vol.7, pp 542, 1968.

57. Leung L.S., "Vertical Pneumatic Conveying: A Flow Regime Diagram and a Review of Choking versus Non-Choking Systems", Powder Technol., Vol.25, pp 185-190, 1980.

58. Leung L.S., "A Quantitative Flow Regime Diagram for Vertical Pneumatic Conveying of Granular Solids", Pneumotransport 5, Paper A3, pp 35-46, 1980.

59. Leung L.S., Wiles R.J. and Nicklin D.J., "Correlation for Predicting Choking Flowrates in Vertical Pneumatic Conveying", Ind. Eng. Chem. Proc. Des. Develop., Vol.10, pp 183-189, 1971.

60. Leung L.S. and Wiles R.J., "A Quantitative Design Procedure for Vertical Pneumatic Conveying Systems", Ind. Eng. Chem. Proc. Des. Devlop., Vol.15, pp 552-557, 1976.

61. Leung L.S. and Wiles R.J., "Design of Vertical Pneumatic Conveying Systems", Pneumotransport 3, Paper C4, pp 47-58, 1976.

62. Maeda M., Ikai S. and Ukon A., "Pneumatic Conveying of Solids: Part 2, On Slip Velocities and Interaction between Wall and Particles in Vertical Lines", Bull. JSME, Vol.17, pp 768-775, 1974.

63. Manley R.St.J. and Mason S.G., "Particle Motions in Sheared Suspensions. II. Collisions of Uniform Spheres", Pulp and Paper Research Institute of Canada, McGill University, Montreal, Canada, pp 354-369, 1952.

64. Matsen J.M., "Mechanisms of Choking and Entrainment", Powder Technol., Vol.32, pp 21-33, 1982.

65. McCarthy H.E. and Olson J.H., "Turbulent Flow of Gas-Solids Suspensions", Ind. Eng. Chem. Fundm., Vol.7, pp 471-483, 1968.

66. McNown J.S. and Lin P.N., Proc. 2nd Midwestern Conf. on Fluid Mechanics, Ohio State Univ., 1952.

67. Mehta N.C., Smith J.M. and Comings E.W., "Pressure Drop in Air-Solid Flow Systems", Ind. Eng. Chem., Vol.49, pp 986-992, 1957.

68. Mogan J.P., Taylor R.W. and Booth F.L., "The Value of the Exponent n in the Richardson and Zaki Equation, for Fine Solids Fluidized with Gases Under Pressure", Powder Technol., Vol.4, pp 286-289, 1970/71.

69. Mogan J.P., Taylor R.W. and Booth F.L., "A Method of Prediction of the Porosities of High-Pressure Gaseous Fluidization Systems", Can. J. Chem. Eng., Vol.47, pp 126, 1969.

70. Munroe H.S., Trans. Am. Inst. Min. Eng., Vol.17, pp 637, 1888.

71. Ottjes J.A., "A Measuring System for Particle Impact Velocities and Application in a Pneumatic Transport Line", Chem. Eng. Sci., Vol.36, pp 1337-1347, 1981.

72. Ottjes J.A., Meeuse G.C. and van Kuijk G.J.L., "Particle Velocity and Pressure Drop in Horizontal and Vertical Pipes", Pneumotransport 3, BHRA, pp D9 109-120, 1976.

73. Reddy K.V.S. and Pei D.C., "Particle Dynamics in Solid-Gas Flow in a Vertical Pipe", Ind. Eng. Chem. Fundam., Vol.8, pp 490-497, 1969.

74. Richardson J.F. and Davies L., "Gas Interchange between Bubbles and the Continuous Phase in Fluidized Bed", Trans. Inst. Chem. Engrs., Vol.44, pp 293, 1966.

75. Richardson J.F. and McLeman M., "Pneumatic Conveying - Part II Solids Velocities and Pressure Gradients in a One-Inch Horizontal Pipe", Trans. Instn. Chem. Engrs., Vol.38, pp 257-256, 1960.

76. Richardson J.F. and Zaki W.N., "Sedimentation and Fluidisation: Part I", Trans. Instn. Chem. Engrs., Vol.32, pp 35-52, 1954.

77. Riethmuller M.L. and Ginoux J.J., "The Application of a Laser Doppler Velocimeter to the Velocity Measurement of Solid Particles Pneumatically Transported", Pneumotransport 2, Paper D3, pp 3-21, 1973.

78. Rowe P.N., Foscolo P.U., Hoffmann A.C. and Yates J.G., "Fine Powders at Low Velocity at Pressures up to 20 Bar with Gases of Different Viscosity", Chem. Eng. Sci., Vol.37, pp 1115-1117, 1982.

79. Shimizu A., Echigo R., Hasegawa S. and Hishida M., "Experimental Study on the Pressure Drop and the Entry Length of the Gas-Solid Suspension Flow in a Circular Tube", Int. J. Multiphase Flow., Vol.4, pp 53-64, 1978.

80. Soo S.L., Trezek G.J., Dimick R.C. and Hohmstreiter G.F., Ind. Eng. Chem. Fundm., Vol.3, pp 98, 1964.

81. Soo S.L., "Fluid Dynamics of Multiphase Systems", Ginn Blaisdell, Massachusetts, Section 4.2, 1967.

82. Smith T.N., "The Spatial Distribution of Spheres Falling in a Viscous Liquid", J. Fluid Mech., Vol.32, pp 203-207, 1968.

83. Smoluchowski M.W., Bull. Int. Acad. Polonaise Sci. Letters, 1A pp 28, 1911.

84. Smoluchowski M.W., "Versuch Einer Mathematischen Theorie Der Koagulationskinetik Kolloider Losungen", Zeitschrift F. Physik. Chemie, Vol.XCII, pp 129-168, 1916.

85. Stemerding S., "The Pneumatic Transport of Cracking Catalyst in Vertical Risers", Chem. Eng. Sci., Vol.17, pp 599-608, 1962.

86. Stokes G.G., "Mathematical and Physical Papers", Vol.3, p.55, Cambridge U.P. 1891.

87. Swaaij W.P.M.V., "Shear Stress on the Wall of a Dense Gas-Solids Risers", Chem. Eng. Sci., Vol.25, pp 1818-1820, 1970.

88. Tomita Y., Yutani S. and Jotake T., "Pressure Drop in Vertical Pneumatic Transport Lines of Powdery Material at High Solids Loading", Powder Technol., Vol.25, pp 101-107, 1980.

89. Torobin L.B. and Gauvin W.H., AIChE Journal, Vol.7, pp 615, 1961.

90. Uchida S., Rept. Int. Sci. Technol. Univ. Tokyo, Vol.3, pp 97, 1949.

91. Uhlherr P.H.T. and Sinclair C.G., "The Effect of Free-Stream Turbulence on the Drag Coefficient of Spheres", Chemeca, pp 1-13, 1970.

92. Van Zuilichem D.J. and de Swart J.G., "Slip Velocity-Measurements by a Radiotracer-Technique in Vertical Conveying Systems", Pneumotransport 2, Paper D4, pp 33-46, 1973.

93. Van Zuilichem D.J., Houben P.J.M., Broekmeijer E. and Stolp W., " Comparison of Some Friction Calculation Methods for Coarse Granular Material", Pneumotransport 5, Paper D1, pp 179-196, 1980.

94. Van Zuilichem D.J., Allersma H.B.G., Stolp W. and de Swart J.G., "Local Densities and Instabilities in a Vertical Conveying System", Pneumotransport 3, Paper D1, pp 1-14, 1976.

95. Vogt E.G. and White R.R., "Friction in the Flow of Suspensions", Ind. Eng. Chem., Vol.40, pp 1731-1738, 1949.

96. Wen C.Y. and Yu Y.H., "Mechanics of Fluidisation", Chem. Eng. Prog. Symp. Ser., Vol.62, pp 100-111, 1966.

97. Wen C.Y. and Hashinger R.F., "Elutriation of Solid Particles from a Dense-Phase Fluidized Bed", AIChE Journal, June, pp 220-226, 1960.

98. Wheeldon J.M. and Williams J.C., "The Analysis of Equilibrium Particle Velocity and Additional Pressure Drop Data for Granular Material from Horizontal and Vertical Light Phase Conveyors with Particular Reference to the Fundamental Equations of Motion and Additional Pressure Drop", Pneumotransport 5, Paper B3, pp 121-154, 1980.

99. Yang W.C., "Estimating the Solid Particle Velocity in Vertical Pneumatic Conveying Lines", Ind. Eng. Chem. Fundam., Vol.12, pp 349-352, 1973.

100. Yang W.C., "A Mathematical Definition of Choking Phenomenon and a Mathematical Model for Predicting Choking Velocity and Choking Voidage", AIChE Journal, Vol.21, pp 1013-1015, 1975.

101. Yerushalmi J., "The Interaction of Gas and Solid in the Fast Fluidized Bed", Pneumotransport 3, Paper E4, pp 4-41, 1976.

102. Yerushalmi J. and Cankurt N.T., "Further Studies of the Regimes of Fluidizations", Powder Technol., Vol.24, pp 187-205, 1979.

103. Yerushalmi J., Turner D.H. and Squires A.M., "The Fast Fluidized Bed", Ind. Eng. Chem. Process. Des. Dev., Vol.15, pp 47-53, 1976.

104. Yerushalmi J., Cankurt N.T., Geldart D. and Liss B., "Flow Regimes in Vertical Gas-Solid Contact Systems", AIChE Symp. Ser., Vol.74, pp 1-13, 1978.

105. Yousfi Y. and Gau G., "Aerodynamique De L'ecoulement Vertical De Suspensions Concentrees Gaz-Solides-I, Regimes D'ecoulement et Stabilite Aerodynamique", Chem. Eng. Sci., Vol.29, pp 1939-1946, 1974.

106. Yousfi Y. and Gau G., "Aerodynamique De L'ecoulement Vertical De Suspensions Concentrees Gaz-Solides-II. Chute De Pression et Vitesse Relative Gaz-Solide", Chem. Eng. Sci., Vol.29, pp 1947-1953, 1974.

APPENDIX (A)

DETAILS OF SIZE ANALYSIS OF MATERIALS USED

Table (A-1) SIZE ANALYSIS OF 96μ GLASS BEADS

Mesh Size (microns)	Mean Diameter (D_p) (microns)	Weight fraction $\Delta\phi_w$
+229	229	0.0011
-229+211	220	0.0014
-211+152	181.5	0.0
-152+124	138	0.2148
-124+104	114	0.1615
-104+ 89	96.5	0.5062
- 89+ 76	82.5	0.0355
- 76+ 53	64.5	0.0568
- 53	26.5	0.0227
		1.0000

$$\text{Surface to volume mean diameter} = \frac{1}{\sum \frac{\Delta\phi_w}{D_p}} = 96\mu$$

Table (A-2) SIZE ANALYSIS OF 173μ SAND

Mesh Size (microns)	Mean Diameter (D_p) (microns)	Weight fraction $\Delta\phi_w$
-295+229	262	0.0668
-229+211	220	0.332
-211+178	194.5	0.2176
-178+152	165	0.2065
-152+104	128	0.1427
-104+ 76	90	0.0243
- 76	38	0.01
		1.0000

$$\text{Surface to volume mean diameter} = \frac{1}{\sum \frac{\Delta\phi_w}{D_p}} = 173\mu$$

Table (A-3) SIZE ANALYSIS OF 644μ GLASS BEADS

Mesh Size (microns)	Mean Diameter (D_p) (microns)	Weight fraction $\Delta\phi_w$
+1001	1001	0.003
-1001+ 853	927	0.0077
- 853+ 711	782	0.1449
- 711+ 599	655	0.6727
- 599+ 500	549.5	0.1549
- 500+ 422	461	0.0131
- 422+ 295	358.5	0.0013
- 295	147.5	0.0024
		1.0000

$$\text{Surface to volume mean diameter} = \frac{1}{\sum \frac{\Delta\phi_w}{D_p}} = 644\mu$$

Table (A-4) SIZE ANALYSIS OF 179μ STEEL SHOT

Mesh Size (microns)	Mean Diameter (D_p) (microns)	Weight fraction $\Delta\phi_w$
-229+211	220	0.0687
-211+178	194.5	0.529
-178+152	165	0.306
-152+124	138	0.094
-124+104	114	0.0
-104+ 76	90	0.002
- 76	38	0.0003
- 295	147.5	0.0024
		1.0000

$$\text{Surface to volume mean diameter} = \frac{1}{\sum \frac{\Delta\phi_w}{D_p}} = 179\mu$$

Table (A-5) SIZE ANALYSIS OF 375μ STEEL SHOT

Mesh Size (microns)	Mean Diameter (D_p) (microns)	Weight fraction $\Delta\phi_w$
-599+500	549.5	0.0111
-500+422	461	0.2773
-422+353	387.5	0.4457
-353+295	324	0.1772
-295+211	253	0.0887
		1.0000

$$\text{Surface to volume mean diameter} = \frac{1}{\sum \frac{\Delta\phi_w}{D_p}} = 375\mu$$

Table (A-6) SIZE ANALYSIS OF 637μ STEEL

Mesh Size (microns)	Mean Diameter (microns)	Weight fraction $\Delta\phi_w$
-1001+ 853	927	0.0001
- 853+ 711	782	0.0313
- 711+ 599	655	0.8157
- 599+ 500	549.5	0.141
- 500+ 422	461	0.0077
- 422+ 353	387.5	0.0029
- 353+ 211	282	0.0013
		1.0000

$$\text{Surface to volume mean diameter} = \frac{1}{\sum \frac{\Delta\phi_w}{D_p}} = 637\mu$$

APPENDIX (B)

EFFECT OF CONCENTRATION ON SLIP VELOCITY

COUNTERCURRENT TRANSPORT DATA

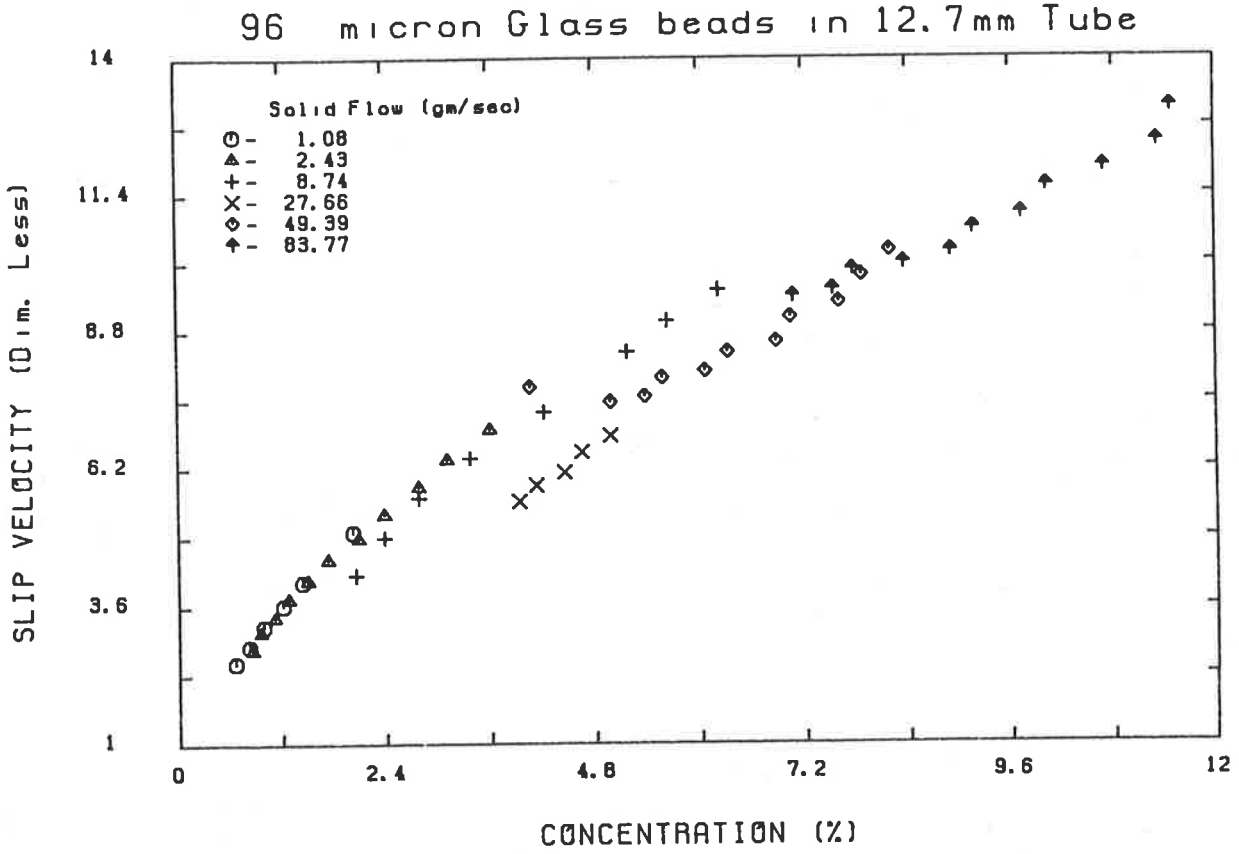
96 micron Glass beads in 12.7mm Tube
Solid Flow (gm/sec)
⊙- 1.08
▲- 2.43
+- 8.74
×- 27.66
◇- 49.39
↑- 83.77
SLIP VELOCITY (Dim. Less)
14
11.4
8.8
6.2
3.6
1
0
2.4
4.8
7.2
9.6
12
CONCENTRATION (%)

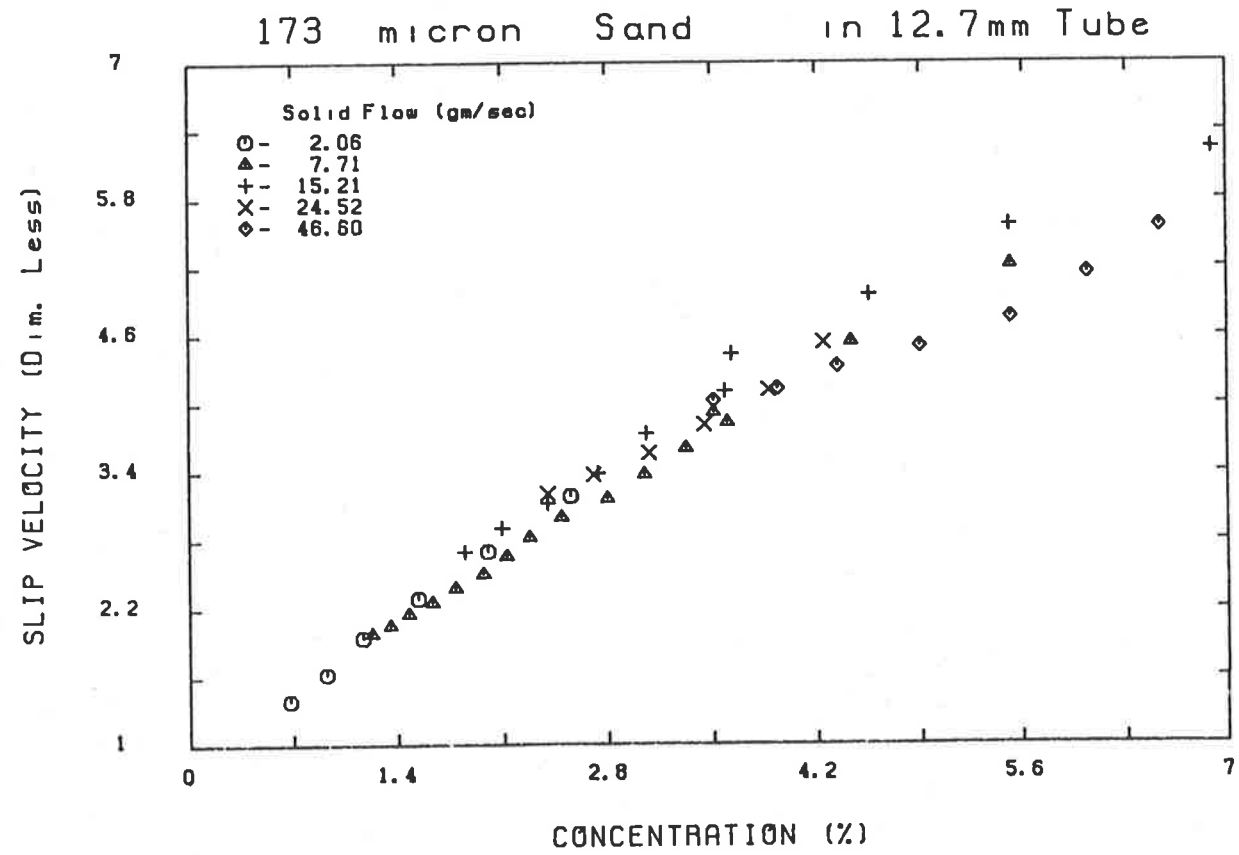
173 micron Sand in 12.7mm Tube
Solid Flow (gm/sec)
⊙- 2.06
▲- 7.71
+- 15.21
×- 24.52
◇- 46.60
SLIP VELOCITY (Dim. Less)
7
5.8
4.6
3.4
2.2
1
0
1.4
2.8
4.2
5.6
7
CONCENTRATION (%)

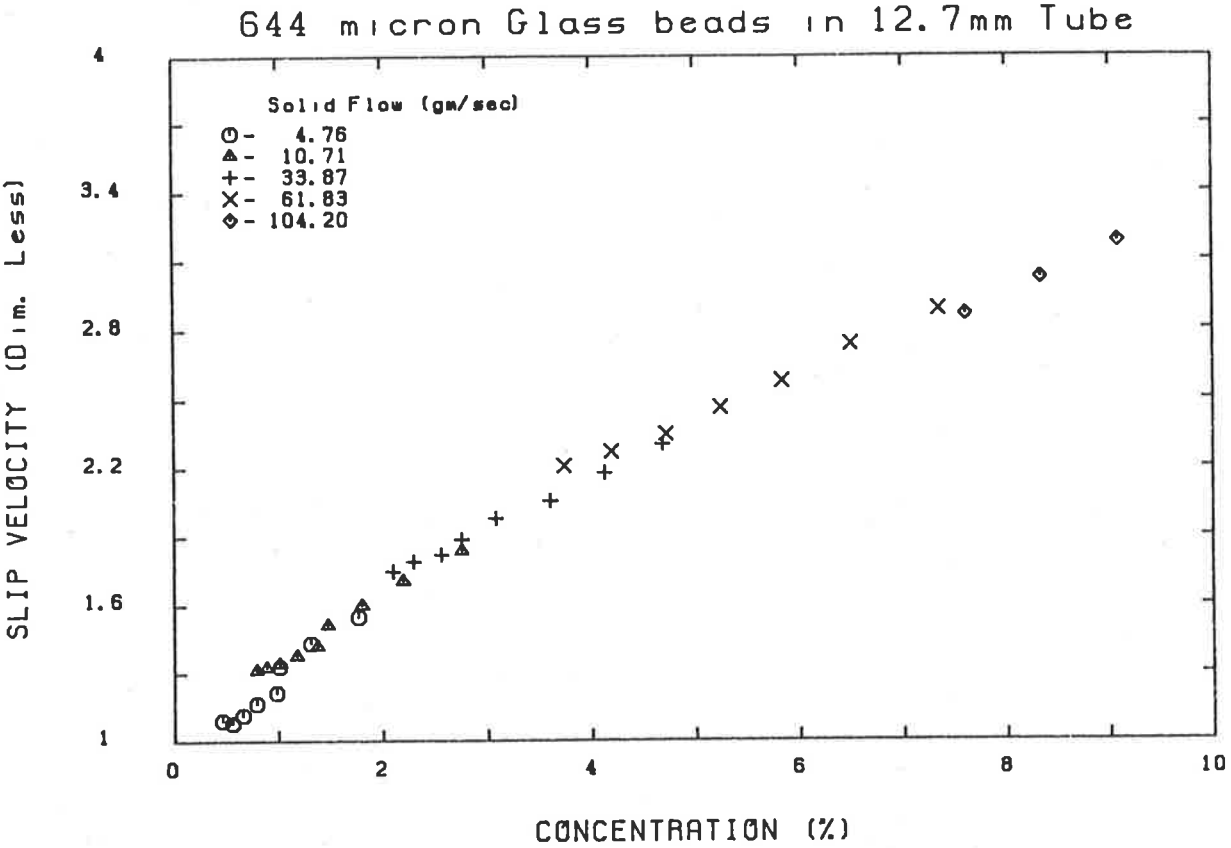
644 micron Glass beads in 12.7mm Tube
Solid Flow (gm/sec)
- 4.76
- 10.71
- 33.87
- 61.83
- 104.20
SLIP VELOCITY (Dim. Less)
CONCENTRATION (%)
1
1.6
2.2
2.8
3.4
4
0
2
4
6
8
10

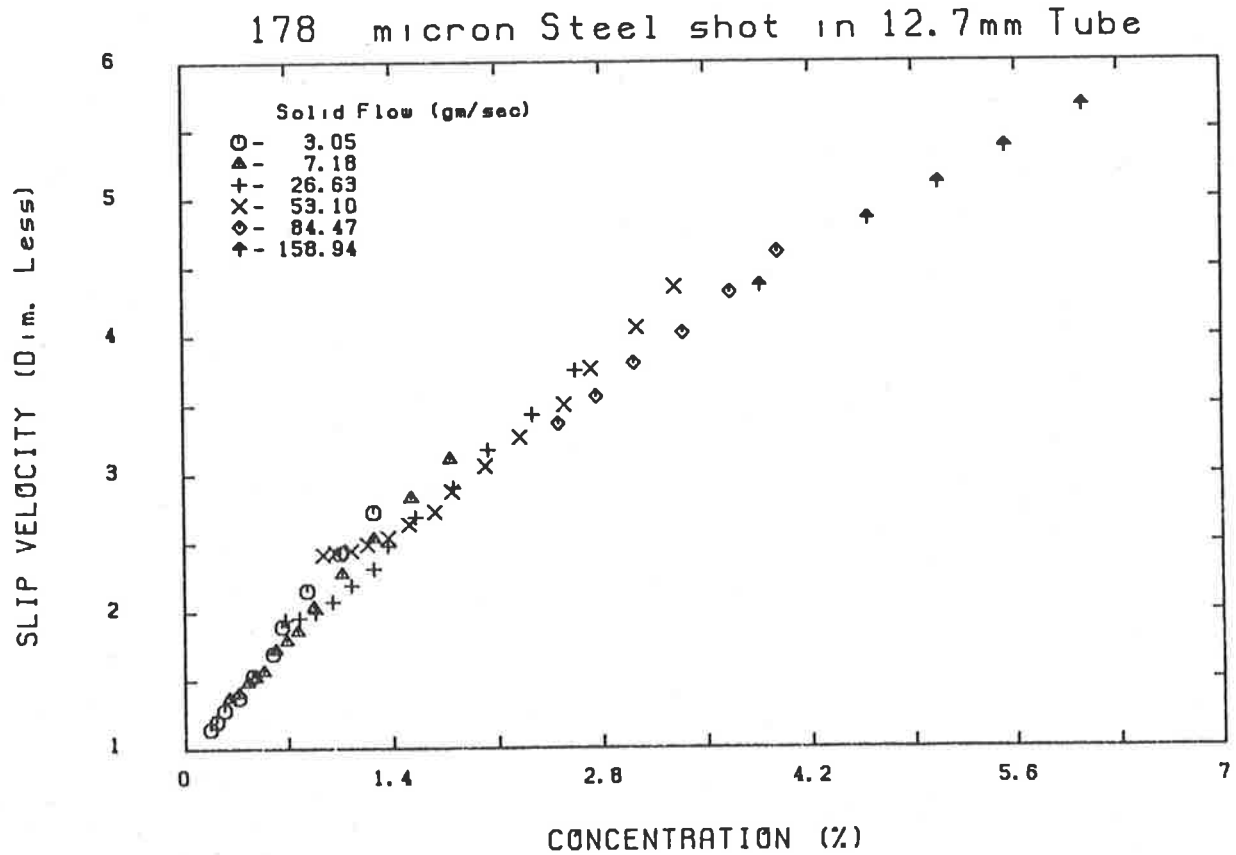
178 micron Steel shot in 12.7mm Tube
Solid Flow (gm/sec)
- 3.05
- 7.18
- 26.63
- 53.10
- 84.47
- 158.94
SLIP VELOCITY (Dim. Less)
CONCENTRATION (%)
1
2
3
4
5
6
0
1.4
2.8
4.2
5.6
7

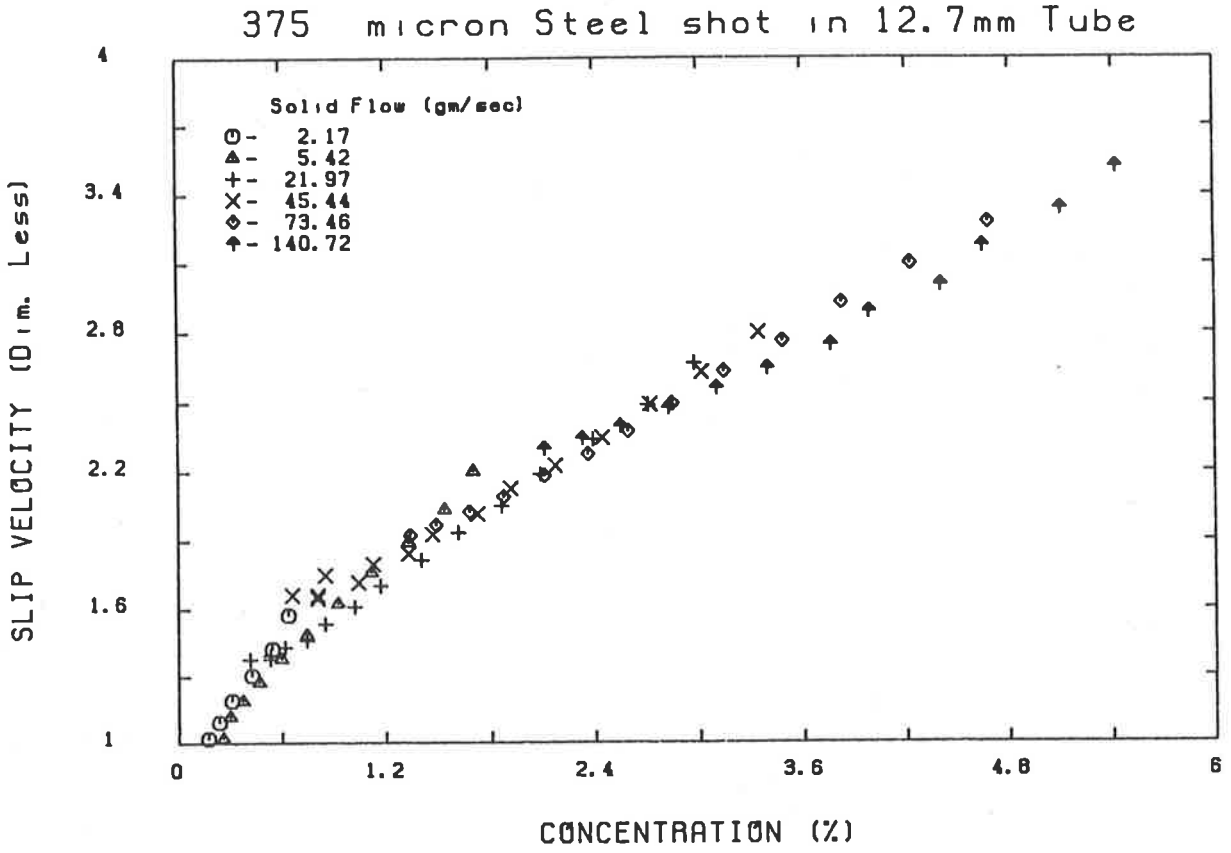
375 micron Steel shot in 12.7mm Tube
Solid Flow (gm/sec)
- 2.17
- 5.42
- 21.97
- 45.44
- 73.46
- 140.72
SLIP VELOCITY (Dim. Less)
CONCENTRATION (%)
4
3.4
2.8
2.2
1.6
1
0
1.2
2.4
3.6
4.8
6

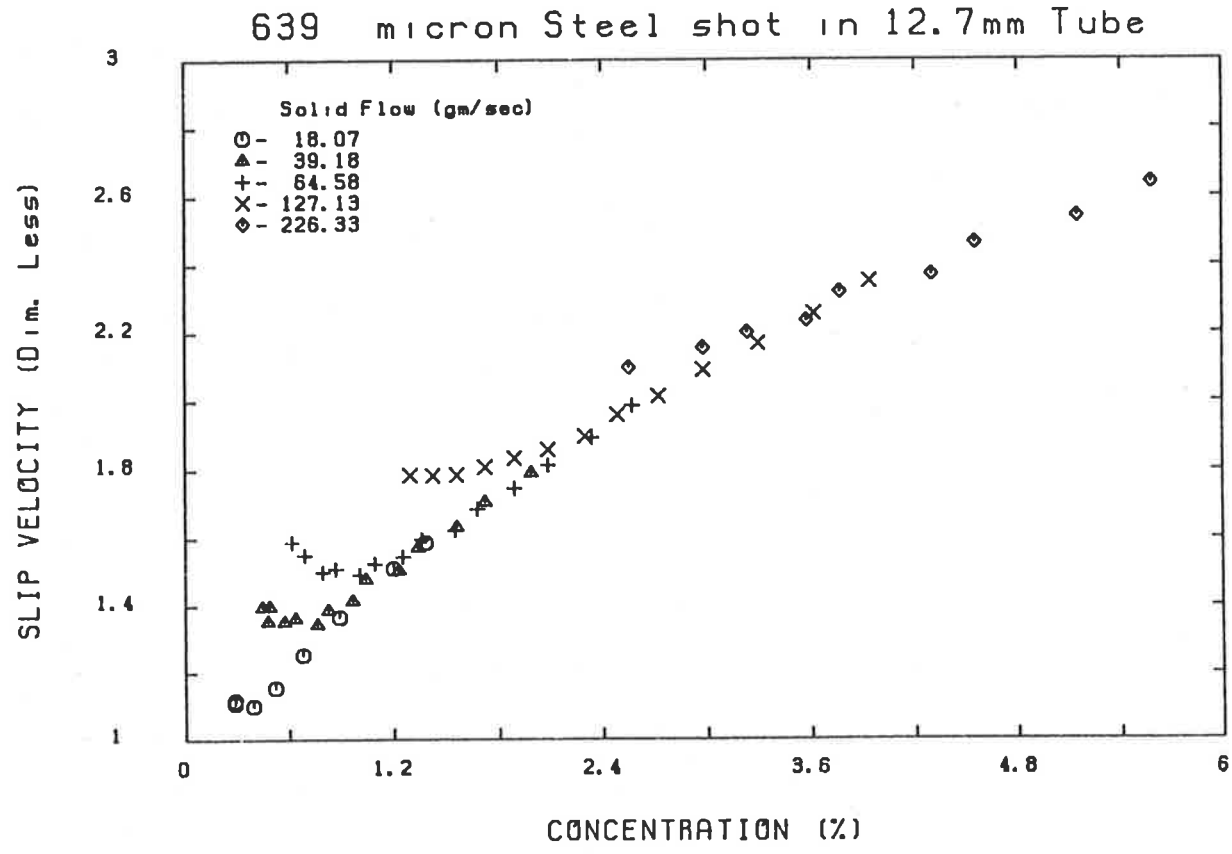
639 micron Steel shot in 12.7mm Tube
Solid Flow (gm/sec)
- 18.07
- 39.18
- 64.58
- 127.13
- 226.33
SLIP VELOCITY (Dim. Less)
CONCENTRATION (%)
3
2.6
2.2
1.8
1.4
1
0
1.2
2.4
3.6
4.8
6

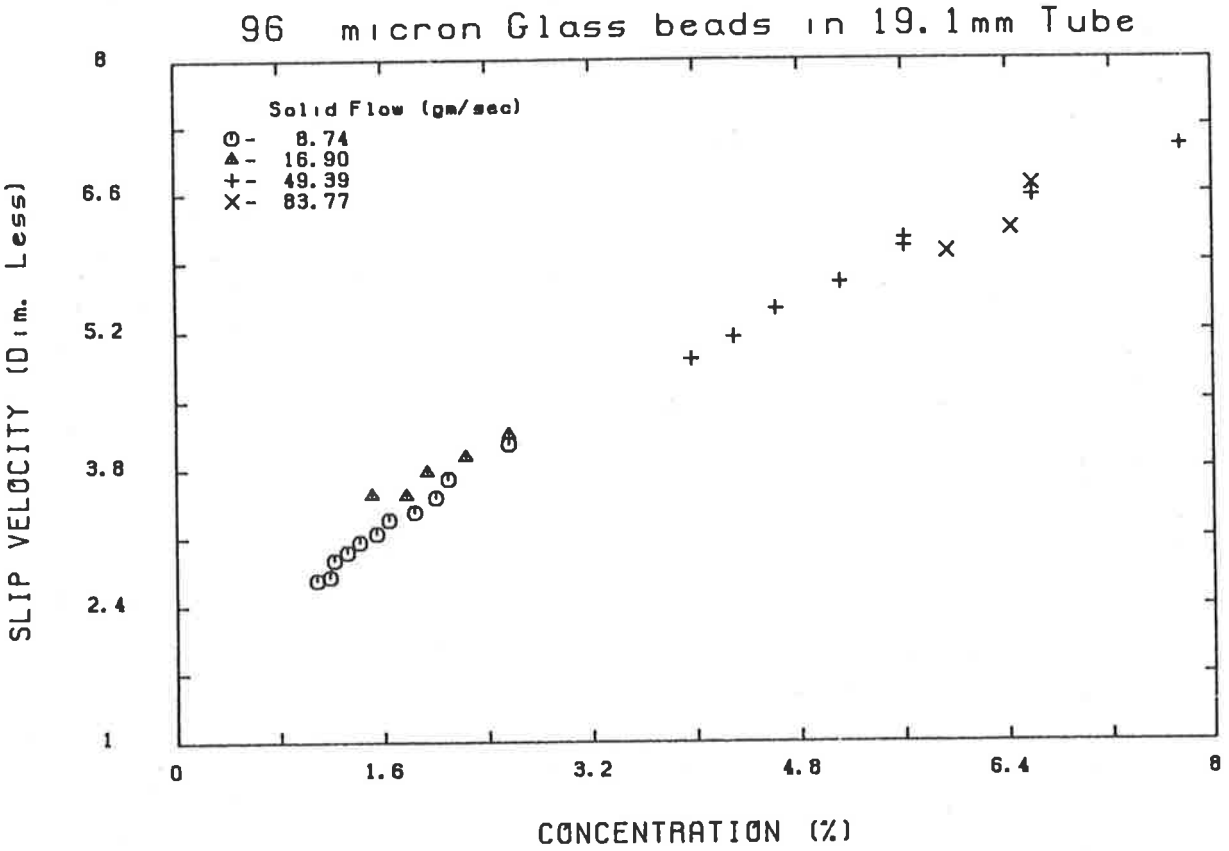
96 micron Glass beads in 19.1mm Tube
Solid Flow (gm/sec)
⊙- 8.74
▲- 16.90
+- 49.39
×- 83.77
SLIP VELOCITY (Dim. Less)
8
6.6
5.2
3.8
2.4
1
0
1.6
3.2
4.8
6.4
8
CONCENTRATION (%)

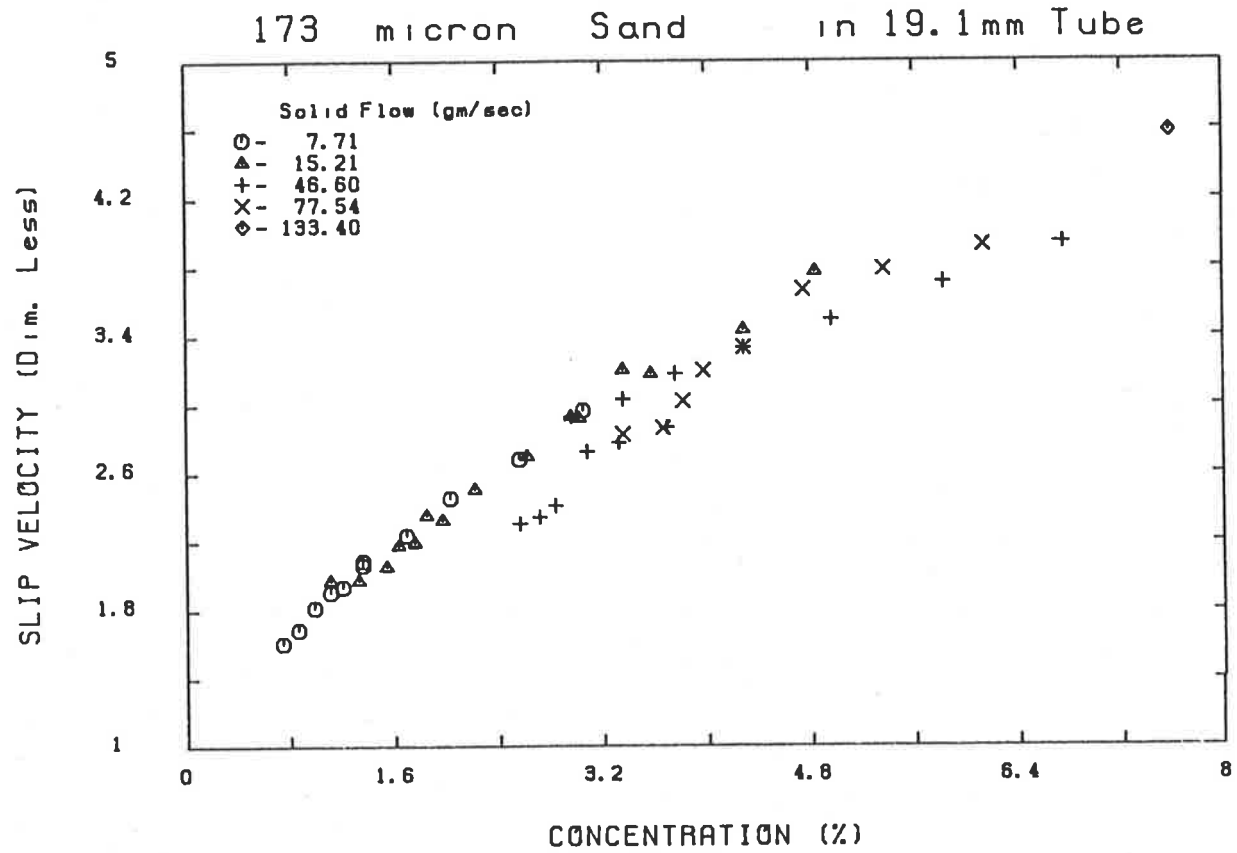
173 micron Sand in 19.1mm Tube
Solid Flow (gm/sec)
⊙- 7.71
▲- 15.21
+- 46.60
×- 77.54
◇- 133.40
SLIP VELOCITY (Dim. Less)
5
4.2
3.4
2.6
1.8
1
0
1.6
3.2
4.8
6.4
8
CONCENTRATION (%)

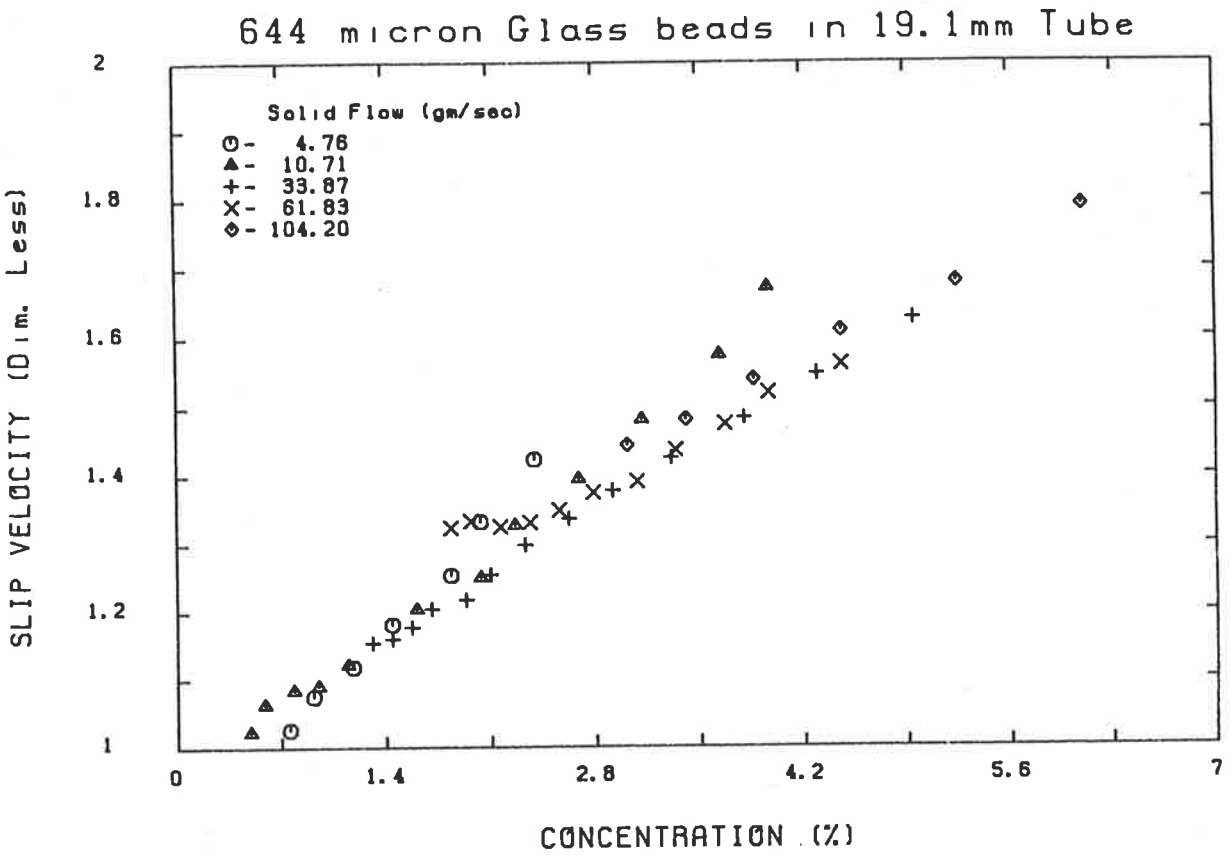
644 micron Glass beads in 19.1mm Tube
Solid Flow (gm/sec)
- 4.76
- 10.71
- 33.87
- 61.83
- 104.20
SLIP VELOCITY (Dim. Less)
CONCENTRATION (%)
2
1.8
1.6
1.4
1.2
1
0
1.4
2.8
4.2
5.6
7

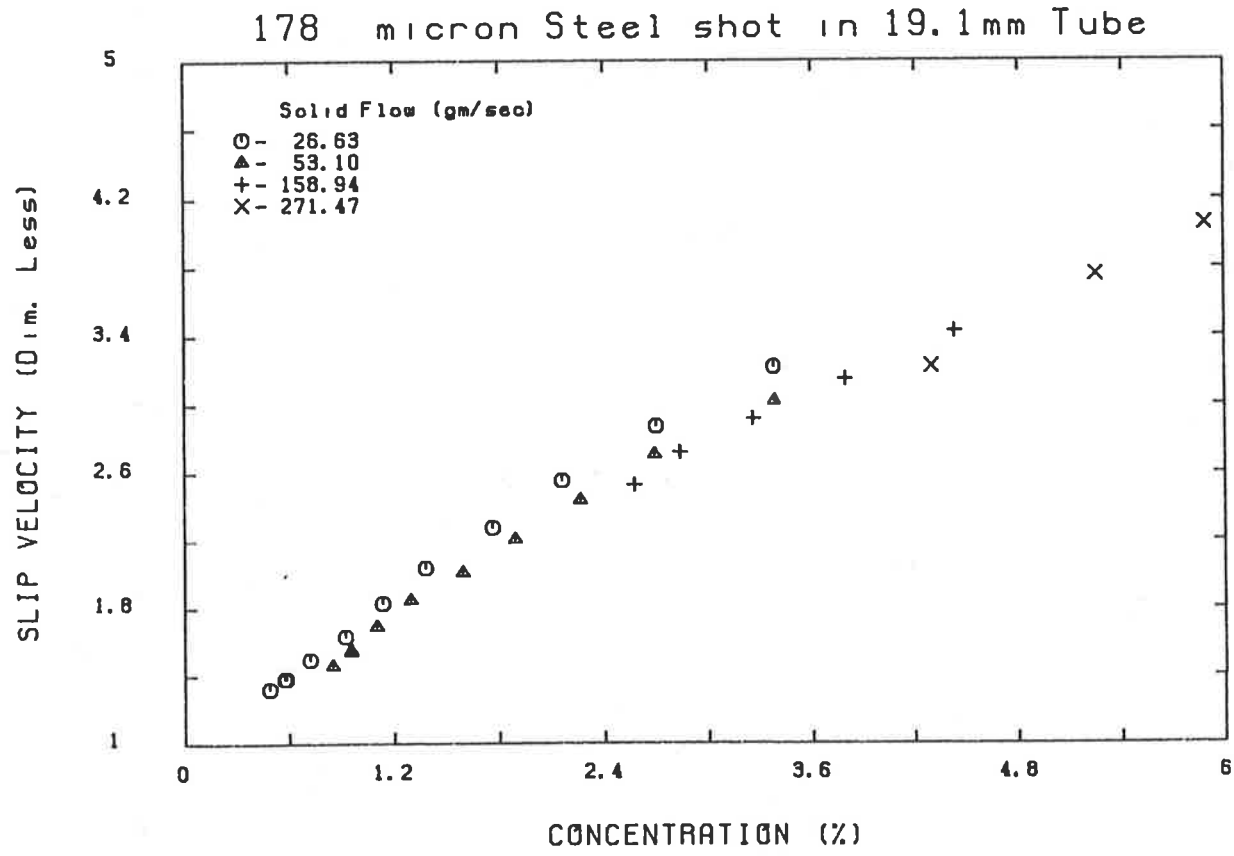
178 micron Steel shot in 19.1mm Tube
Solid Flow (gm/sec)
- 26.63
- 53.10
- 158.94
- 271.47
SLIP VELOCITY (Dim. Less)
CONCENTRATION (%)
5
4.2
3.4
2.6
1.8
1
0
1.2
2.4
3.6
4.8
6

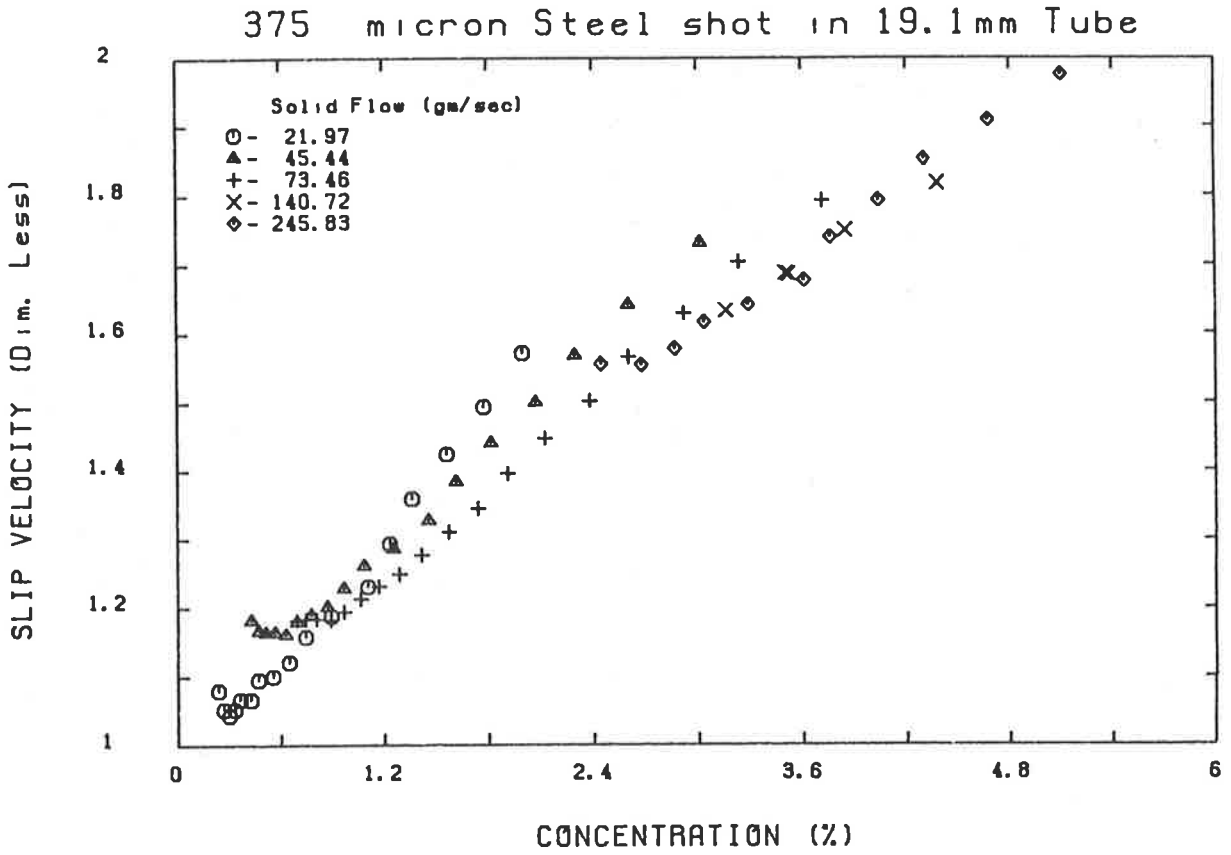
375 micron Steel shot in 19.1mm Tube
Solid Flow (gm/sec)
- 21.97
- 45.44
- 73.46
- 140.72
- 245.83
SLIP VELOCITY (Dim. Less)
CONCENTRATION (%)
2
1.8
1.6
1.4
1.2
1
0
1.2
2.4
3.6
4.8
6

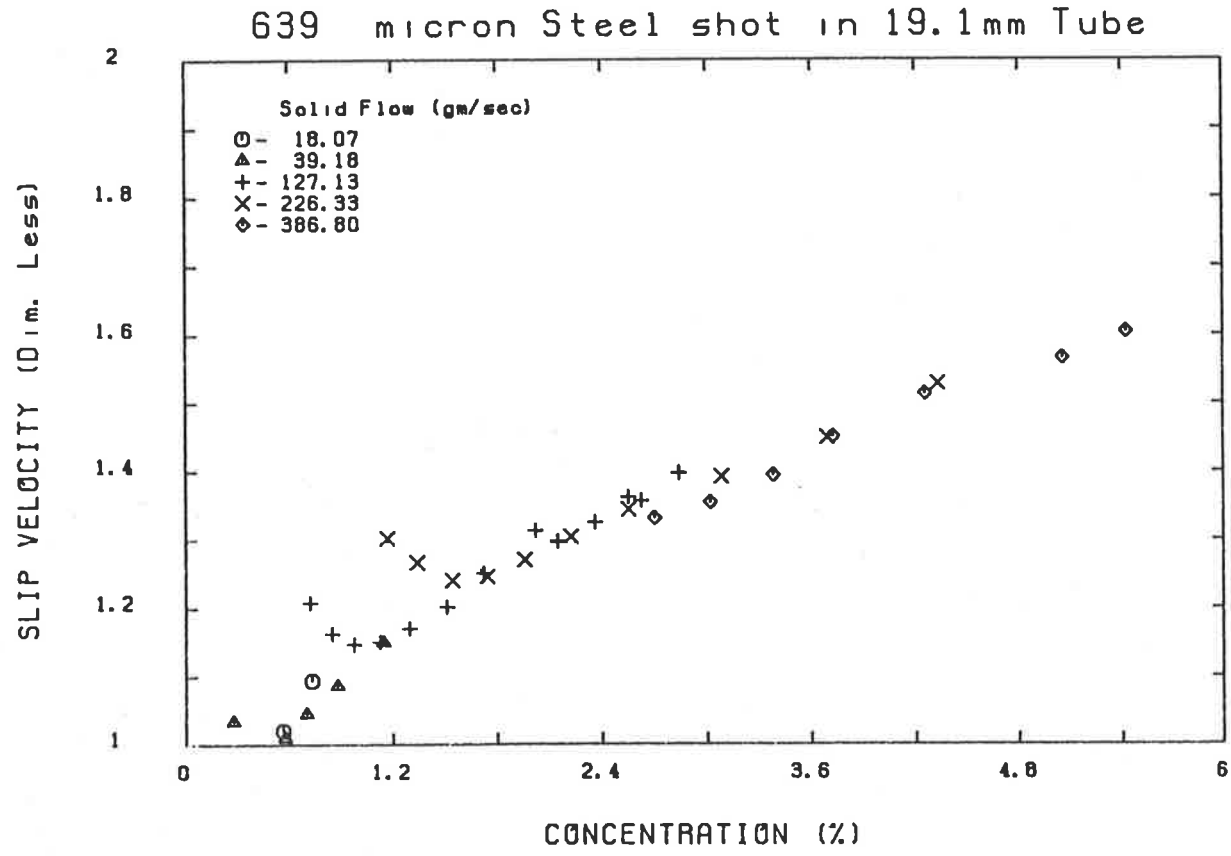
639 micron Steel shot in 19.1mm Tube
Solid Flow (gm/sec)
- 18.07
- 39.18
- 127.13
- 226.33
- 386.80
SLIP VELOCITY (Dim. Less)
CONCENTRATION (%)
2
1.8
1.6
1.4
1.2
1
0
1.2
2.4
3.6
4.8
6

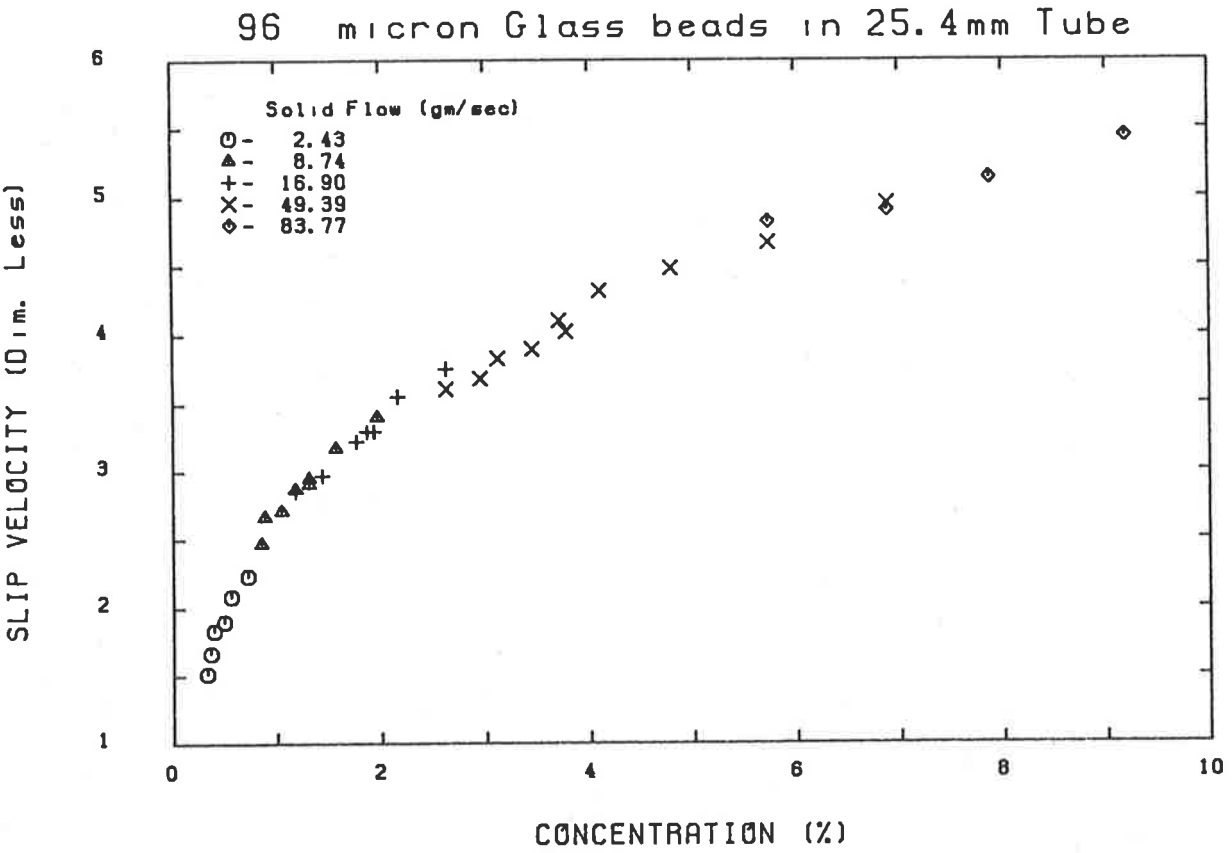
96 micron Glass beads in 25.4mm Tube
Solid Flow (gm/sec)
- 2.43
- 8.74
- 16.90
- 49.39
- 83.77
SLIP VELOCITY (Dim. Less)
CONCENTRATION (%)
1
2
3
4
5
6
0
2
4
6
8
10

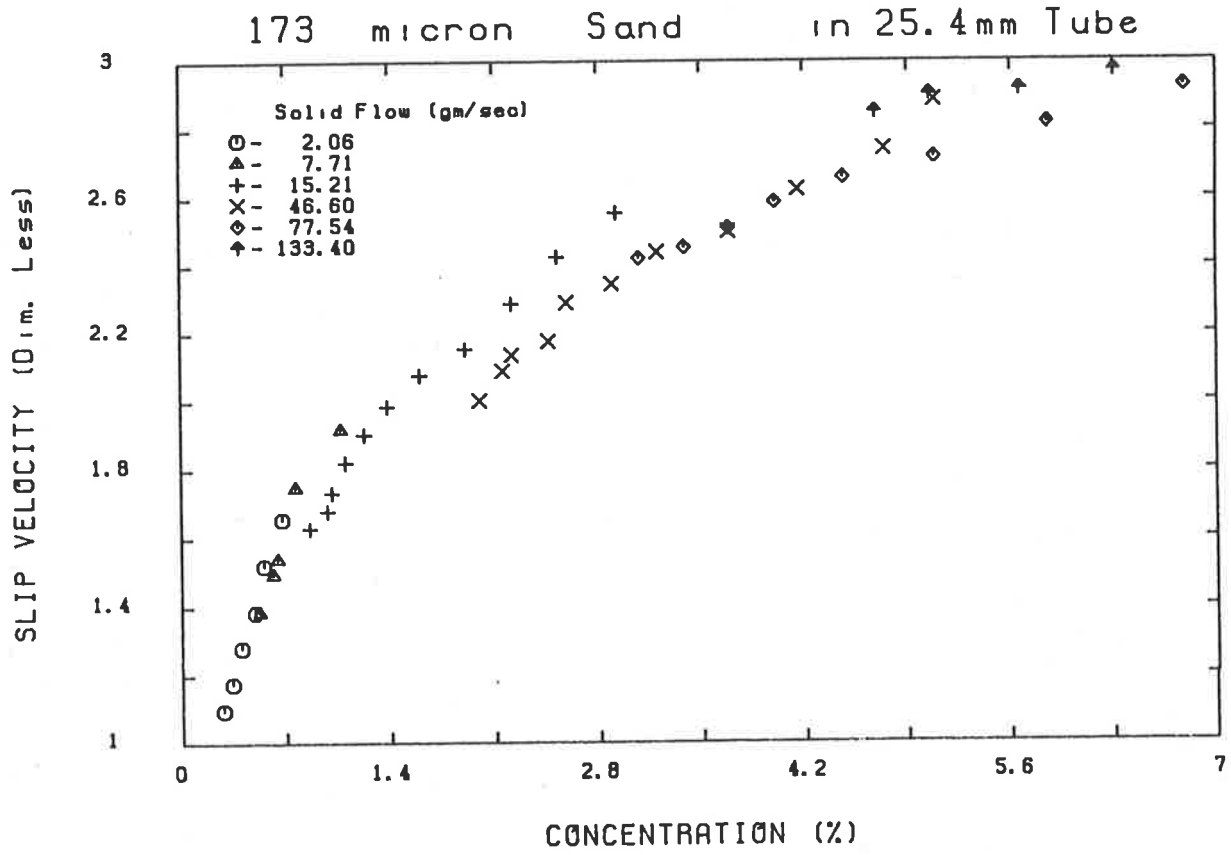
173 micron Sand in 25.4mm Tube
Solid Flow (gm/sec)
- 2.06
- 7.71
- 15.21
- 46.60
- 77.54
- 133.40
SLIP VELOCITY (Dim. Less)
CONCENTRATION (%)
1
1.4
1.8
2.2
2.6
3
0
1.4
2.8
4.2
5.6
7

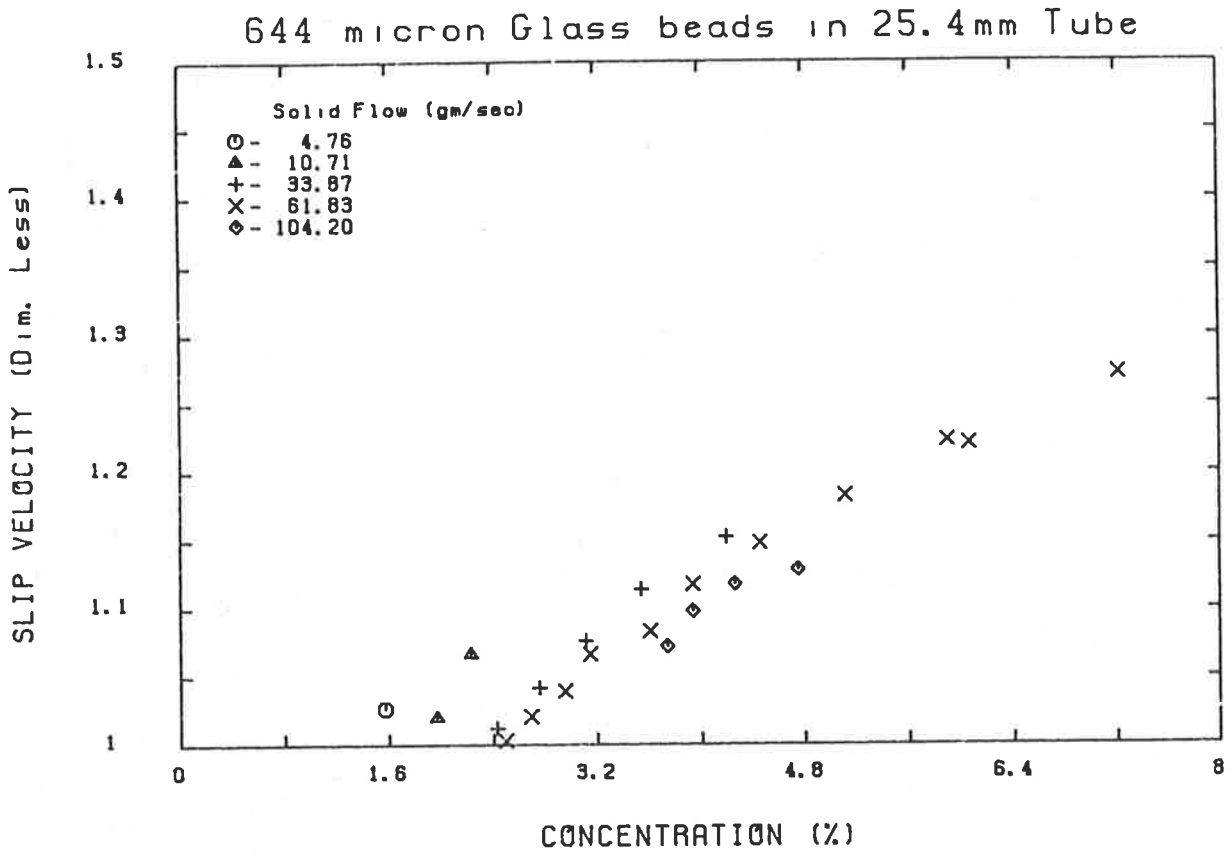
644 micron Glass beads in 25.4mm Tube
Solid Flow (gm/sec)
- 4.76
- 10.71
- 33.87
- 61.83
- 104.20
SLIP VELOCITY (Dim. Less)
1.5
1.4
1.3
1.2
1.1
1
0
1.6
3.2
4.8
6.4
8
CONCENTRATION (%)

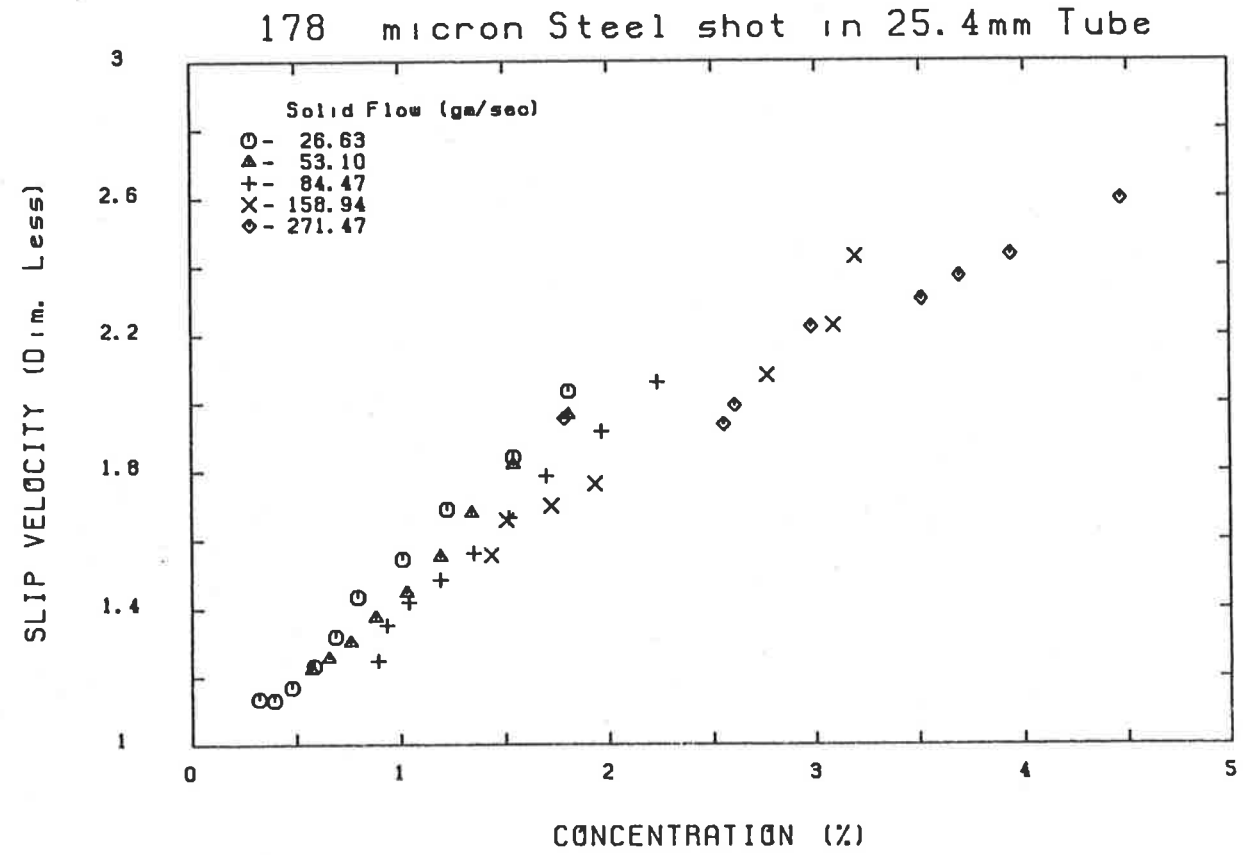
178 micron Steel shot in 25.4mm Tube
Solid Flow (gm/sec)
- 26.63
- 53.10
- 84.47
- 158.94
- 271.47
SLIP VELOCITY (Dim. Less)
3
2.6
2.2
1.8
1.4
1
0
1
2
3
4
5
CONCENTRATION (%)

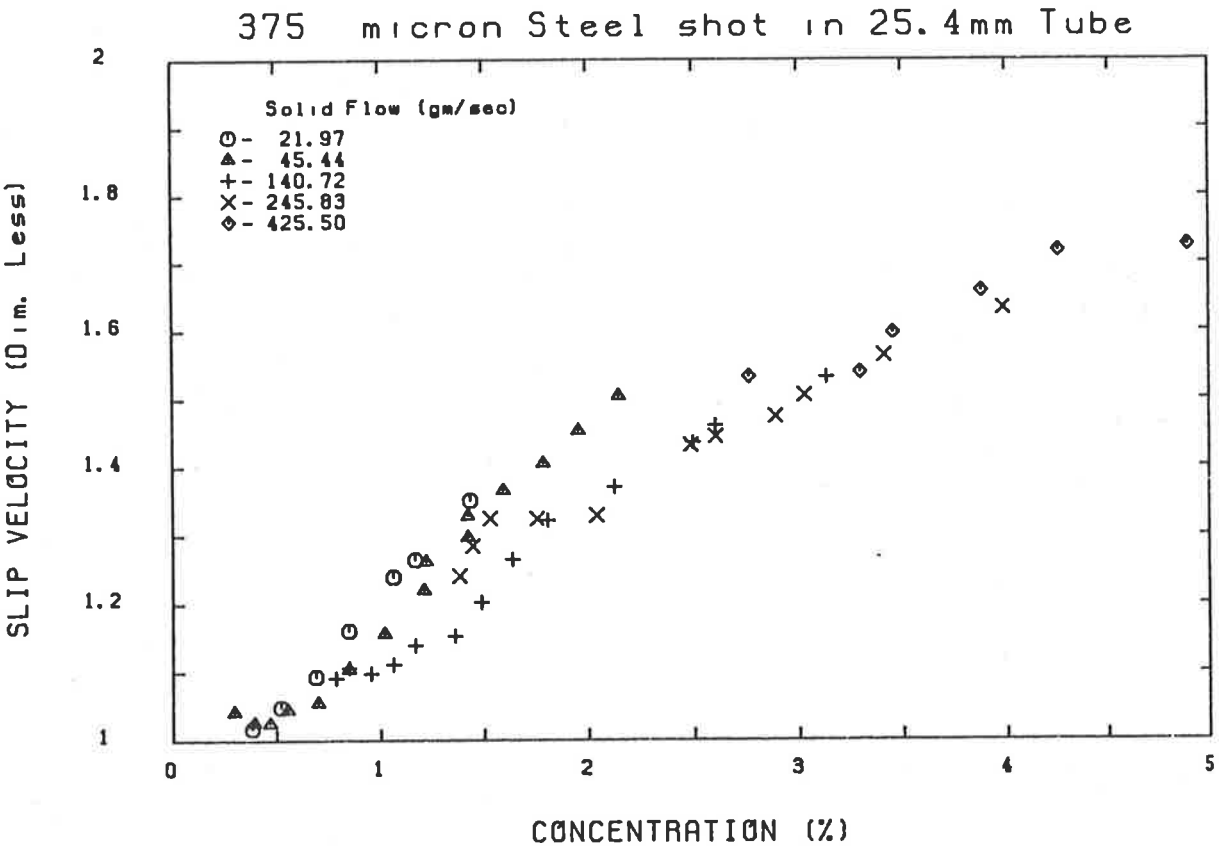
375 micron Steel shot in 25.4mm Tube
Solid Flow (gm/sec)
⊙- 21.97
▲- 45.44
+- 140.72
×- 245.83
◇- 425.50
SLIP VELOCITY (Dim. Less)
CONCENTRATION (%)
2
1.8
1.6
1.4
1.2
1
0
1
2
3
4
5

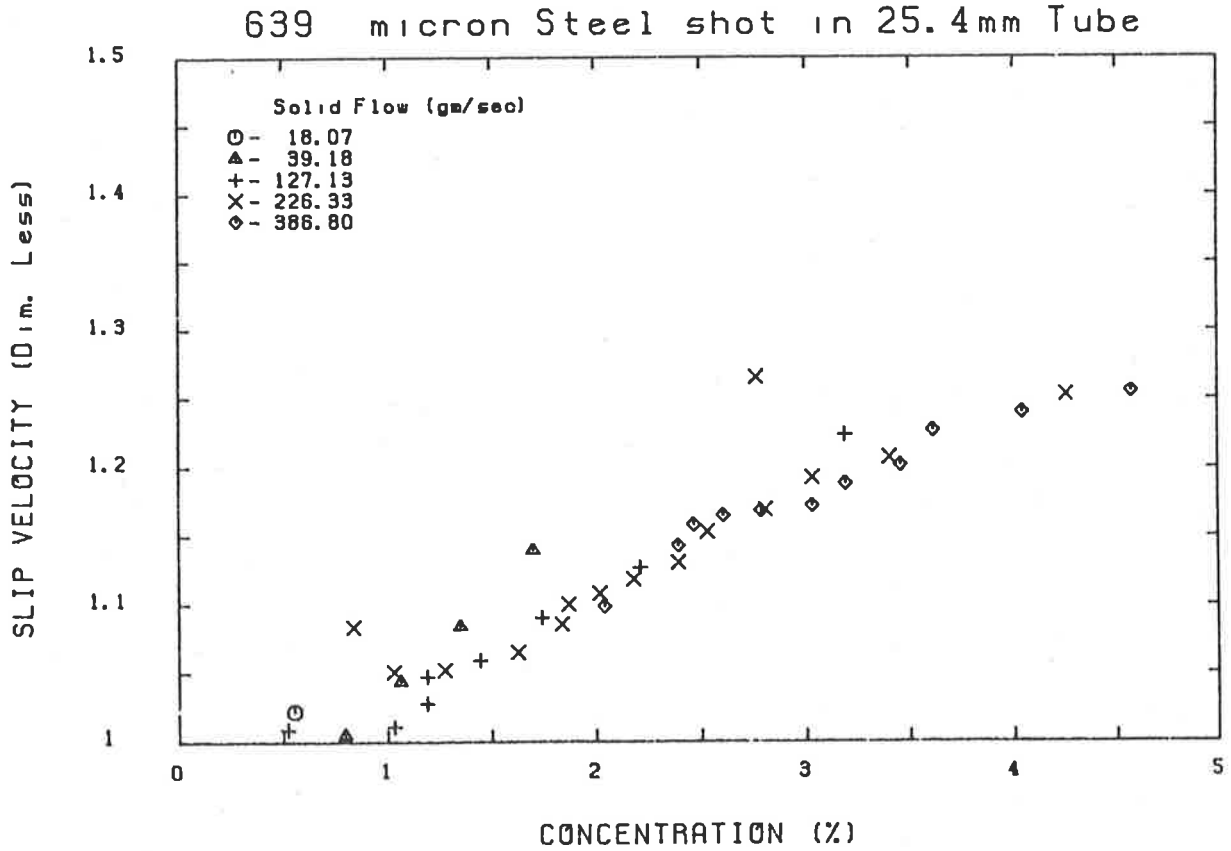
639 micron Steel shot in 25.4mm Tube
Solid Flow (gm/sec)
⊙- 18.07
▲- 39.18
+- 127.13
×- 226.33
◇- 386.80
SLIP VELOCITY (Dim. Less)
CONCENTRATION (%)
1.5
1.4
1.3
1.2
1.1
1
0
1
2
3
4
5

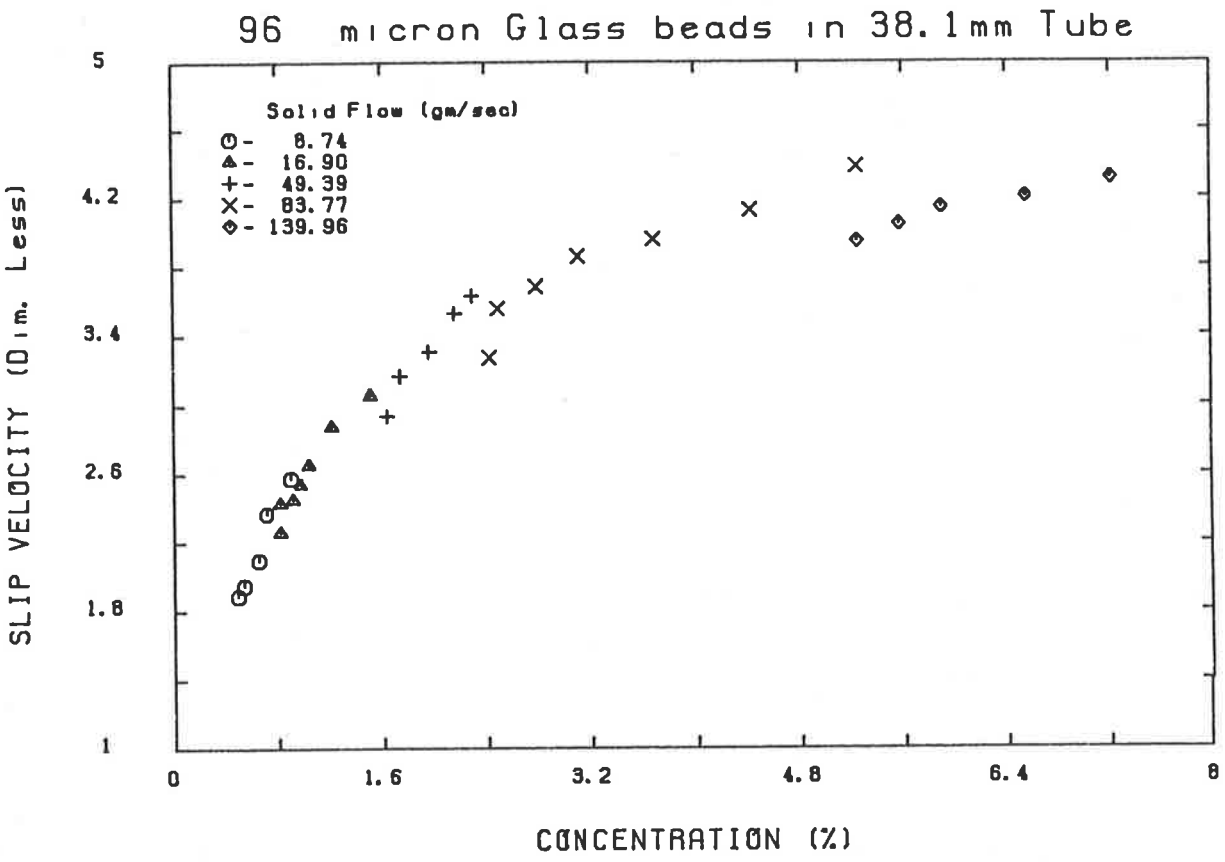
96 micron Glass beads in 38.1mm Tube
Solid Flow (gm/sec)
⊙- 8.74
▲- 16.90
+- 49.39
×- 83.77
◇- 139.96
SLIP VELOCITY (Dim. Less)
CONCENTRATION (%)
5
4.2
3.4
2.6
1.8
1
0
1.6
3.2
4.8
6.4
8

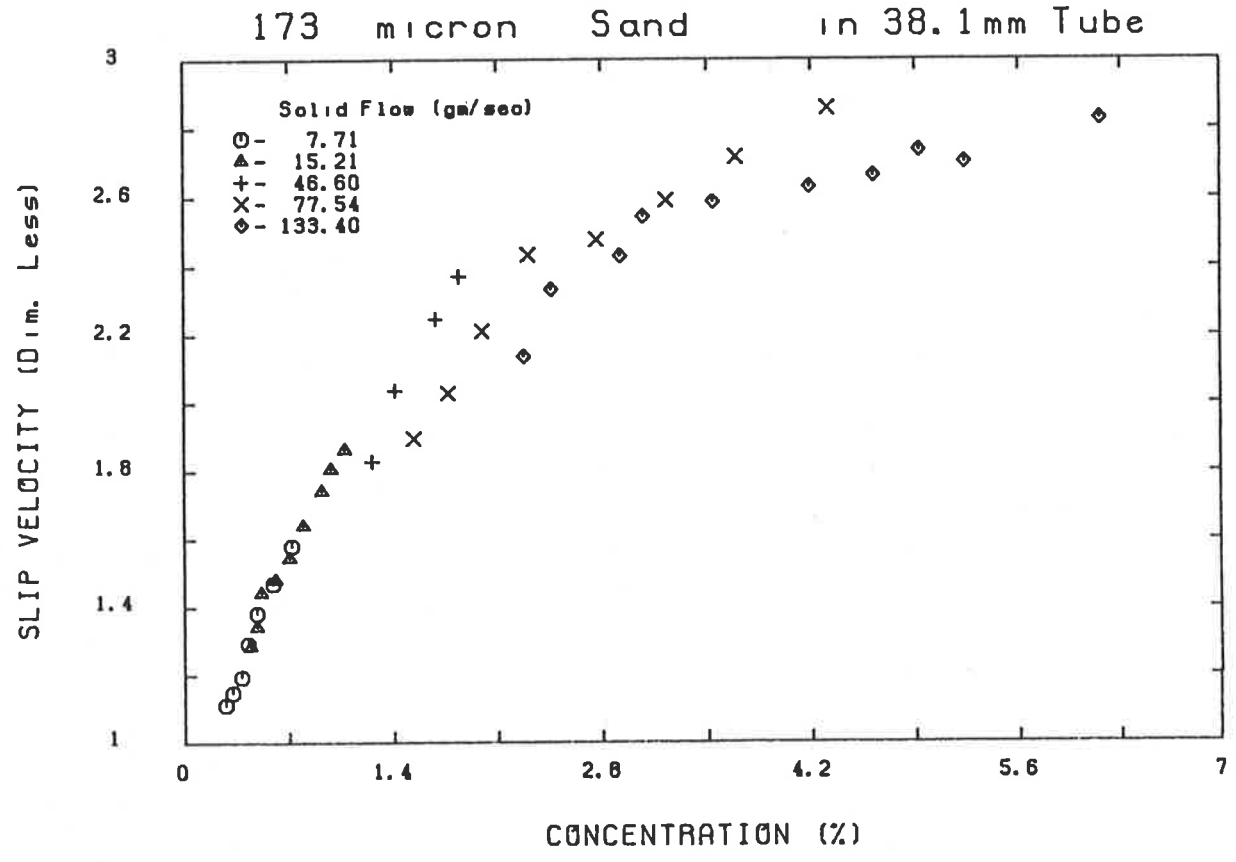
173 micron Sand in 38.1mm Tube
Solid Flow (gm/sec)
⊙- 7.71
▲- 15.21
+- 46.60
×- 77.54
◇- 133.40
SLIP VELOCITY (Dim. Less)
CONCENTRATION (%)
3
2.6
2.2
1.8
1.4
1
0
1.4
2.8
4.2
5.6
7

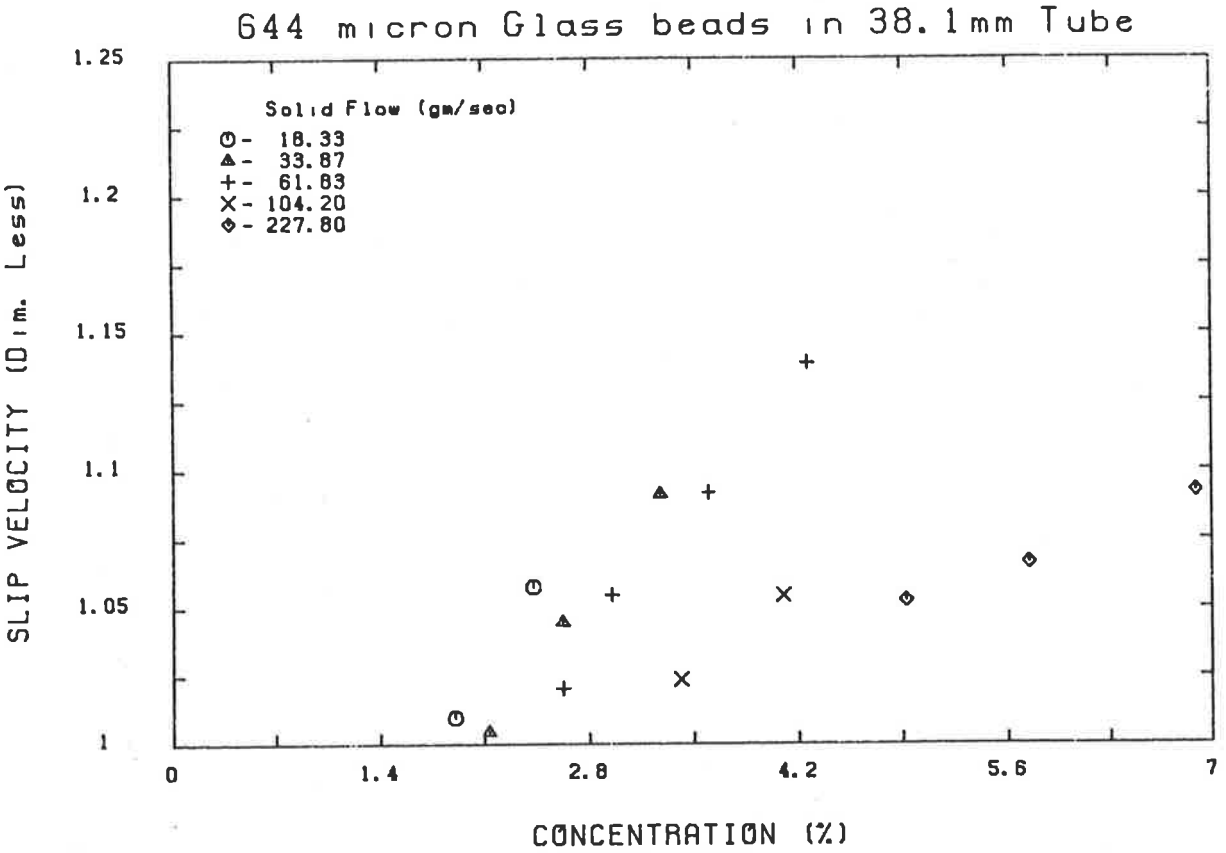
644 micron Glass beads in 38.1mm Tube
Solid Flow (gm/sec)
⊙- 18.33
▲- 33.87
+- 61.83
X- 104.20
◇- 227.80
SLIP VELOCITY (Dim. Less)
1.25
1.2
1.15
1.1
1.05
1
0
1.4
2.8
4.2
5.6
7
CONCENTRATION (%)

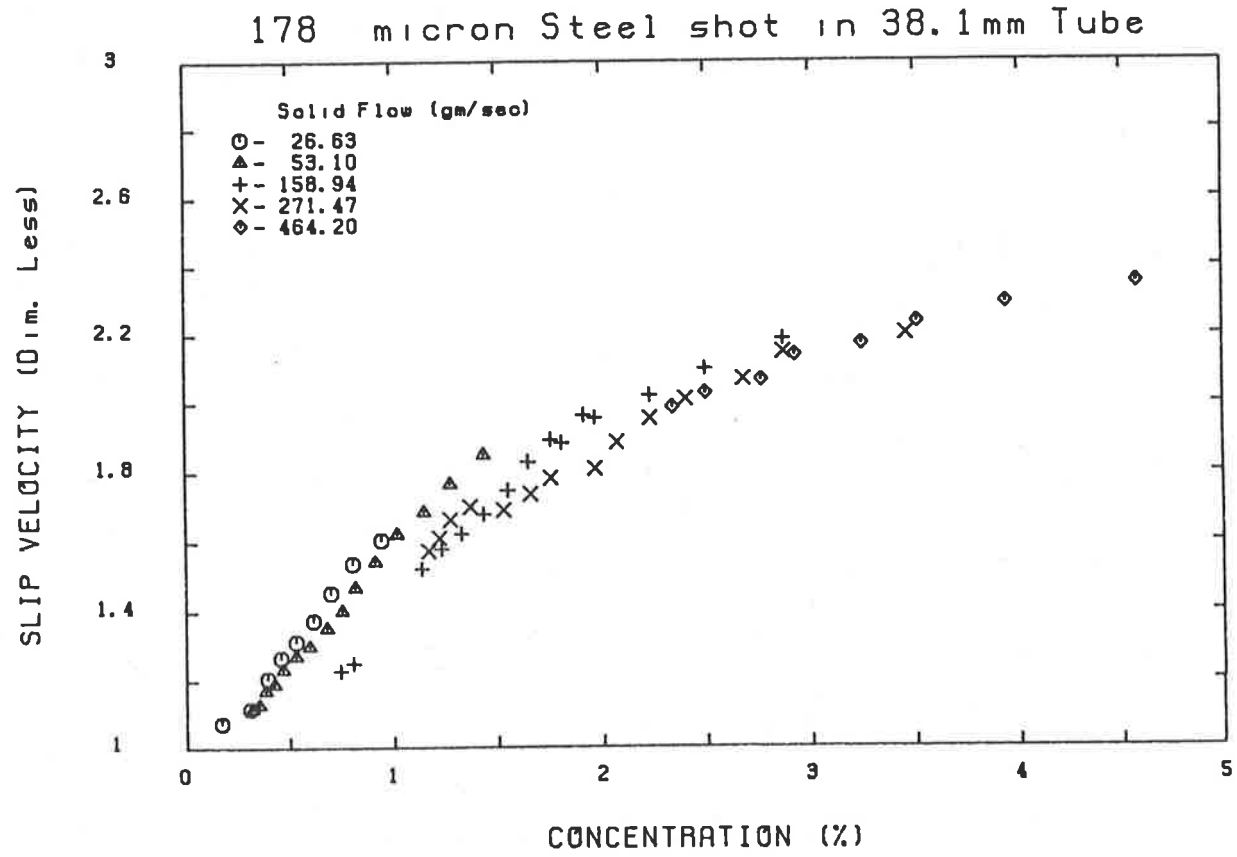
178 micron Steel shot in 38.1mm Tube
Solid Flow (gm/sec)
⊙- 26.63
▲- 53.10
+- 158.94
X- 271.47
◇- 464.20
SLIP VELOCITY (Dim. Less)
3
2.6
2.2
1.8
1.4
1
0
1
2
3
4
5
CONCENTRATION (%)

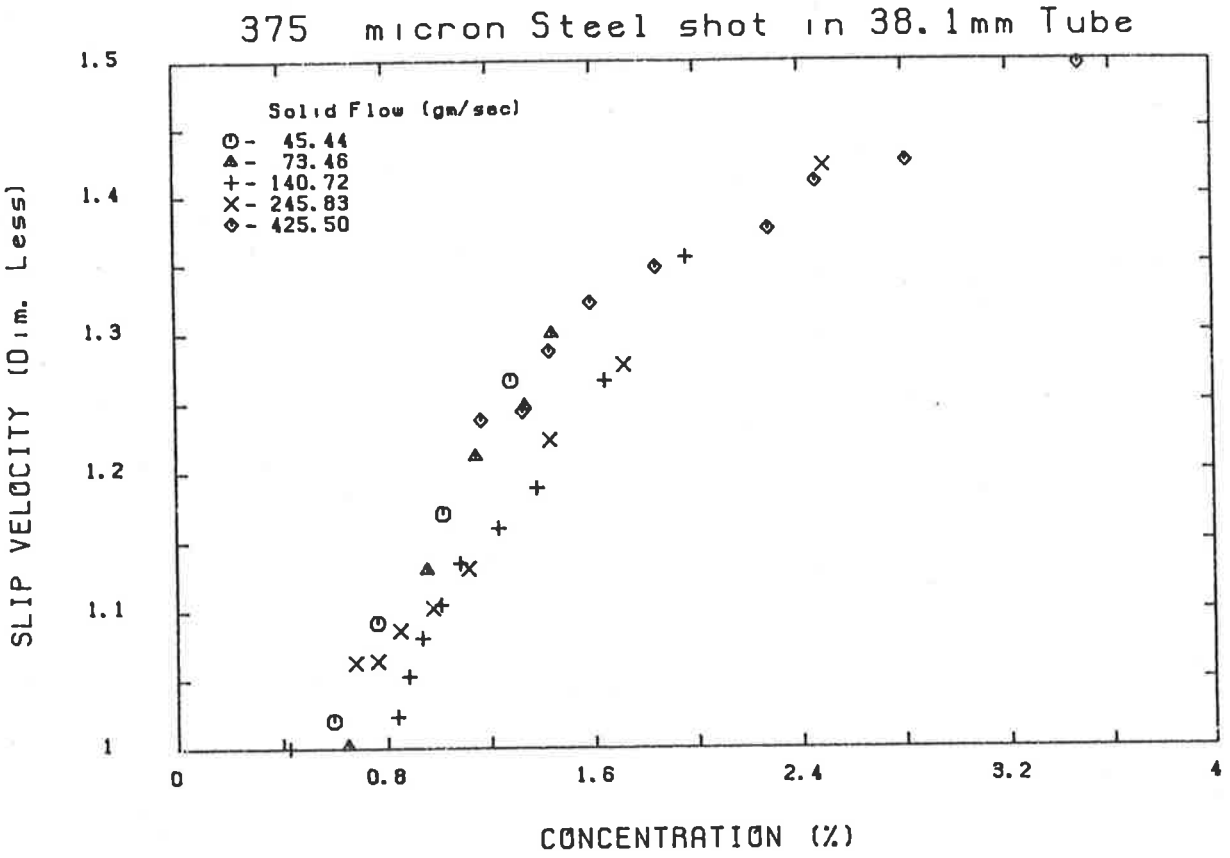
375 micron Steel shot in 38.1mm Tube
Solid Flow (gm/sec)
- 45.44
- 73.46
- 140.72
- 245.83
- 425.50
SLIP VELOCITY (Dim. Less)
CONCENTRATION (%)
1.5
1.4
1.3
1.2
1.1
1
0
0.8
1.6
2.4
3.2
4

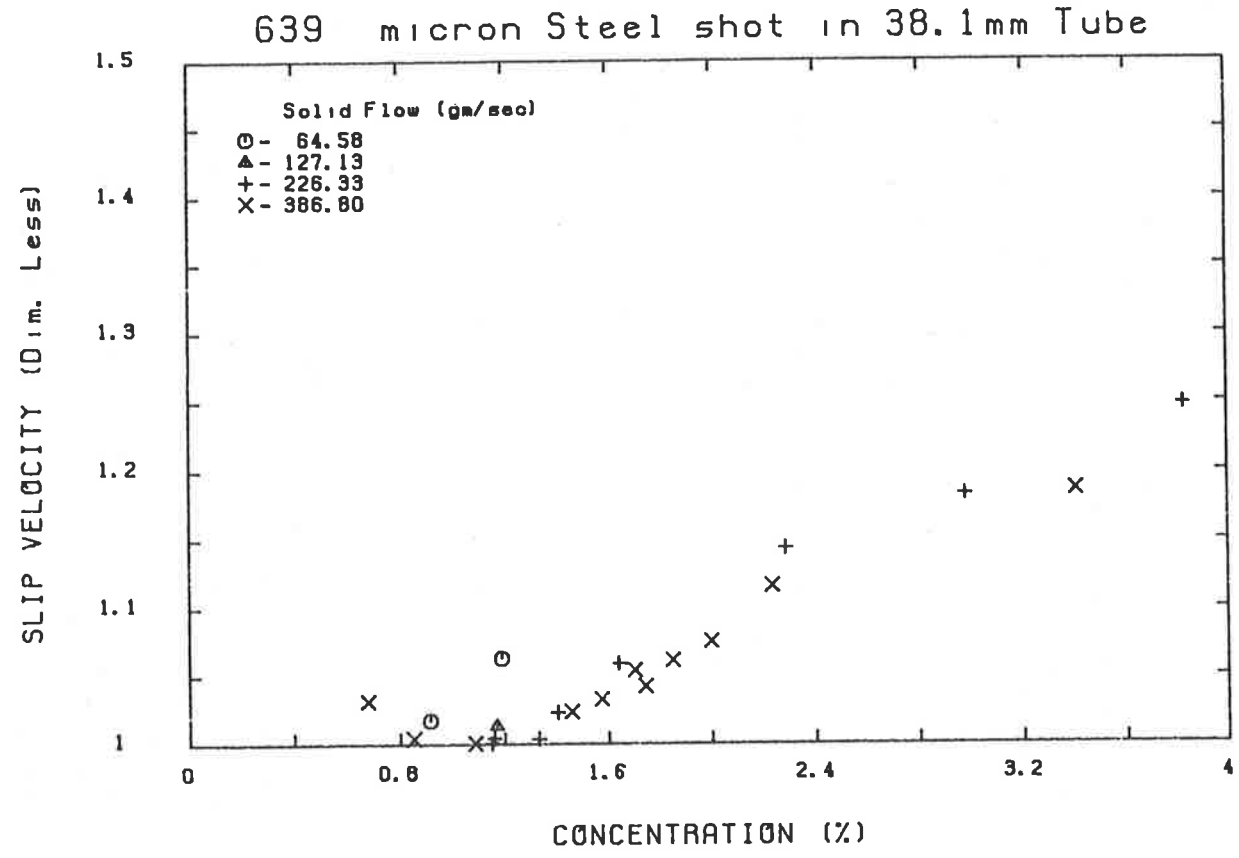
639 micron Steel shot in 38.1mm Tube
Solid Flow (gm/sec)
- 64.58
- 127.13
- 226.33
- 386.80
SLIP VELOCITY (Dim. Less)
CONCENTRATION (%)
1.5
1.4
1.3
1.2
1.1
1
0
0.8
1.6
2.4
3.2
4

APPENDIX (C)

EFFECT OF PARTICLE PROPERTIES ON SLIP VELOCITY

COUNTERCURRENT TRANSPORT DATA

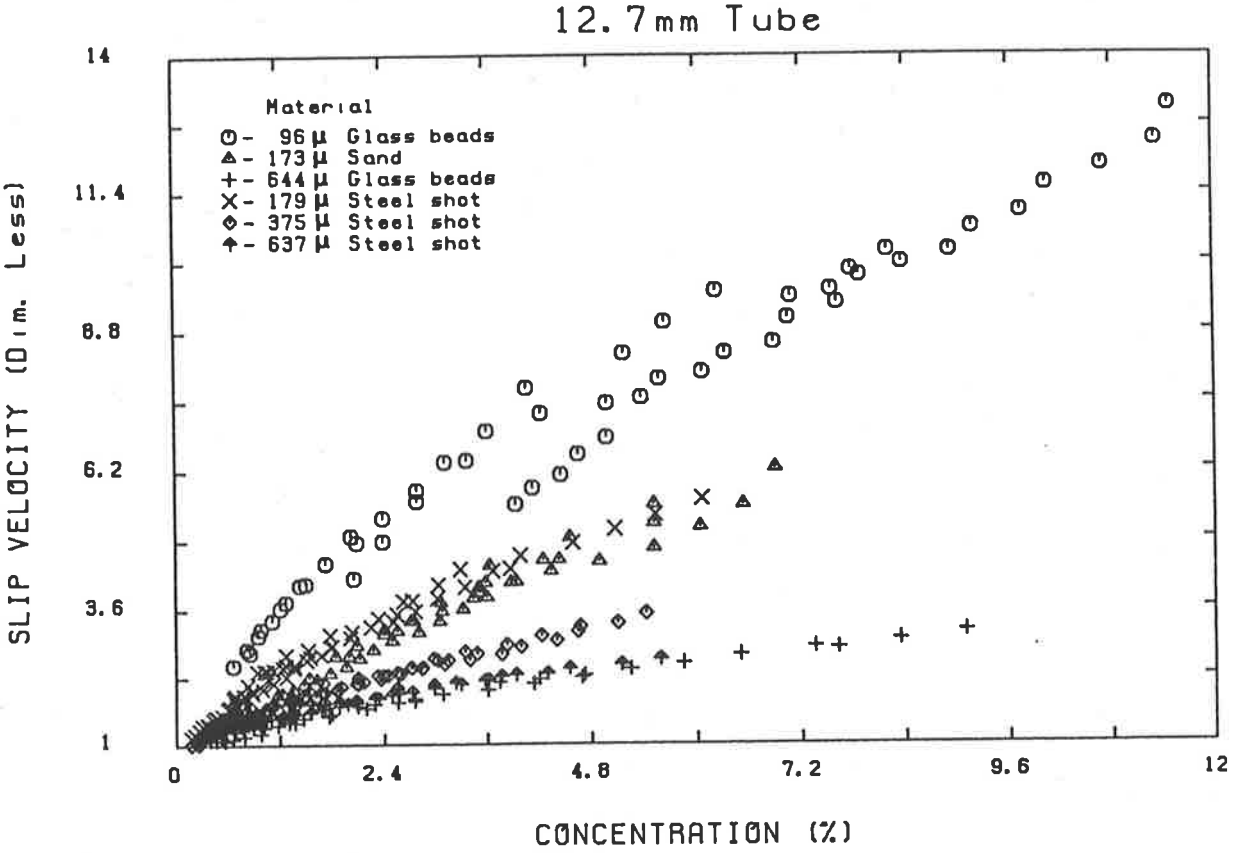
12.7mm Tube
Material
- 96 µ Glass beads
- 173 µ Sand
- 644 µ Glass beads
- 179 µ Steel shot
- 375 µ Steel shot
- 637 µ Steel shot
SLIP VELOCITY (Dim. Less)
14
11.4
8.8
6.2
3.6
1
0
2.4
4.8
7.2
9.6
12
CONCENTRATION (%)

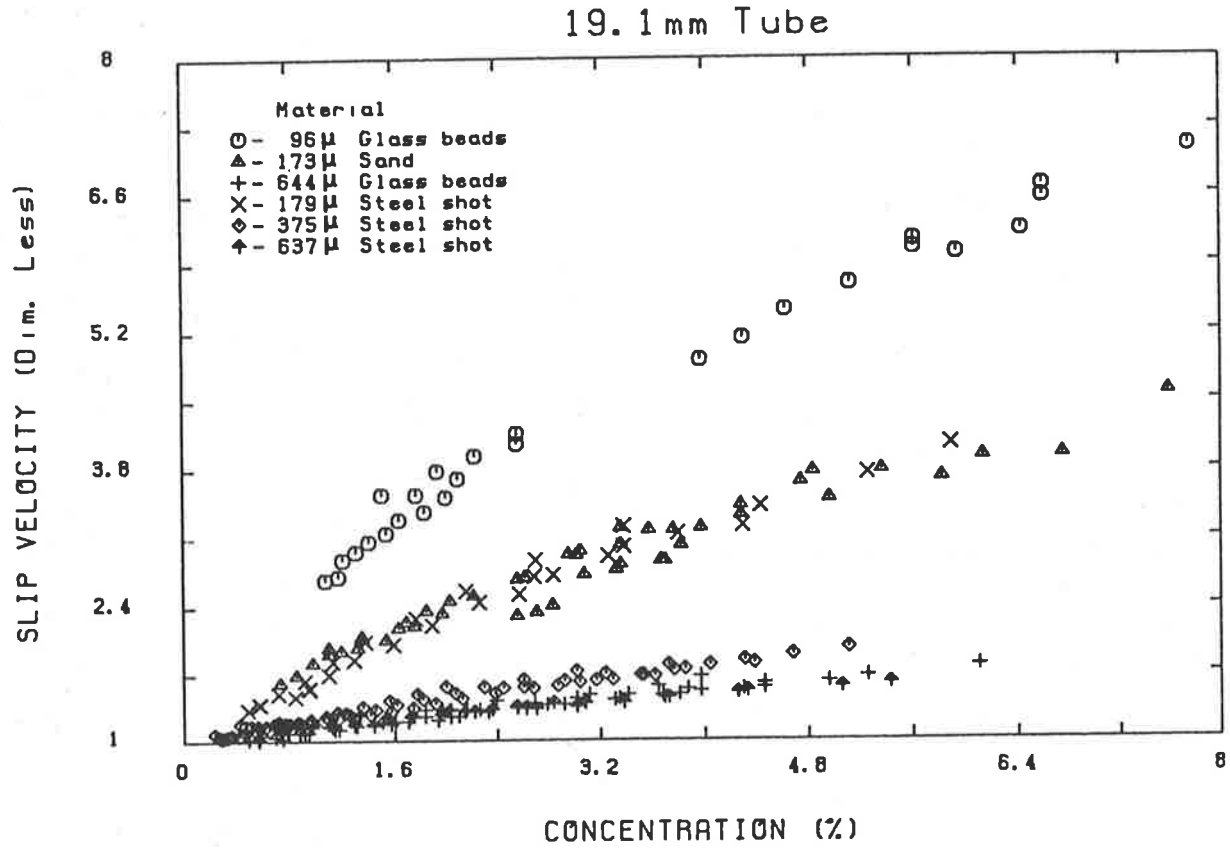
19.1mm Tube
Material
- 96 µ Glass beads
- 173 µ Sand
- 644 µ Glass beads
- 179 µ Steel shot
- 375 µ Steel shot
- 637 µ Steel shot
SLIP VELOCITY (Dim. Less)
8
6.6
5.2
3.8
2.4
1
0
1.6
3.2
4.8
6.4
8
CONCENTRATION (%)

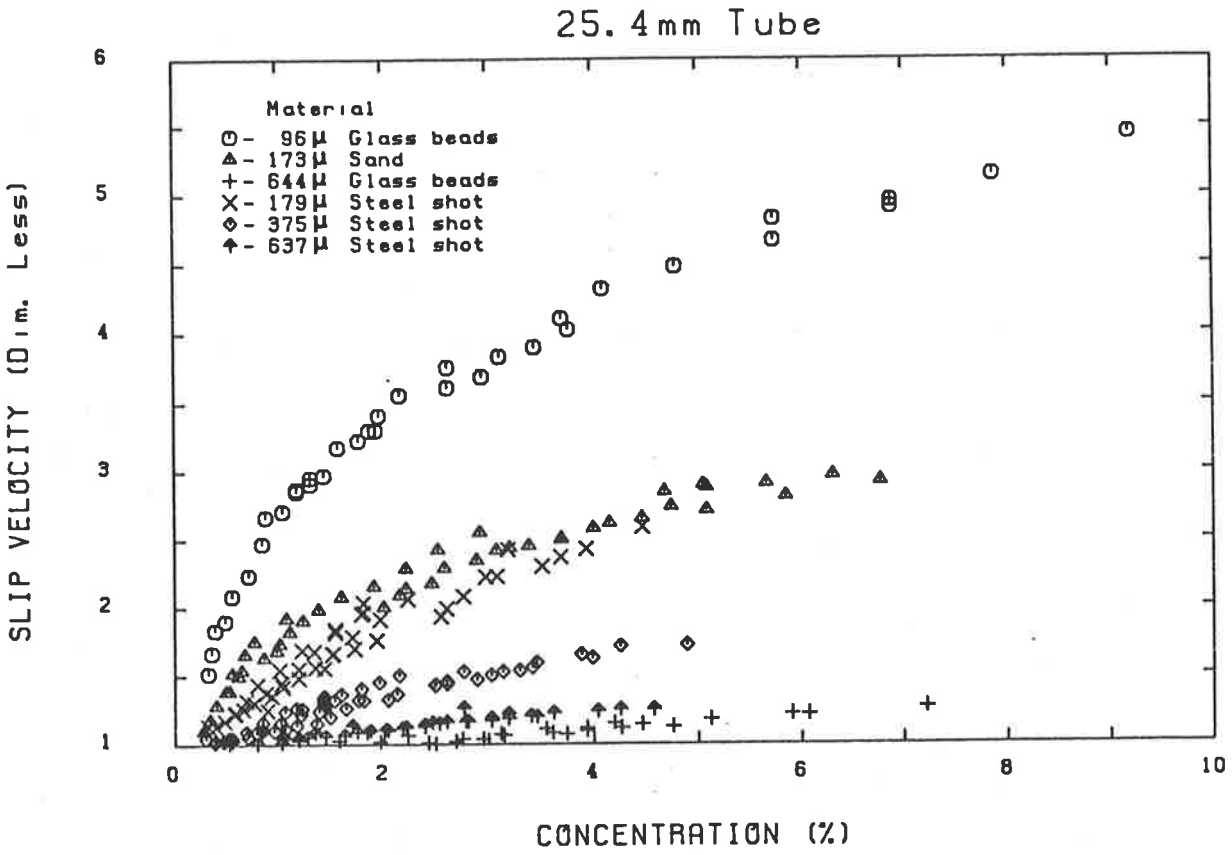
25.4mm Tube
Material
⊙- 96μ Glass beads
△- 173μ Sand
+- 644μ Glass beads
×- 179μ Steel shot
◇- 375μ Steel shot
↑- 637μ Steel shot
SLIP VELOCITY (Dim. Less)
CONCENTRATION (%)
1
2
3
4
5
6
0
2
4
6
8
10

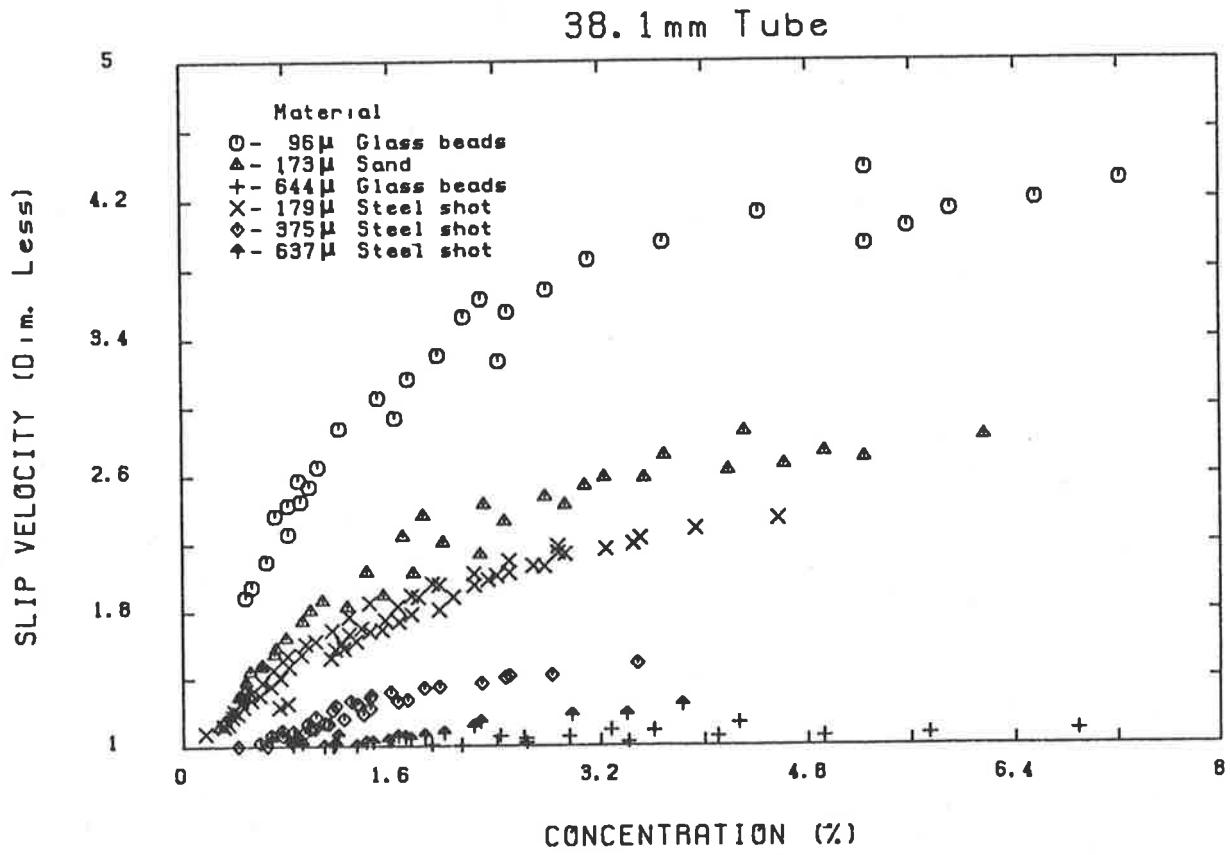
38.1mm Tube
Material
⊙- 96μ Glass beads
△- 173μ Sand
+- 644μ Glass beads
×- 179μ Steel shot
◇- 375μ Steel shot
↑- 637μ Steel shot
SLIP VELOCITY (Dim. Less)
CONCENTRATION (%)
1
1.8
2.6
3.4
4.2
5
0
1.6
3.2
4.8
6.4
8

APPENDIX (D)

EFFECT OF TUBE DIAMETER ON SLIP VELOCITY COUNTERCURRENT TRANSPORT DATA

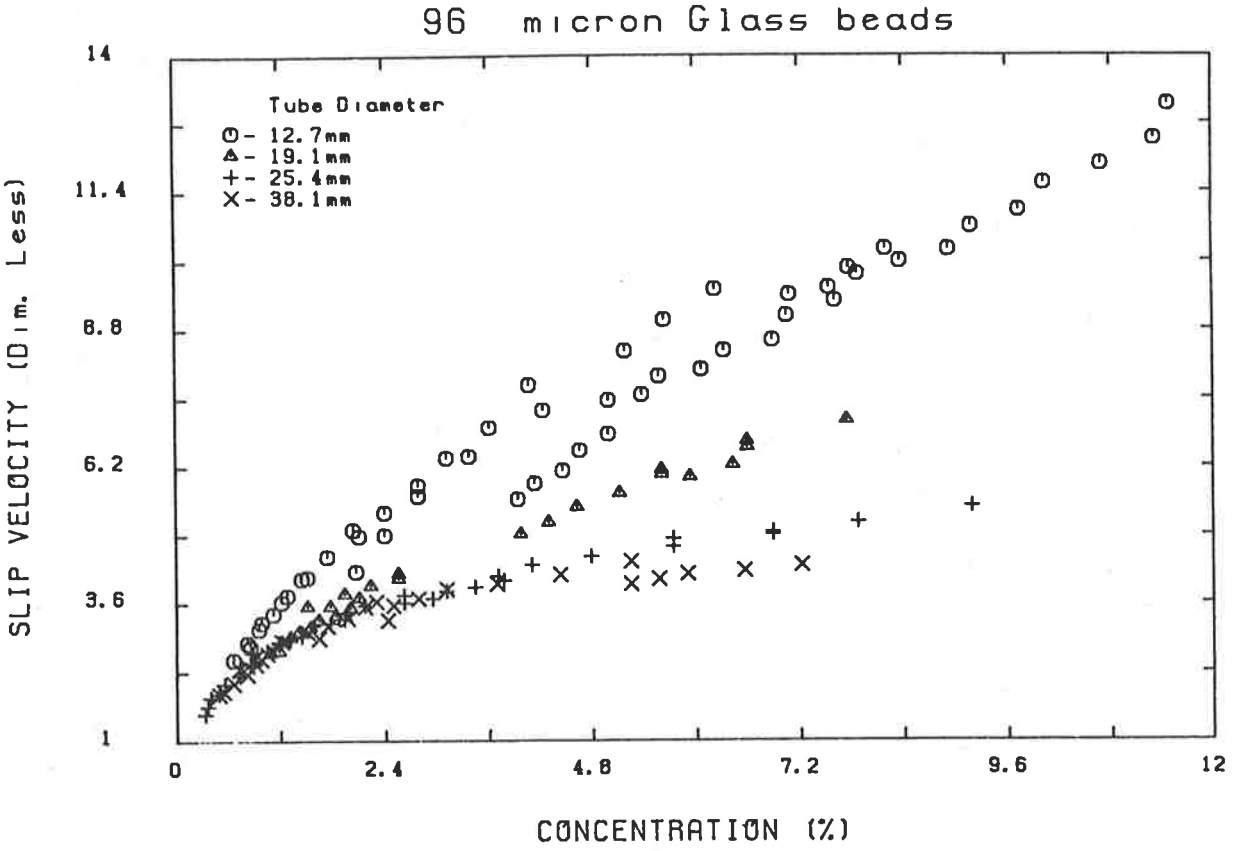
96 micron Glass beads
Tube Diameter
O- 12.7mm
Δ- 19.1mm
+- 25.4mm
X- 38.1mm
SLIP VELOCITY (Dim. Less)
14
11.4
8.8
6.2
3.6
1
0
2.4
4.8
7.2
9.6
12
CONCENTRATION (%)

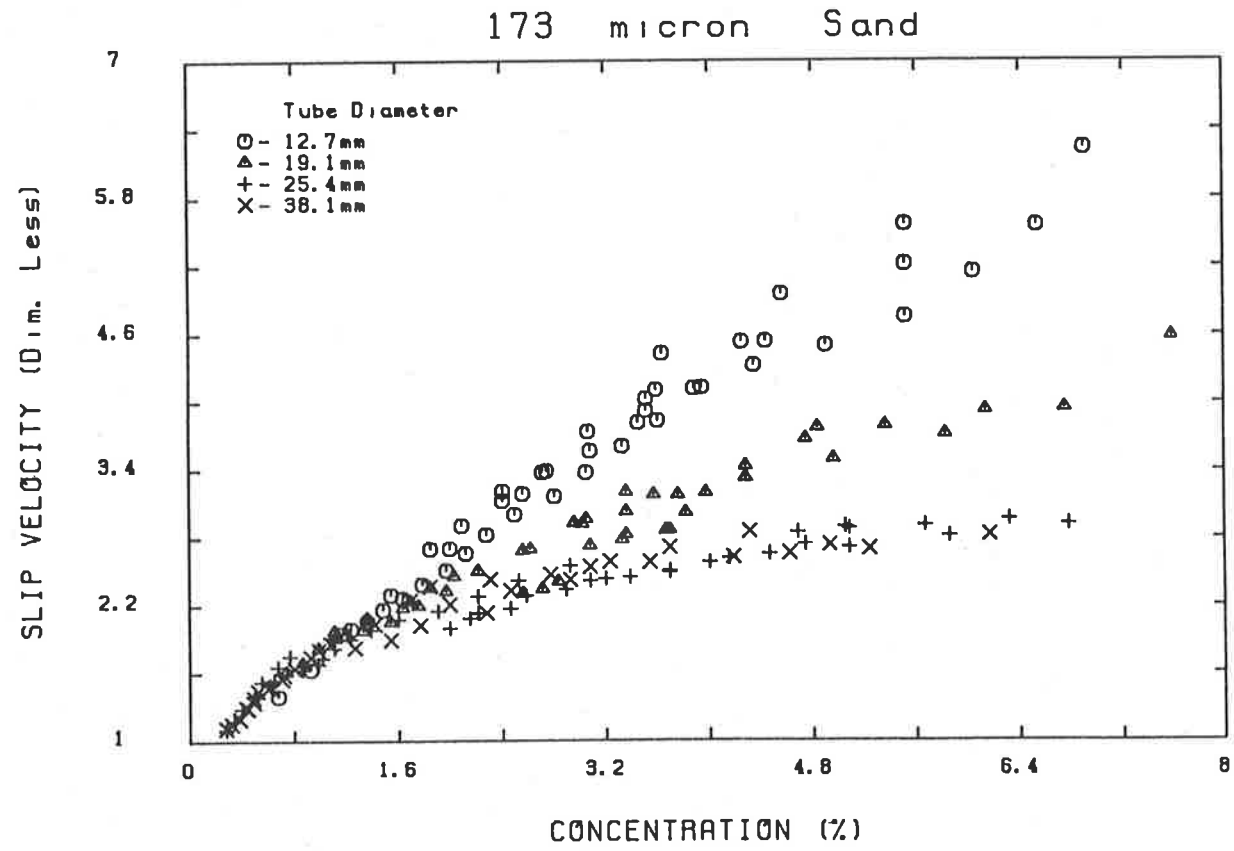
173 micron Sand
Tube Diameter
O- 12.7mm
Δ- 19.1mm
+- 25.4mm
X- 38.1mm
SLIP VELOCITY (Dim. Less)
7
5.8
4.6
3.4
2.2
1
0
1.6
3.2
4.8
6.4
8
CONCENTRATION (%)

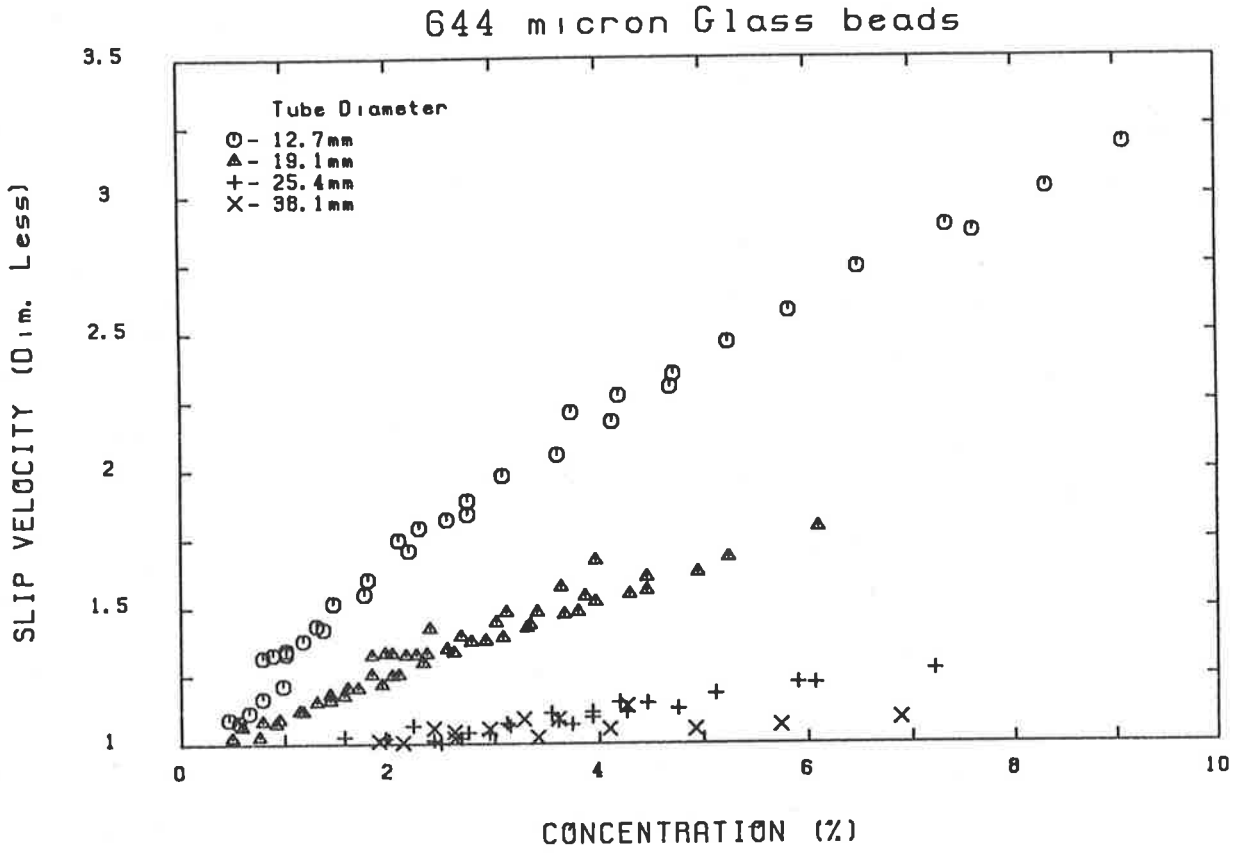
644 micron Glass beads
Tube Diameter
O- 12.7mm
Δ- 19.1mm
+- 25.4mm
X- 38.1mm
SLIP VELOCITY (Dim. Less)
CONCENTRATION (%)
3.5
3
2.5
2
1.5
1
0
2
4
6
8
10

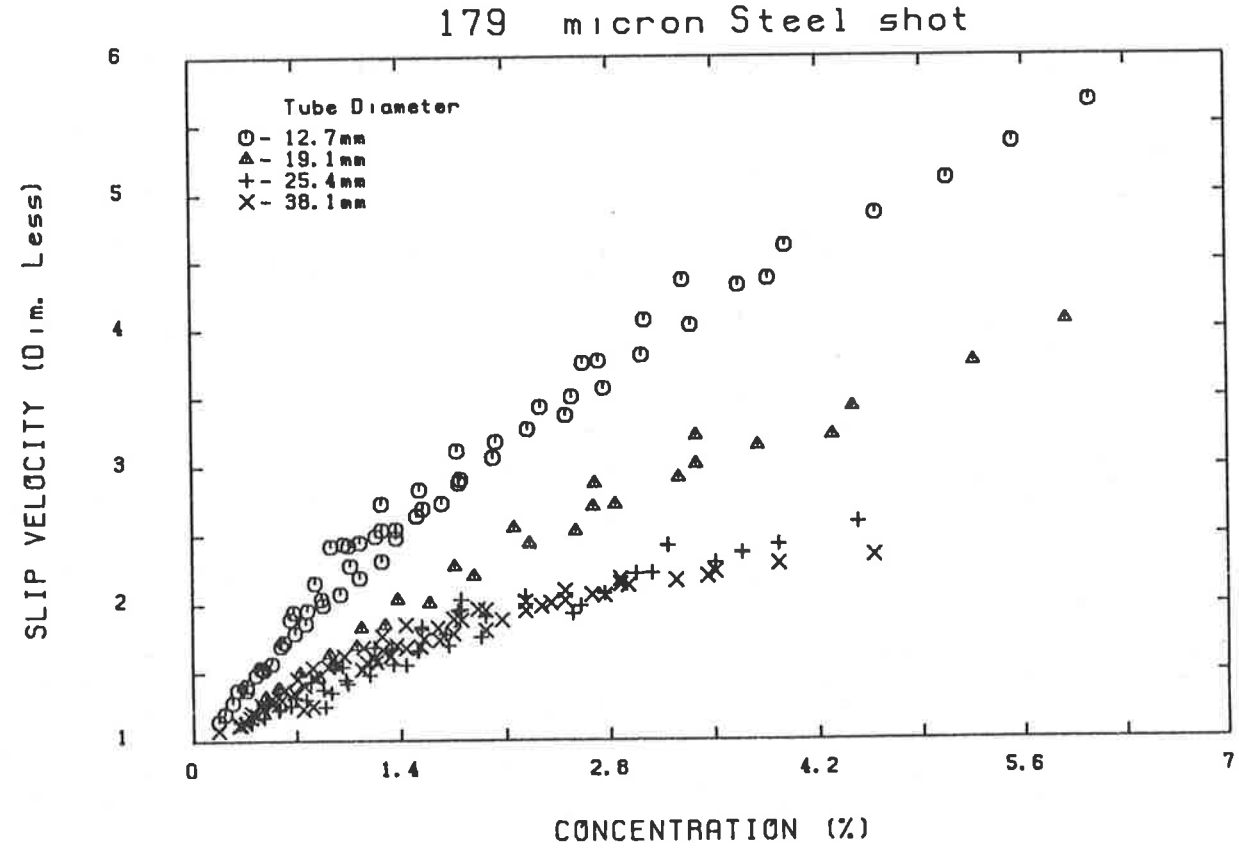
179 micron Steel shot
Tube Diameter
O- 12.7mm
Δ- 19.1mm
+- 25.4mm
X- 38.1mm
SLIP VELOCITY (Dim. Less)
CONCENTRATION (%)
6
5
4
3
2
1
0
1.4
2.8
4.2
5.6
7

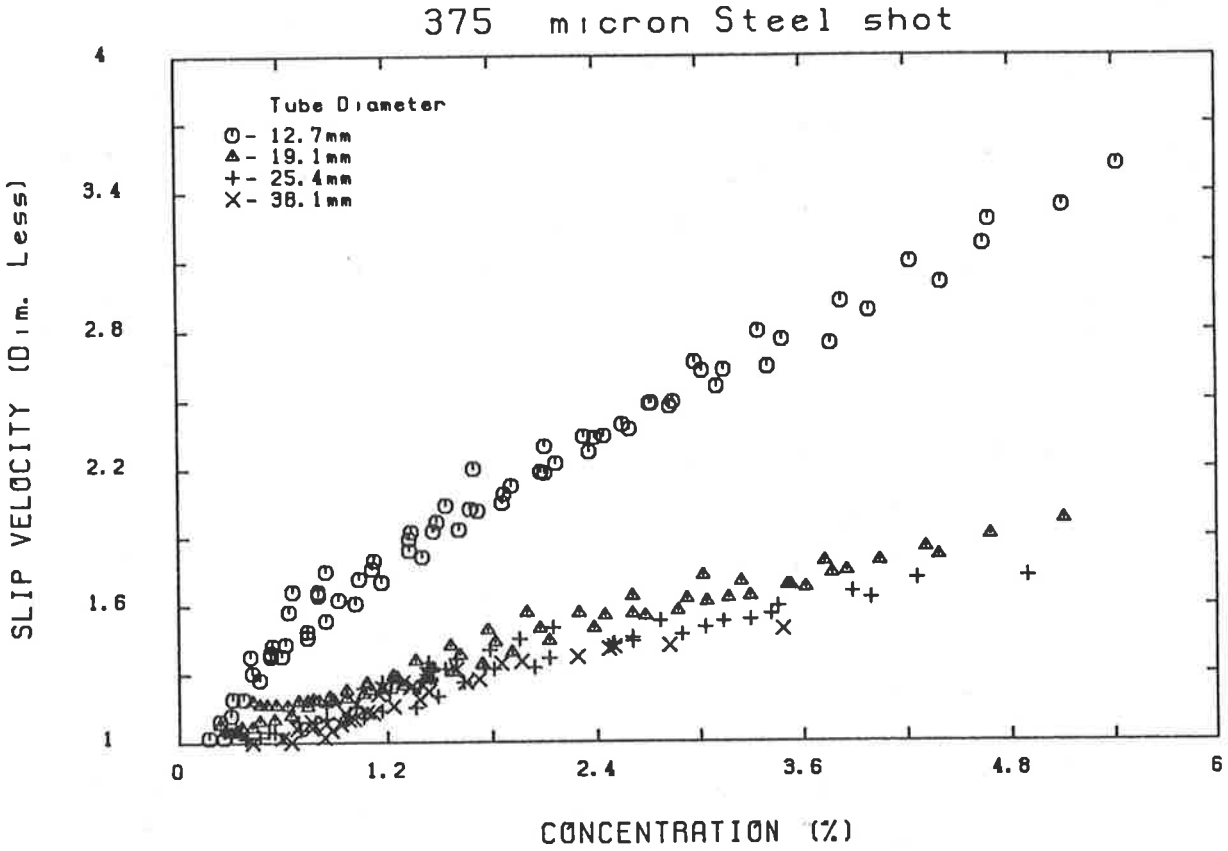
375 micron Steel shot
Tube Diameter
O- 12.7mm
Δ- 19.1mm
+- 25.4mm
X- 38.1mm
SLIP VELOCITY (Dim. Less)
CONCENTRATION (%)
4
3.4
2.8
2.2
1.6
1
0
1.2
2.4
3.6
4.8
6

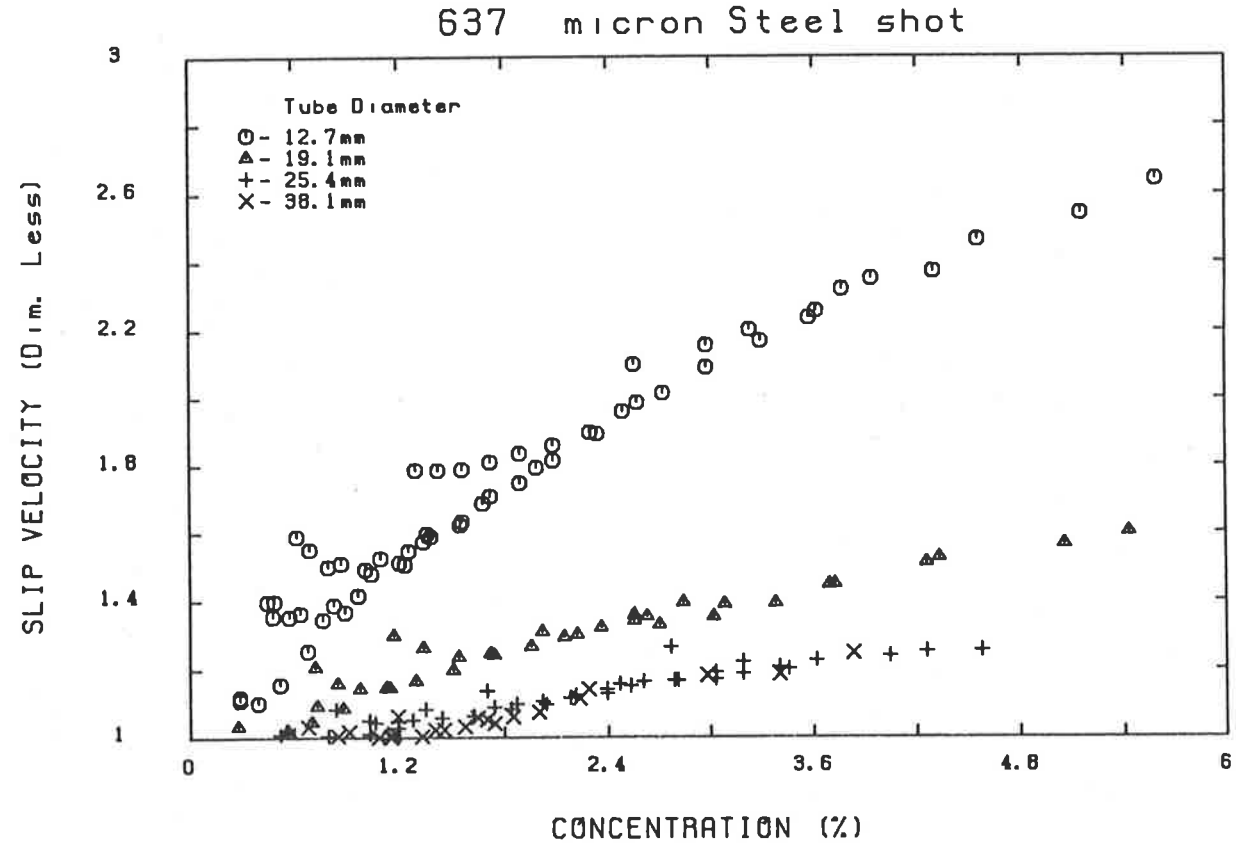
637 micron Steel shot
Tube Diameter
O- 12.7mm
Δ- 19.1mm
+- 25.4mm
X- 38.1mm
SLIP VELOCITY (Dim. Less)
CONCENTRATION (%)
3
2.6
2.2
1.8
1.4
1
0
1.2
2.4
3.6
4.8
6

APPENDIX (E)

TEST OF GRADIENT COAGULATION MODEL

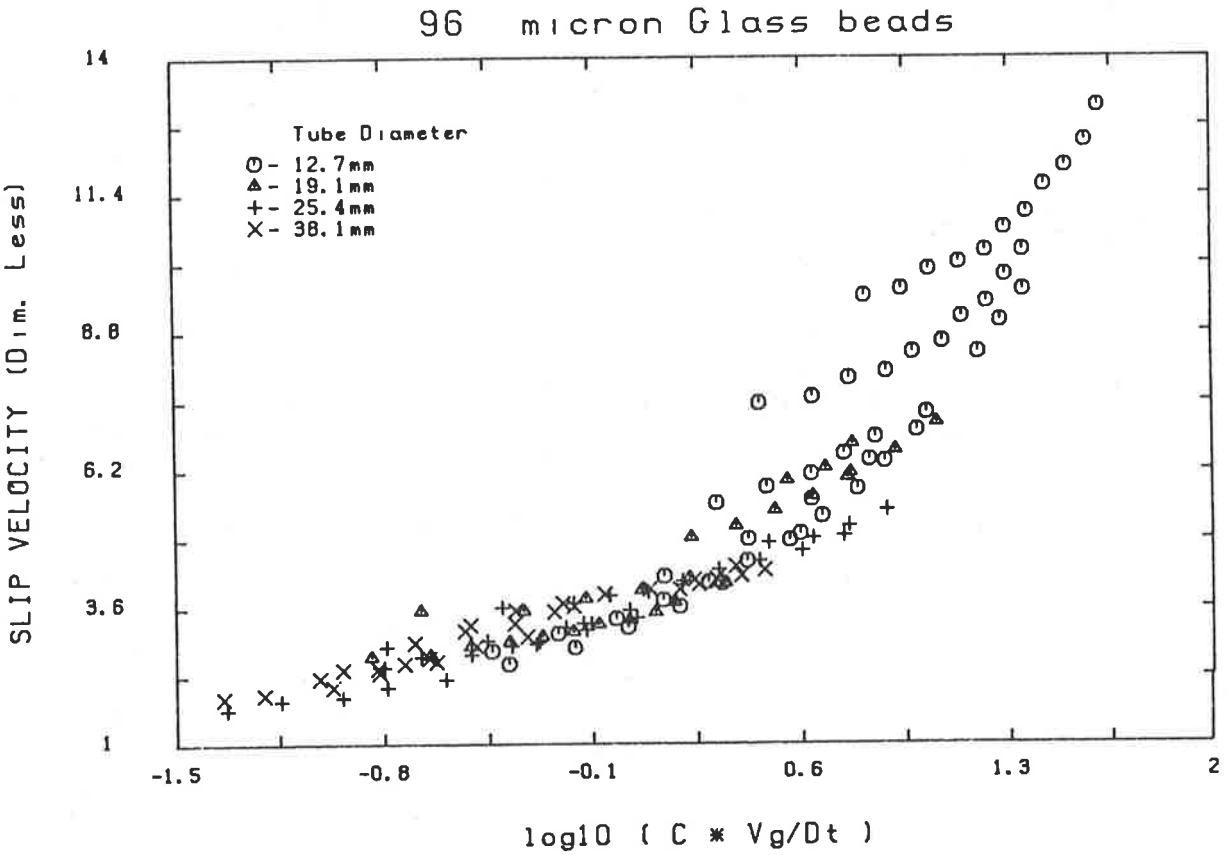
96 micron Glass beads
Tube Diameter
O- 12.7mm
Δ- 19.1mm
+- 25.4mm
X- 38.1mm
SLIP VELOCITY (Dim. Less)
14
11.4
8.8
6.2
3.6
1
-1.5
-0.8
-0.1
0.6
1.3
2
log10 (C * Vg/Dt)

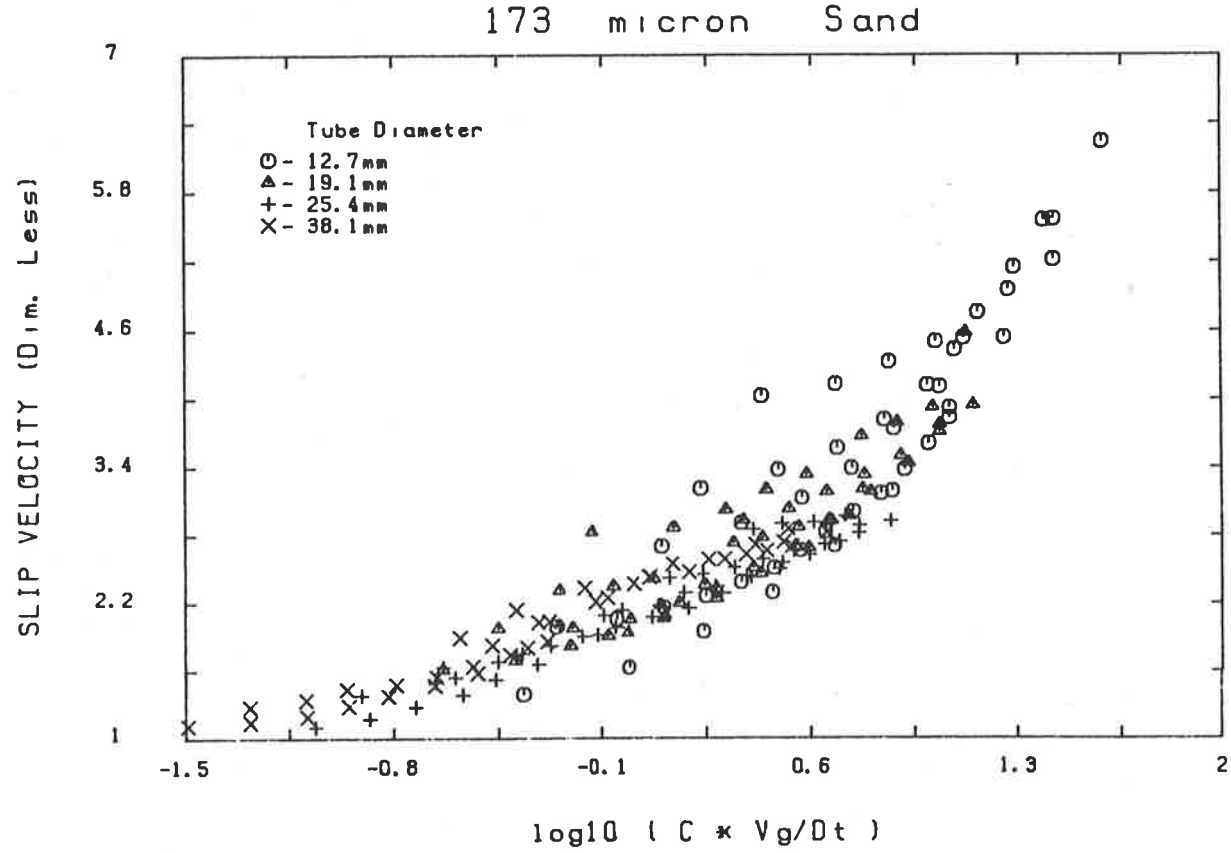
173 micron Sand
Tube Diameter
O- 12.7mm
Δ- 19.1mm
+- 25.4mm
X- 38.1mm
SLIP VELOCITY (Dim. Less)
7
5.8
4.6
3.4
2.2
1
-1.5
-0.8
-0.1
0.6
1.3
2
log10 (C * Vg/Dt)

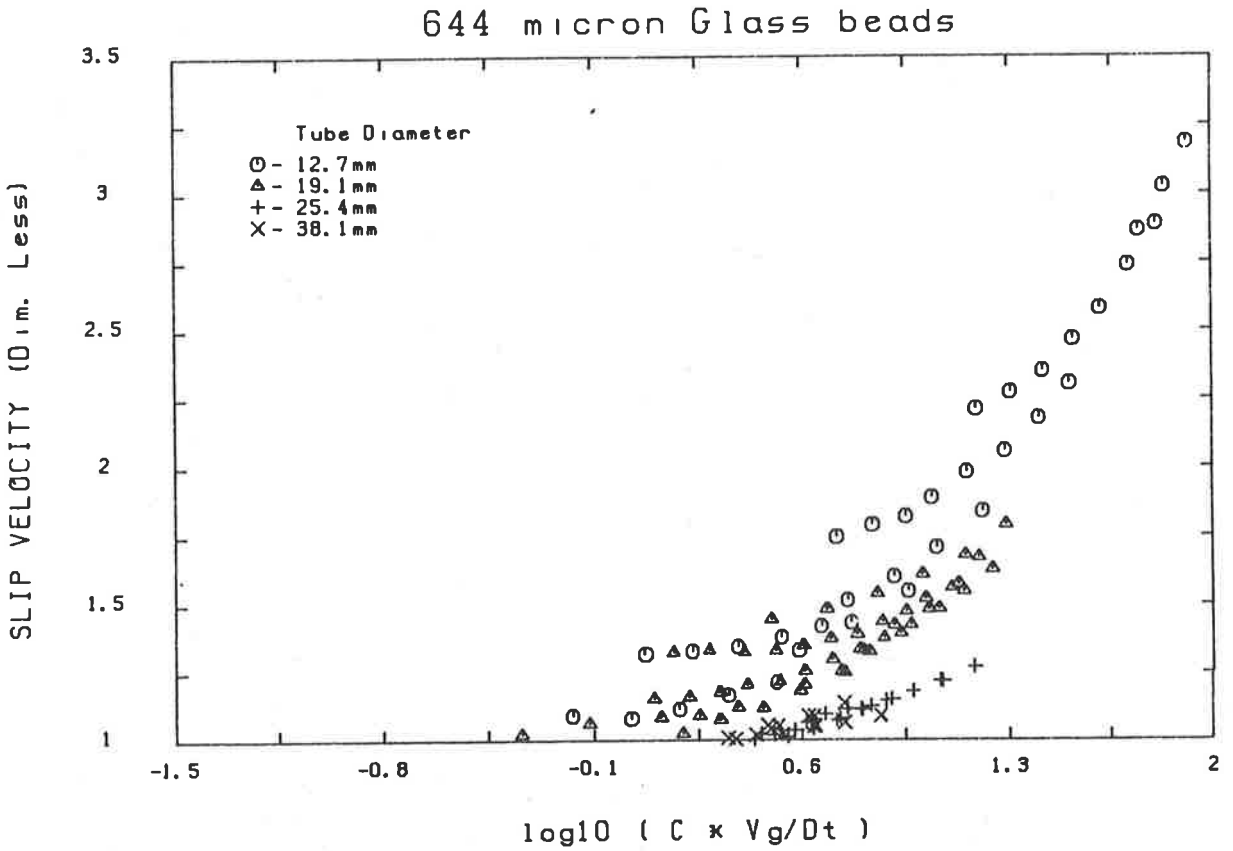
644 micron Glass beads
Tube Diameter
O - 12.7mm
Δ - 19.1mm
+ - 25.4mm
X - 38.1mm
SLIP VELOCITY (Dim. Less)
3.5
3
2.5
2
1.5
1
-1.5
-0.8
-0.1
0.6
1.3
2
log10 (C * Vg/Dt)

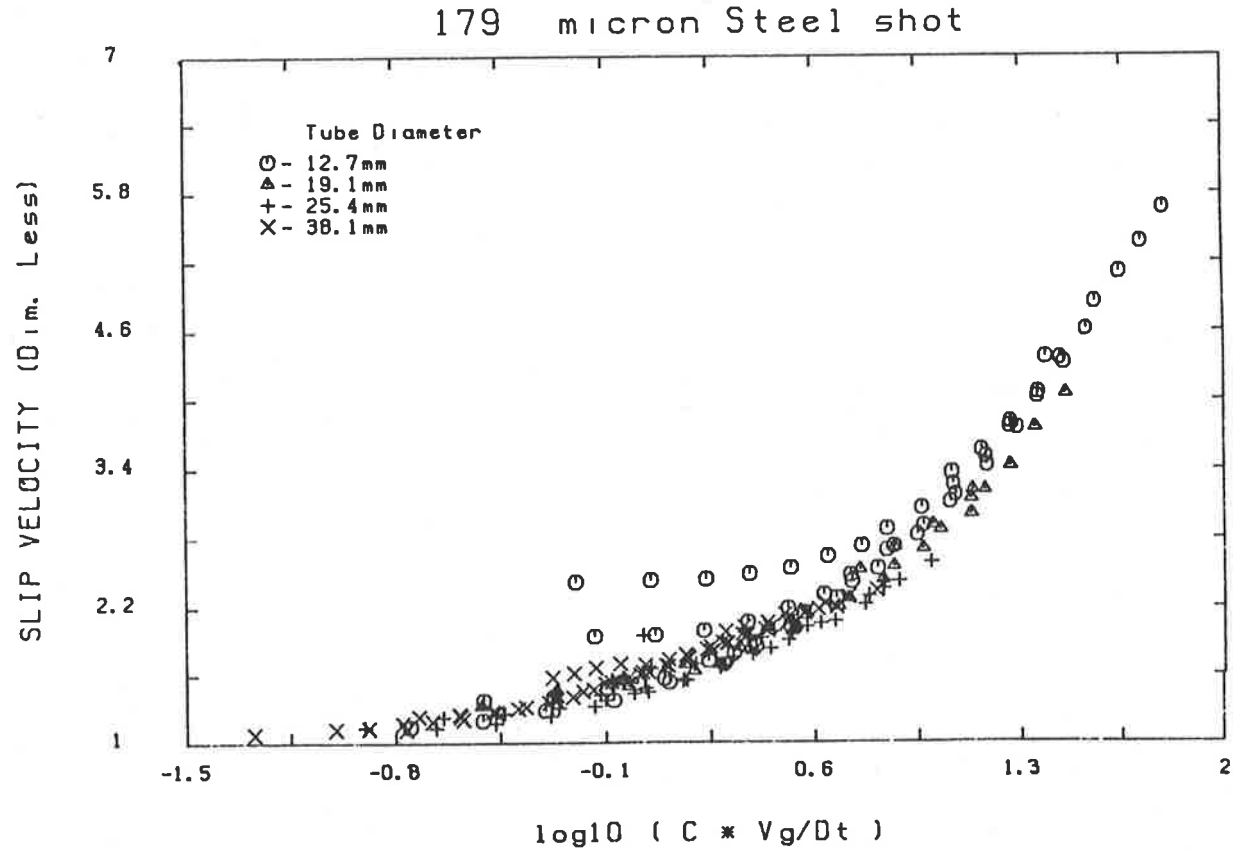
179 micron Steel shot
Tube Diameter
O - 12.7mm
Δ - 19.1mm
+ - 25.4mm
X - 38.1mm
SLIP VELOCITY (Dim. Less)
7
5.8
4.6
3.4
2.2
1
-1.5
-0.8
-0.1
0.6
1.3
2
log10 (C * Vg/Dt)

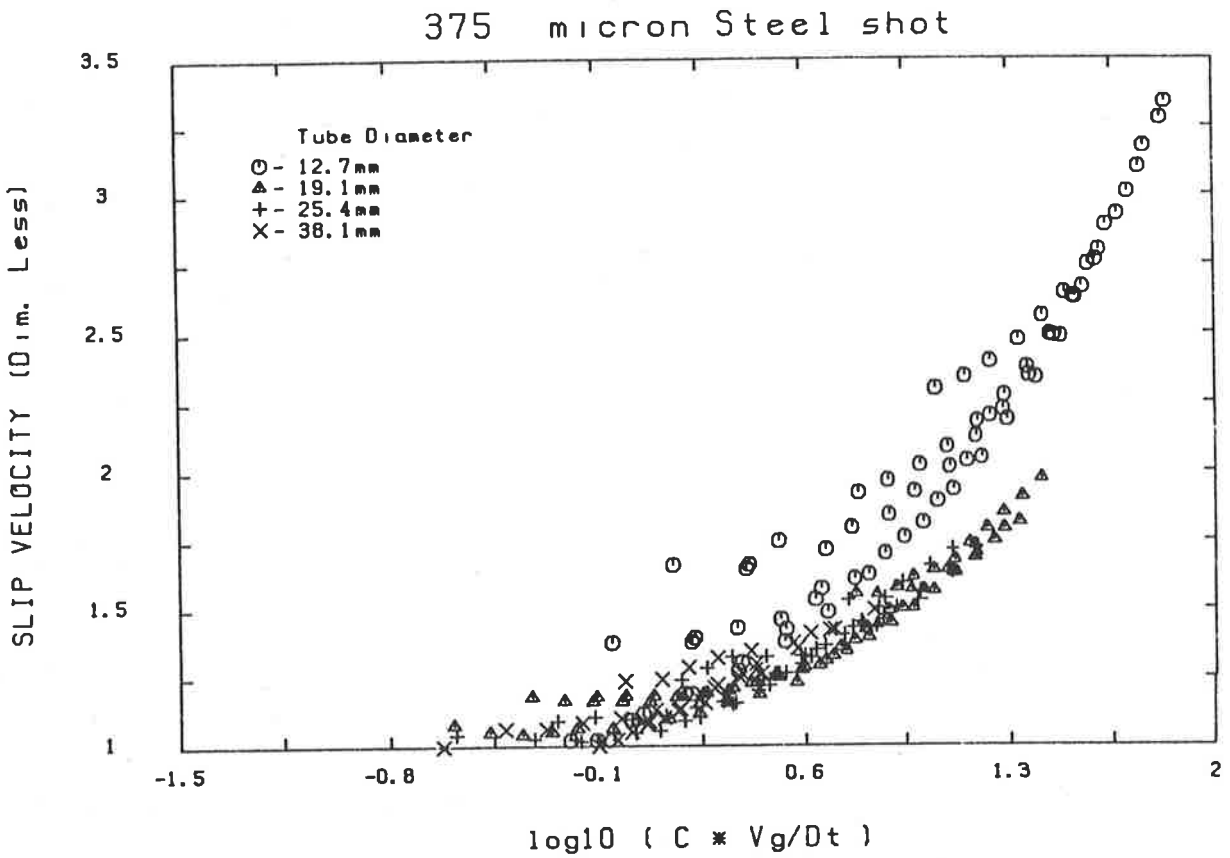
375 micron Steel shot
Tube Diameter
O - 12.7mm
Δ - 19.1mm
+ - 25.4mm
X - 38.1mm
SLIP VELOCITY (Dim. Less)
3.5
3
2.5
2
1.5
1
-1.5
-0.8
-0.1
0.6
1.3
2
log10 (C * Vg/Dt)

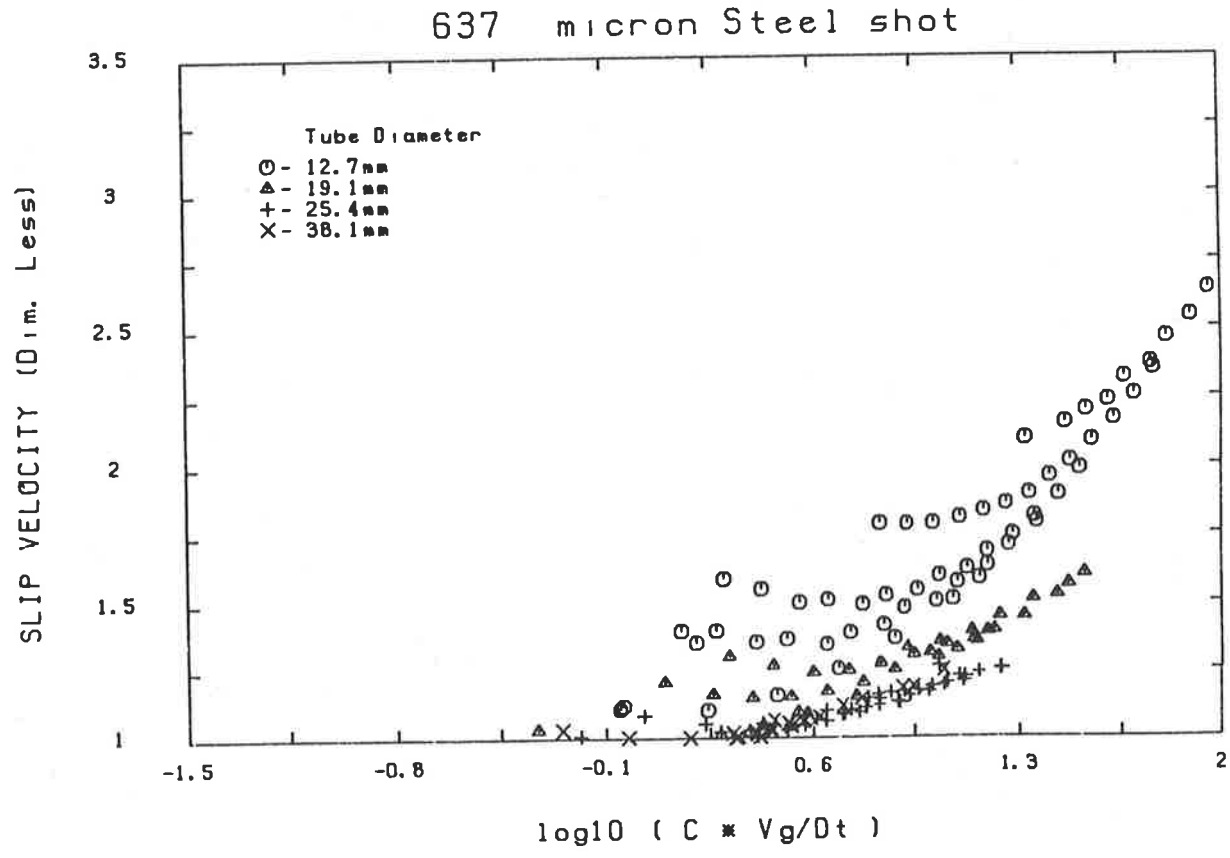
637 micron Steel shot
Tube Diameter
O - 12.7mm
Δ - 19.1mm
+ - 25.4mm
X - 38.1mm
SLIP VELOCITY (Dim. Less)
3.5
3
2.5
2
1.5
1
-1.5
-0.8
-0.1
0.6
1.3
2
log10 (C * Vg/Dt)

APPENDIX (F)

EFFECT OF TRANSPORT VELOCITY
ON
CONCENTRATION-SLIP VELOCITY MAPS

COCURRENT TRANSPORT DATA

(Countercurrent data is also presented for comparison)

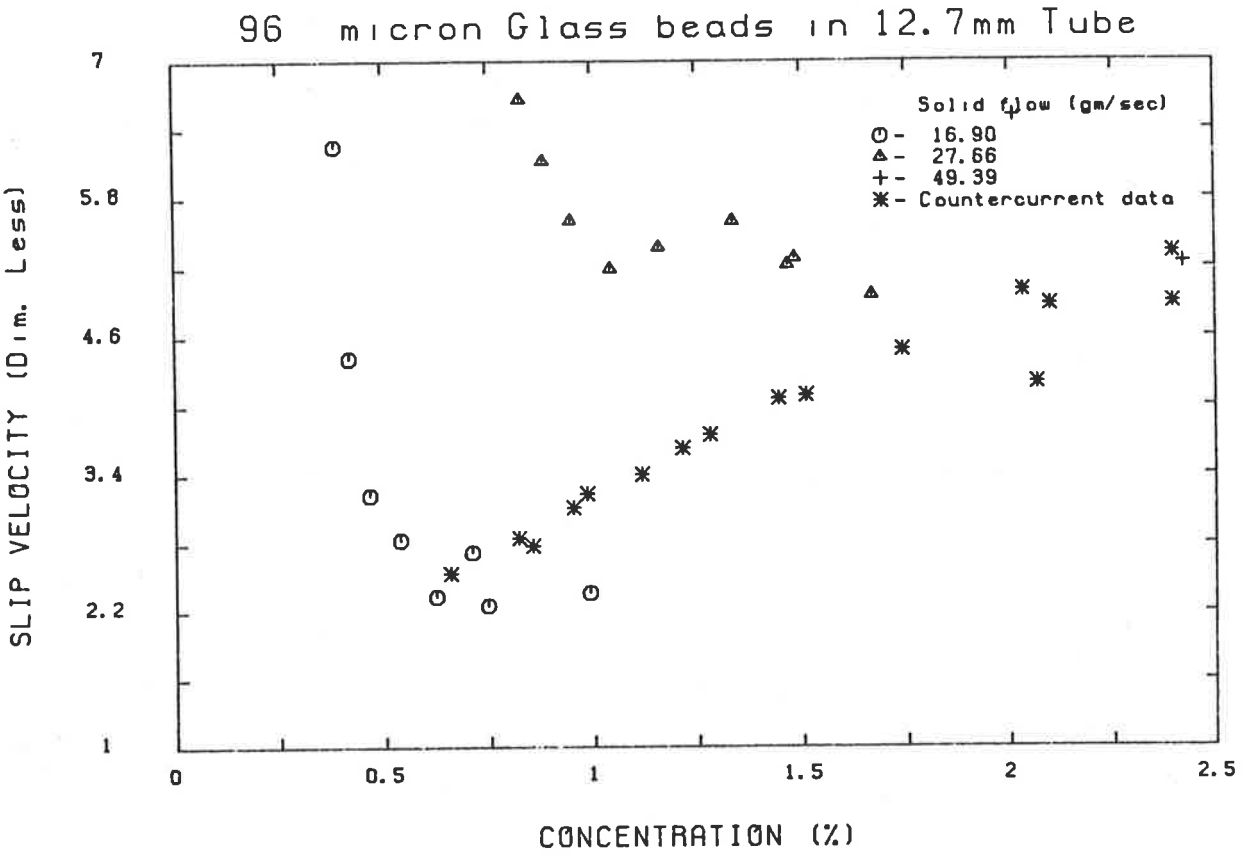
96 micron Glass beads in 12.7mm Tube
Solid flow (gm/sec)
- 16.90
- 27.66
- 49.39
- Countercurrent data
SLIP VELOCITY (Dim. Less)
CONCENTRATION (%)
7
5.8
4.6
3.4
2.2
1
0
0.5
1
1.5
2
2.5

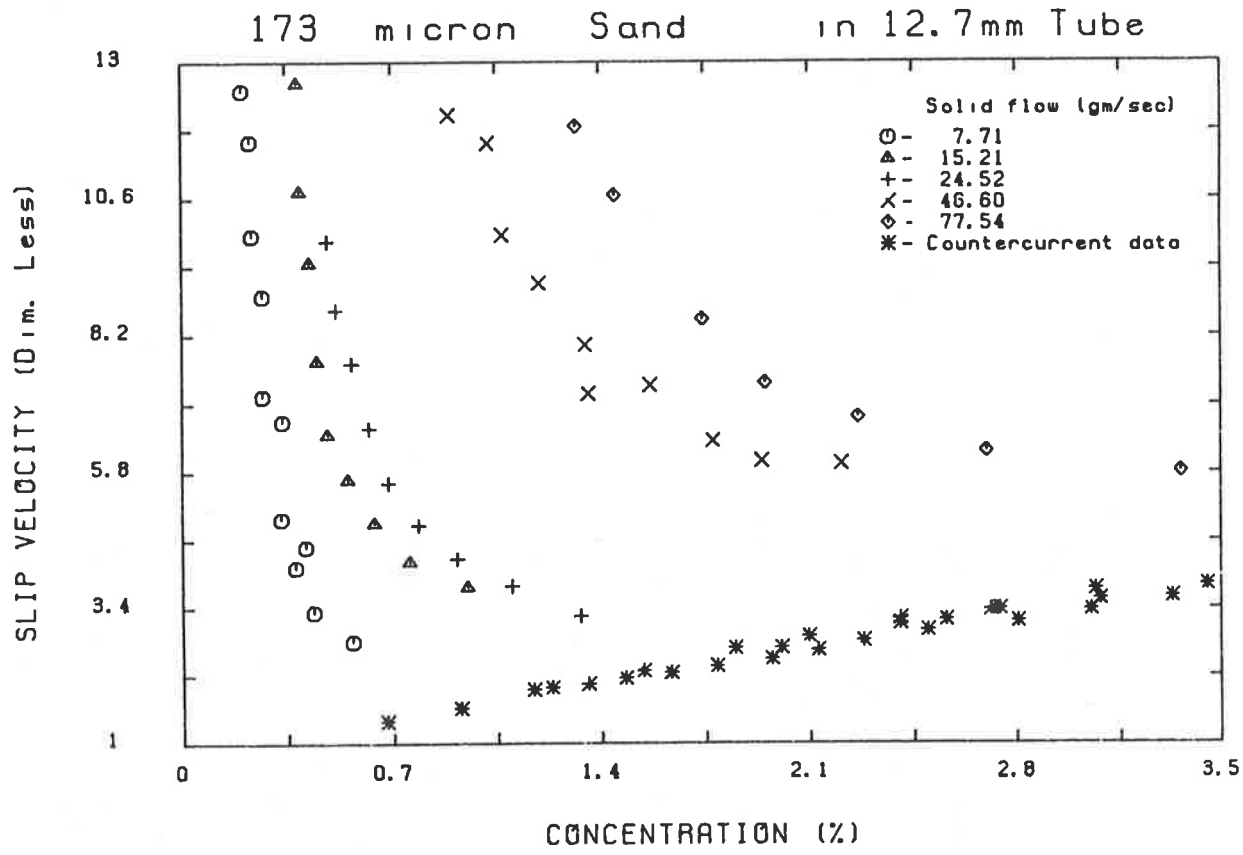
173 micron Sand in 12.7mm Tube
Solid flow (gm/sec)
- 7.71
- 15.21
- 24.52
- 46.60
- 77.54
- Countercurrent data
SLIP VELOCITY (Dim. Less)
CONCENTRATION (%)
13
10.6
8.2
5.8
3.4
1
0
0.7
1.4
2.1
2.8
3.5

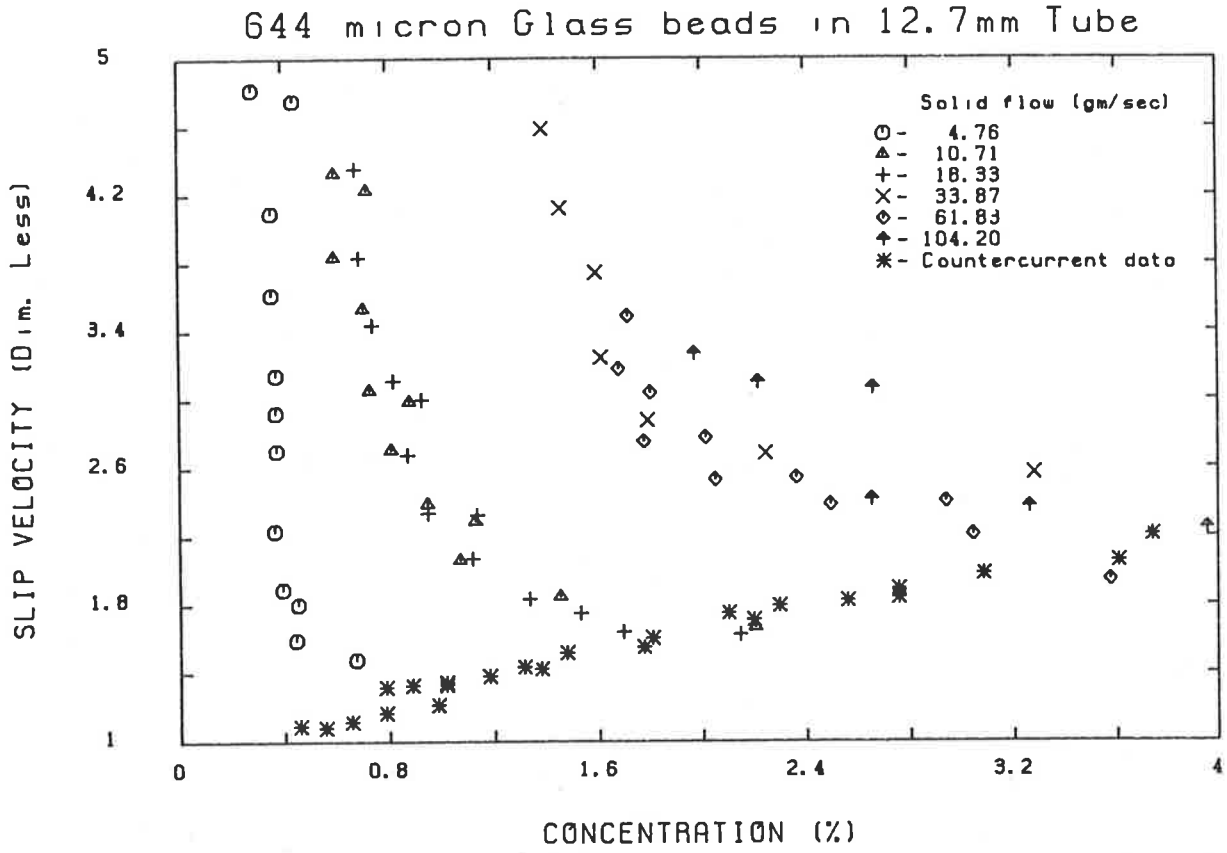
644 micron Glass beads in 12.7mm Tube
SLIP VELOCITY (Dim. Less)
CONCENTRATION (%)
Solid flow (gm/sec)
- 4.76
- 10.71
- 18.33
- 33.87
- 61.83
- 104.20
- Countercurrent data
5
4.2
3.4
2.6
1.8
1
0
0.8
1.6
2.4
3.2
4

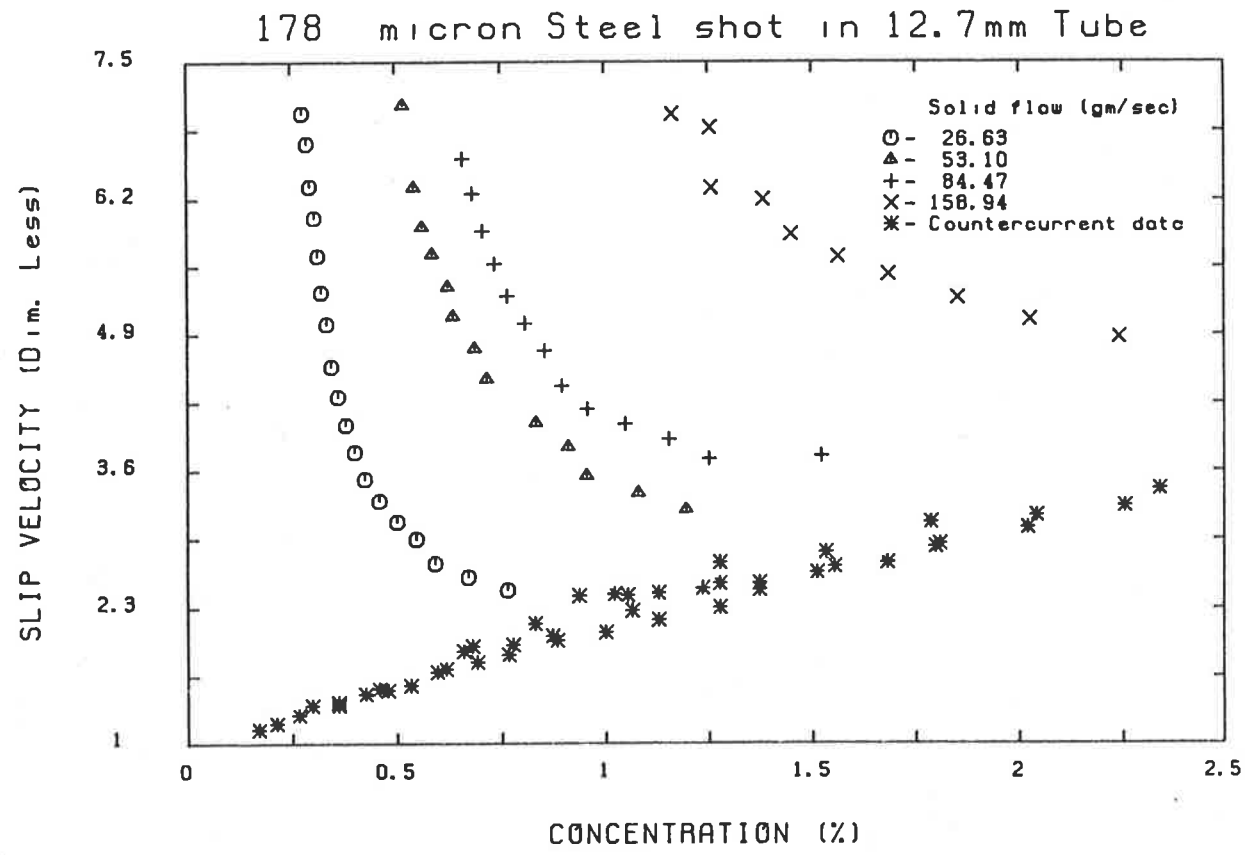
178 micron Steel shot in 12.7mm Tube
SLIP VELOCITY (Dim. Less)
CONCENTRATION (%)
Solid flow (gm/sec)
- 26.63
- 53.10
- 84.47
- 158.94
- Countercurrent data
7.5
6.2
4.9
3.6
2.3
1
0
0.5
1
1.5
2
2.5

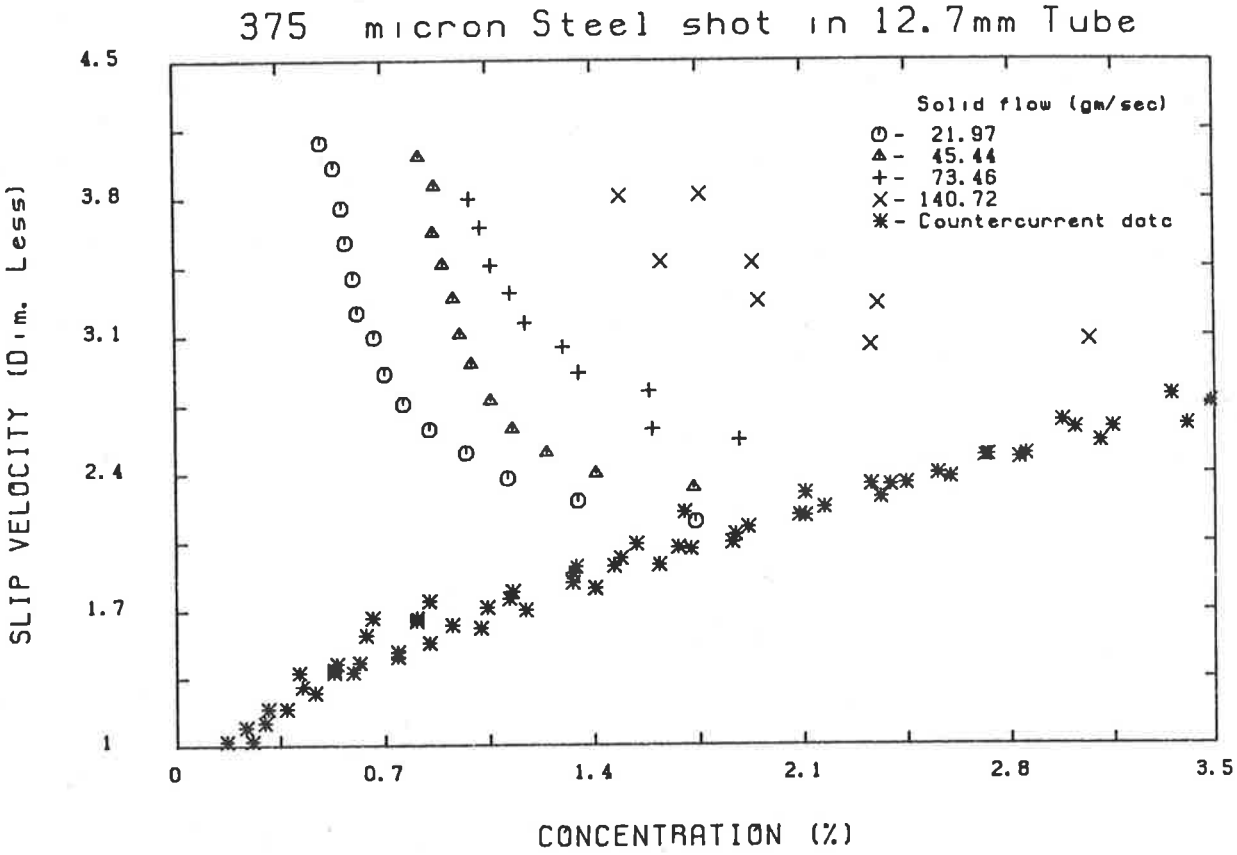
375 micron Steel shot in 12.7mm Tube
Solid flow (gm/sec)
- 21.97
- 45.44
- 73.46
- 140.72
- Countercurrent data
SLIP VELOCITY (Dim. Less)
4.5
3.8
3.1
2.4
1.7
1
0
0.7
1.4
2.1
2.8
3.5
CONCENTRATION (%)

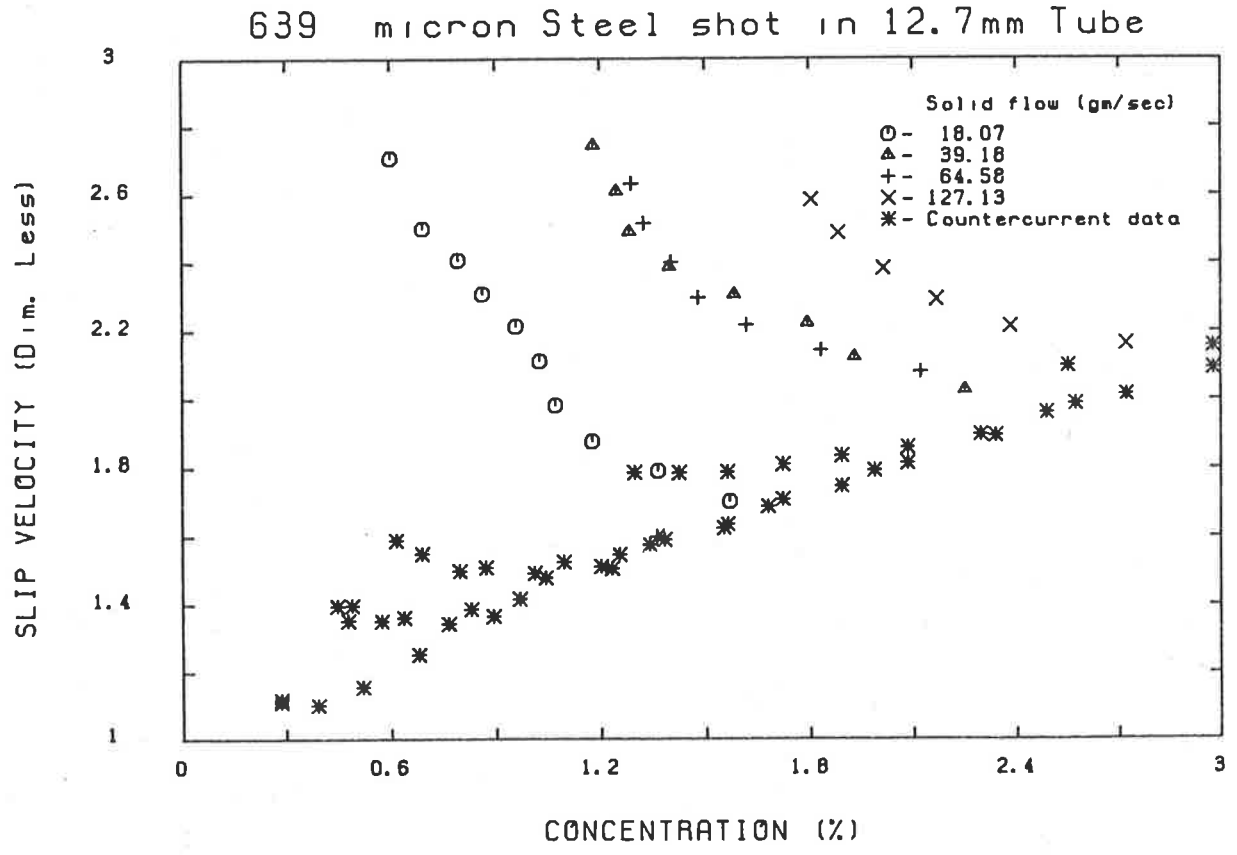
639 micron Steel shot in 12.7mm Tube
Solid flow (gm/sec)
- 18.07
- 39.18
- 64.58
- 127.13
- Countercurrent data
SLIP VELOCITY (Dim. Less)
3
2.6
2.2
1.8
1.4
1
0
0.6
1.2
1.8
2.4
3
CONCENTRATION (%)

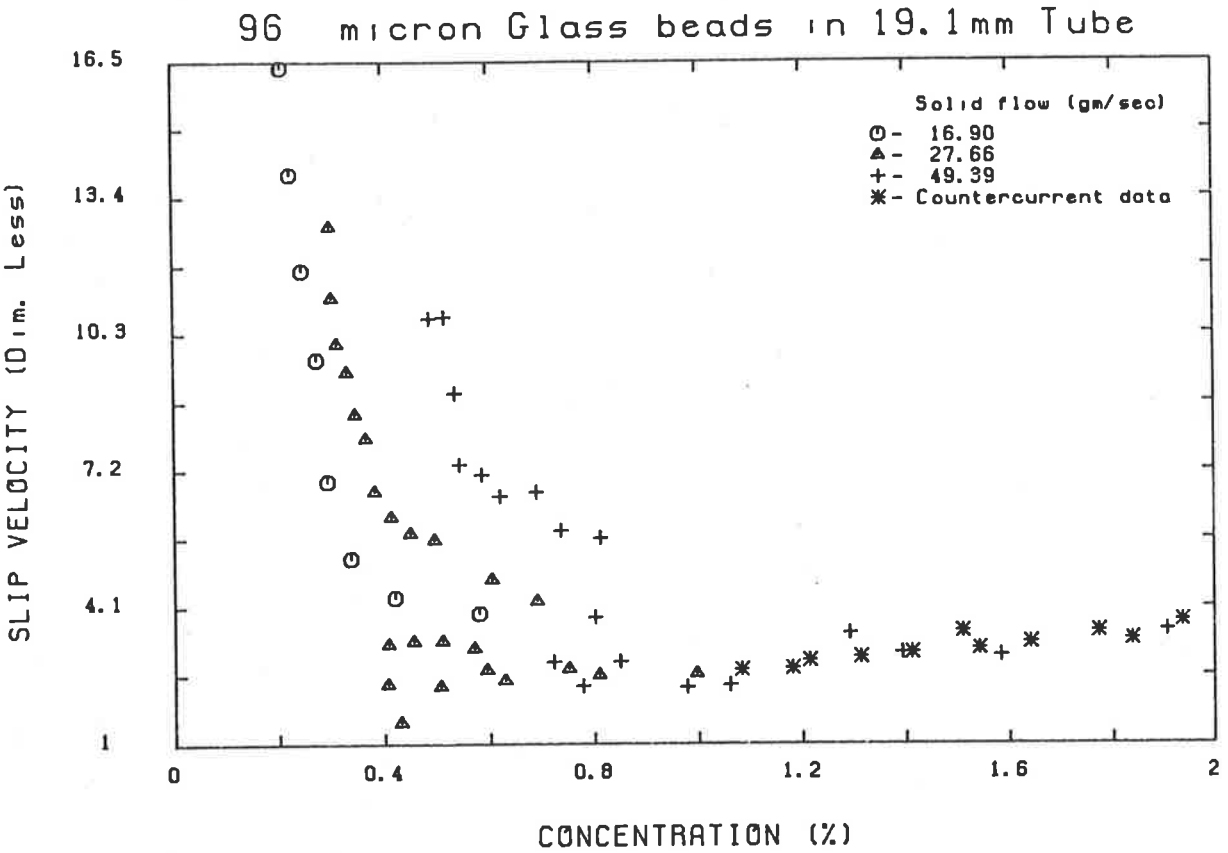
96 micron Glass beads in 19.1mm Tube
Solid flow (gm/sec)
⊙- 16.90
△- 27.66
+- 49.39
✱- Countercurrent data
SLIP VELOCITY (Dim. Less)
16.5
13.4
10.3
7.2
4.1
1
0
0.4
0.8
1.2
1.6
2
CONCENTRATION (%)

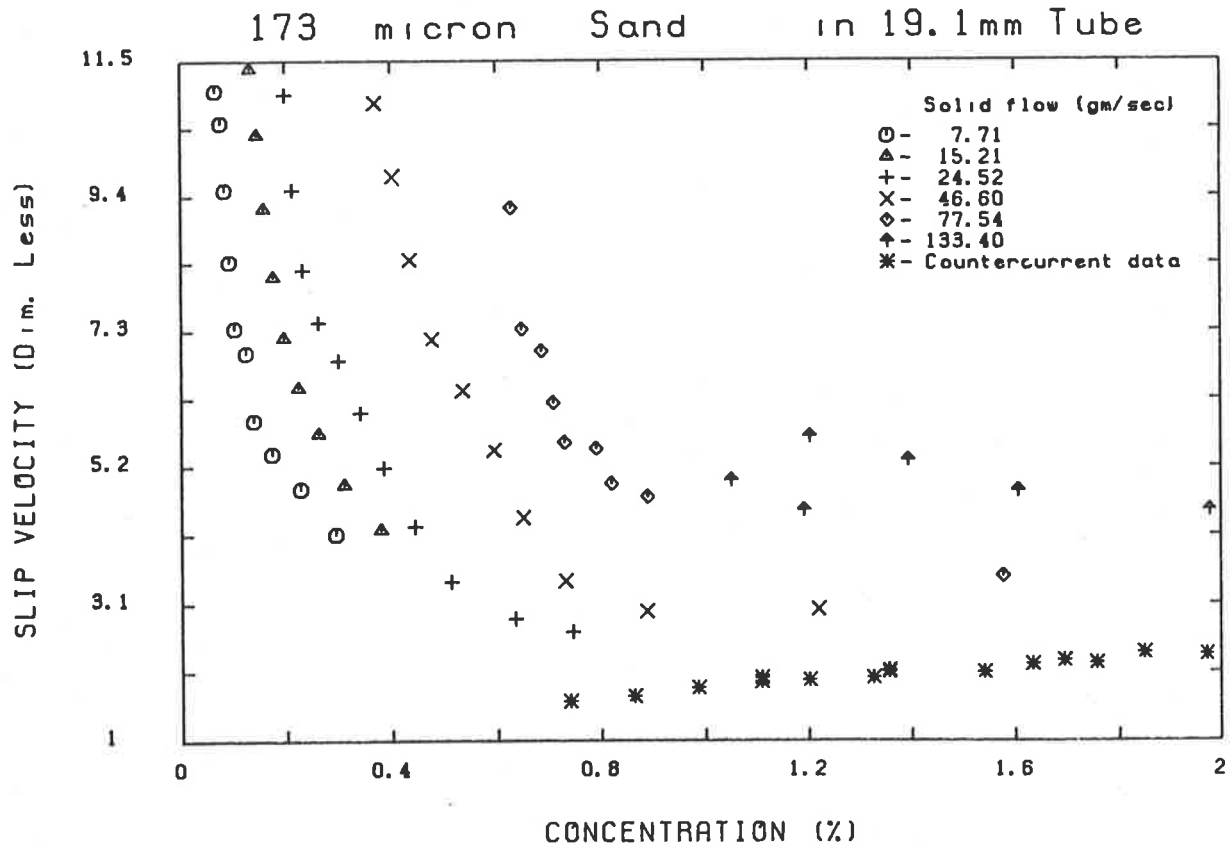
173 micron Sand in 19.1mm Tube
Solid flow (gm/sec)
⊙- 7.71
△- 15.21
+- 24.52
×- 46.60
◇- 77.54
♠- 133.40
✱- Countercurrent data
SLIP VELOCITY (Dim. Less)
11.5
9.4
7.3
5.2
3.1
1
0
0.4
0.8
1.2
1.6
2
CONCENTRATION (%)

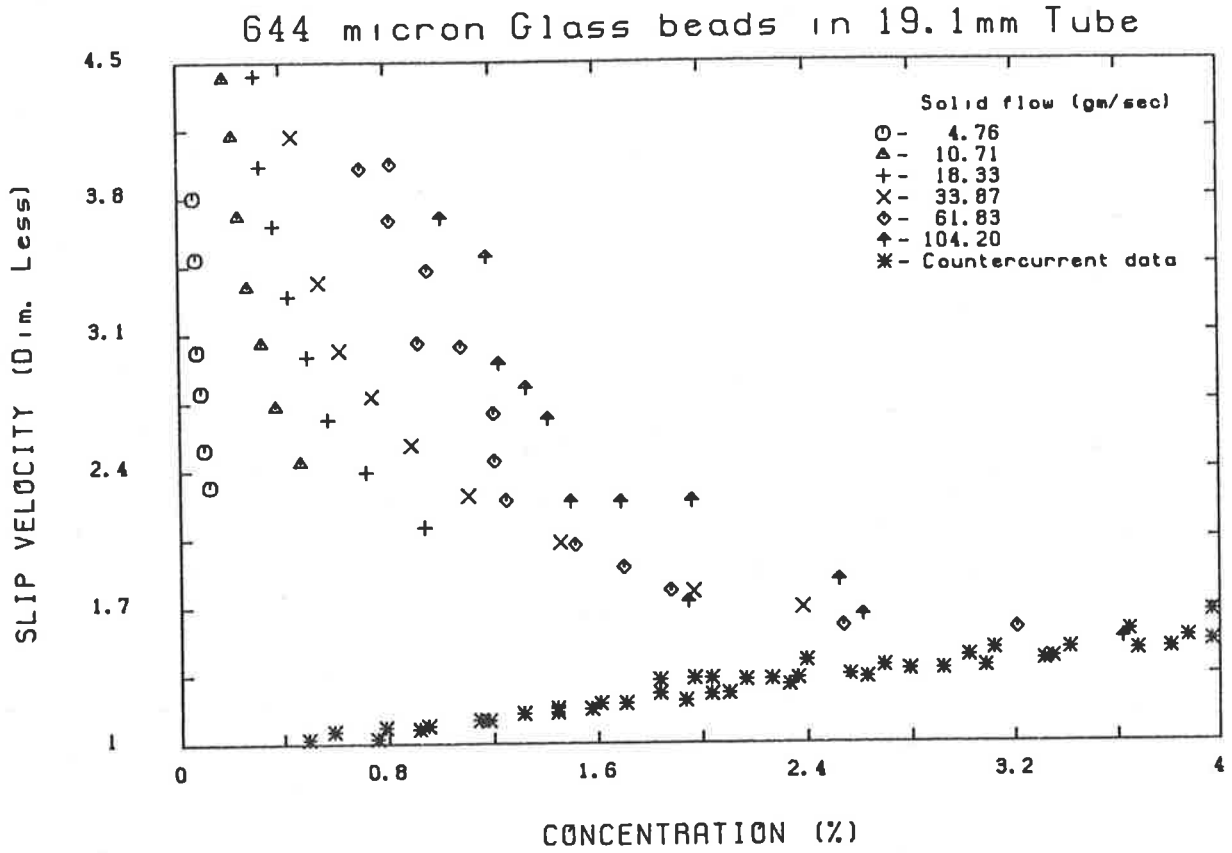
644 micron Glass beads in 19.1mm Tube
Solid flow (gm/sec)
- 4.76
- 10.71
- 18.33
- 33.87
- 61.83
- 104.20
- Countercurrent data
SLIP VELOCITY (Dim. Less)
CONCENTRATION (%)
4.5
3.8
3.1
2.4
1.7
1
0
0.8
1.6
2.4
3.2
4

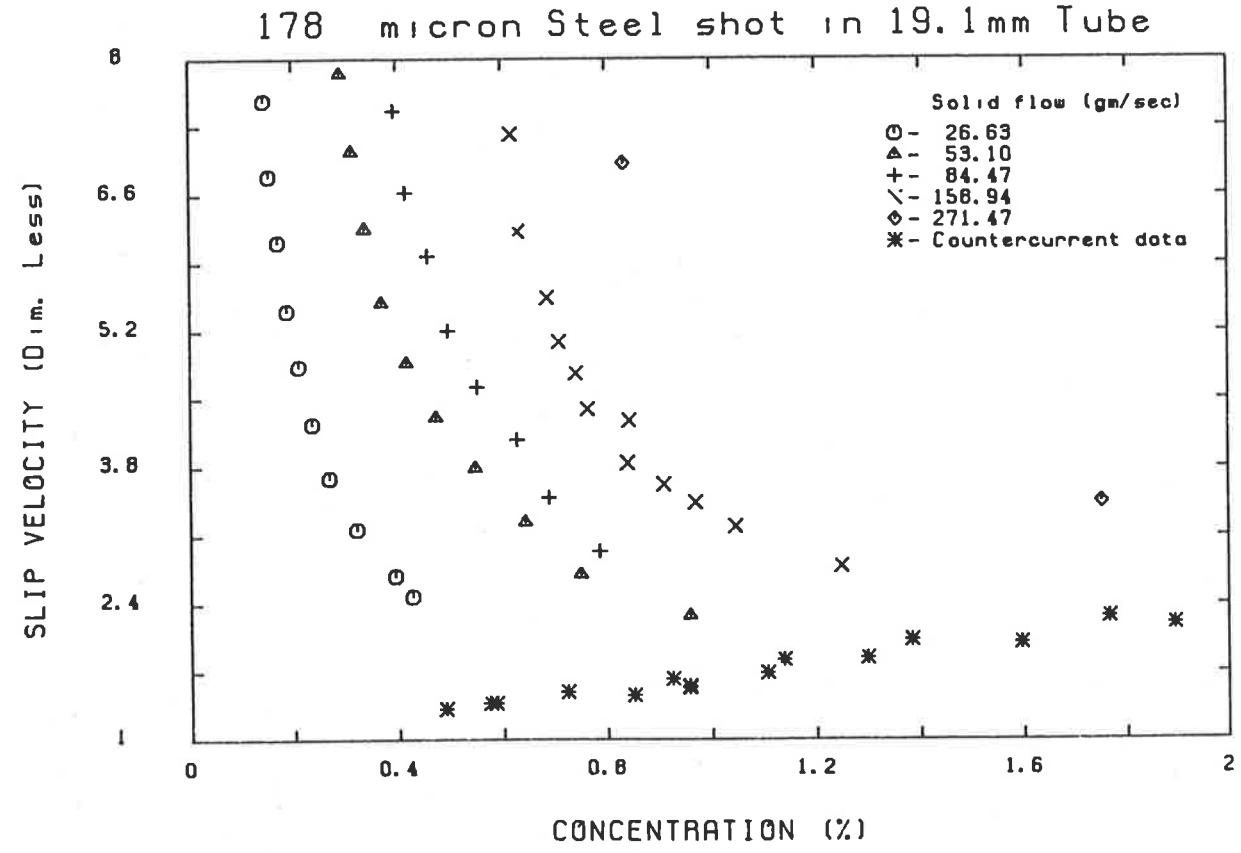
178 micron Steel shot in 19.1mm Tube
Solid flow (gm/sec)
- 26.63
- 53.10
- 84.47
- 156.94
- 271.47
- Countercurrent data
SLIP VELOCITY (Dim. Less)
CONCENTRATION (%)
8
6.6
5.2
3.8
2.4
1
0
0.4
0.8
1.2
1.6
2

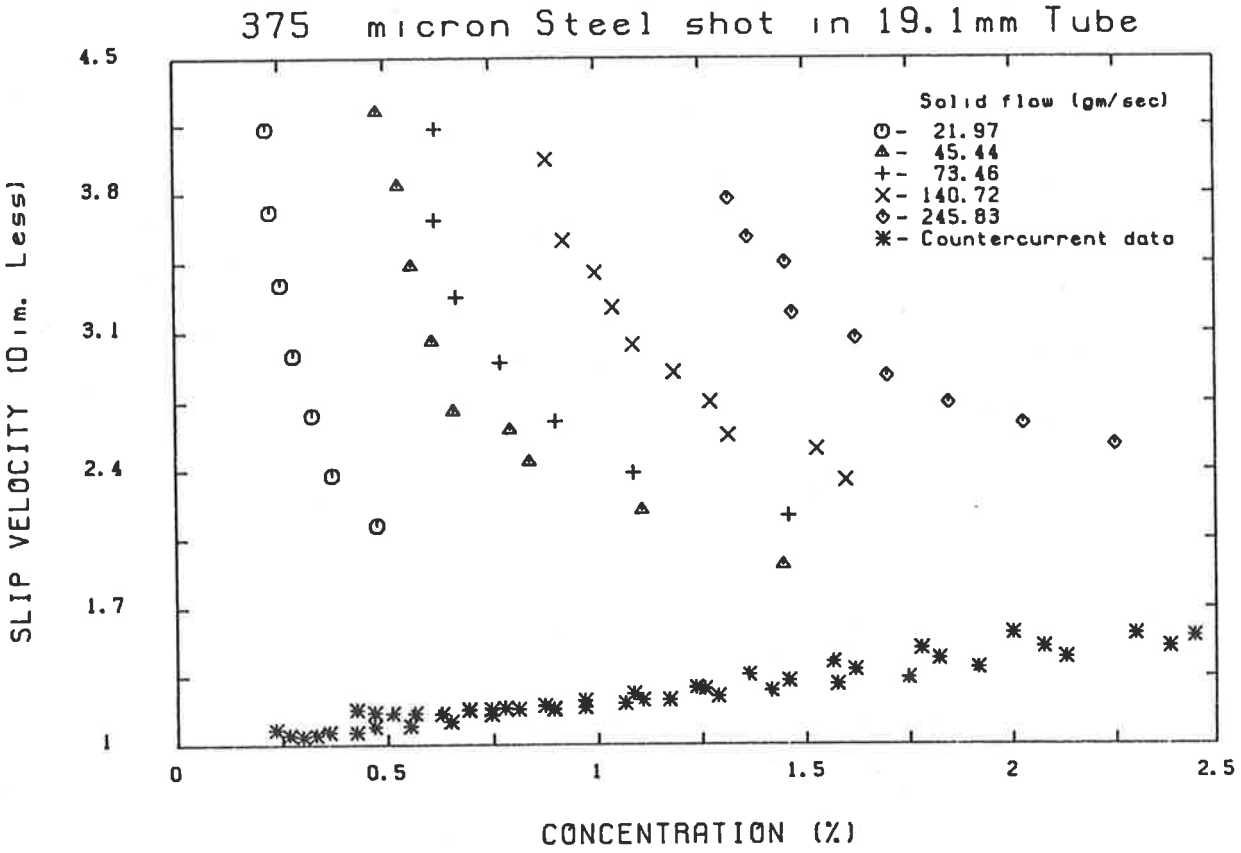
375 micron Steel shot in 19.1mm Tube
SLIP VELOCITY (Dim. Less)
CONCENTRATION (%)
Solid flow (gm/sec)
- 21.97
- 45.44
- 73.46
- 140.72
- 245.83
- Countercurrent data
4.5
3.8
3.1
2.4
1.7
1
0
0.5
1
1.5
2
2.5

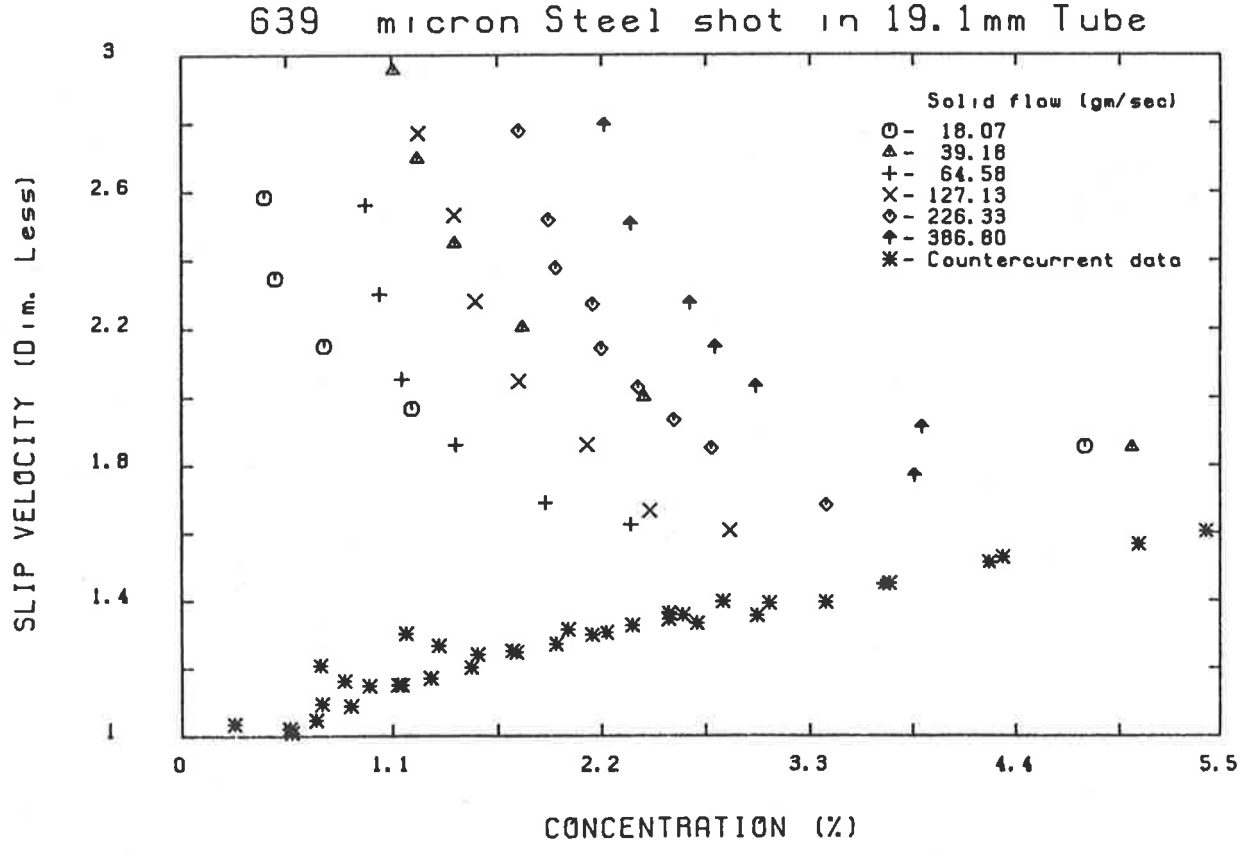
639 micron Steel shot in 19.1mm Tube
SLIP VELOCITY (Dim. Less)
CONCENTRATION (%)
Solid flow (gm/sec)
- 18.07
- 39.18
- 64.58
- 127.13
- 226.33
- 386.80
- Countercurrent data
3
2.6
2.2
1.8
1.4
1
0
1.1
2.2
3.3
4.4
5.5

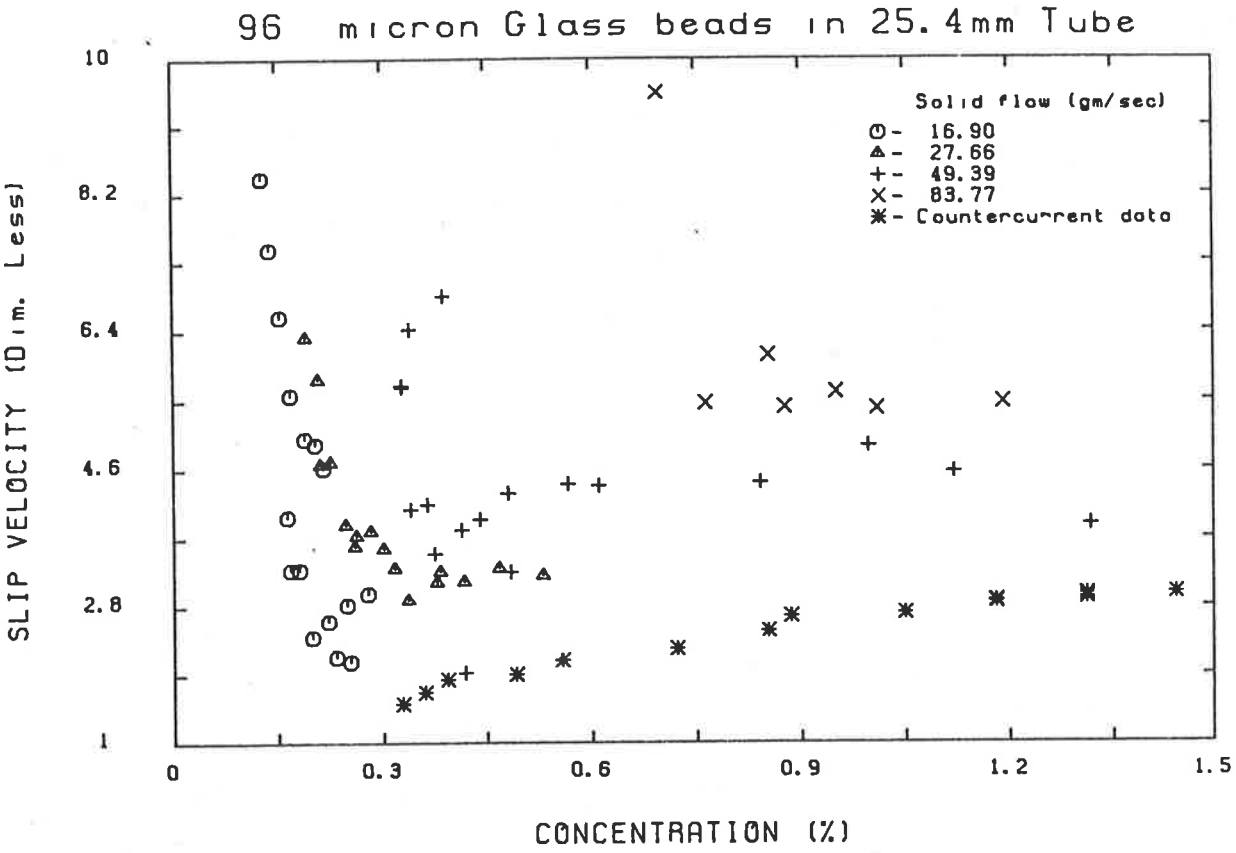
96 micron Glass beads in 25.4mm Tube
Solid flow (gm/sec)
⊙- 16.90
△- 27.66
+- 49.39
×- 83.77
✱- Countercurrent data
SLIP VELOCITY (Dim. Less)
10
8.2
6.4
4.6
2.8
1
0
0.3
0.6
0.9
1.2
1.5
CONCENTRATION (%)

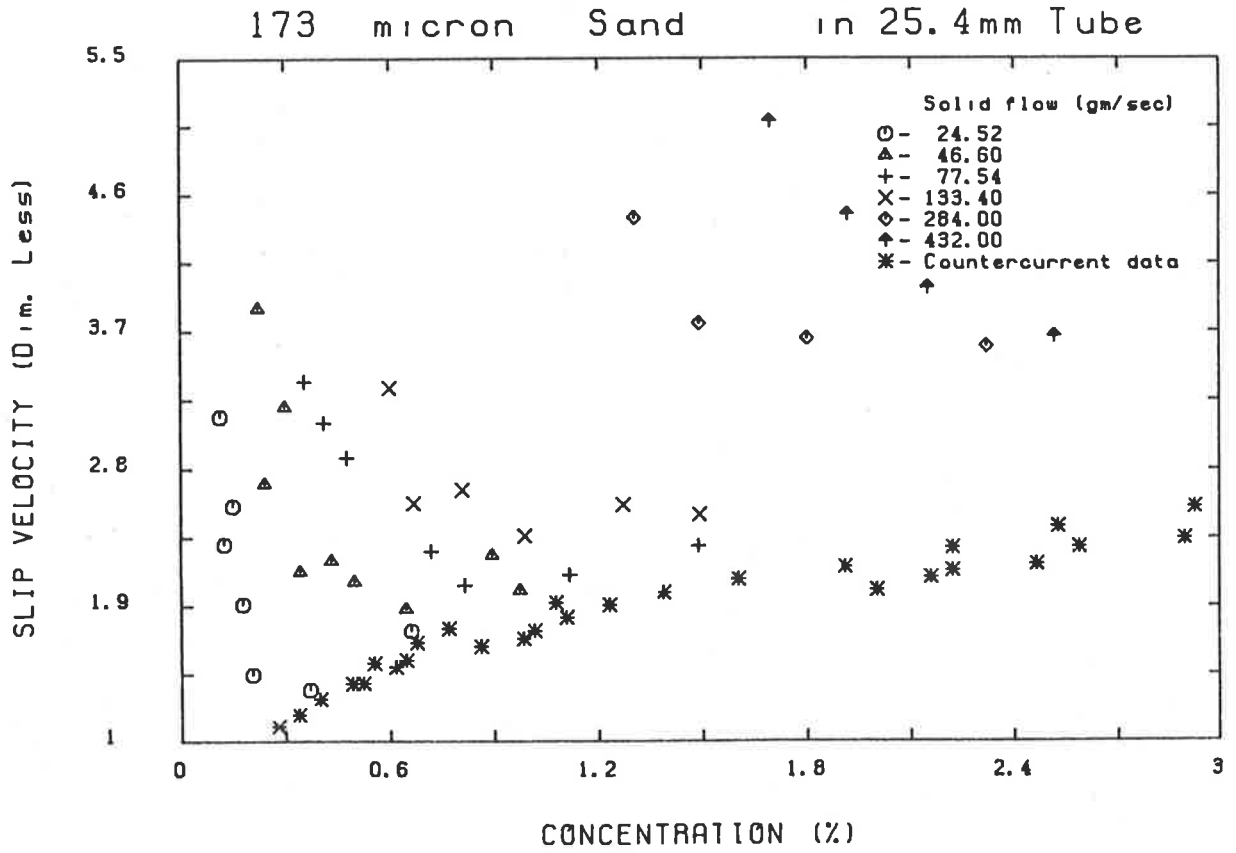
173 micron Sand in 25.4mm Tube
Solid flow (gm/sec)
⊙- 24.52
△- 46.60
+- 77.54
×- 133.40
◇- 284.00
↑- 432.00
✱- Countercurrent data
SLIP VELOCITY (Dim. Less)
5.5
4.6
3.7
2.8
1.9
1
0
0.6
1.2
1.8
2.4
3
CONCENTRATION (%)

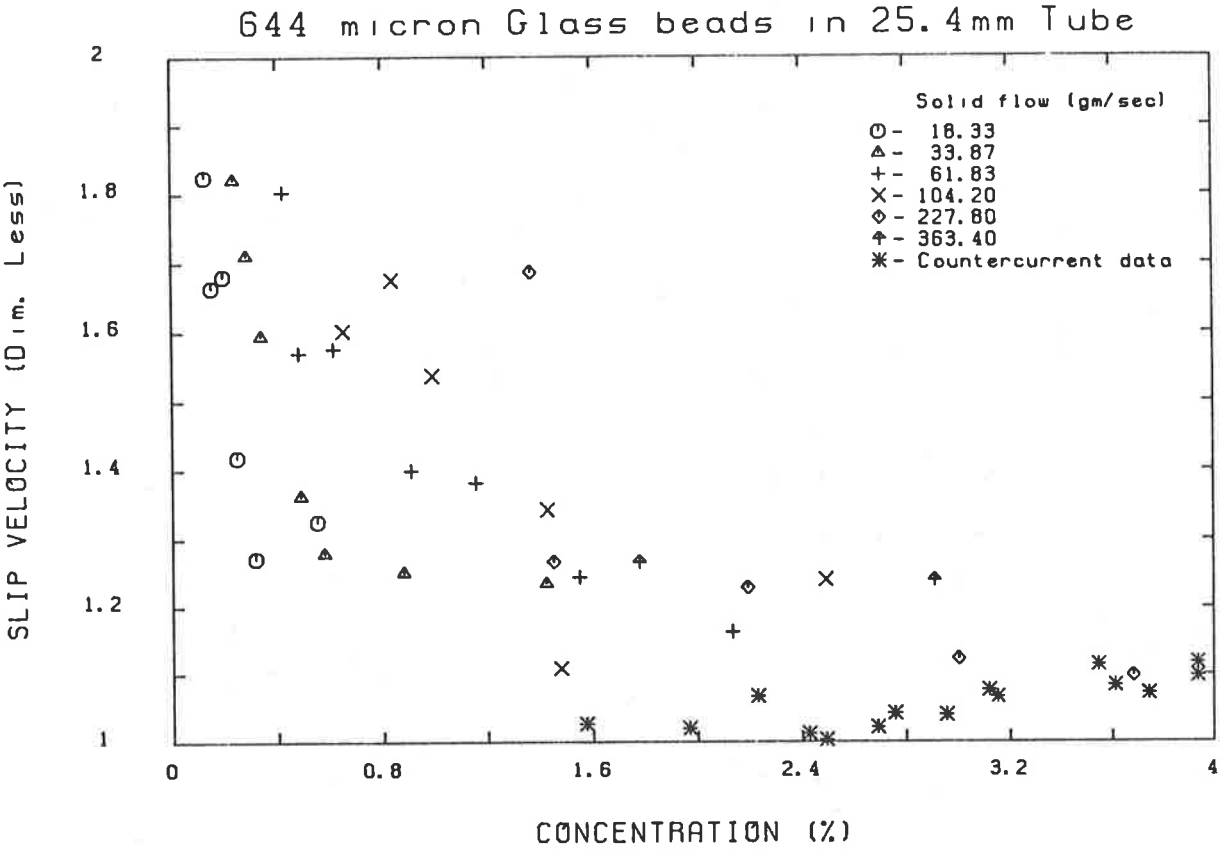
644 micron Glass beads in 25.4mm Tube
Solid flow (gm/sec)
- 18.33
- 33.87
- 61.83
- 104.20
- 227.80
- 363.40
- Countercurrent data
SLIP VELOCITY (Dim. Less)
CONCENTRATION (%)
2
1.8
1.6
1.4
1.2
1
0
0.8
1.6
2.4
3.2
4

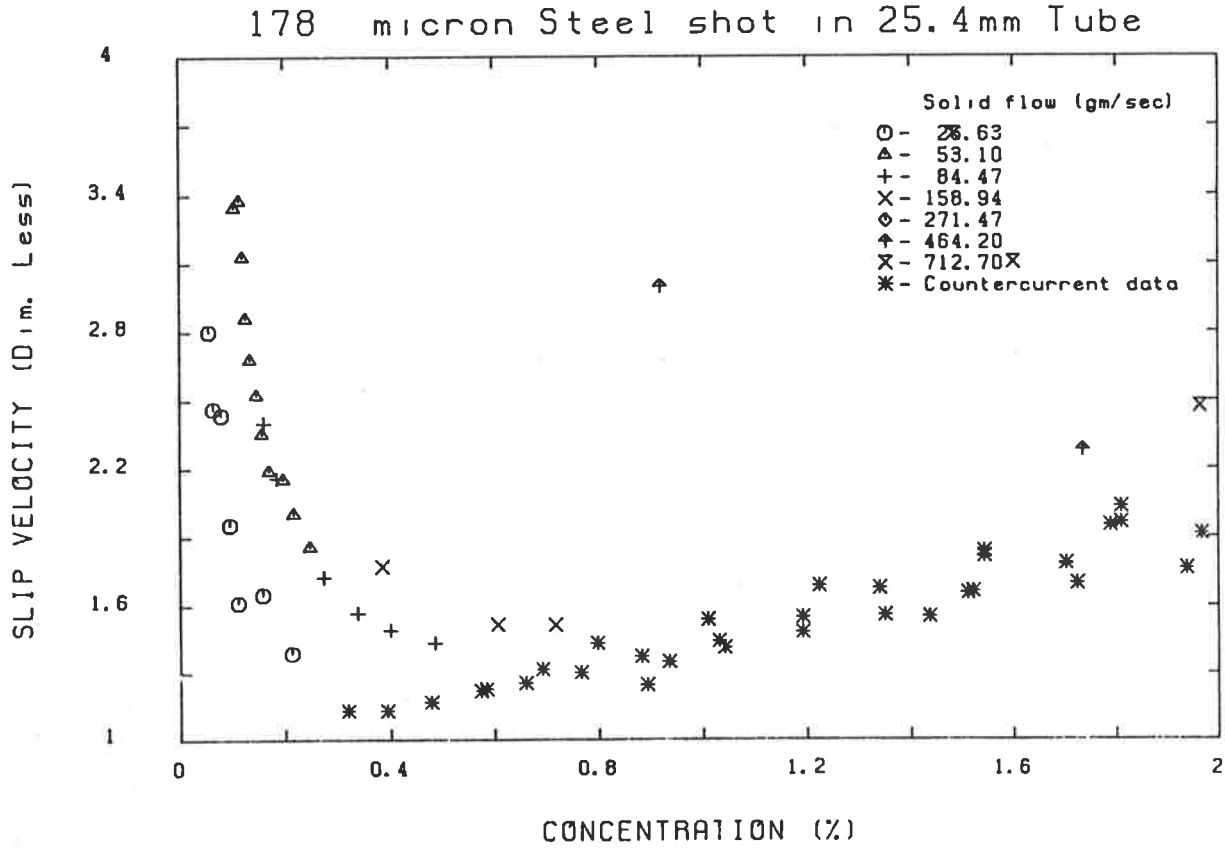
178 micron Steel shot in 25.4mm Tube
Solid flow (gm/sec)
- 26.63
- 53.10
- 84.47
- 158.94
- 271.47
- 464.20
- 712.70
- Countercurrent data
SLIP VELOCITY (Dim. Less)
CONCENTRATION (%)
4
3.4
2.8
2.2
1.6
1
0
0.4
0.8
1.2
1.6
2

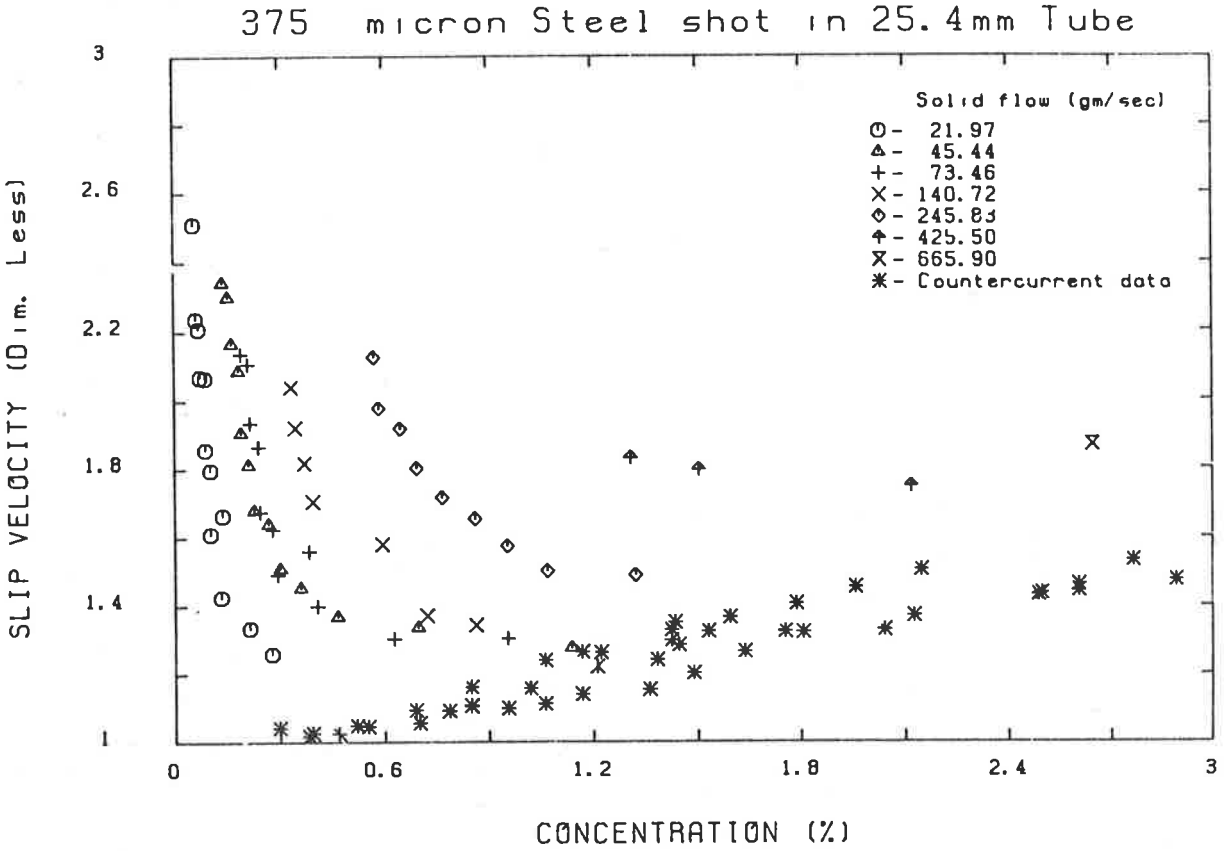
375 micron Steel shot in 25.4mm Tube
Solid flow (gm/sec)
- 21.97
- 45.44
- 73.46
- 140.72
- 245.83
- 425.50
- 665.90
- Countercurrent data
SLIP VELOCITY (Dim. Less)
CONCENTRATION (%)
3
2.6
2.2
1.8
1.4
1
0
0.6
1.2
1.8
2.4
3

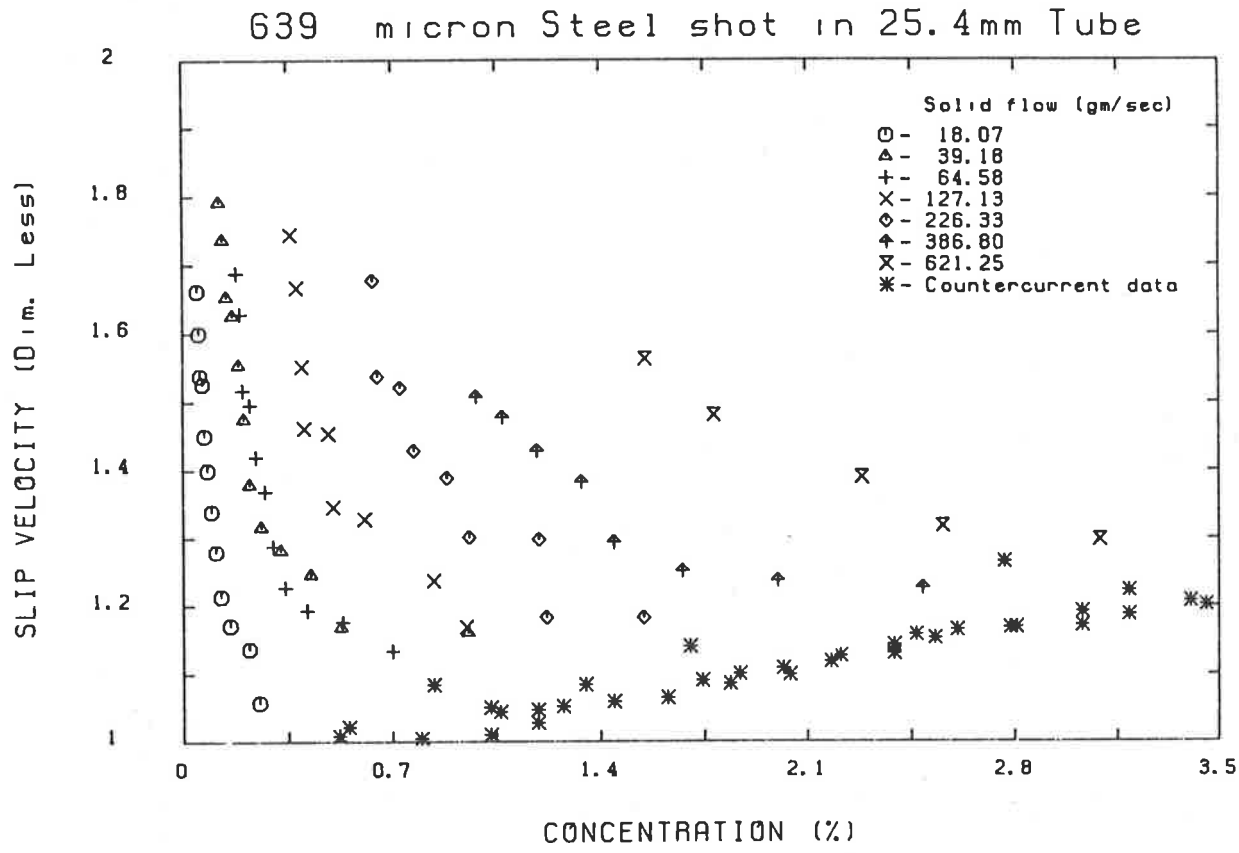
639 micron Steel shot in 25.4mm Tube
Solid flow (gm/sec)
- 18.07
- 39.18
- 64.58
- 127.13
- 226.33
- 386.80
- 621.25
- Countercurrent data
SLIP VELOCITY (Dim. Less)
CONCENTRATION (%)
2
1.8
1.6
1.4
1.2
1
0
0.7
1.4
2.1
2.8
3.5

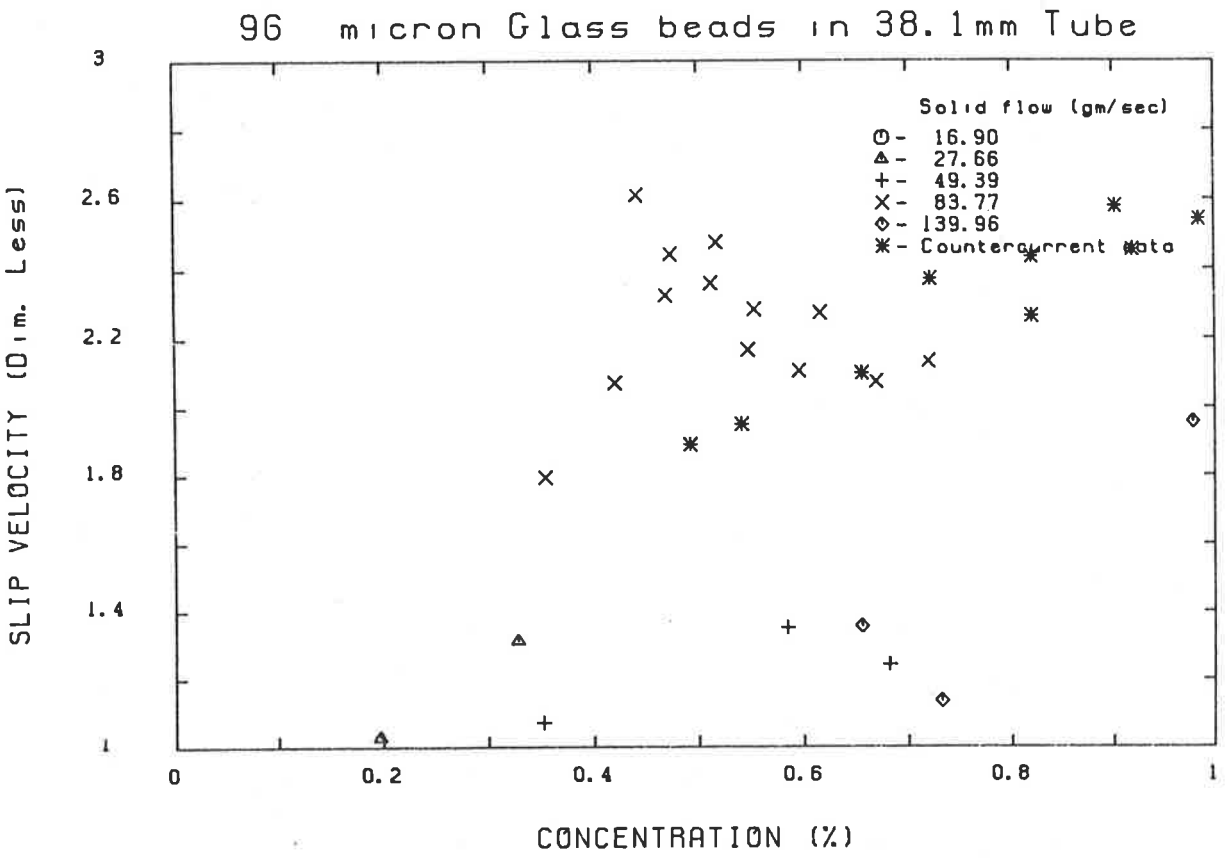
96 micron Glass beads in 38.1mm Tube
Solid flow (gm/sec)
- 16.90
- 27.66
- 49.39
- 83.77
- 139.96
- Countercurrent data
SLIP VELOCITY (Dim. Less)
CONCENTRATION (%)
3
2.6
2.2
1.8
1.4
1
0
0.2
0.4
0.6
0.8
1

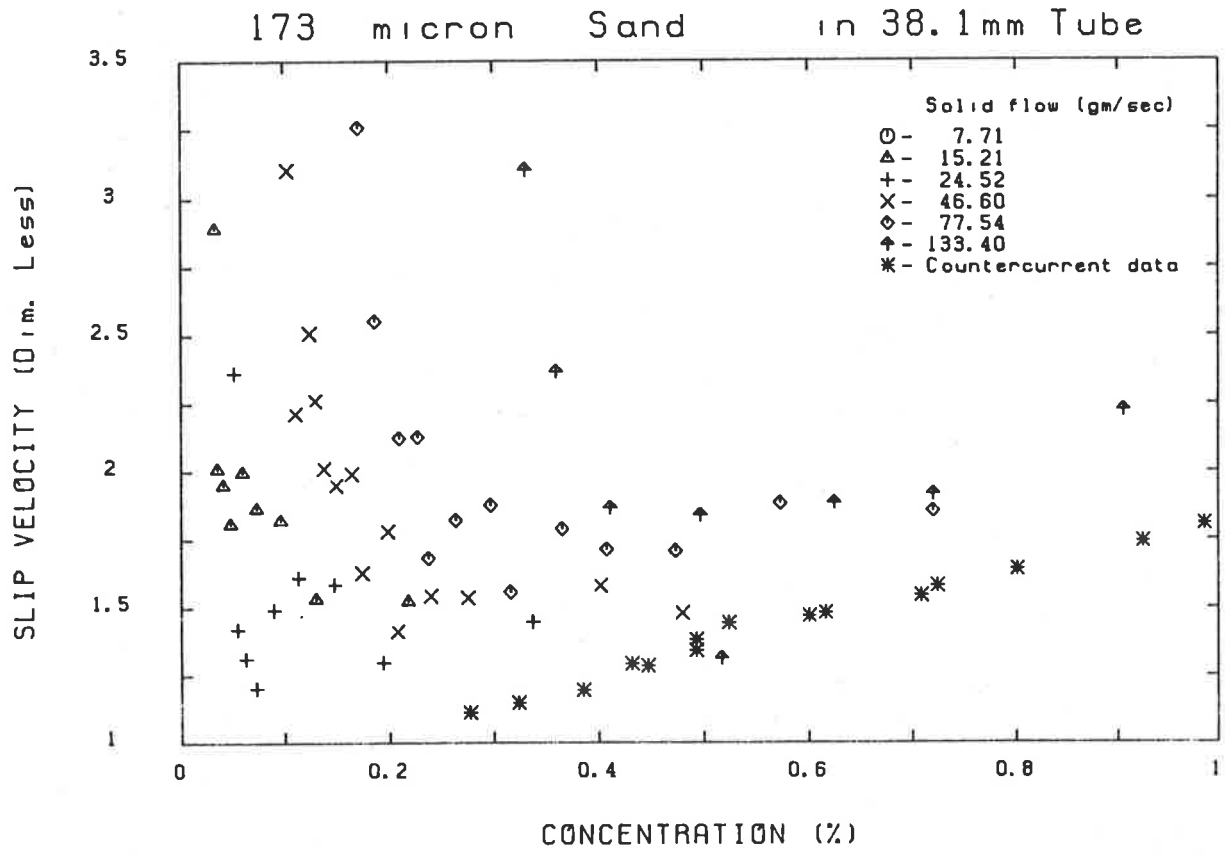
173 micron Sand in 38.1mm Tube
Solid flow (gm/sec)
- 7.71
- 15.21
- 24.52
- 46.60
- 77.54
- 133.40
- Countercurrent data
SLIP VELOCITY (Dim. Less)
CONCENTRATION (%)
3.5
3
2.5
2
1.5
1
0
0.2
0.4
0.6
0.8
1

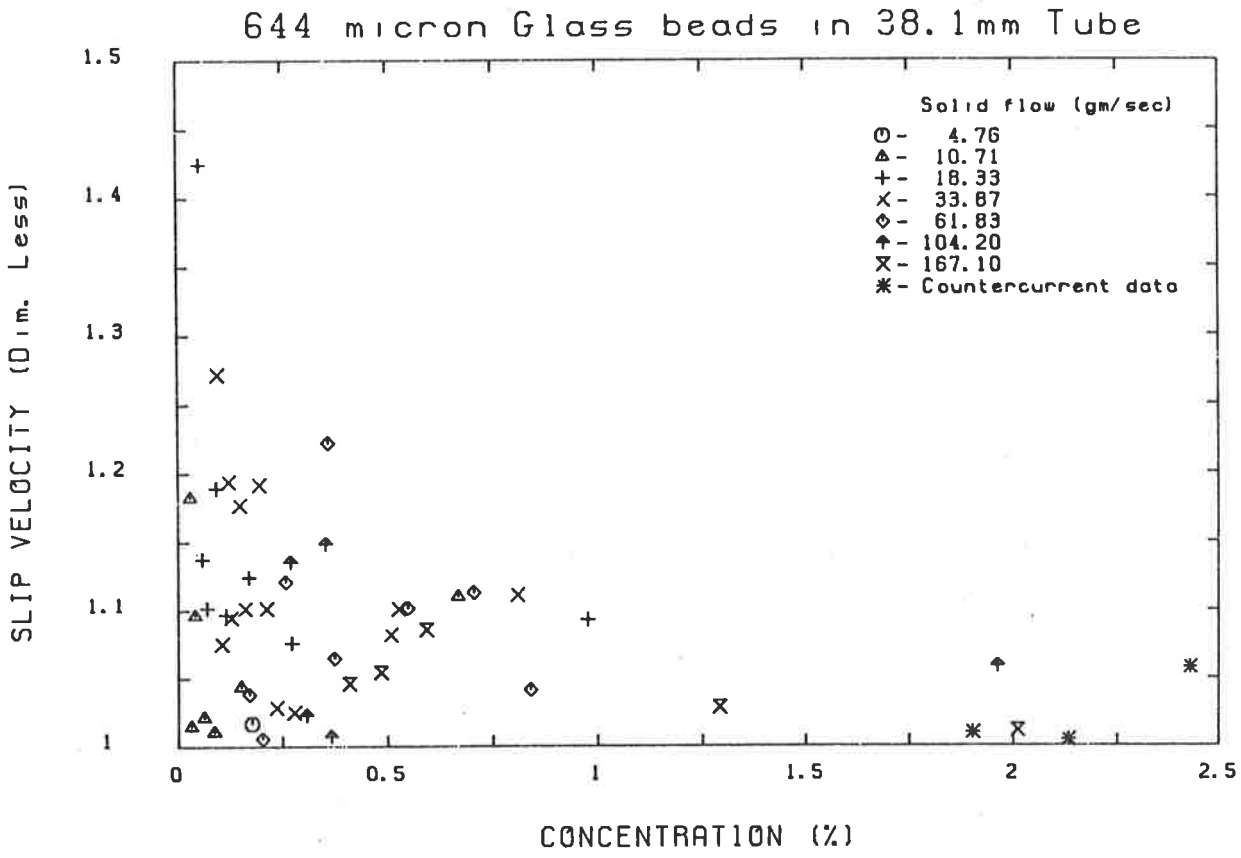
644 micron Glass beads in 38.1mm Tube
SLIP VELOCITY (Dim. Less)
CONCENTRATION (%)
Solid flow (gm/sec)
- 4.76
- 10.71
- 18.33
- 33.87
- 61.83
- 104.20
- 167.10
- Countercurrent data
1.5
1.4
1.3
1.2
1.1
1
0
0.5
1
1.5
2
2.5

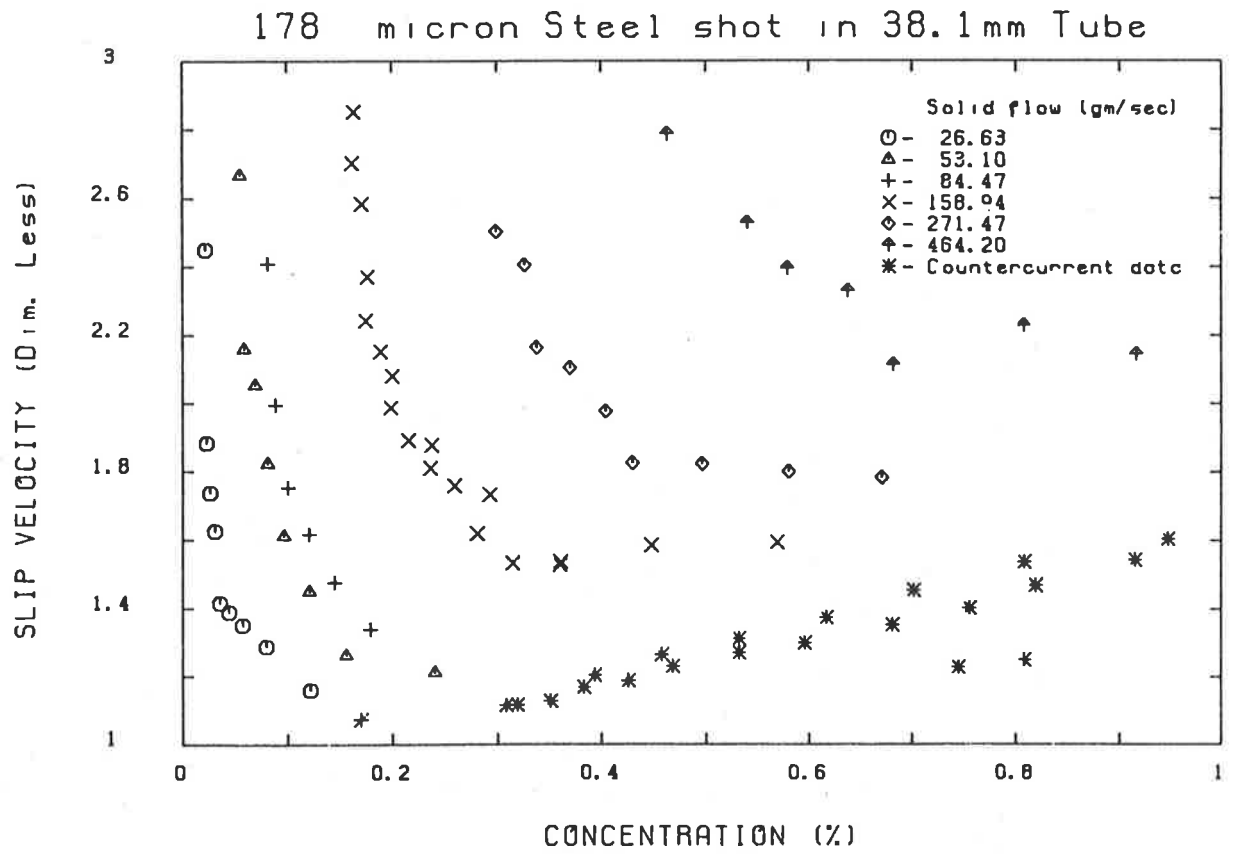
178 micron Steel shot in 38.1mm Tube
SLIP VELOCITY (Dim. Less)
CONCENTRATION (%)
Solid flow (gm/sec)
- 26.63
- 53.10
- 84.47
- 158.94
- 271.47
- 464.20
- Countercurrent data
3
2.6
2.2
1.8
1.4
1
0
0.2
0.4
0.6
0.8
1

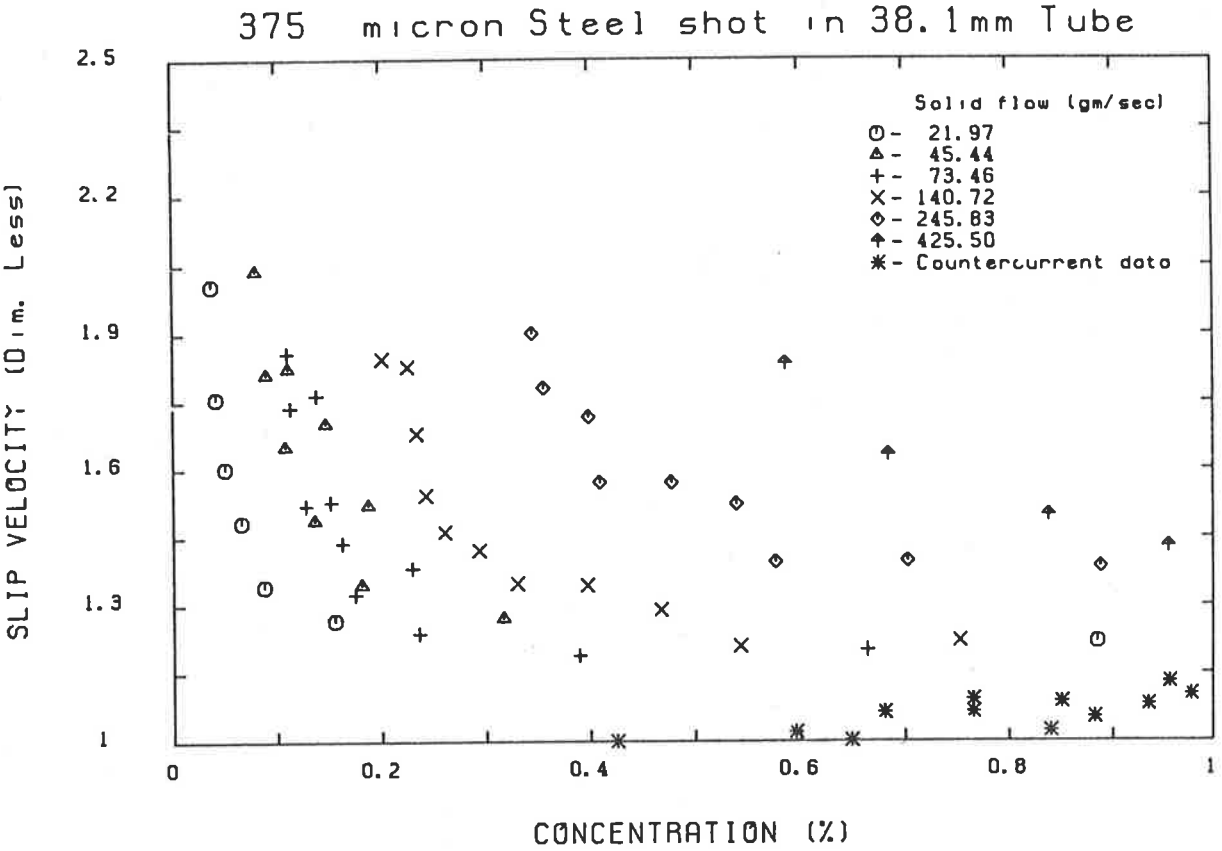
375 micron Steel shot in 38.1mm Tube
SLIP VELOCITY (Dim. Less)
CONCENTRATION (%)
Solid flow (gm/sec)
- 21.97
- 45.44
- 73.46
- 140.72
- 245.83
- 425.50
- Countercurrent data
2.5
2.2
1.9
1.6
1.3
1
0
0.2
0.4
0.6
0.8
1

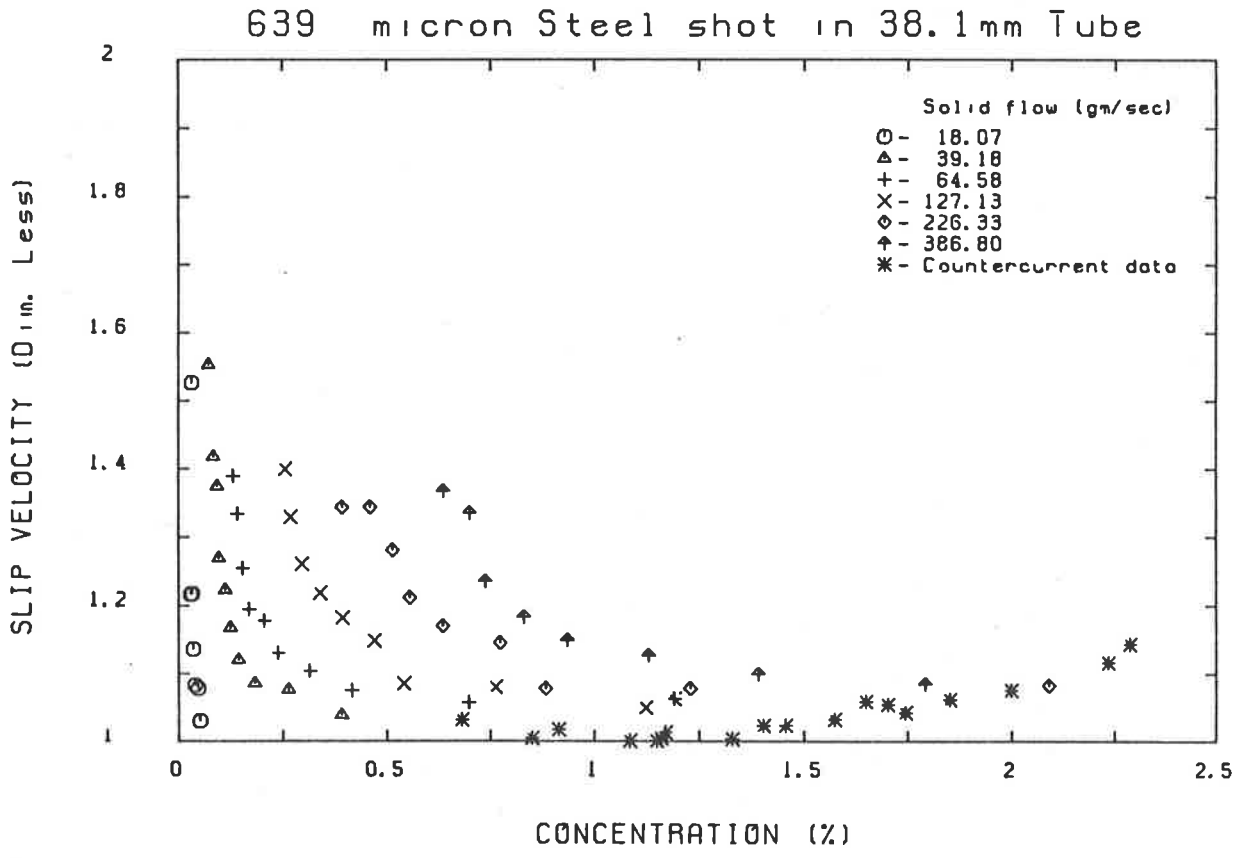
639 micron Steel shot in 38.1mm Tube
SLIP VELOCITY (Dim. Less)
CONCENTRATION (%)
Solid flow (gm/sec)
- 18.07
- 39.18
- 64.58
- 127.13
- 226.33
- 386.80
- Countercurrent data
2
1.8
1.6
1.4
1.2
1
0
0.5
1
1.5
2
2.5

APPENDIX (G)

VARIATION OF SLIP VELOCITY DUE TO WALL FRICTION WITH TRANSPORT VELOCITY

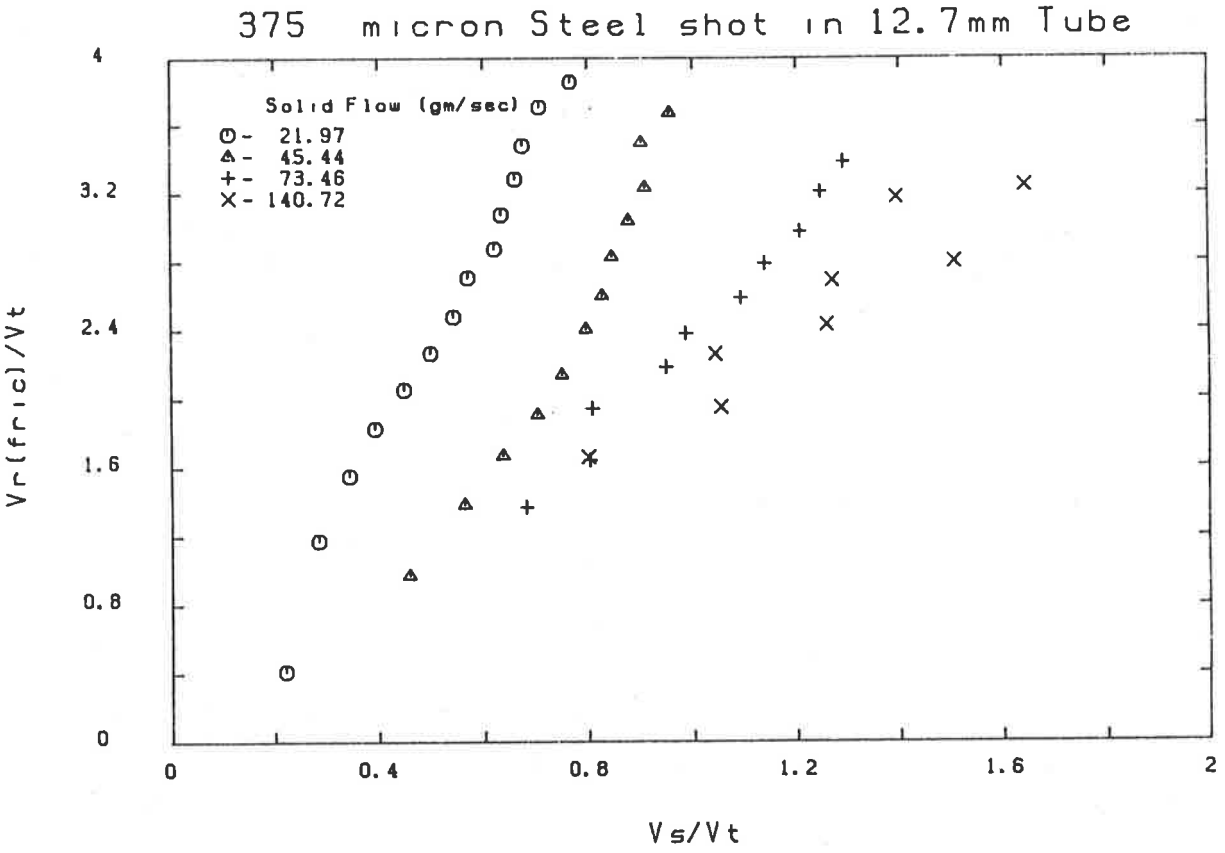
375 micron Steel shot in 12.7mm Tube
Solid Flow (gm/sec)
- 21.97
- 45.44
- 73.46
- 140.72
Vr(fric)/Vt
Vs/Vt
0
0.8
1.6
2.4
3.2
4
0.4
1.2
2

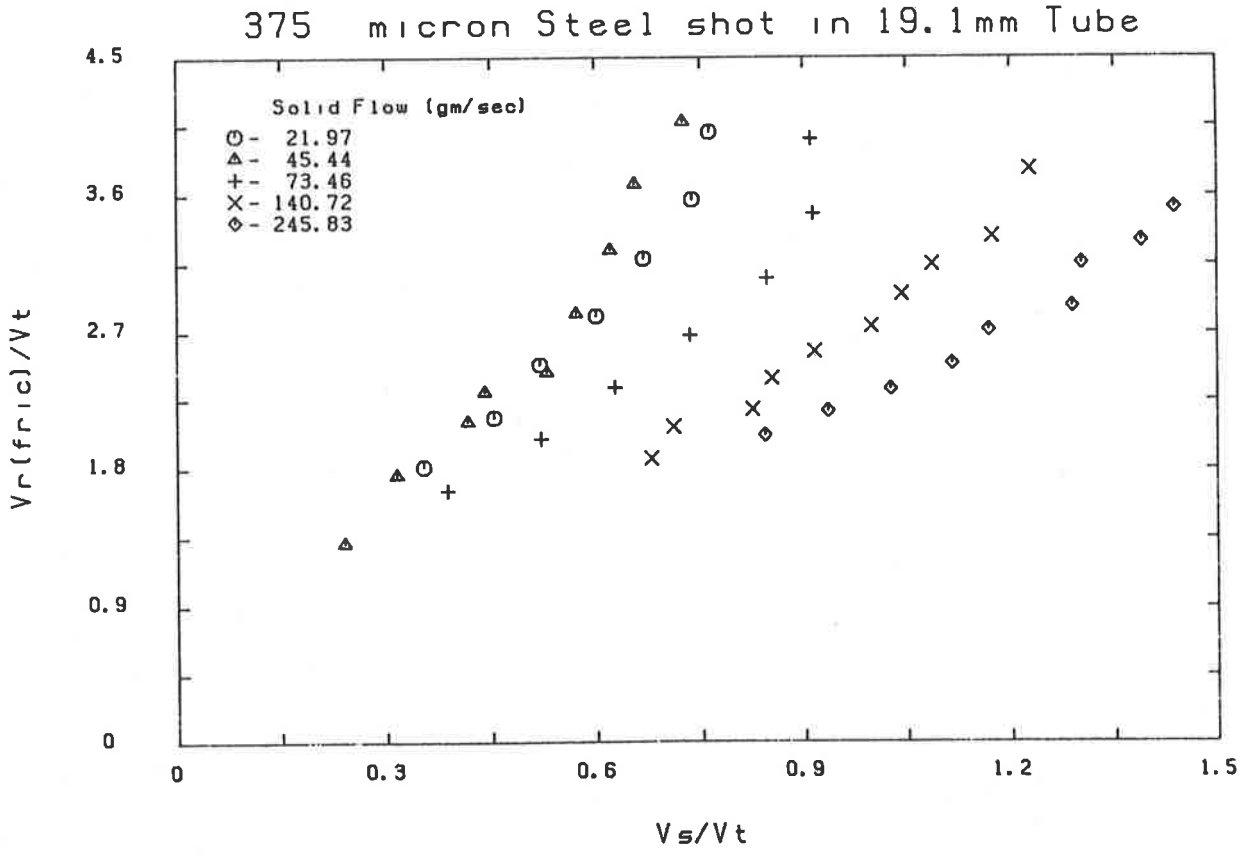
375 micron Steel shot in 19.1mm Tube
Solid Flow (gm/sec)
- 21.97
- 45.44
- 73.46
- 140.72
- 245.83
Vr(fric)/Vt
Vs/Vt
0
0.9
1.8
2.7
3.6
4.5
0.3
0.6
1.2
1.5

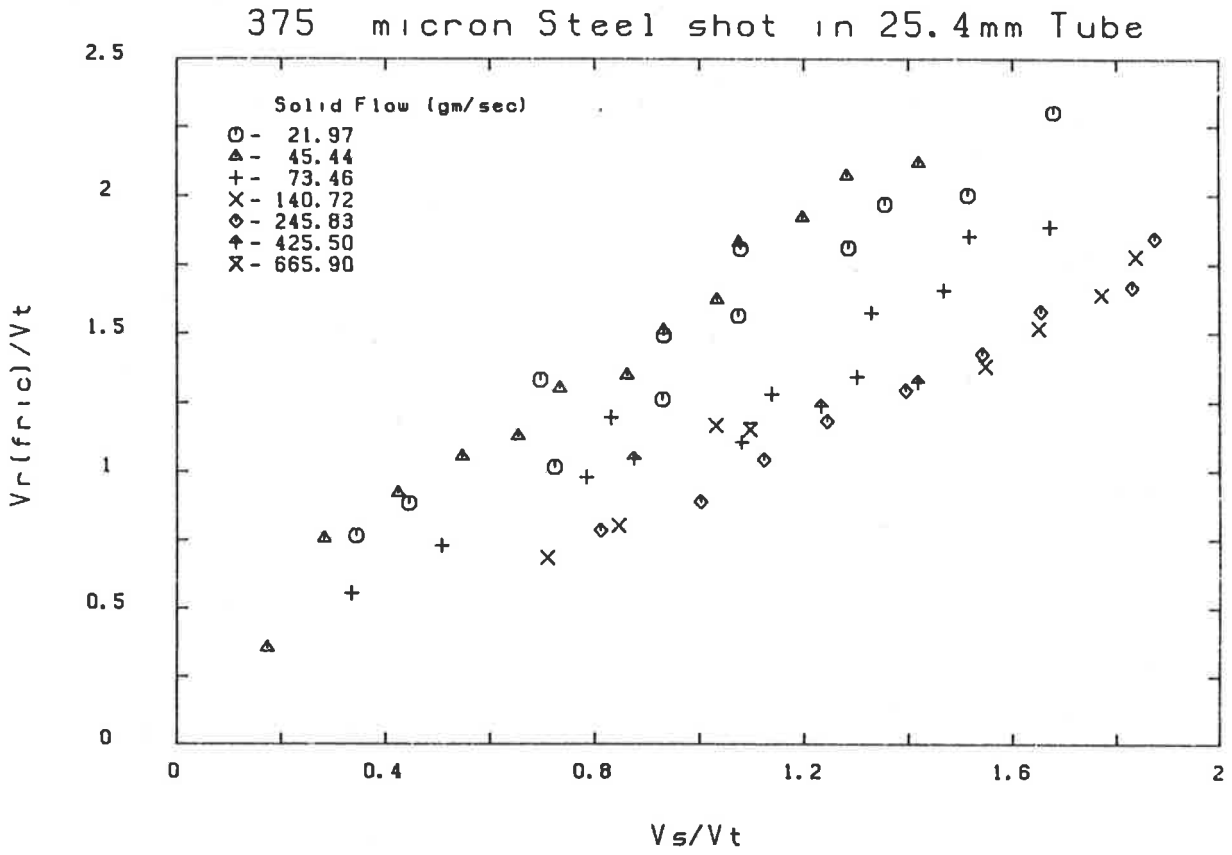
375 micron Steel shot in 25.4mm Tube
Solid Flow (gm/sec)
- 21.97
- 45.44
- 73.46
- 140.72
- 245.83
- 425.50
- 665.90
Vr(fric)/Vt
Vs/Vt
0
0.5
1
1.5
2
2.5
0.4
0.8
1.2
1.6

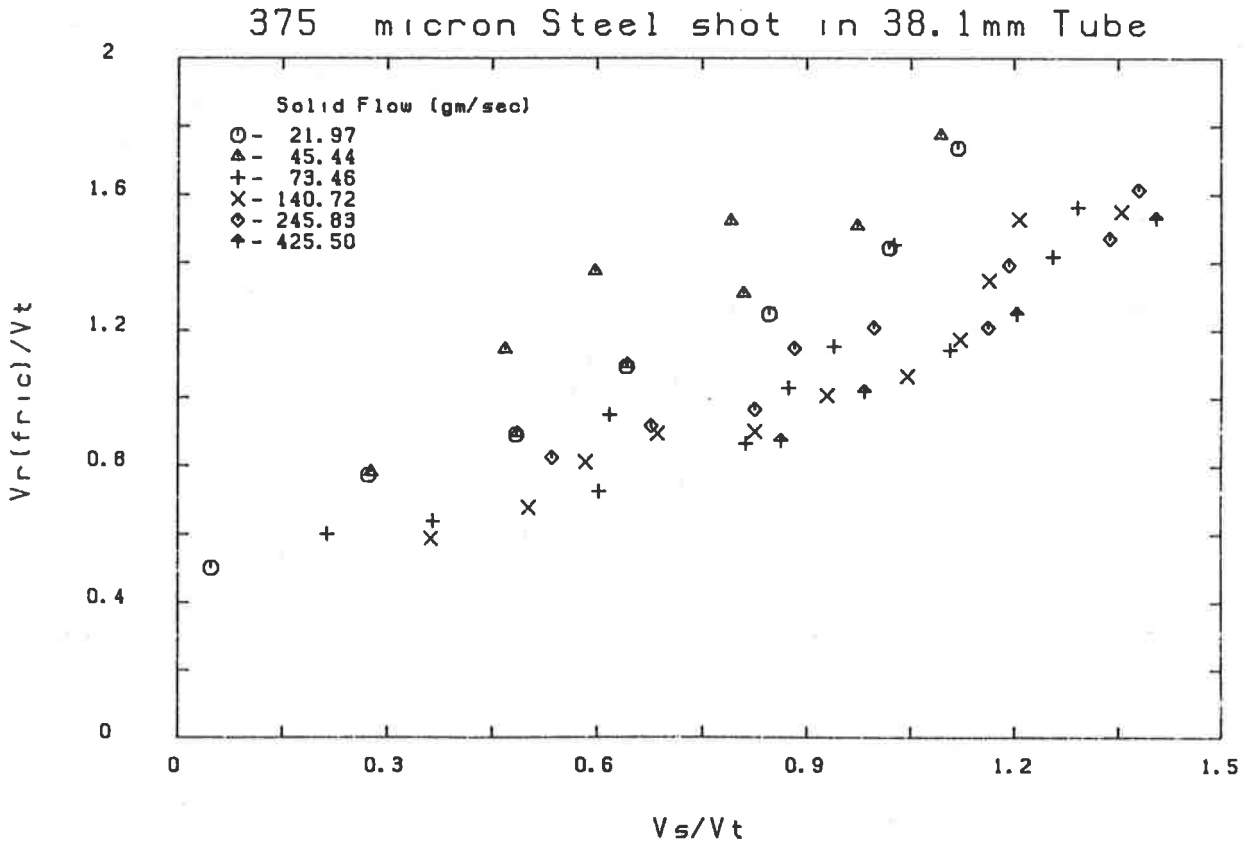
375 micron Steel shot in 38.1mm Tube
Solid Flow (gm/sec)
- 21.97
- 45.44
- 73.46
- 140.72
- 245.83
- 425.50
Vr(fric)/Vt
Vs/Vt
0
0.4
0.8
1.2
1.6
2
0.3
0.6
0.9
1.5

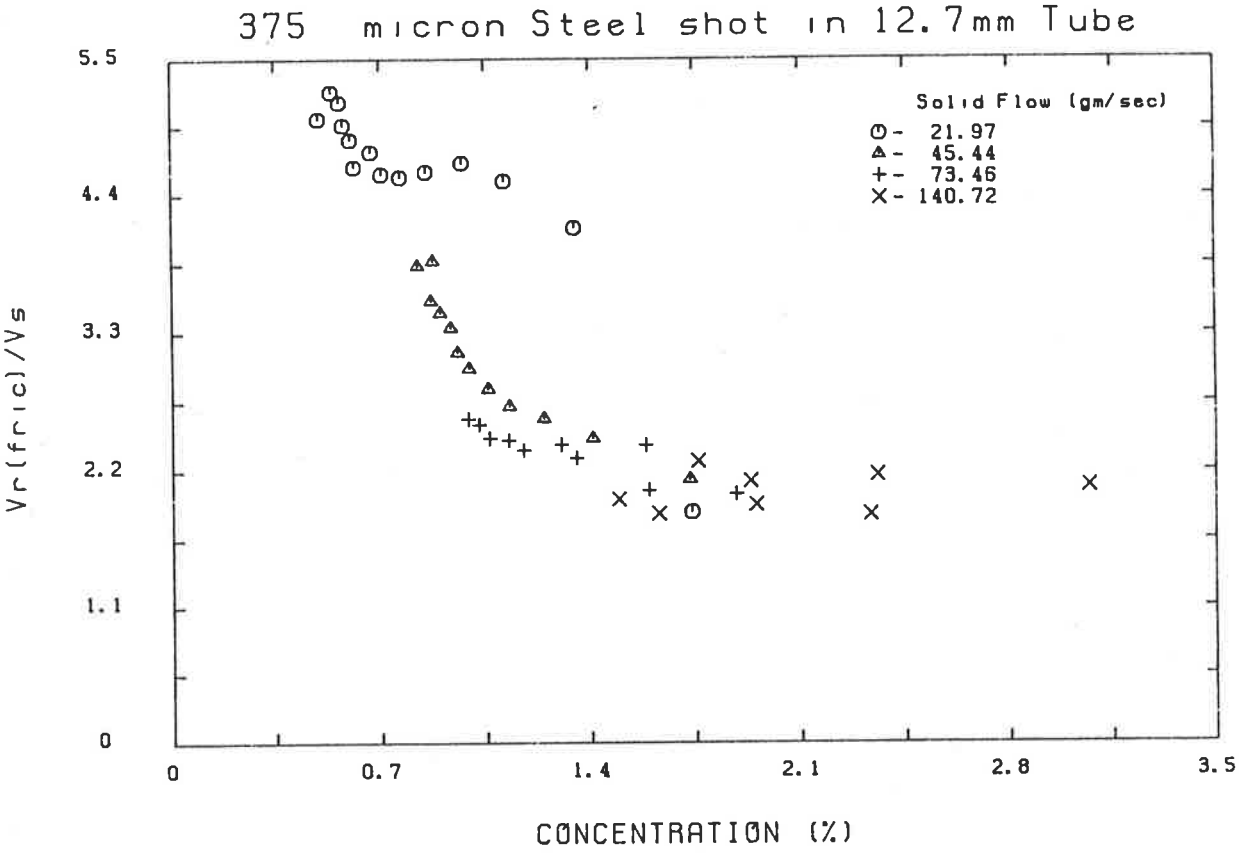
375 micron Steel shot in 12.7mm Tube
Solid Flow (gm/sec)
- 21.97
- 45.44
- 73.46
- 140.72
Vr(fric)/Vs
5.5
4.4
3.3
2.2
1.1
0
0
0.7
1.4
2.1
2.8
3.5
CONCENTRATION (%)

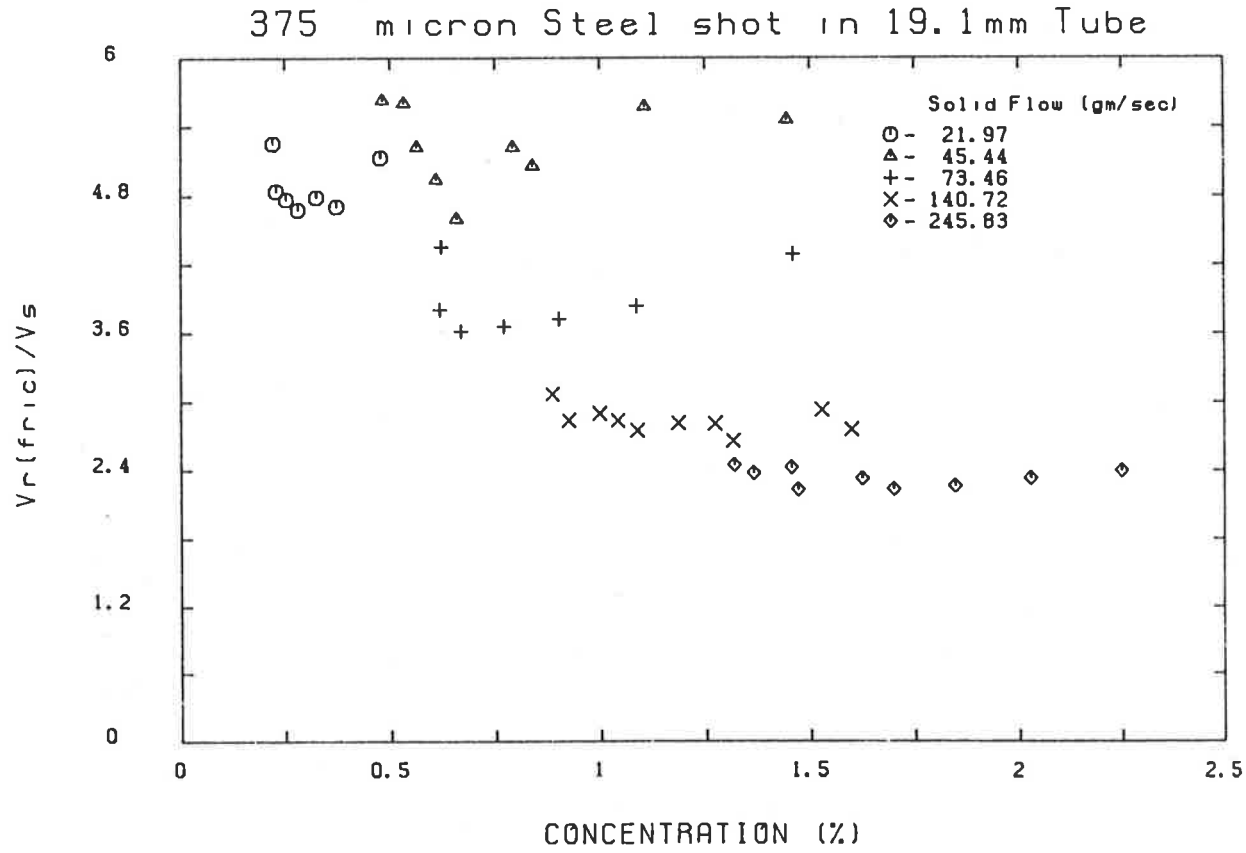
375 micron Steel shot in 19.1mm Tube
Solid Flow (gm/sec)
- 21.97
- 45.44
- 73.46
- 140.72
- 245.83
Vr(fric)/Vs
6
4.8
3.6
2.4
1.2
0
0
0.5
1
1.5
2
2.5
CONCENTRATION (%)

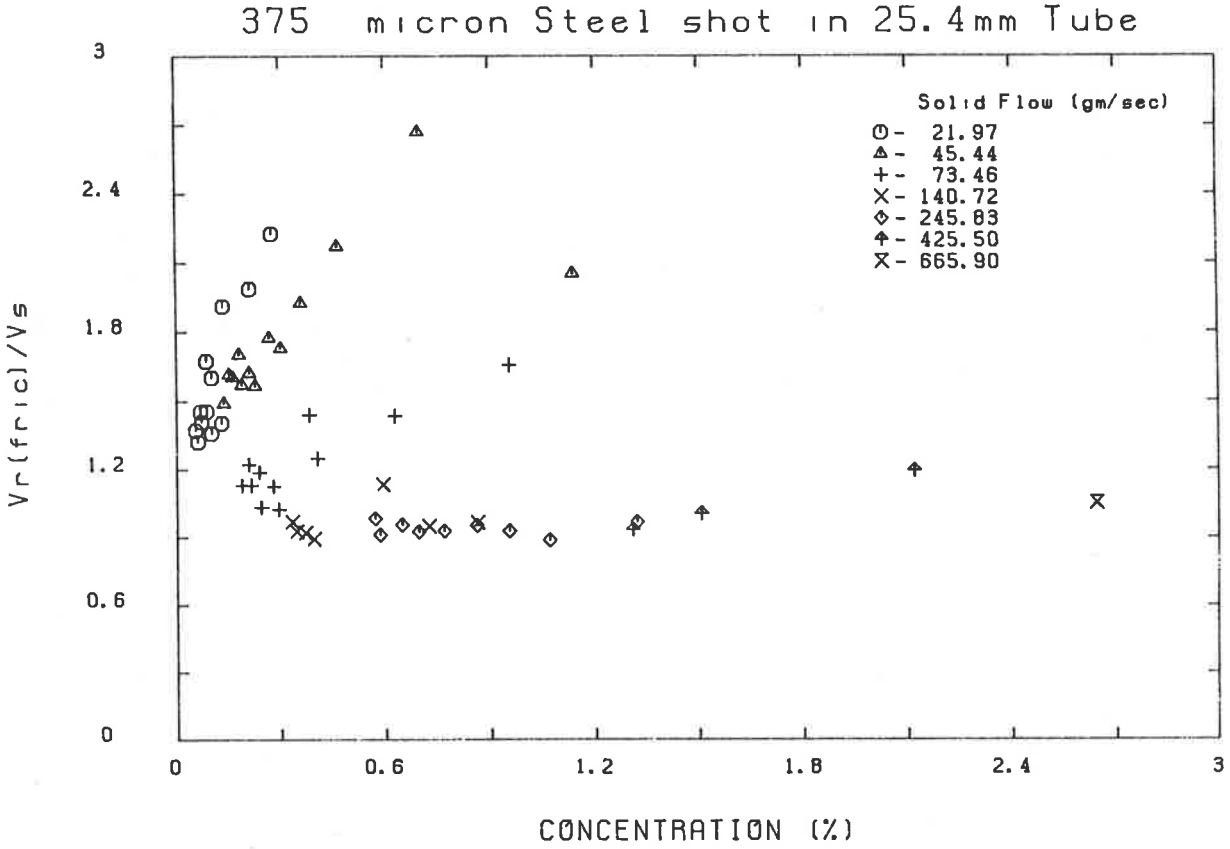
375 micron Steel shot in 25.4mm Tube
Solid Flow (gm/sec)
- 21.97
- 45.44
- 73.46
- 140.72
- 245.83
- 425.50
- 665.90
Vr(fric)/Vs
CONCENTRATION (%)
0
0.6
1.2
1.8
2.4
3

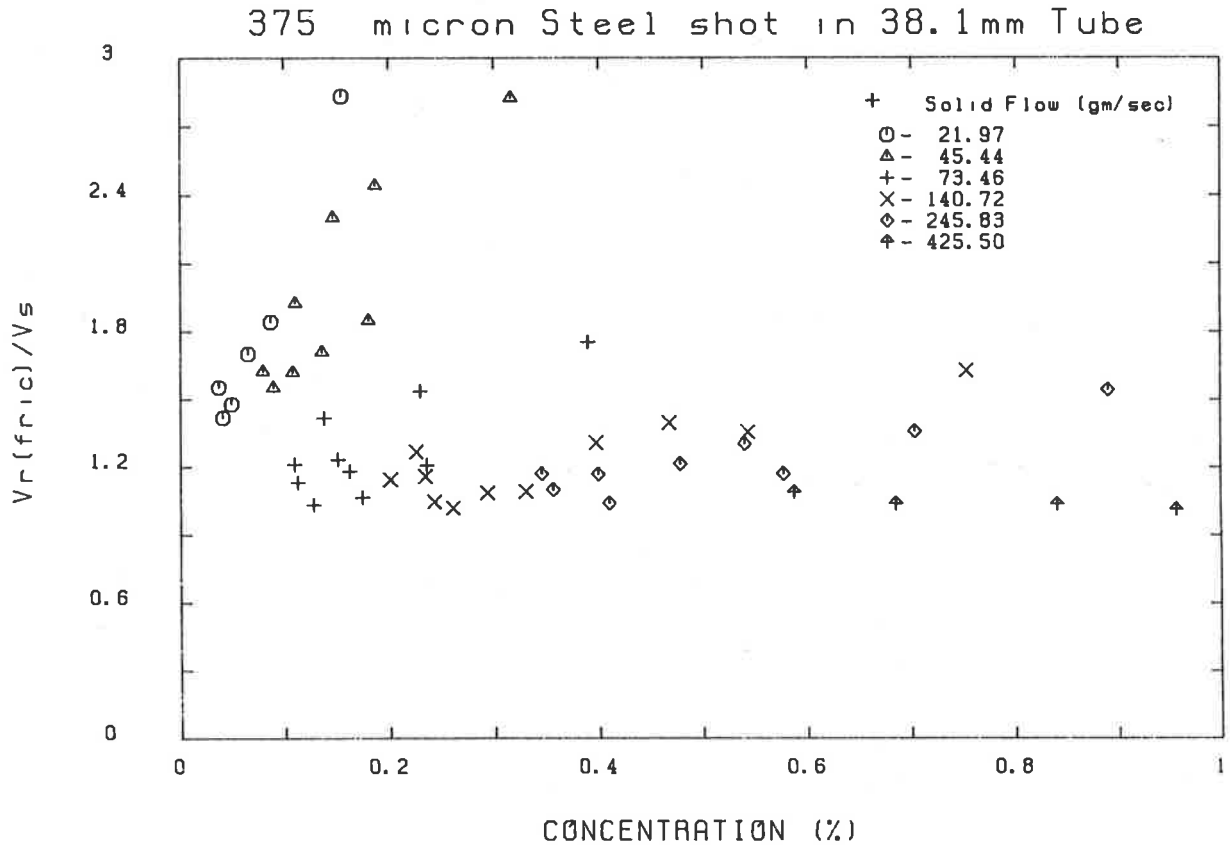
375 micron Steel shot in 38.1mm Tube
Solid Flow (gm/sec)
- 21.97
- 45.44
- 73.46
- 140.72
- 245.83
- 425.50
Vr(fric)/Vs
CONCENTRATION (%)
0
0.2
0.4
0.6
0.8
1
1.2
1.8
2.4
3